The Government of
The Republic of the Union of Myanmar
Ministry of Education

Department of Higher Education (Lower Myanmar)
and
Department of Higher Education (Upper Myanmar)

Universities Research Journal

Vol. 4, No. 3 December, 2011

Contents

The Government of
The Republic of the Union of Myanmar
Ministry of Education

Department of Higher Education (Lower Myanmar)
and
Department of Higher Education (Upper Myanmar)

Universities Research Journal

Vol. 4, No. 3 December, 2011

Chemical Analysis and α-Glucosidase Inhibitory Effect of Bizat Leaves (*Eupatorium odoratum* Linn.)

Hla Ngwe[1], Sandar Kyin[2] and Hla Hla Nyo[2]

Abstract

This research deals with the investigation of some chemical properties and the α-glucosidase inhibitory effect of ethanol extract and watery extract from Bizat leaf (*Eupatorium odoratum* Linn.). The Bizat leaf sample was collected from Pyay University campus. The 50% inhibitory concentration (IC_{50}) values of watery and ethanol extracts from Bizat leaves on α-glucosidase enzyme activity were found to be 0.14 and 0.31 μg/mL, respectively, lower than that of standard metformin (IC_{50}=0.42 μg/mL) under conditions. Therefore, both watery and ethanol extracts from Bizat leaf were observed to be more effective than standard drug α-glucosidase inhibitor metformin to inhibit the α-glucosidase enzyme activity.

Key words: α-glucosidase inhibitory effect, Bizat leaf, *Eupatorium odoratum* Linn.

Introduction

Nowadays, people suffered from diabetes mellitus are rapidly increasing. It is also one of the six prior major diseases: diabetes, tuberculosis, hypertension, malaria, diarrhoea and dysentery recorded in Myanmar. Most of the people have tried to use herbal drugs for management or for the treatment of the diseases. There are two common types of diabetes: Type I diabetes (insulin-dependent diabetes) and Type II diabetes (non-insulin dependent diabetes). Postprandial hyperglycaemia plays an important role in the development of Type II diabetes mellitus. Control of postprandial hyperglycaemia is thought to be very important in the treatment of diabetes.

α-Glucosidase and diabetes

α-Glucosidase is one of glucosidases located in the brush-border surface membrane of intestinal cells and body fluids. As it is the key enzyme of carbohydrate digestion increasing the blood glucose level, it is

1. Professor, Dr, Department of Chemistry, Pyay University
2. Assistant Lecturer, Dr, Department of Chemistry, Pyay University

one of the facts to develop the Type II diabetes after a meal (Fallah. *et al*., 2008)

α-Glucosidase inhibitors

α-Glucosidase inhibitors act directly to reduce the sharp increases in glucose level that occur immediately following ingestion of a meal. By using α-Glucosidase inhibitors, postprandial hyperglycaemia could be controlled or managed (Cannel *et al*., 1987). α-Glucosidase inhibitors, a class of diabetes drugs, also known as "starch blockers" function by slowing the absorption of certain simple sugar molecules in the gastrointestinal tract to reduce or to delay the sharp rise in blood glucose level after a meal. Acarbose (brand name Precose), miglitol (Glyset), voglibose (Volix and others) and emiglitate have been approved to use as antidiabetes drugs. Metformin (Glucophage and others) or sulfonylureas (Diabinese, DiaBeta, Glynase, Micronase, Glucotrol, Glucotrol XL, Amaryl) have been reported to be more effective at managing blood glucose (Website 1). Numbers of research on the investigation of the effective natural α-Glucosidase inhibitors from herbals with antidiabetic potential have been reported.

Testing the effect of herbs with anti-diabetic potential on α-Glucosidase is a common procedure in herbal research laboratories by using UV-visible spectroscopy. This bio-assay is useful to screen and to elucidate the mechanism of action of hypoglycaemic herbs.

Recently, in Myanmar *Eupatorium odoratum* Linn. (Bi-zat) flowering with purple colour is claimed as a medicinal plant to use for the treatment of Type II diabetes. It is widely distributed in Myanmar. It has been proposed as a traditionally useful medicinal plant for the treatment of various kinds of diseases such as skin disease, cancer and diabetes etc. Scientific investigation on treatment of boil, infected by *Stapylococcus aureus* has already been done using ethanol and pet-ether extracts and it was found that this plant has high potency for the treatment of skin disease (Nwe Thin Ni, 2004 a). It has also been found that it is flavonoid in its rich in leaves (Nwe Thin Ni, 2004 b). However, there is no scientific evidence that this plant can be used for the treatment of diabetes.

***Eupatorium odoratum* Linn.**

Myanmar name – Bizat
Botanical name - *Eupatorium odoratum* Linn.
Family name - Asteraceae

English name – Triffid-weed

Part used - leaves

Eupatorium odoratum is distributed through India, Indochina and common in all tropical countries. In Myanmar, it can be widely found anywhere. It is (up to 9 feet) shrubby with rather large, lanceolate, leaf blades coarsely toothed, especially near the base on long leafless branches which are spreading from the axils. These flowers are white, flowering time from August to October in the Western Countries, whereas in Myanmar, it is from November to March (Wealth of India, 1952).

The plant of *Eupatorium odoratum* consists of terpenoids, steroids, flavonoids and tannins. According to the literature, steroids, terpenoids and 13 flavonoids such as 2-hydroxy-3,4,4',5',6'-pentamethoxy chalone, 4,2'-dihydroxy-4',5',6'-trimethoxy chalone, 2'-hydroxy-4,4',5',6'-tetramethoxy chalone, 6'-hyroxy-4,2',3',4'–tetramethoxy chalone, 4'-methoxy 5,7-dihydroxy flavonone, kaempferol, quercetin and kaempferol -4'–methyl ether, etc., are present in this plants.

Application of *Eupatorium odoratum* Linn.s

Indigenous cellulosic raw materials for the production of pulp, paper and board were obtained from *Eupatorium odoratum* Linn. The whole plant is reported to possess medicinal properties. Bitterness of the plant can cure blood clotting. A decoction of the leaves is used for lactogogue and it is valued in native medicine as a cure for malaria and as a cough remedy. Cancer is also found to be cured by the decoction of the leaves of this plant. Not only this property but also rejuvenation power restoration was found and practised by natives of Myanmar. The fresh juices of the leaves can cure fresh cuts very easily. It is like tincture iodine for the cuts. The part of leaves are used externally in traditional medicine as a wound healing, skin abscess, diuretic, cathartic, intermittent, fever, ulcers, bilious, catarrh and influenza.

The present research focused on some chemical analyses and on scientific study of the antidiabetic property of Bizat leaves via the investigation of the inhibitory effect on α-glucosidase activity using ethanol extract and watery extract.

Materials and Methods

Eupatorium odoratum Linn. (Bizat) leaves were collected from Pyay University Campus in April, 2010. It was identified at Department of

Botany, University of Yangon. The collected Bizat leaves were air-dried at room temperature after cleaning. These dried leaves were then powdered and stored in air-tight glass bottle. The chemicals used in this research were "British Drug House Chemical Ltd., Poole, England", "Kanto Chemical Co., Inc., Japan", and Hopkins and Williams Ltd., England".

Some Chemical Analyses of Bizat Leaves

Some nutritional values such as moisture, ash, fat, protein, crude fiber and carbohydrate contents of the sample were determined by appropriate reported methods (AOAC, 1990). The elements present in dried powdered samples were qualitatively determined by EDXRF (Energy Dispersive X-Ray Fluorescence) technique using Shimadzu EDX-700 spectrometer in Universities' Research Center, Yangon University. In order to find out the types of organic constituents present in the sample, preliminary phytochemical investigation: tests for alkaloids (Trease and Evans, 1980), α-amino acids (Marini-Bettolo *et al.*, 1981), carbohydrates (Molish's Test) (Shriner *et al*., 1980), cyanogenic glycosides (Trease and Evans, 1980), flavonoids (Robinson, 1983), glycosides (Marini-Bettolo *et al.*, 1981), organic acids (Robinson, 1983), reducing sugars (Finar, 1973), saponins (Shriner *et al*., 1980), steroids, tannins and terpenoids (Tin Wa, 1972) was carried out according to the appropriate reported methods.

Screening of Inhibitory Effect of Bizat Leaf on α - Glucosidase Enzyme Activity

α-Glucosidase enzyme was extracted from imgerminated flint corn seed and this was used for screening of the inhibitory effect of Bizat leaf ethanol and watery extracts.

The effect of ethanol extract and watery extract from Bizat leaves on α-glucosidase enzyme activity was investigated by determining the α - glucosidase inhibitory effect on the production of glucose from sucrose at 505 nm wavelength (Astumi *et al*., 1990). This experiment was done in triplicate for each sample solution. Absorbance values obtained were used to calculate percent inhibition and 50% inhibitory concentrations.

(i) Preparation of test sample solution

2 mg of each extract and 10 ml of distilled water were thoroughly mixed with vortex mixer. The mixture solution was filtered and the stock solution was obtained. Then the test sample solutions were prepared in

different concentrations: 0.125, 0.25, 0.5, 1.0, 2.0 µg/mL by serial dilution method.

(ii) Reagents required

(i) α - glucosidase enzyme

10 mg dissolved in 100 ml distilled water.

(ii) Substrate – sucrose dissolved in distilled water (37 mM)

(iii) Glucose oxidase reagent (commercial kit)

Glucose oxidase in special buffer

(iv) 6 % dimethyl sulfoside (DMSO)

(iii) Procedure

Firstly, the control solution was prepared by mixing 1 mL of sucrose, 1 mL of enzyme and 1 mL of DMSO with vortex mixer and incubated for 30 min at 37 ºC followed by addition of glucose oxidase reagent (0.5 mL). After the incubation of the above mixture at 37 ºC for 30 min, the reaction was stopped by immersing the test tube into a boiling water bath for 10 min and allowed to cool to room temperature. Secondly, the background solution was prepared by mixing 1 mL of sucrose and 1 mL of 6% DMSO with vortex mixer according to the above procedure. Finally, the test solution was prepared by mixing 1 mL of sucrose, 1 mL of sample solution and 1 mL of 6% DMSO with vortex mixer and incubated for 30 min at 37 ºC followed by addition of 1 mL of enzyme. After the incubation of the above mixture at 37 ºC for 30 min, glucose oxidase reagent (0.5 mL) was added. Then the above mixture was incubated at 37 ºC for 30 min and the reaction was stopped by immersing the test tube into a boiling water bath for 10 min and allowed to cool to room temperature. Absorbance for all solutions was measured by using a UV-7504 spectrophotometer at 505 nm. Antidiabetic drug metformin was used as a standard.

From the absorbance values, percent inhibition of the sample on α-glucosidase enzyme activity and average percent inhibition on α-glucosidase enzyme activity were calculated by using following equations (Kurihara *et al.*,. 1994).

$$\%\ \ inhibition = \frac{A_c - A - A_b}{A_c} x100$$

Where,

% Inhibition = percent inhibition of tests sample on α-glucosidase enzyme activity

A_c = absorbance of control solution

A_b = absorbance of background solution

A = absorbance of test sample solution

The IC_{50}, 50% inhibitory concentration of the sample on α - glucosidase enzyme activity was calculated by Linear Progressive Excel Program.

Results and Discussion

In this section, the resultant data obtained from the preliminary phytochemical investigation, some chemical analyses and determination of α-glucosidase inhibitory effect of watery and ethanol extracts from Bizat leaves will be discussed.

Preliminary phytochemical investigation indicated the presence of α–amino acids, carbohydrates, flavonoids, glycosides, phenolic compounds, reducing sugars, saponins, steroids, tannins and terpenoids in Bizat leaves. There is no cyanogenic glycosides found in this sample and it can be so inferred that Bizat leaves may be free from harmful effect due to the toxic property of cyanogenic glycosides. Chemical analyses revealed that the dried Bizat leaves contained 7.70% of moisture, 12.40 % of ash, 4.0 % of fats, 6.80% of fiber, 8.75% of proteins and 60.35 % of carbohydrates, based on dry weight.

α- Glucosidase inhibitory effect of Bizat leaves

α - Glucosidase enzyme can produce the glucose and fructose from sucrose by enzymatic hydrolysis.

$$\text{Sucrose} \xrightarrow{\alpha - glucosidase} \text{Glucose + Fructose}$$

Therefore, the presence or absence of α-glucosidase enzyme inhibition effect of a sample can be demonstrated by the subsequent enzymatic production of glucose from the substrate sucrose. If glucose is not produced from sucrose by α - glucosidase in the presence of the herbal extract, it can be inferred that the sample has the α-glucosidase inhibitory effect, ie., it is an enzyme inhibitor. If the glucose is still formed from the

sucrose by α-glucosidase enzyme in the presence of the herbal extract, the herbal may not possess the α-glucosidase inhibitory effect. The principle of this method can be expressed as follows:

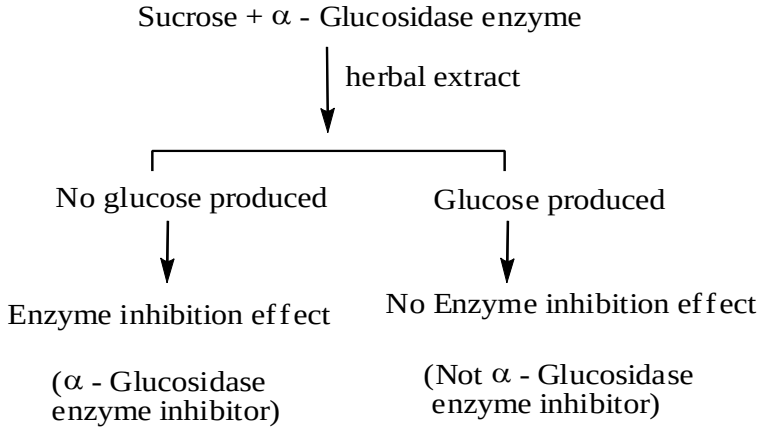

The formation of glucose can be quantitatively determined by using UV-visible spectrophotometric technique. Glucose oxidase enzyme oxidizes the glucose into gluconic acid and hydrogen peroxide is also obtained. The produced hydrogen peroxide induces oxidative condensation between phenol and 4-aminoantiphyrine in the presence of peroxidase (POD), so a red colour is produced. The amount of glucose contained in a test sample is determined by measuring the absorbance of the red colour at 505 nm (Yuhoo, 2004).

The reaction involved in the process can be shown as follows:

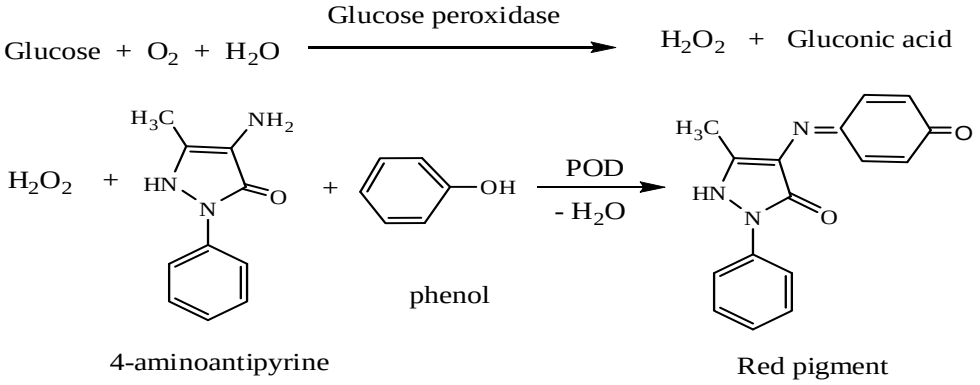

The absorbance of the red pigment will be increased with increasing amount of glucose. Hence, the lower the absorbance value, the lower the glucose content.

The absorbance of the red pigment formed from the glucose that produced from sucrose by α-glucosidase enzymatic hydrolysis, was found to be higher than that for the glucose produced from sucrose by α - glucosidase enzymatic hydrolysis in the presence of watery and ethanol extracts of Bizat leaves. This observation indicated that the extracts has the inhibitory effect on the α-glucosidase enzyme activity. The absorbance values of red pigment formed from the glucose decreased after addition with crude extracts of Bizat.

From the absorbance values, the resultant percent inhibition effects of the corresponding crude extract and standard drugs in various concentrations (0.125, 0.25, 0.5, 1.0, 2.0 µg/mL) on α-glucosidase enzyme activity are shown in Table 1. It was also found that the percent inhibition of crude extract was increased with increasing the concentrations as illustrated in (Figure 1).

From the percent inhibition, the respective IC_{50} values were calculated from the plot of percent inhibition vs different concentrations using Linear Progressive Excel Program and the results are tabulated in Table 1. Comparative study was also made on the IC_{50} values for watery and ethanol extracts from Bizat leaves with standard drug metformin. Since the lower the IC_{50} values the higher the inhibitory effect, the α-glucosidase inhibitory effect of Bizat watery extract (IC_{50}=0.14 µg/mL) was found to be highest, followed by EtOH extract (IC_{50}= 0.31 µg/mL) and then by standard drug metformin (IC_{50} = 0.42 µg/mL) as described in Figure 2.

Table 1 Percent inhibition of crude extracts from Bizat leaves and standard metformin in various concentrations on α-glucosidase enzyme activity and the corresponding IC_{50}

Sample	% inhibition in different concentrations (µg/mL)					IC_{50} (µg/mL)
	0.125	0.25	0.5	1.0	2.0	
Ethanol extract	23.70	47.21	57.95	69.40	73.25	0.31
Watery extract	48.02	63.73	72.95	79.43	85.41	0.14
Metformin	38.85	45.25	51.85	58.29	74.07	0.42

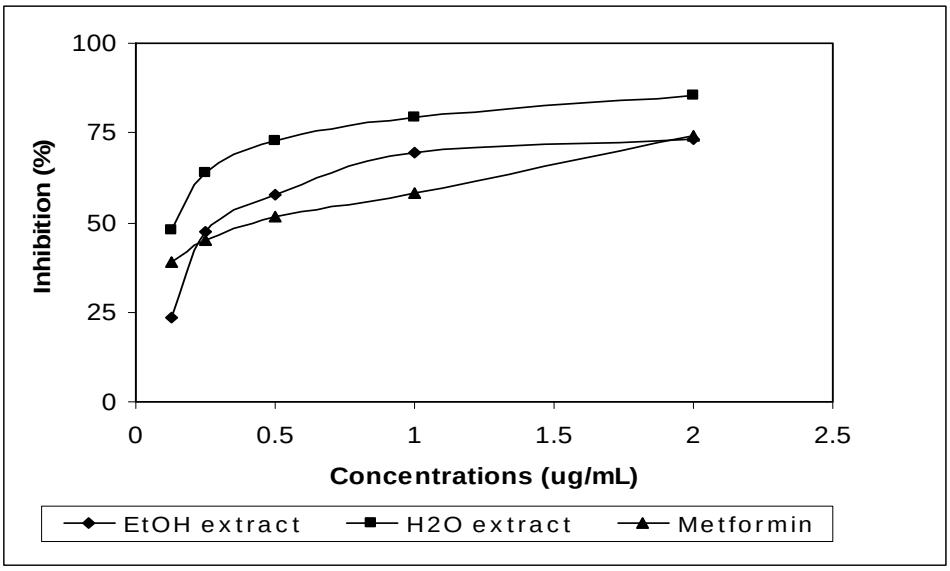

Figure 1 A plot of percent inhibition on α - glucosidase vs different concentrations of Bizat leaves extracts and standard metformin

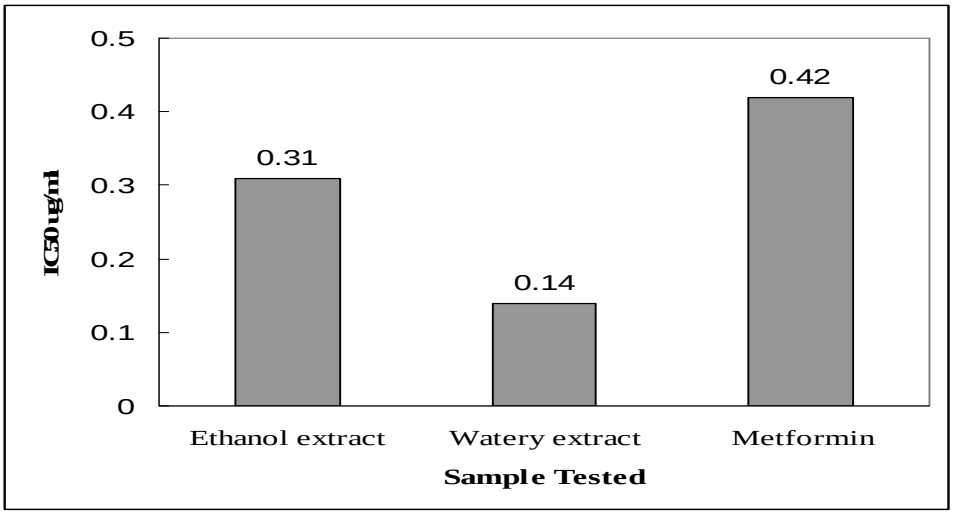

Figure 2 Comparison of the IC_{50} values of watery and ethanol extracts from Bizat leaves with standard drug metformin

Conclusion

From the overall assessment of the present research work, the following inferences could be deduced.

Preliminary phytochemical tests revealed the presence of α–amino acids, carbohydrates, flavonoids, glycosides, phenolic compounds, reducing sugars, saponins, steroids, tannins and terpenoids in Bizat leaves. In addition, Bi-zat leaves may be free from toxic effect due to the absence of the harmful cyanogenic glycosides.

The Bizat leaves contained 7.70% of moisture, 12.40 % of ash, 4.0 % of fats, 6.80% of fibre, 8.75% of proteins and 60.35 % of carbohydrates, based on dry weight.

The watery extract (IC_{50} = 0.14 µg/mL) and EtOH extract (IC_{50} = 0.31 µg/mL) from Bizat leaves possessed the inhibition effect on α - glucosidase enzyme activity and these extracts were found to be more effective to inhibit the α-glucosidase enzyme activity than standard drug metformin (IC_{50} = 0.42 µg/mL). This observation indirectly shows that *Eupatorium odoratum* Linn. (Bizat) leaves may possess the antidiabetes activity and may be effectively used as a natural α-glucosidase inhibitor or may be useful in the formulation of antidiabetes drugs to control or to manage the Type II diabetes mellitus.

This research will contribute to develop the role of formulation of antidiabetes drugs from medicinal plants to control or to manage the Type II diabetes mellitus.

Acknowledgements

The authors wish to thank Rector U Win Myint and Pro-Rector Dr. Than Than Win, University of Pyay and Professor Dr. Daw Hla Hla Than, Head of Department of Chemistry, Pyay University for their kind provision of the opportunity to submit this research paper.

References

AOAC, (1990), Methods of Analysis, Association of Official Analytical Chemists, 3rd Edn, Washington D.C.

Astumi, S.K., Umezawa, H. and Iinuma, H., (1990), "Production, Isoaltion and Structure Determination of a Novel β-Glucosidase Inhibitor, Cyclophellitol", *Phellinussp J. Antibiot.*, **43(1),** 49-53

Cannel, R.T., Kellam, S.J. and Owsianka, A. M. (1987), "Microalgae and Cyanobacteria as a Source of Glycosidase Inhibitor", *J. Gen Microbiol.*, **133**, 1701-1705

Fallah, H., Sharifi-far, H. and Mirtajaddini, M., (2008), "The Inhibitory Effect of Some Iranian Plants Extracts on the Alpha Glucosidase", *Iranian Journal of Basic Medical Science"*, **11 (1)**, 1-9.

Finar, I. L., (1973), "Organic Chemistry", 6th. Edn., 1, Longmans Group Limited, London

Kurihara, H., Sasaki, M. and Hatano, M., (1994), "A New Screening Method for Glucosidase Inhibitors and its Application to Algal Extracts", *Fisheries Science*, **60(6)**, 759-761.

Marini Bettolo, G.B., Nicolettic, M. and Patamia, M. and Patamia, M., (1981), "Plant Screening by Chemistry and Chromatographic Procedure Under Field Conditions", *J. Chromato.*, **121**, 213-214

Nwe Thin Ni, (2004 a), "Investigation of antibacterial activity and minimum inhibitory concentration of *Eupatorium odoratum* Linn. (Taw-bizat)", Submitted in School Family Day, Research Paper Reading Section (10.8.2004)

Nwe Thin Ni, (2004 b), "Isolation of bioflavonoid compounds from *Eupatorium odoratum* Linn. (Taw-bizat)", *J of MAAS* , Vol. 1. No.1

Robinson, T., (1983), "The Organic Constituents of Higher Plants", 5th Edn., Cordus Press, North Amberst, 285-286

Shriner, R.L., Fuson, R.C., Curtin, D.Y. and Morrill, T.C., (1980), "The Systematic Identification of Organic Compounds", A Laboratory Manual, John Wiley and Sons, New York, 385-425

Tin Wa, (1972), "Phytochemical Screening Methods and Procedures", *Phytochemical Bulletin of Botanical Society of America Inc.*, **5(3),** 4-10

Trease, G. E. and Evans, W. C. (1980), "Pharmacognosy", 1st. Ed., Spottiswoode, Ballantyne Ltd., London, 108-529

Wealth of India, (1952), " A Dictionary of Indian Raw Materials and Industrial Products , Council of Scientific and Industrial Research, New Delhi, Vol.1,p-1332

Yuhoo, L., (2004),"Effect of *Salacia oblonga* root and *Punica granatum* Flower on α-Glucosidase Activity", Herbal Medicine Practical, The University of Sydney

Online Material

Website 1: http://www.Website Diabetes Drugs Alpha Glucosidase Inhibitors Diabetes self M. htm. (2010)

Structural Elucidation of Bioactive Organic Compound Isolated from the Root of *Clerodendrum bracteatum* Wall (Phet-nan)

Thida Win[1] and San San Htay[2]

Abstract

In this research paper, one Myanmar Traditional Indigenous Medicinal Plant, namely *Clerodendrum bracteatum* Wall. (Phet-nan) was selected for chemical investigations. The preliminary phytochemical screening of the root of this plant and antimicrobial activities of the crude extract in various solvent systems were determined. In addition, a pure colorless needle shape crystal compound (SSH-1) was separated by Thin Layer and Column Chromatographic methods. The yield percent is found to be (8.15 mg, 0.2%) based upon the ethyl acetate crude extract. The melting point of this compound is 247-249 °C. The pure organic compound (SSH-1) was also screened for the antibacterial activities employing two species of microorganisms utilizing agar-well diffusion method. It was found to have medium activities on two types of micro organisms such as *Bacillus subtilis* and *Staphylococcus aureus*. It was also reconfirmed by phytochemical test which gave positive test for steroid. Furthermore, the molecular formula of this pure organic compound could be assigned as ($C_{28}H_{47}O_2N$) based upon some advanced spectroscopic methods, such as FT IR, ^{1}H NMR (500 MHz), ^{13}C NMR (125 MHz), DEPT, and EI-mass spectral data. The complete structure of isolated compound (SSH-1) including nine chiral centers could be elucidated by DQF-COSY, HMQC, HMBC, expanded ^{1}H NMR, NOESY, and EI-MS, respectively.

Key words: *Clerodendrum bracteatum* Wall., Phet-nan, steroid, DEPT, DQF-COSY, HMQC, HMBC

Introduction

In most developing countries, the flora remains unexplored from the point of view of practical utilization, yet past experience shows the many valuable drugs have been derived from plants. Information that a plant is used in traditional medicine is often an indication that it is worth scientific study. A number of approaches are available to the natural products

1. Pro-rector, Dr, Kyaukse University
2. Assistant Lecturer, Dr, Department of Chemistry, Kyaukse University

researcher who may be interested in discovering new and useful drug derived from plants (WHO, 1990 a).

Thus, if history is an indicator, when drugs derived from higher plants are being developed, it must be accepted that the end product will most probably have to be produced commercially by extraction and not by synthesis. If this is true, an abundant and easily accessible source of starting material must be available so that it can be collected and shipped to a processing point without undue difficulty or expense (WHO, 1990 a).

As chemical technology improved, the active constituents were isolated from plants, were structurally characterized, and in due course, many were synthesized in the laboratory. Sometimes, more active, better tolerated drugs were produced by chemical modifications (semi-synthesis), or by total synthesis of analogues of the active principles.

Research on medicinal plants has continued to be an area of major interest for the last several decades. In the United States, industrial chemists began a program in 1995 to look for new drugs in plant (WHO, 1990 b). Also in Myanmar the study of traditional indigenous medicinal plants and their usage in therapy play a very important role. These plants may have biologically active principles. The plant kingdom constituents are invaluable source of new chemical products which may be important due to their bioactive properties and their potential uses in medicines. One of Myanmar Indigenous Medicinal plants, *Clerodendrum bracteatum* Wall., Phet-nan, was used as astringent. But for chemically investigation no one reported in literature. Therefore, in the present study, isolation and elucidation of antibacterial steroid compound from the root of *Clerodendrum bracteatum* Wall. were performed.

Botanical Description

Family : Verbenaceae
Scientific name : *Clerodendrum bracteatum* Wall.
Local name : Phet-nan
Habit : Small Tree or Shrub
Medicinal uses : Inflammation, Dedandruff, Antipruritus
Parts used : root
Flowering time : July – November

Properties and Uses

Paste made from the plant is used as an astringent. Juice extract is applied to kill lice and remove dandruff. In the rural area of the Myanmar, bark or root of decotion is used to treat inflammation (Changkija, 1999).

Materials and Methods

In this research work, commercial grade reagents from BDH, and Merck, were used except ethanol, methanol, n-hexane and ethyl acetate, which were distilled for two times before they were applied. The advanced instruments are FT–IR Spectrometer (Hyper-IR, SHIMADZU), ^{1}H NMR Spectrometer (500MHz, JEOL, Japan), ^{13}C NMR Spectrometer (125 MHz, JEOL, Japan), and EI-MS Spectrometer (Finnigan MAT SSQ 710, USA) which are used in the characterization of samples and elucidation of pure compound. Analytical preparative thin layer chromatography was performed by using precoated silica gel (Merck, Co. Inc, Kieselgel 60 F_{254}). Silica gel 60 (70 to 230 mesh ASTM) was used for column chromatography.

Sample Collection

In this research work, Phet-nan was collected from Pyin Oo Lwin Township, Mandalay Region. Firstly, it was identified by the botanists of Department of Botany, University of Mandalay. The roots of Phet-nan were cut into small pieces and then allowed to dry in air. Those pieces were stored in a well stoppered bottle and used throughout the experiment.

Preliminary Phytochemical Screening

It was done on root sample according to the standard methods (Priestman and Edwards, 1953, Finar, 1964, and Vogel, 1956, 1966).

Antimicrobial Activities on Crude Extract

The study of antimicrobial activities was performed by agar-well diffusion method. In this experiment, six micro organisms, *Bacillus subtils, Staphylococcus aureus, Pseudomonas aeruginosa, Bacillus pumalis, Candida albicans,* and *Mycobacterium* species were selected.

Extraction and Isolation of Unknown Compound (SSH–1) from Phet-nan

The air dried powder sample (500 g) was percolated with (1500 mL) 95% ethanol for about two months. Percolated solution was filtered and concentrated. The residue was dissolved in 300 mL of ethyl acetate. When ethyl acetate extract was filtered and evaporated, the crude sample (4.2 g) was obtained. It was fractionated by column chromatography over SiO_2 (70-230 mesh), eluting with n-hexane : ethyl acetate in various volume ratios. Totally (188) fractions were collected. Then, the fractions with same R_f values were combined to yield 13 fractions. The major fraction (20 mg) was rechromatographed with the same procedure. Five combined fractions were obtained. Among them, the fraction (c) was found to be pure one. It was further purified by recrystallization using n-hexane: ethyl acetate (1:1 v/v) to provide pure compound (8.15 mg) as colorless crystal. Total yield of pure compound (SSH-1) was 0.2% based upon ethyl acetate crude extract.

Melting Point Determination of Pure Compound (SSH-1)

A few pure crystal was powdered and inserted into the capillary tube and the melting point was determined by the help of electric melting point apparatus.

Antibacterial Activity of Pure Compound (SSH-1)

Antibacterial activities of pure compound (SSH-1) were examined by using agar well diffusion method at DCPT. These results gave rise to the activity of the pure isolated compound (SSH-1).

Spectroscopic Studies of Pure Compound (SSH-1)

Spectroscopic data of isolated compound (SSH-1) were recorded by using advanced spectroscopic methods such as FT-IR, ^{1}H Nuclear Magnetic Resonance, ^{13}C Nuclear Magnetic Resonance, Distortionless Enhancement by Polarization Transfer (DEPT), Double Quantum Filter Correlation Spectroscopy (DQF-COSY), Hetero nuclear Multiple Quantum Coherence (HMQC), Hetero nuclear Multiple Bond Coherence (HMBC), Electron Impact Mass Spectroscopy (EI-MS) and Nuclear Over Hauser Effect Spectroscopy (NOESY).

Results and Discussions

The root of one Myanmar Indigenous Medicinal plant, Phet-nan, responded for a variety of constituents such as alkaloid, flavonoid, terpene, glycoside, phenolic compound and steroid in phytochemical test. Moreover, the ethyl acetate solvent extract of the plant material (Phet-nan) responded high activities on six selected organisms such as *Bacillus subtilis, Staphylococcus aureus, Pseudomonas aeruginosa, Bacillus pumalis, Candida albicans,* and *Mycobacterium* species. The colorless needle shape crystal (SSH-1)(0.85 mg) could be isolated utilizing modern separation methods. The yield percent was 0.2 % based upon ethyl acetate crude extract. Melting point is found to be 247-249°C. This pure compound (SSH-1) gave rise to positive for steroid test. The isolated compound (SSH-1) responded to medium antibacterial activities on *Bacillus subtilis* and *Staphylococcus aureus.*

Molecular Formula Determination of Compound (SSH-1)

The molecular formula of compound (SSH-1) could be determined by using some modern spectroscopic methods such as FT–IR, ^{1}H NMR (500 MHz), ^{13}C NMR (125 MHz), DEPT, HMQC, and EI mass spectral data, respectively.

Hence, FT–IR spectrum of compound (SSH-1) gave an information that unknown compound (SSH–1) contains –OH group (3463.9 cm^{-1}), NH

group (3255.6 cm^{-1}), sp^3 hydrocarbon (3070.5 cm^{-1}), carbonyl group (1689.5 cm^{-1}) , gem-dimethyl group (1373.2 cm^{-1}), cis or Z and trans or E alkenic functional groups (941.2 cm^{-1} and 887.2 cm^{-1}) respectively. The ^1H NMR (500 MHz) spectrum of SSH-1 indicates the total number of protons 45 in this compound. ^{13}C NMR (125 MHz) spectrum informs the total number of carbons 28 in this compound. In accordance with DEPT spectral data, seven sp^3 methyl carbons, eight sp^3 methylene carbons, six sp^3 methine carbons, four sp^3 quaternary carbons and one sp^2 quaternary carbon, one sp^2 methylene carbon and one carbonyl carbon could be detected. ^1H NMR (500 MHz) and ^{13}C NMR (125 MHz) spectral data reveal the partial molecular formula to be C_{28} H_{45} and partial molecular mass is 381. In the FT-IR spectrum, this unknown compound should consist of at least one –OH group and one carbonyl group. Hence, the partial molecular formula could be extended as C_{28} H_{46} O_2 and the partial molecular mass is 414. In the EI-mass spectrum, the molecular ion peak (m/z 429) represents its molecular mass. Therefore, the remaining molecular mass is (429–414=15). Hence, the remaining group should be secondary amine (>NH). Thus, the real molecular formula of this unknown compound (SSH–1) can be represented as C_{28} H_{47} O_2N which agrees with the nitrogen rule. The Hydrogen Deficiency Index (HDI) is 6.

Structure Elucidation of Compound (SSH–1)

The structure of compound (SSH–1) could be elucidated by using FT-IR, HMQC, DEPT, DQF-COSY and HMBC spectral data. In DEPT and HMQC spectral data, sp^2 alkenic protons (δ 4.56 ppm) and (δ 4.69 ppm) directly attach to sp^2 carbon (δ 109.50 ppm) as downward position which give rise to the exomethylene fragment. Moreover, in the DQF-COSY spectrum, the observation of long range (W) coupling between methyl protons (δ 1.65 ppm) and the exomethylene protons (δ 4.56 ppm and δ 4.69 ppm) attached to sp^2 carbon (δ 109.50 ppm) leads to the existence of this fragment (a).

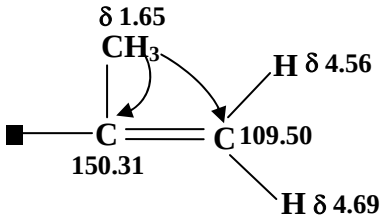

fragment (a)

By using DQF-COSY and HMBC spectra fragment (b) including A, B, C three rings could be elucidated. Furthermore, in HMBC spectrum, β ^{1}H-C long range signal and W long range signal occur both of methine proton (δ 1.51 ppm) and geminal methylene protons (δ 1.81 ppm) with carbonyl carbon (δ 177.21 ppm) producing the extended fragment (b).

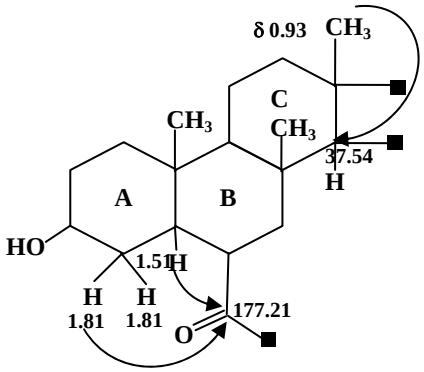

fragment (b)

In addition, in HMBC spectrum, methyl protons (δ 0.87 ppm) of gemdimethyl group have β ^{1}H–C long range signal with sp^{3} quaternary carbon (δ 40.21 ppm) and methine proton (δ 2.12 ppm) of long chain responds α ^{1}H-C long range coupling with sp^{3} quaternary carbon (δ 41.95 ppm) which leads to fragment (c).

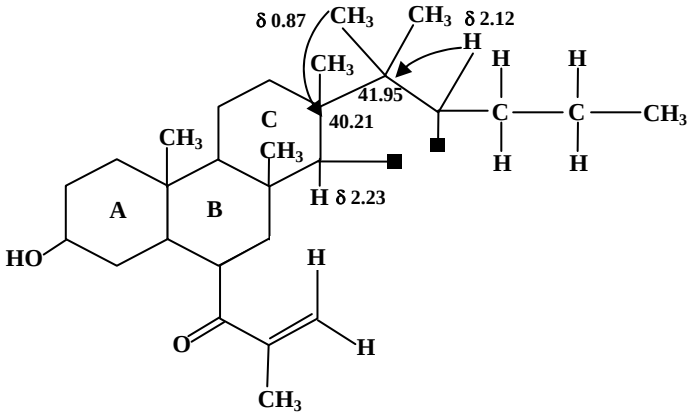

fragment (c)

In fragment (c), the down field chemical shift values of methine proton (δ 2.23 ppm) and (δ 2.12 ppm) lead to the attachment of NH group. It could be confirmed by FT-IR spectrum, the appearance of NH group at 3255.6 cm^{-1} could be assigned by the logical correlation of NH group to the down field chemical shift values of sp^3 methine proton (δ 2.23 ppm) and (δ 2.12 ppm) giving rise to the reasonable following planar structure. Its IUPAC name is 1-(3-hydroxy-8, 10, 13, 17, 17-penta-methyl-16-propyl-hexadecahydro-naphtho{1,2-g}indole-6-yl)-2-methyl propenone.

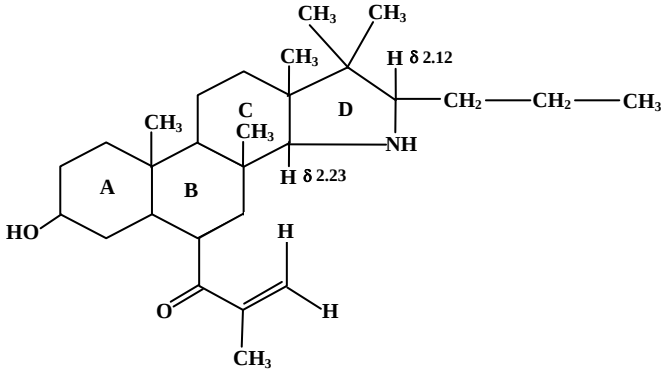

Planar Structure

Conformational Analysis of Compound (SSH-1)

The splitting pattern and J values of junction methine proton (δ 1.51 ppm, dt, J = 5.4, 11.3 Hz) in proton NMR spectrum displays axial

orientation of this methine proton and chair conformation of ring A and B could be assigned in trans decalin type two rings.

According to the NOESY spectrum and Proton NMR ring A, ring B and ring C are chair forms and ring D envelope like one.

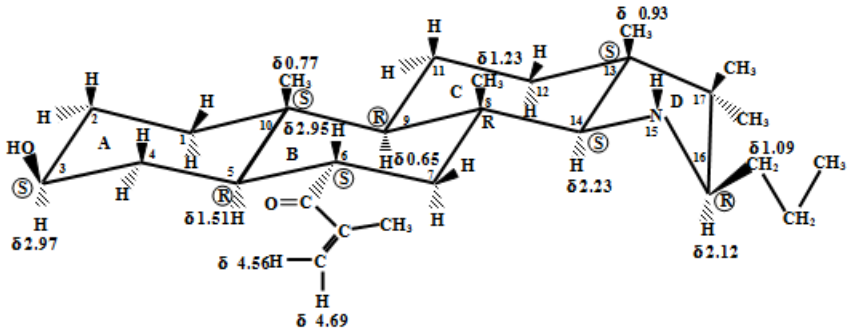

Hence the absolute confirmations of nine chiral centres could be assigned as (C_3- S, C_5- R, C_6-S, C_8-R, C_9 –R, C_{10}- S, C_{13}-S, C_{14}- S, C_{16}-R), respectively. IUPAC name of this compound (SSH-1) is (3-hydroxy-8,10,13,17,17-penta-methyl-16-propyl-hexadecahydro-naphtho{1,2-g} indole-6-yl)-2-methyl propenone.

Conclusion

In this paper, isolation of steroid type compound (SSH-1) from the ethyl acetate extract of root of one Myanmar Indigenous Medicinal plant, *Clerodendrum bracteatum* Wall. (Myanmar name: Phet-nan) was reported for the first time. This steroid compound responds to medium antibacterial activities on *Bacillus subtilis* and *staphylococcus aureus.* Moreover, the molecular formula of compound could be determined as C_{28} H_{47} O_2 N by some advanced spectroscopic methods such as FI IR, ^{1}H NMR (500 MHz), ^{13}C NMR (125MHz), HMQC and EI-mass, spectral data. In addition, the structural elucidation of this compound (SSH-1) and its conformational analysis was done by using some modern spectroscopic techniques such as DQF-COSY, HMQC, HMBC, NOESY and the fragmentation behaviors of EI-mass spectral data. In the structural elucidation of compound (SSH-1), DQF-COSY and HMBC spectra displays the assignment of planar structure of rings A, B, C, and D which were reported in Results and Discussion. In

the conformational analysis of compound (SSH-1), the observation of the coupling constant (J=11.3 Hz) between the two methine protons (δ 1.51 ppm and δ 2.95 ppm) indicates the axial orientation of those two protons. Hence, the two six member rings (A and B) are assigned as chair conformers. According to model study, the trans decalin type ring (A, B) junction C_5, axial proton must be oriented below the plane of the two rings and C_6, axial proton (δ 2.95 ppm) lies upper plane of ring B. NOESY spectrum indicates that all of these three methyl signals lie upper plane of their respective rings. The present research work suggests that the root of Phet-nan might be a potential source of antibacterial activity.

Acknowledgements

The authors would like to express sincere thanks to Professor Dr. Mya Aye, and Prof Dr. Myint Myint Sein, Department of Chemistry, University of Mandalay for providing research facilities and for their close supervision and suggestions. Special thanks are due to Rector Dr. Myint Lwin, Kyaukse University for his encouragement. Sincere thanks are also due to Associate Professor Dr. Y. Takaya, Mejio University, Japan for his invaluable helps and encouragement.

References

Changkija, S., (1999), "Folk Medicinal Plants of the Nagas in India", *Asian Folklore Studies*, 58, 250-230.

Finar.I.L., (1964), "Organic Chemistry", The English Language Book Society and Longmans. Green and Co., Ltd. 304.

Priestman, J. and Edwards, F.C.G.,(1953), "Aids to Qualitatives Pharmaceutical Analysis", Pag nd Bros (Norwish) Ltd., London, 98.

World Health Organization,(1990a), "Medicinal Plant in Geneva", *World Health Forum*, **11**(1).

World Health Organization, (1990b), "Medicinal plants in Vietnam", Western Pacific Series No. 3, WHO Regional Office for the Western Pacific, Manila, (ISBN 92 9061 101 4)

Vogel, A.I., (1956), " A Text Book of Practical Organic Chemistry", The English Language Book Society and Longmans. Green and Co., Ltd., 454.

Vogel, A.I., (1966), "Practical Quantitative Organic Analysis", 2nd Edition, Longman, William Clowes and Sons Ltd., 89.

Some Chemical Properties and Antimicrobial Activities of Dani –Ye (Fermented Nypa Sap) Obtained by Traditional Tapping Process

Aye Aye Myint

Abstract

Nypa frutican Wurmb. palm (Dani) has historically provided many useful products such as leaves, sap and fruits to traditional people living near or in coastal and mangrove forests. This research work deals with the processing of nypa sap (Dani-Ye-Cho) by traditional tapping method (Dani Kyauk) and fermentation of Dani-Ye-Cho with lack of chemical agent. Fresh sap from the selected palm yielded 0.5 L per day per tree. Phytochemical constituents in fresh sap and fermented sap investigated by chemical tests were α amino acids, carbohydrates, glycosides, reducing sugar and saponin. Some sensory characters and chemical properties were determined by standard methods. During 5 days changes of pH (6.5- 4.5) and reducing sugar content in fermented sap (26.80% - 21.5%) were recorded. On second day, alcohol formation of primary alcoholic–OH in fermented sap was qualitatively detected by chemical tests. Screening of antimicrobial activity on fresh and fermented Dani-Ye by paper disc method was carried out. The ten tested organisms used in this study were *Agrobacterium tumefaciens, Aspergillus flavus, Bacillus subtilis, Candida albicans, Escherichia coli, Micrococcus leteus, Pseudomonas fluorescens, Salmonella typhi, Staphylococcus aureus* and *Xanthomonas oryzae.* Fermented nypa sap showed more potent antimicrobial activity against all tested organisms with the range of inhibition zone diameter (14-24mm) than those of fresh sap against all test organisms except *Escherichia coli* and *Bacillus subtilis* with the range of inhibition zone diameter 10-15mm.

Key words : *Nypa frutican*, sap, traditional tapping, fermentation, reducing sugar, antimicrobial activity

Introduction

Nypa fruticans Wurmb. Dani , is one of the versatile palm found naturally in mangrove forests of Asia (Maung Maung Aye, 1995).Some large scale commercial interest is also currently developing for nypa products such as alcohol, sugar syrup, brown sugar , vinegar and fermented beverage in many countries (Burkill, 1993, Giesen, *et al*, 2006). In this paper, selection and preparation of mature nypa palm for traditional tapping process (locally called Dani kyauk), the collection of fresh sap,

Professor(Head) , Dr., Department of Chemistry, Myeik University

fermentation process , changes of sensory parameters and some chemical properties vs time and antimicrobial activities of fresh and fermented sap have been reported.

Botanical Aspects

Botanical name	*Nypa fruticans* Wurmb.
Myanmar name	Dani
Family	Arcaceae
Subfamily	Nypodeae
Genus	*Nypa*
Habit	Shrub
Parts used	The whole plant
	Sap

Description and Distribution

Nypa is the latinised of ‘nipah”, means shrubby, referring to its stemless appearance (Duke, 2006). Palm–shaped leaves are very long (5 - 9 m). Flowers appear on a long stalk (1m) as an inflorescence. Female flowers are encased in bracts and resemble a cone. Male flowers appear as a long spike and when ripe is golden yellow with sticky pollen. Fruits are chestnut brown, in cluster forming a globular shape (20-25cm). The fruits are fibrous and air cavities in the seed coat and fruit coat help keep the seedling afloat. The 'stem' of this palm is mostly horizontal and even underground. The sap is extracted from the inflorescence is called 'toddy', a typical local alcoholic drink (Tomlinson, 1986). Nypa fully matures within 5-6 years but bears fruits after three years or earlier. Plant native is Philippines, Malaysia, Indonesia, India and Myanmar. Figure 1 shows the selected mature *Nypa fruticans* palm in the mangrove forest near Taungpyo creek, Myeik,Tanintharyi Region.

(i) Taungpyo creek , Myeik

(ii) Mature palm with fruits

(iii) Flowering cone

(iv) Stalk bearing globular fruits

Figure 1. *Nypa frutican* Palm

Chemical Constituents

Most tapped palm trees give a sap very rich in sugar 10% to 20% according to species and individual variation, whereas in Asia the sap is used either as fresh juice or processed into a large array of products, wine, alcohol, arak, sugar and vinegar, etc. (Dalibard,1999). Nypa sap contained sucrose, protein, minerals as ash, calcium, phosphorous, iron, copper and vitamins (Gibbs,1911). The presence of non-essential amino acids, glycine, glutamic acid, alanine, proline, tyrosine and essential amino acids; methonine and leucine were detected in Pa-Ohn-Ye (Ei Ei Phyu Sin, 2002).

Alcohol from Nypa Sap by Fermentation

The quality and alcohol content of fermented sap depend on the conditions of alcohol fermentation process. The morning collection of sap is less fermented and contains more sucrose. During tapping process starch in Nypa stalk is broken down into sugar and are transport upwards toward the

stem apex (Fox, 1977). The polysaccharide formed was converted into glucose by fermentation. The fermentation of glucose to alcohol was carried out by using traditional method.

$$C_{12}H_{22}O_{11} + H_2O \xrightarrow{\text{yeast}} 4CH_3CH_2OH + 4CO_2$$

Sucrose Ethanol

$$C_6H_{12}O_6 \xrightarrow{\text{yeast}} 2\,CH_3CH_2OH + 2CO_2$$

Glucose Ethanol

Uses of *Nypa fruticans*

The long feathery leaves have traditionally been used as thatching materials for roof shingles, walls for dwelling poultry, acne , rest houses and picnic hut in resort area. Nypa palm leaves can also be used to make baskets, hats, mats, raincoats, brooms, floats for fish nets, fishing poles and ropes. The young leaves are used for smoking (Hamilton and Murphy,1988). In Malayan medicine, it is useful for the treatment for herpes and the juice from young shoot is effective for open sores. In Kalimintan, the ash "garm nipah" of the roots or leaves, was used to treat both toothache and headache (Burkill,1993). Brown sugar and fermented product; vinegar can be used in domestic cooking, industry and for preserving food. The Steering Committee on Canadian liquid Renewable Fuels report that Nypa alcohol may be mixed with petrol at 1:4 ratio and used directly in standard petrol engines without carburetor modification. Currently the Department of Primary Industry of Papua Guinea is planning alcohol from Nypa palm project and alco-gas from Nypa palm as an energy source is under study in Philippines (Päivoke,1985).

Materials and Methods

Preparation of Fresh Nypa Sap by Traditional Tapping Process

Figure 2 performed the traditional tapping process, locally known as "Dani Kyauk" in Myeik to prepare fresh sap; Dani -Ye- Cho. About 5-year old Nypa palm trees bearing globular fruits were selected .Before tapping, some old leaves were removed from the infloresence stalk. The treated stalk at a distance of about 45 cm from the base was then slowly tapped with legs (i.e, kicked) for several times twice a day. The process

was repeated until the stalk became swollen. Then the phloem of the stalk was cut at least three times at the swollen section. In every tapping step, a thin slice of 2mm thickness was cut off . On the first day, the fresh sap slowly oozed out from the smooth surface of the cut. After overnight, the frothing was followed by exudation. On the third day, the sweet smell of clear golden brown color sap (Dani -Ye -Cho) was slowly collected with the sterilized bamboo culm in the inclined position. Depending on the long term tapping process, the sap was successfully collected for about one month. It yields 0.5 L per tree per day.

Fermentation of Fresh Nypa Sap

Freshly collected sap samples (~100 mL) in each conical flask (250mL) were kept and stored at (31 ±1°C) for 5 days to allow natural fermentation in a close chamber. The flasks were carefully closed to prevent frothing of fermentation. The changes of sensory during storage was observed and recorded.

Phytochemical Investigation on Fresh and Fermented in Nypa Sap

The phytochemical constituents in both fresh and fermented Nypa sap were investigated according to the standard procedures (Tin Wa, 1972; Vogel, 1966; Robinson, 1983; Harbone,1984).

(a)Selection of palm

(i) Inflorence stalk of *Nypa frutican* (ii)Cleaning the base of the plant

(b)Kicking (Tapping) process for good exudation

(iii)Tapping (kicking) the stalk (iv) Cutting about 2mm slice

(c) Collection of sap

(vi) Exudation of sap (vii) Collection of sap in sterilized bamboo culm

Figure 2. Collection of Nypa sap by traditional tapping process

Detection of Alcohol in Fermented Nypa Sap by Chemical Reactions

The fermentation capacity in term of alcohol production was the highest in ***Nypa fruticans*** sap. Formation of alcohol and functional group -OH, the hydroxyl group was preliminarily detected by chemical reaction tests ; Xanthate, Oxidation and Lucas tests (Vogel,1966) . Then the –OH of primary alcohol was confirmed by specific qualitative tests namely ethyl acetate and iodoform test.

Determination of Some Sensory in Nypa Sap During Storage

Sensory characteristics such as color (visual), odor and taste of freshly collected Nypa sap was monitored daily during storage at

(31 ±1°C) for 5 days (Table 1).

Determination of Some Chemical Properties of Nypa Sap During Fermentation

Changes of pH in fermented sap in 5 days were recorded by pH meter (Table 2). Reducing sugar content and ascorbic acid content in fermented sap were also determined by iodotitrimetric method (Pearson, 1962, Vogel,1966). Elemental analysis was carried out by AAS (Perkin Elmer 800).

Determination of Antimicrobial Activity

In vitro antimicrobial activity of both fresh and fermented Nypa sap was screened by paper disc diffusion method (Cruckshank, 1960, Prescott, *et al*.,1999).

Ten tested organisms

Agrobacterium tumefaciens, Aspergillus flavus, Bacillus subtilis, Candida albicans, Escherichia coli, Micrococcus leteus, Pseudomonas fluorescens, Salmonella typhi, Staphylococcus aureus and Xanthomonas oryzae

Results and Discussion

Selection of Samples

Nypa fruticans palm is a useful, versatile and fairly common component of mangrove forests of Asia and Oceania. Nypa sap was natural abundance and traditional liquors in Myeik , Tanintharyi Region.

Traditional Tapping Process

Nypa fruticans sap was prepared by traditional tapping (kicking) process as described in Figure 2. “Traditional Tapping process” was carried out because nature has made this product in such a way that it cannot be manufactured in the mills, It can be produced in the cottages. The average yield of fresh sap was 0.5 L per tree per day during process studies. Sap yields depend on the skills of the tapper. Tapping the inflorescence is produced throughout South East Asia on all species of tapped palm trees. Usually, if the sap is used for drink and sugar production it will be collected twice a day as fermentation has to be avoided as far as possible (Kovoor, 1983). Traditionally lime and bark or leaves of various species, and smoke can be used as anti-fermenting agents.

Qualitative Chemical Analysis of Fresh and Fermented Nypa Sap

The detected phytochemical constituents in the fresh and fermented *Nypa fruticans* sap sample were α amino acid, carbohydrates, glycoside, phenolic compound, reducing sugar and saponin . Reactions of an alcohol can involve the breaking of either two bonds; the C-OH bond, with removal of the –OH group; the O-H bond with removal of –H. The results of the preliminary chemical reactions tests showed the presence of primary alcoholic -OH group in fermented sap as follows: yellow precipitate obtained by Xanthate , color product obtained by oxidation test and no oily layer observed by Lucas test. Then the –OH of primary alcohol was confirmed by specific qualitative tests namely ethyl acetate and iodoform test. The formation of fruity odour of ethyl acetate and yellow crystals indicated the presence of primary alcoholic group in fermented sap. The fermented sap must contain primary alcohol.

Sensory Changes of Fermented Sap During Storage

The sap of Nypa palm was collected twice a day and observed the changes of sensory was observed for 5 days. After only two hours, the sap, like wine, has sweet taste and aromatic. First, the formation of bubbles were observed and the clear sap with sweetish smell became turbid. On the second day it turned sour and frothing stopped. After three days the smell of fermented sap became stronger and sour .The observation was recorded in Table 1.

Table 1. Changes of Some Sensory in Fermented Sap During Storage at 31±1˚ C for 5 days

Time (Day)	Taste	Colour (visual)	Odour
0	Sweet	Colorless	Aroma
1	Bitter sweet	Light straw	Pleasant
2	Bitter sour	Light brown	Pungent
3	Sour	Light brown	Pungent
4	Sour	Brown	Strong
5	Sour	Brown	Putrefaction

Changes of Some Chemical Parameters of Fermented Sap During Storage

For 5 days , changes of some sensory properties such as taste, color and odor in fermented sap were daily monitored. On the 2nd day it was found to be more acceptable than the others. After three days the sap became putrefaction and readily contaminated. The decreasing range of pH as increasing time was recorded 6.5-4.3. Specific gravity was varied from1.04 to 1.22. Reducing sugar content in fresh sap reduced from 26.8 to 21.5% during storage. The content of ascorbic acid was found to be gradually increased from 16 to 22 mg as increasing fermentation time. The results were recorded in Table 2 and Figures 3,4 and 5. Natural fermented sap was found to be enriched nutrient minerals. The AAS analysis of fermented sap revealed that it contains 0.16 ppm zinc, 0.18 ppm manganese, 0.28 ppm copper, 0.80 ppm lead, 14.0 ppm lithium, 60.2 ppm sodium, 110.0 ppm calcium, 5.7 ppm iron and 200.0 ppm potassium.

Table 2. Changes of Some Physicochemical Properties of Fermented Sap During Storage

Time (Day)	pH	Specific Gravity	Reducing Sugar (%)	Ascorbic Acid (mg)
0	6.5	1.22	26.8	16.0
1	6.0	1.20	25.6	18.8
2	5.6	1.20	24.4	19.0
3	5.2	1.16	23.0	19.5
4	4.8	1.12	22.5	20.7
5	4.3	1.04	21.5	22.6

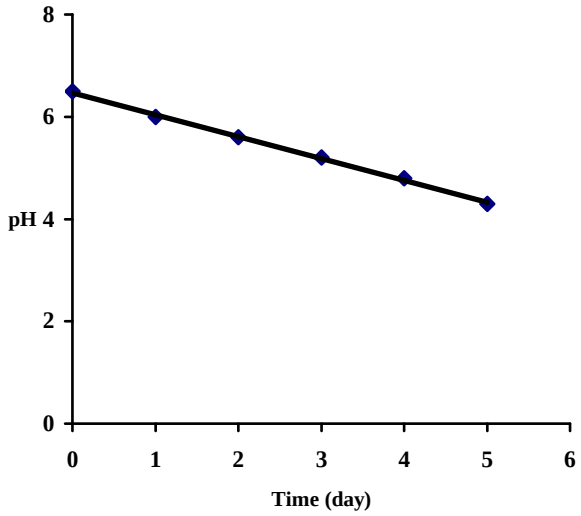

Figure 3 Changes of pH in fermented sap vs fermentation time

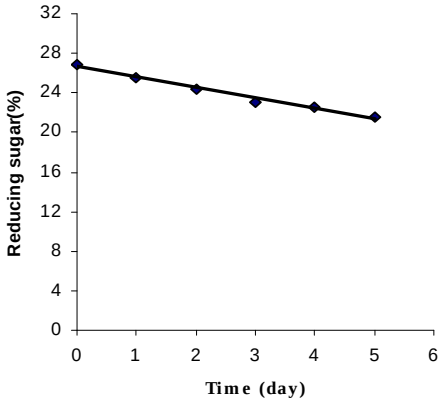

Figure 4 Changes of reducing sugar content in fermented sap vs fermentation time

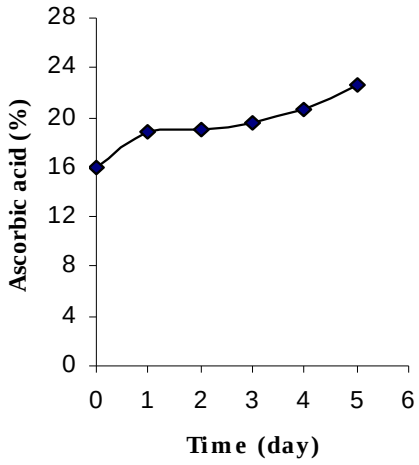

Figure 5 Changes of ascorbic acid content in fermented sap vs fermentation time

Antimicrobial Activity

Fermented nypa sap inhibits the activity of all tested organisms with the range of inhibition zone diameter (14-24 mm) whereas fresh nypa sap showed mild activity against all organisms except *Bacillus subtilis* and *Escherichia coli* with the range of inhibition zone diameter between 10-15mm as shown in Figure 6. In decreasing order of antimicrobial activity of fermented sap was observed as *Salmonella typhi* (24mm), *Aspergillus flavus*, (20mm) *Pseudomonas fluorescens* (20mm), *Bacillus subtilis* (18mm) , *Xanthomonas oryzae* (18mm), *Candida albicans* (16mm), *Agrobacterium tumefaciens* (16mm), *Staphylococcus aureus* (15mm), *Escherichia coli* (14mm), *and Micrococcus leteus* (14mm).

Based on these results, the more acceptable fermented nypa sap on 2rd day should be used to consume as safe nutritious food as well as an antimicrobial agent related to their respective microorganisms for bronchitis, typhoid fever, food poison, skin infection and alimentary tract infection. The comparison of inhibition zone diameters for two types of nypa sap are shown in Figure 6.

Table 3 Diameter of Inhibitory Zone for Antimicrobial Activity of Fresh and Fermented Nypa Sap

Test Organisms	Diameter of Inhibitory Zone (mm)	
	Fresh sap	Fermented sap
Agrobacterium tumefaciens	15	16
Aspergillus flavus	12	20
Bacillus subtilis	0	18
Candida albicans	14	16
Escherichia coli	0	14
Micrococcus letus	12	14
Pseudomonas fluorescenns	14	20
Salmonella typhi	12	24
Staphylococcus aureus	10	15
Xanthomonas oryzae	12	18

10 mm ~ 14 mm (+), 15 mm ~ 19 mm (++), 20 mm above (+++)

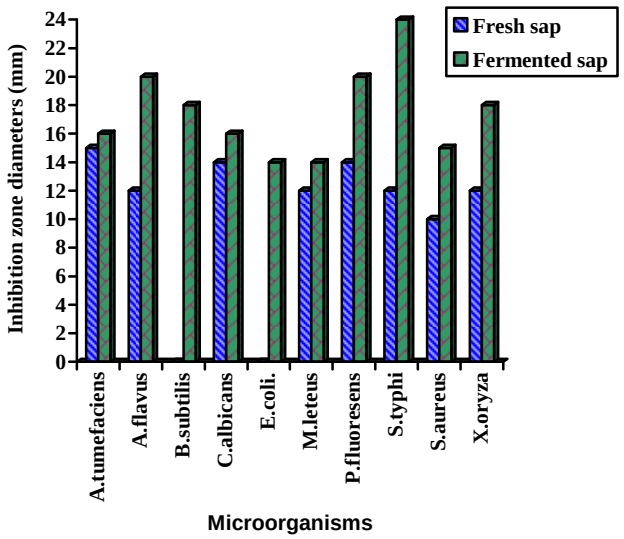

Figure 6. A bar graph diagram of inhibition zone diameters for antimicrobial activity of fresh and fermented nypa sap against ten microorganisms

Conclusion

Nypa frutican palms (Dani) from Taungpyo, Myeik were selected for process studies of fresh nypa sap. Fresh sap was collected from infloresence stalk by traditional tapping process, locally known as "Dani-Kyauk". This method is cost effective for production of sugar syrup and alcohol with lack of chemical agents. The average yield was 0.5 L per day per tree. Based on the sensory characters, fermented sap on 2^{nd} day storage was acceptable for chemical analysis. Phytochemical investigations indicate the presence of sugar, α- amino acids, carbohydrates, glycosides, phenolic compounds, and saponin in fresh and fermented nypa sap samples. Starch was not detected. The formation of alcohol in fermented sap was qualitatively detected by xanthate, oxidation and Lucas tests. Then the results of ethyl acetate and iodoform tests confirmed the presence of primary alcohol in fermented sap. During study period pH decreased from 6.5 to 4.3 whereas reducing sugar content in fermented sap decreased from 26.8% to 21.5%. Specific gravity was in the range between 1.04-1.22. The content of ascorbic acid increased from 16 to 22.6 mg as increasing fermentation time. Investigation on antimicrobial activity of fresh and fermented sap by paper disc diffusion method revealed that fresh sap inhibited the growth of tested organisms namely *Agrobacterium tumefaciens, Aspergillus flavus, Candida albican, Micrococcus leteus, Pseudomonas fluorescens, Salmonella typhi, Staphylococcus aureus and Xanthomonas oryzae* except *Bacillus subtilis* and *Escherichia coli* with the inhibition zone diameters ranged between 10mm-15mm. Fermented sap on second day exhibited the antimicrobial activity against all tested organisms with the range between 14-24mm.Generally antimicrobial activity of fermented sap was found to be more potent than that of fresh sap.

Acknowledgements

The author would like to acknowledge Dr. Myint Swe, Rector, Myeik University for his kind permission to carry out this research. Sincere thanks are due to all the participants who helped in this study. The author also express sincere gratitude to Major Shwe Pyi Hein, Director, Fermentation Department, Development Centre of Pharmaceutical Technology, Ministry of Industry (1), for providing research facilities for the investigation of antimicrobial activitiy. Special thanks are due to U Nyan Tun, Lecturer, Universities' Research Center, for AAS analysis.

References

Burkill, I. H., (1993). "A Dictionary of the Economic Products of the Malay Peninsula." 3rd Printing. Publication Unit, Ministry of Agriculture, Malaysia, Kuala Lumpur. Volume **1**: 1-1240

Cruckshank,(1960), "Handbook of Bacteriology",10thEdn, E&S.Living Stone Ltd.,Edinburgh

Duke, N., (2006), "Australia's Mangroves. The Authoritative Guide to Australia's Mangrove Plants," University of Queensland, Queensland. p.200

Ei Ei Phyu Sin, (2002), "Amino acid Determination in Toddy Juice and Glutamate Determination in Taste Intensifier Powders", M Sc. Thesis, Department of Chemistry, University of Yangon

Fox ,J. F.,(1977), "Harvest of the Palm, Ecological Change in Eastern Indonesia," Harvard University Press, Cambridge, England. p. 290

Gibbs, H.D., (1911), " A Study of Some Palms of Commercial Importance with Special Reference to the Saps and their Uses," Philipp. *J. Sci. Sect*. A, **6**: 99-145

Hamilton ,L. S. and Murphy, D. H., (1988). " Use and Management of Nipa Palm (*Nypa fruticans*, Arecaceae): a Review" ,*Economic Botany*, **42**(**2**): 206-213

Harbone,J.B., (1984)," Phytochemical Methods-A Guide to Modern Techniques of Plant Analysis", 2nd Ed., Chapman and Hall, New York, 120-122

Kovoor, A., (1983), "The Palmyrah Palm: Potential and Perspectives. FAO Plant Production and Protection Paper", No 52. FAO, Rome. p. 77

Maung Maung Aye, (1995), "Mangrove Ecosystems, Some Economic and Natural Benefits", Versatile Palm Research Paper, Department of Geography, UDE, Yangon, p.9

Päivöke, A. E. A., (1985), "Tapping Practices and Sap Yields of the Nipa Palm (*Nipa fruticans*) in Papua New Guinea," Agriculture, Ecosystems and and Environment. **13**:59-72

Pearson,D.,(1962), "Chemical Analysis of Foods", 4th Ed. , Trindall and Cox Company Ltd.London.

Prescott,L,T., Harley,T.P., and Klein, D.A.,(1999),' Microbiology", Mc Graw Hill Book Co. Inc. New York

Robinson, T., (1983), " The Organic Constituents of Plants", 5th Ed., Cordus Press, North America, p.63-68

Tin Wa, (1972), "Phytochemical Screening Methods and Procedures", *Phytochemical Bulletin of Botanical Society of America*, Inc., **5**(**3**), 4-10

Tomlinson, P.B., (1986), "The Botany of Mangroves", Cambridge University Press. USA. p.419

Vogel, A.I, (1966), "A Text Book of Practical Organic Chemistry", 3rd Ed, Longmans, Green & Co. Ltd, London

Online Materials

Dalibard, C. (1999), "Overall View on the Tradition of Tapping Trees and Prospects for Animal Production," Livestock Research for Rural Development(11)1: http://www.cipav.org.co/lrrd/lrrd7/2/5.ht

Giesen, W., Stephan, W., Max, Z., and Liesbeth S., (2006), " Mangrove Guidebook for Southeast Asia", (PDF online) RAP Publication 2006/07, Food and Agriculture Organization of the United Nations Regional Office for Asia and the Pacific Bangkok. http://www.fao.org.co/docrep

Chemical Analysis of Local Zircon Concentrate and Preparation of Zirconium Oxychloride Octahydrate

Ni Ni Aung

Abstract

Zircon is one of the most valuable mineral ore for production of important intermediate compound, zirconium oxychloride, and zirconium metal. Zircon has been found in heavy sands of river beds and ocean beaches in Myanmar. This work deals with the systematic study using locally available zircon concentrate from Moemeik Myitsone area; and the optimal conditions for the production of zirconium oxychloride from zircon were investigated. It was found that samples of zircon concentrate consist of 65.53 % of ZrO_2, 25.23 % of SiO_2, 0.34 % of FeO, 0.216 % of Fe_2O_3, 0.74 % of TiO_2 and 1.6 % of HfO_2. The process for the production of zirconium oxychloride, $ZrOCl_2.8H_2O$ from zircon concentrate involves (i) fluxing with alkali, (ii) treating with 1:10 w/v ratio of concentrated hydrochloric acid and (iii) repeated crystallization via hydroxide gel. Within a fluxing time of one and half hour the optimal conditions for the fluxing of zircon was found to be 1:4 w/w ratio of zircon to sodium hydroxide at 650 ºC. Repeated crystallization via hydroxide gel was able to upgrade the purity of zirconium oxychloride up to 99.24 % with the yield % of about 69.8. It was characterized by XRD, EDXRF, FT IR, TG-DTA and chemical analysis. This work initiating with local zircon concentrate provides an efficient method for the production of an important zirconium oxychloride, of high purity which is justifiable to be used in the synthesis of zirconium sol and other zirconium compounds, and extraction of zirconium metal.

Keywords: zircon, analysis, zirconiumoxychloride $ZrOCl_2.8H_2O$, hydroxide gel

Introduction

Zirconium is classified in subgroup IV B of the periodic table with its sister metallic elements, titanium and hafnium. Zirconium forms a very stable oxide. The principal valence state of zirconium is +4, its only stable valence in aqueous solutions. Zirconium compounds commonly exhibit coordinations of 6, 7 and 8.

Associate Professor, Dr., Department of Chemistry, Taungoo University

Zirconium is found in at least 37 different mineral forms but the predominant commercial source is the mineral zircon, zirconium orthosilicate. Other current mineral sources are baddeleyite and eudialyte (Nielsen *et al*., 1984).Although so widely distributed , large workable deposits are rare .

The largest commercial sources of zircon are in Kerala State in India, Sri Lanka, the east and west Coast of Australia, on the Trial Ridge in Florida, and at Richards Bay in the Republic of South Africa. These heavy mineral sands are processed for the recovery of the titanium bearing minerals ilmenite, rutile, and leucoxene, and the zircon is obtained as a co-product (Nielsen *et al*., 1984).

Most gem grade zircon comes from several eastern Asian countries, where it is found in placer deposits of rounded waterworn stones. These countries are Sri Lanka, Myanmar, Vietnam, Cambodia, Thailand, Madagascar and Brazil (Watt, 1980).

In Myanmar, zircon sand can be found in northern Shan State, Sagaing Region and Tanintharyi Region, occurring mostly as beach sands. In Mogoke Area, Mandalay Region, it occurres as a crystal zircon, hyacinth, accompanied by ruby and other gem-gravels, and it also occurred as heavy mineral sand, consisting of zircon, samarskite, uranite and monazite. Heavy sand containing monazite and zircon etc, radioactive bearing mineral (pegmatite) are also found in Sagaing Region. The presence of monazite (ThO_2) and zircon in heavy sand are also found in Dawei, Tanintharyi Region, as tailings from tin-tungsten ore dressing (United Nations, 1996). Mostly zircon can be found in heavy sand, of which promising deposits are in Myitsone Area, Moemeik Township, northern Shan State. It is also found in Rakhine Coast but further investigation and exploration should be undertaken.

Zirconium oxide dichloride, $ZrOCl_2.8H_2O$, commonly called zirconium oxychloride, is really a hydroxyl chloride, $[Zr_4(OH)_8.16H_2O]Cl_8.12H_2O$.Zirconyl chloride is the most commonly used zirconium compound from which to derive other zirconium compounds: hydrous oxide, carbonated hydrous oxide, acetate, sulfate, glycolate, lactate, and others. Its solutions precipitate acid dyes, and can be used to prepare high quality pigment toners and to improve the properties of color lakes. Zirconyl chloride is also important precursor for the production of advanced ceramic, zirconia and for the production of zirconium metal.

Materials and Methods

The chemicals used were of analytical and reagent grade. They were procured from British Drug House Chemical Ltd, Poole, England (BDH), Kanto Chemical Co. Ltd. Japan, and Sigma, Aldrich Co. Ltd., Poole, England. The chemicals were used as received unless otherwise stated.

In all analytical procedures of the experiments, recommended standard methods and techniques were applied (Vogel, 1961; Maxwell, 1968; Dean, 1995). All analytical determinations, instrumental analyses and monitoring of the process system were carried out by FT IR Spectrophotometer, Perkin Elmer 1600, Shimadzu model IR-408 TG-DTA, Hi-TGA 2950 Thermogravimetric Analyzer; X-ray Diffractometer, XRD - Rigaku - D - Max - 2200, Japan; EDXRF Spectrometer (Shimadzu EDX - 700) ; UV-visible Spectrometer, Ciba - Corning 259; Electromicroscope, BX 51 Biological Microscope attached by Olympus, PM 20 Automatic Photomicrographic System; AAS Perkin Elmer A.Analyst 800 AAS, Germany.

Sample Collection: The principal source of the sample is the heavy sand collected from Myitsone area, Moemeik Township, Northern Shan State. Figure 1 shows the location and site of the sample collecting area. Sample collected is pale yellow in colour. The sample used in this investigation is zircon concentrate. The beneficiated sample was subjected to dressing process such as screening, magnetic separation, high-tension separation, ball milling and air drying and then grinding (100mesh). The powdered sample (approximately 147 μm) were stored in plastic containers.

Representative sample was taken systematically by Coning and Quartering method.

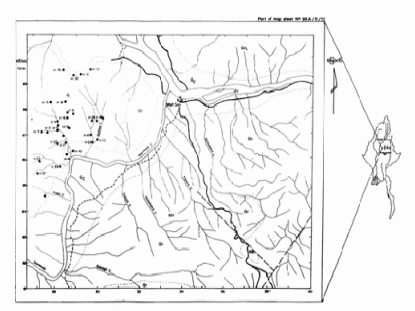

Figure 1. Location map of zircon sample

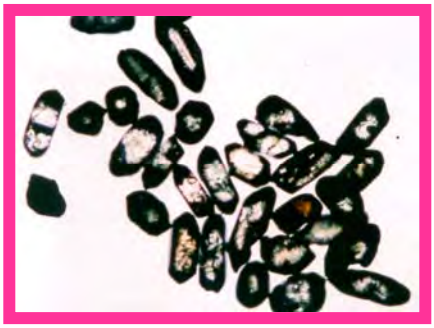

Figure 2. EM photograph of Zircon concentrate

Characterization of Zircon Sample: The powdered zircon concentrate was subjected to characterization by electromicroscope, XRD and EDXRF Technique.

Determination of Zirconium Content: Zirconium dioxide in zircon sample was determined by gravimetric analysis of fusion with a mixture of anhydrous sodium carbonate and sodium peroxide and precipitated with 15% mandelic acid solution.

Determination of Titanium ,Total Iron , Silica and Other Trace Elements : Titanium dioxide in zircon was determined by colorimetric method . By preparing the calibration curve of standard TiO_2 solution ,and the Ti content was determined from maximun absorbance λ_{max} at 410 nm.The total iron content was determined by using Zimmermann-Reinhardt solution and titrated with 0.1 N potassium permanganate solution . The silica content was determined by gravimetric determination of fusion with sodium carbonate .Other trace elements in zircon concentrate were determined by the atomic absorption spectroscopic technique.

Preparation of Zirconium Oxychloride : The unit process of fusion with alkali and extraction with hydrochloric acid was used for the extraction of zirconiun oxychloride from zircon . The altered process , crystallization via hydroxide gel was carried out to obtain purified $ZrOCl_2 .8H_2O$. In order to find out the optimal conditions for the preparation of zirconium oxychloride, the sample was fused with sodium hydroxide with respect to variation of NaOH to zircon ratio within 1:1 to 5:1 w/w ratios. Fusion temperatures were varied from 600ºC to 800°C and fusion periods were varied from 1 to 3 hr.Crystallization conditions were carried out by (i) recrystallization for several times and (ii) repeated crystallization via hydroxide gel methods.

Characterization of Prepared Zirconium Oxychloride : The extracted compound , zirconium oxychloride , was confirmed and characterized by electromicroscope, XRD , EDXRF, FT IR , TG-DTA and chemical analysis.

Results and Discussion

Analytical Assay of Zircon Sample: The authenticity as zircon, $ZrSiO_4$, was obvious by the XRD pattern as presented in Figure 3. The authenticity of the presence of zircon can be known by matched spectra included in the diffractograms. The high intensity and well resolution of the peaks regarding zircon sample indicated that the sample is a high purity type of zircon.

The presence of a high content of ZrO_2 in the sample is augmented by the semiquantitative data of EDXRF, shown in Figure 4. The data, although based on relative abundance present in the matrix, indicate high ZrO_2, content about 97%.

The chemical analytical assay data of the sample is shown in Table 1. Although the analytical data is semiquantitative in XRF technique the percent content of ZrO_2 is comparable with that of chemical analysis. It was observed that from XRF data and chemical analysis data, local zircon was high grade zircon.

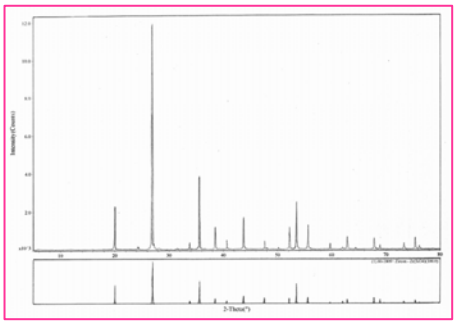

Figure 3 . XRD diffractogram of of zircon sample

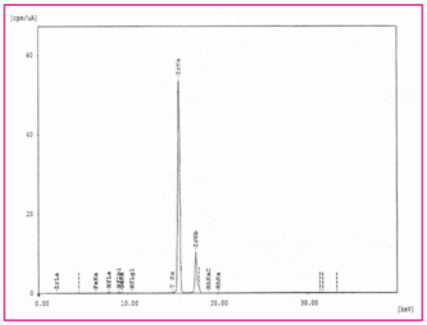

Figure 4 . EDXRF spectrum of zircon sample

In the analytical assay determination, all chemical methods for the determination of zirconium actually give the amount of zirconium plus hafnium. The latter can be determined only by physical methods such as emission spectroscopy or X-ray spectrography. From the XRF determination (Figure 4.) the hafnia content was found to be ca 1.6% in the sample. It is a common observation; that the zirconium and hafnium ratio is 100:2 in the

zircon sample. The chemical analysis gives the composition of zirconium plus hafnium.

From the observation of XRD diffractogram, semiquantitative data of EDXRF and analytical assay data, it was observed that the zircon concentrate from Moemeik Myitsone Area is of a high grade sample.

On the Aspect of the Preparation of $ZrOCl_2.8H_2O$: Tables 2 – 4 showed optimal conditions for preparation of zirconium oxychloride , the investigated data as regard to the optimal conditions, found out with respect to the digestion step where NaOH was used as fluxing agent. The nature of digestion primarily depends on the fluxed mass cake where different proportions of NaOH to sample were used in Table 2. It shows that the fluxed mass, which decomposed by using different caustic soda to sample ratio, can give rise to different yields of $ZrOCl_2$. It can be observed that 4:1 caustic soda to sample ratio shows optimal yield of 69.42%.

Based on the ratio of 4:1 NaOH to sample, the effect of fusion temperature and time of fusion were found out. Thus, Tables 3 and 4 show the optimal fusion temperature to be 650˚C and optimal fusion time to be 1.5 hr. At these optimal conditions the highest yield of $ZrOCl_2$ was achieved. It was observed that the optimum ratio of NaOH and zircon is 4:1. At lower ratio, the sample cannot be decomposed completely and at greater value, the yield was drop of little significance. The ratio above (5:1), sodium silicate interfered as a gel and it was difficult to filter and the separation is incomplete.

Table 1. Analytical assay results of zircon concentrate from Moemeik Myitsone area

Constituent	Content (%)	Method of Assay
ZrO_2	65.530 ± 0.02	Chemical analysis
SiO_2	25.234 ± 0.003	Chemical analysis
Fe_2O_3	0.2165 ± 0.002	Chemical analysis
FeO	0.3419 ± 0.001	Chemical analysis
TiO_2	0.7424 ± 0.002	Spectrophotometric
HfO_2	1.608	XRF

Constituent	Content (%)	Method of Assay
Cu	0.0014 ± 0.0002	AAS
Pb	0.0015 ± 0.0002	AAS
Zn	0.0024 ± 0.0002	AAS
Mn	0.0043 ± 0.0002	AAS
Ni	0.0025 ± 0.0001	AAS
Mg	0.0038 ± 0.0002	AAS
Ag	ND	AAS
Co	ND	AAS

ND = less than 0.0001 % for Ag and Co

At the fluxing temperature below 600˚C, yield of $ZrOCl_2$ is lower than at the high temperature. It was due to the incomplete fusion of the sample. At temperature higher than 650˚C, yield of $ZrOCl_2$ became low. It was due to the effect of high temperature, which favours various composition of oxide and silicozirconate formation when hydrolysed it formed zirconic acid or silicozirconic acid gelation. Table 4 shows the yield of $ZrOCl_2$ from fused mass by variation of fluxing time. At a short time fusion, the sample could not be fused completely and at longer time it did not change significantly. Thus, the optimal conditions for decomposition of zircon for the extraction of $ZrOCl_2$ by fluxing with alkali were 4:1 NaOH to zircon ratio, temperature 650˚C and 1.5 hr heating time. The fused mass product was washed with deionized water and the moist cake was extracted with concentrated HCl by the ratio of 1:10 w/v.

Table 2. Yield percents of zirconium oxychloride from different NaOH to sample ratio fused mass

NaOH: Sample (w /w)	Fusion Temperature (°C)	Fusion time (hr)	Yield (%)
1:1	650	2	63.25 ± 0.02
2:1	650	2	64.54 ± 0.02
3:1	650	2	65.14 ± 0.02
4:1	650	2	69.42 ± 0.02
5:1	650	2	69.37 ± 0.02

Table 3. Yield percents of zirconium oxychloride from fused mass by variation of fusion temperature

NaOH: Sample (w /w)	Fusion Temperature (°C)	Fusion time (hr)	Yield (%)
4:1	600	2	65.69 ± 0.02
4:1	650	2	69.82 ± 0.02
4:1	700	2	52.58 ± 0.02
4:1	750	2	51.05 ± 0.02
4:1	800	2	51.02 ± 0.02

Table 4. Yield percents of zirconium oxychloride from fused mass by variation of fluxing time

NaOH: Sample (w /w)	Fusion Temperature (ºC)	Fusion time (hr)	Yield (%)
4:1	650	1	65.45 ± 0.02
4:1	650	1.5	69.87 ± 0.02
4:1	650	2	69.52 ± 0.02
4:1	650	2.5	69.51 ± 0.02
4:1	650	3	68.24 ± 0.02

Figures 5 and 6 are XRD diffractograms of extracted compound obtained from fifth time recrystallization and the extracted compound from repeated crystallization via hydroxide gel. Recrystallization is an important step to obtain desired crystals because the crystals from recrystallization route can be formed as mixture of crystals, such as hexahydrated, trihydrated and mixture of both hydrated crystals. In the crystallization via hydroxide gel route, it is considered that the desired crystals formed were only octahydrated crystals.

Studies on the Characterization of Zirconium Oxychloride Octahydrate: EM photograph (Figure 7) shows the extracted compound that has needle shape. Figures 8 and 9 show the EDXRF spectra of $ZrOCl_2.8H_2O$ obtained from 5^{th} time of recrystallization and crystallization via the hydroxide gel method. It was observed that, the crystal from hydroxide gel was more of a purer form than others (based on semi-quantitative data of EDXRF spectra). It shows 98% purity. Table 5 shows the percent purity and elemental data of $ZrOCl_2.8H_2O$. From these data, crystal from hydroxide gels, $ZrOCl_2.8H_2O$ are more purified than recrystallization process. The percent purity of extracted compound was found to be 99.24% based on chemical analysis.

Figure 10 is FT-IR spectrum of extracted compound . This spectrum was identical to the reference standard $ZrOCl_2.8H_2O$ spectrum (Nyquist and Kagal,1991). At the frequency range of 3650-3200 cm^{-1}, the very broad band

was observed. It was due to the stretching vibration of free - OH group of water molecule and polymeric -OH group. At 1619 cm^{-1} was due to the bending vibration of -OH group and 1010 cm^{-1} was due to the vibration of bridging - O - group attached with metal zirconium atom. Very broad overlapping band at 731-486 cm^{-1} can be referred to the monoclinic form of zirconia. In this spectrum, frequency at 850 cm^{-1} band was not observed. Thus, the compound has no = O bonding. Therefore, the extracted compound contained metal -O- bridging group, polymeric -OH and monoclinic character.

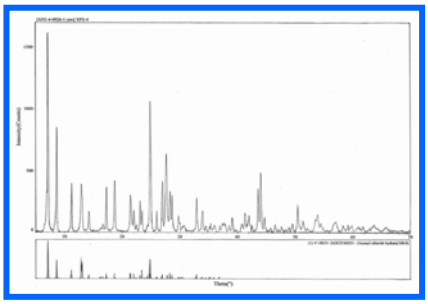

Figure 5. XRD diffractogram of extracted zirconium oxychloride by 5 th time recrystallization

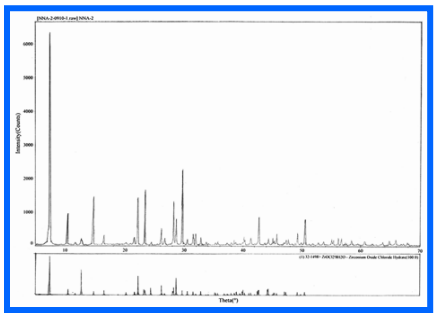

Figure 6. XRD diffractogram of extracted zirconium oxychloride by repeated crystallization

Figure 11 shows the TG-DTA curves for the decomposition of extracted $ZrOCl_2.8H_2O$ crystals. The compound is found to have decomposed into zirconia in two steps. It is shown by the DTA curve in Figure 11. There exists an exothermic peak at about 80˚C, which corresponds to the elimination of surface water and at about 160˚C dehydration of interstitial water of the compound occurred. The corresponding weight loss obtained from the TGA curve is about 44%. It is in agreement with the 8 moles of water molecules. There is an exothermic peak in the DTA profile around 400˚C. The exothermic peak may be attributed to the decomposition of compound with libration of HCl and transformation to zirconia.

Figure 7. EM photograph of zirconium oxychloride

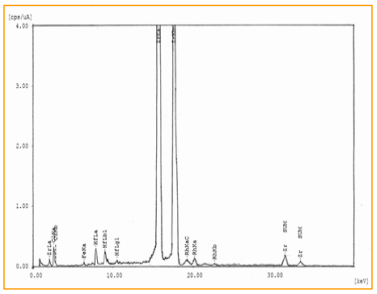

Figure 8. EDXRF spectrum of extracted zirconium oxychloride by 5th time recrystallization

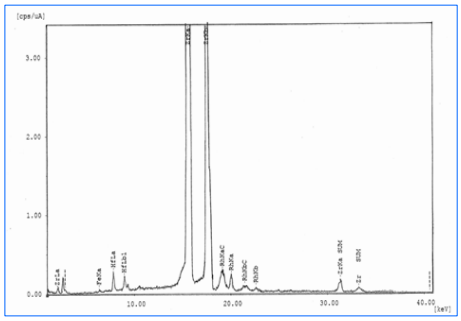

Figure 9. ED-XRF spectrum of extracted zirconium oxychloride

Table5. Percent purity and elemental data of extracted zirconium oxychloride

Extracted Compound	Zr (%)		Hf (%)	Fe (%)	Ni (%)	SiO_2 (%)
	Chemical*	XRF	XRF	AAS	AAS	(Chemical)
5 times Recrystallization $ZrOCl_2$	97.43 ± 0.01	95.51 ± 0.01	1.47	0.0020 ± 0.0002	0.0010 ± 0.0001	0.70 ± 0.001
Recrystallization *via* hydroxide gel $ZrOCl_2$	99.24 ± 0.01	98.45 ± 0.01	1.33	ND	-	-

ND - less than 0.0001 % for Fe

* Hf may also be included

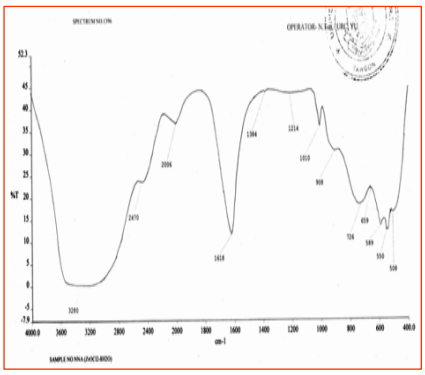

Figure 10 FT IR spectrum of zirconium oxychloride

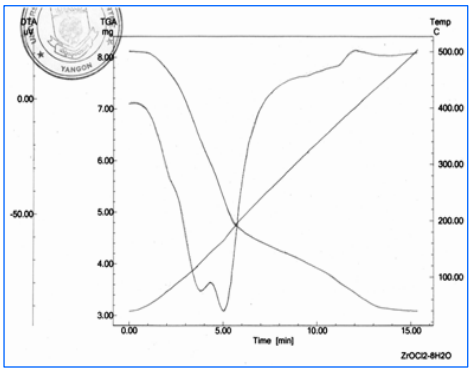

Figure 11 TG-DTA thermogram of zirconium oxychloride

Conclusion

The results of this investigation revealed that local zircon concentrate has high zirconia content . It consists of 65.53% ZrO_2, 25.23% SiO_2, 0.34% FeO, 0.216% Fe_2O_3, 0.74% TiO_2, 1.6% HfO_2 and trace amounts of other elements. It is High Zircon.

It is evident from the results of investigation that $ZrOCl_2.8H_2O$ can be extracted from hydroxide gel that was more pure (99.24%) than it is from recrystallization for several times (97.43% purity). Hf content in extracted $ZrOCl_2.8H_2O$ was found to be 1.33%. Prepared zirconium oxychloride was characterized by conventional and modern instrumental techniques. From XRD diffractogram, it was confirmed that the extracted compound is pure $ZrOCl_2.8H_2O$ crystalline form. From EM photograph , it was observed that the compound is needle shape crystal . FT-IR spectrum of $ZrOCl_2.8H_2O$ indicates the existence of surface water and interstitial water which shows very broad band at 3650 cm^{-1} - 3000 cm^{-1}, and monoclinic zirconia was also confirmed by the band at 731-486 cm^{-1}. From TG-DTA thermogram, the compound was in octahydrated form. It was dehydrated (surface water) at 160˚C and further decomposition was completed at 400˚C. The XRD diffractogram of prepared $ZrOCl_2.8H_2O$ did not indicate any major impurities. According to the chemical analysis data by conventional and modern instrumental techniques, it did not contain other trace elements. Therefore, the extracted compound is justifiable to be used for the synthesis of zirconium sols, other zirconium compounds and extraction of zirconium metal.

Acknowledgements

The author would like to express sincere thanks to Dr.Aung Thu,, Rector, Dr. Khin Myo Naung, Professor and Head, and Dr. Mya Hnin Kyaing, Professor, Department of Chemistry, Taungoo University for giving the opportunity to present this paper.

References

Dean, J. A., (1995), "Analytical Chemistry Hand Book“, McGraw-Hill Inc., New York.

Maxwell, J.A, (1968), "Rock and Mineral Analysis" Interscience Publishers, New York

Nielsen, R.H., Schlewitz, J. H. and Nielsen, H., (1984), "KirkOthmer Encyclopedia of Chemical Technology", 3rd Edn., A Wiley-Interscience Publication, John Wiley & Sons, New York, Vol. 24

Nyquist, R. A. and Kagel, R. O., (1991), "Infrared Spectra of Inorganic Compounds", Academic Press, Inc., New York

United Nations, (1996), "Atlas of Mineral Resources of the Escape Region“, 12, Geology and Mineral Resources of Myanmar, United Nations, New York.

Vogel, A. I., (1961), "A Text-Book of Quantitative Inorganic Analysis" 3rd Edn., Longmans, Green and Co. Ltd, London.

Watt, J.G., (1980), "Mineral Facts and Problems“, U.S. Bur. Mines, Bulletin 671, U.S. Government Printing Office, Washington D.C. p.1045-1060.

Spectrophotometric Study on Complex Formation of 2-Ethanolimino- 2-pentylidino-4-one Ligand with Co^{2+}, Zn^{2+}, and Pb^{2+} Ions

Than Than Oo[1], Kyaw Naing[2] and San San Myint[3]

Abstract

In this research, the complex formation of the prepared 2-ethanolimino-2-pentylidino-4-one ligand (ELPO) with Co^{2+}, Zn^{2+}, and Pb^{2+} ions were investigated spectrophotometrically. The ELPO ligand was prepared by the condensation reaction of monoethanolamine and acetylacetone (mole ratio of 1:1). The resultant product is brown color (yield% = 95.03) and the melting point is 70°C. The purity of the prepared ELPO ligand was characterized by using melting point, uv-visible and FT IR spectroscopy. FT IR data indicated that the presence of –OH, $-CH_2-$, $-CH_3$, >C=O and >C=N groups. The peak at 1550 cm^{-1} clearly indicated the >C=N group, that is result from the condensation reaction. The visible spectrum of the prepared ligand showed two strong absorption peaks at 454nm and 390nm. These are related to the electronic transition of electrons in >C=N, >C=O and –OH groups. The λmax values for all complexes were found at 464nm. The color stability of all complexes were found to be stable at least for 72 hr. The standard calibration curve for each complex was constructed using standard solutions. The complexes of Co^{2+}, Zn^{2+}, and Pb^{2+} in aqueous solutions follow the Beer's law in the concentration range of $2.23–11.26\times10^{-4}$M, $1.14–6.2\times10^{-4}$M and $2.24–17.9\times10^{-5}$M respectively. All complexes were found to be 1:2 (M: ELPO) formation. The stability constants of Pb^{2+}, Zn^{2+}, and Co^{2+} were determined to be 172×10^6, 44.1×10^6, and 3.43×10^6 respectively.

Key words: 2-ethanolimino-2-pentylidino-4-one ligand (ELPO), monoethanolamine, acetylacetone, Beer's Law, stability constant, spectroscopy

Introduction

The study of "co-ordination chemistry" is the study of "inorganic chemistry" of all alkali and alkaline earth metals, transition metals, lanthanides, and metalloids. A complex in general is any species formed by specific association of molecules or ions by donor-acceptor interaction

1. Lecturer, Department of Chemistry, East Yangon University
2. Professor, Dr, Department of Chemistry, University of Yangon
3. Lecturer, Dr, Department of Chemistry, University of Yangon

(Cox, 2000).Co-ordination complex is a compound in which metal atoms or ions are bonded via co-ordinate covalent bonds to anions or neutral molecules that supply electron pair. A molecule or ion bound to a metal atom or ion through co-ordination of its ion electron pairs is called ligand (Oxtoby *et al.*, 1999). Ligands can be characterized as monodentate and multidentate. A monodentate ligand is one which is attached to the metal atom by a bond from only one donor atom of the ligand (Jolly, 1991). Multidentate ligand may be bound to the metal by means of two or more donor groups where upon a ring structure is formed. The strongest complexing agents are those that are multidentates. (Hamilton *et al.*, 1969).

Metal complexes often have spectacular colors. These colors are caused by electronic transitions by the absorption of light. Most transitions that are related to colored metal complexes are either “d-d transition” or “charge transfer band”. These phenomena can be observed with aid of electronic spectroscopy, also known colloquially as “uv-vis”. As compared with the other techniques, spectrophotometry is very simple, rapid and less expensive for the determination of elements in a variety of samples.

Classification of Co-ordination Chemistry

The area of co-ordination chemistry can be classified according to the nature of the ligands. Ligands in classical co-ordination chemistry bind to metal via their lone pair of electrons (eg. H_2O, NH_3, Cl^-, CN^-, etc). In organometallic chemistry, ligands are organic (alkenes, alkynes, alkyls) as well as organic like ligand such as phosphines, hydrides, and CO. [eg. (C_5H_5) Fe $(CO)_2$ CH_3]. In biochemistry, ligands are those including the side chain of amino acids and many cofactors such as porphyrins (eg. Hemoglobin). In cluster chemistry, ligands are all of the above but also include other metals as ligand [eg. Ru_3 $(CO)_{12}$].

The Stability of Complexes

The stability of metal complexes are determined by many factors including metal ion size and electronic configuration, ligand basicity and ring size, and donor atom orbital energies. The higher the electronegativity of the central ion, the greater is the stability of its complexes. For negative ligands, the higher the charge and smaller the size, the more stable is the complex formed (Prakash *et al*., 1983). The stabilities of complexes are generally increased by the co-ordination of polydentate ligands. The co-ordination of such ligands produces ring structures, the metal atom forming

part of the ring: this process is known as chelation. One factor of great important in chelation is the size of chelate ring produced(Graddon, 1968).The complex resulting from co-ordination with the chelating ligand is much more thermodynamically stable.Qualitatively, the greater the association, the greater the stability of the compound. The magnitude of the (Stability or formation) equilibrium constant for the association, quantitatively expressed the stability.

Importance of Metal Complexes

Among the ions of transition elements, iron, cobalt, copper, manganese, molybdenum and zinc play important role in the biochemistry of the human body. Knowledge of the structure, type of bonding and properties of complex ions is becoming more and more important to the chemists. Metal complexation is of widespread interests. It is studied not only by inorganic chemists, but by physical and organic chemists and by biochemists, pharmacologists, molecular biologists and environmentalists.

Materials and Methods

Preparation of 2-Ethanolimino -2-pentylidino-4-one (ELPO) Ligand

The ELPO ligand was prepared by dissolving 3 mL of ethanolamine in ethanolic acetylacetone solution (5:30, v/v) and stirring for 5 hrs at room temperature and then for 1hr at 55ºC. The resulting reddish brown color solutions was evaporated to 65ºC and then cool to room temperature to crystallize out brown color ELPO ligand.

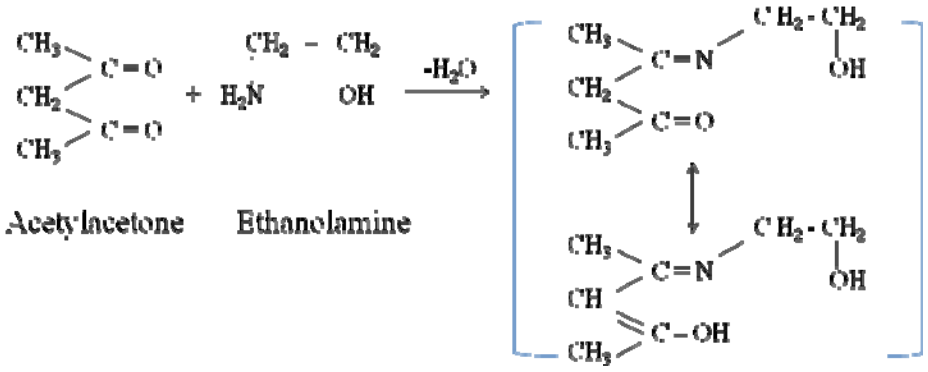

2-ethanolimino -2-pentylidino-4-one (ELPO) ligand

Reagents and Solutions

A stock solution of ELPO ligand (0.1M) was prepared by dissolving 3.575 g ELPO ligand in deionized water and the volume made up to the mark of 250 mL volumetric flask. The 0.006M stock solutions of metal ions (Co^{2+}, Zn^{2+}, and Pb^{2+}) were prepared by dissolving 0.3569 g of $CoCl_2$. $6H_2O$, (BDH), 0.4313g of $ZnSO_4$. $7H_2O$ (BDH) and 0.4968g of Pb $(NO_3)_2$ (BDH) in deionized water and the volumes made up to the mark of 250mLvolumetric flask for each(Vogel, 1968).

Procedure for Spectrophotometric Measurement of Metal-ELPO Complexes

A 2.5mL of solution A [mixture of 0.3mL ELPO ligand (0.1M) +9.7mL H_2O] was placed in a cell. A 0.1mL of solution B [mixture of 0.3mL ELPO ligand (0.1M) + 9.7mL M^{2+} solution (0.006M)] was added into the solution A in each time by using 20µL micro-pipette. The measurements of the respective absorbance values in each time were recorded until the constant absorbance value was obtained. Absorbances were measured by using uv-vis spectrophotometers (Apel PD-303uv, Japan) and (uv 1800 Shimadzu, Japan).

Results and Discussion

Characterization of ELPO Ligand

FT IR spectrum of ELPO ligand is shown in Figure 1. FT IR data indicated that the presence of – OH,-CH_2-, CH_3-, >C=O and >C=N groups, which result from the condensation reaction. The absorption spectra of prepared ELPO ligand and the starting reagents (monoethanolamine and acetylacetone) are shown in Figure-2. The absorption maximum of the prepared ligand showed two strong peaks at 454nm and 390nm. These two peaks related to the electronic transition of electrons in > C=N, >C=O, and –OH groups. These groups show the resonance structures and shift to the lower energy (longer wavelength). The molar extinction coefficients were 3.65mol^{-1} dm^3 cm^{-1} and 7.18 mol^{-1} dm^3 cm^{-1} respectively. There is no absorption of monoethanolamine and acetylacetone in that region. The melting point of prepared ELPO ligand was found to be 70ºC and the yield percent was 95.03.

The Spectrophotometric Studies of Metal-ELPO Complexes

The absorption spectra of ELPO complexes of Co (II), Zn (II), and Pb(II) are shown in Figures 3 and 4. The λ_{max} values for all complexes were found at 464nm. The standard calibration curve for each complex was shown in Figures 5, 6, and 7. The Co (II)-ELPO complex in aqueous solution follows the Beer's law between 2.23-11.26 $\times 10^{-4}$M. The aqueous solution of Zn (II)-ELPO complex obeys the Beer's law between 1.14-6.23$\times 10^{-4}$M. The Pb(II)-ELPO complex in aqueous solutions obeys the Beer's law in the concentration range of 2.24 – 17.9 $\times 10^{-5}$M.

The reaction time for maximum complex formation was found to be 100min for all complexes. After attaining the maximum absorbance, color stability remains constant for more than three days. The complex formation of the metal-ELPO complexes were studied at various metal ion concentrations and concentration of ELPO ligand was kept constant. Relationship between log $\frac{\Delta A_{int}}{\Delta A_{com} - A_{int}}$ and log [M^{2+}] at 464nm curve was plotted for metal-ELPO complexes as shown in Figures 8, 9, and 10. By applying the Bunton's equation, the stoichiometric compositions and stability constants of the complexes were determined (Fiedler, *et al*., 2004).

Bunton (1991) equation

$$\text{Log } \frac{\Delta A_{int}}{\Delta A_{com} - A_{int}} = \log K_{eq} + n \log [Co^{2+}]$$

ΔA_{int} = Absorbance of Co(II)-ELPO complex

ΔA_{com} = Absorbance of Co(II)-ELPO complex at maximum complex formation.

K_{eq} = equilibrium constant

n = ligand number

Similar calculations were carried out for ELPO complexes of Zn(II) and Pb(II). All complexes were found to be 1:2 (M: ELPO) formation. The stability constants of Co^{2+}, Zn^{2+}, and Pb^{2+} were determined to be 3.43 $\times 10^6$; 44.1 $\times 10^6$; and 172 $\times 10^6$ respectively. From these data, the highest stable complex was Pb(II)-ELPO complex and the lowest one was Co(II)-ELPO complex. Therefore, the prepared ELPO ligand can be used for the selected separation of Pb^{2+} from the mixture of metal ions in aqueous solutions.

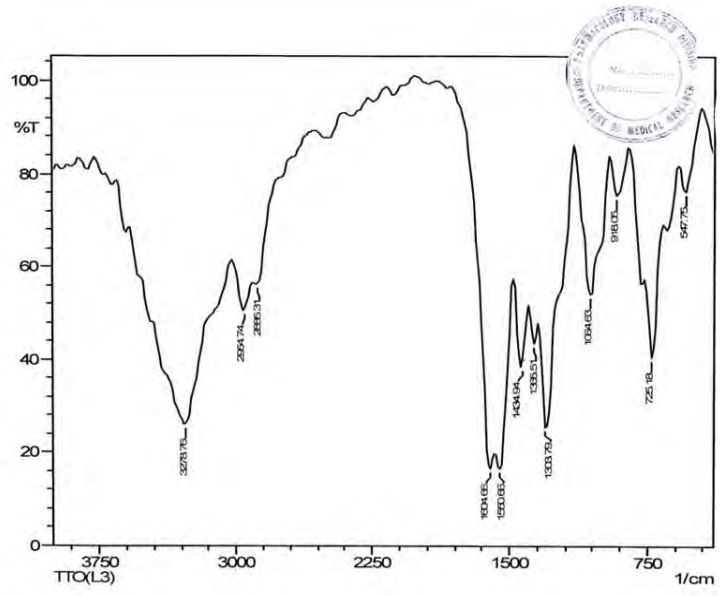

Figure 1. FT-IR spectrum of 2-ethanolimino-2-pentylidino-4-one ligand (ELPO)

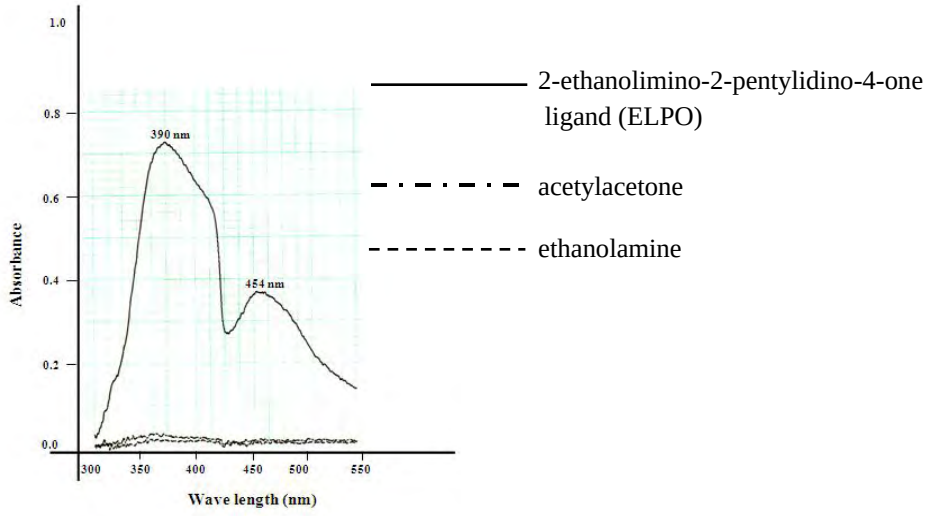

Figure 2. Absorption spectrum of 2-ethanolimino-2-pentylidino-4-one ligand (ELPO)

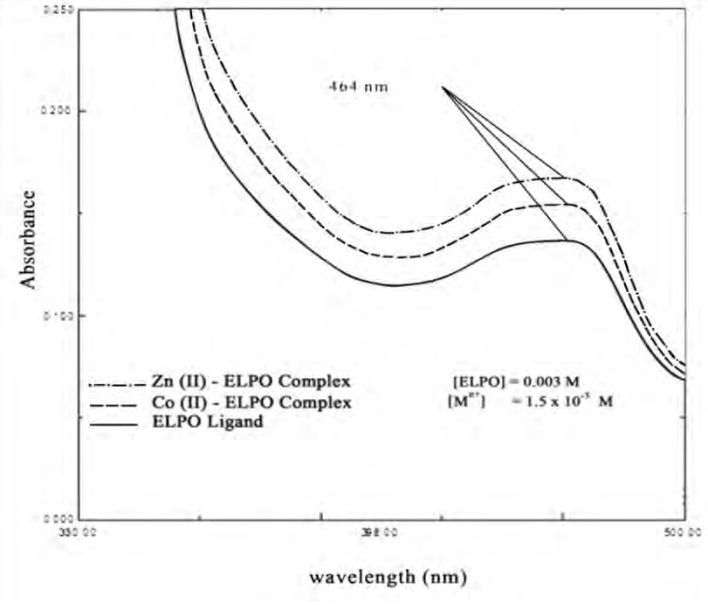

Figure 3. Absorption spectra of ELPO complexes of Co(II) and Zn(II)

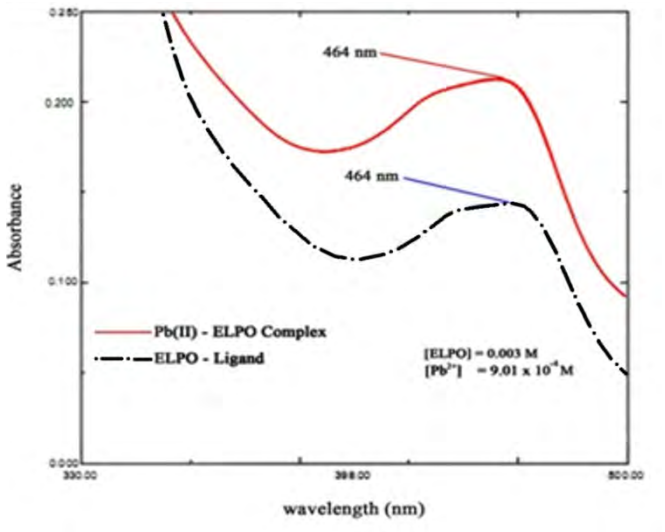

Figure 4. Absorption spectra of Pb(II)- ELPO complex

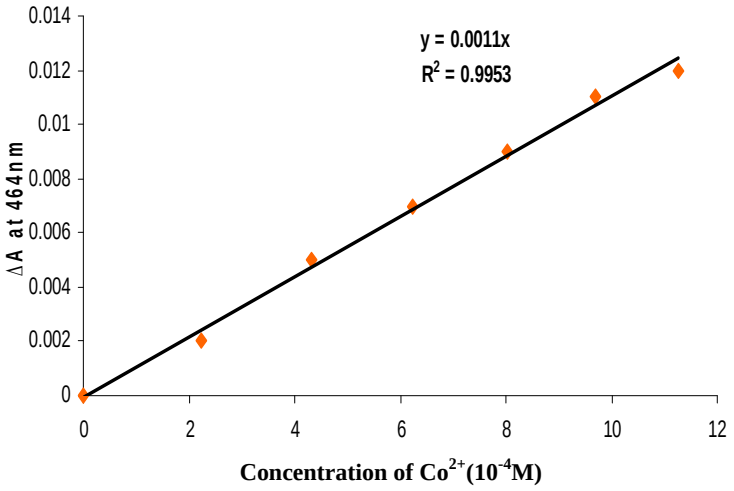

Figure 5. Standard calibration curve for Co(II)-ELPO complex

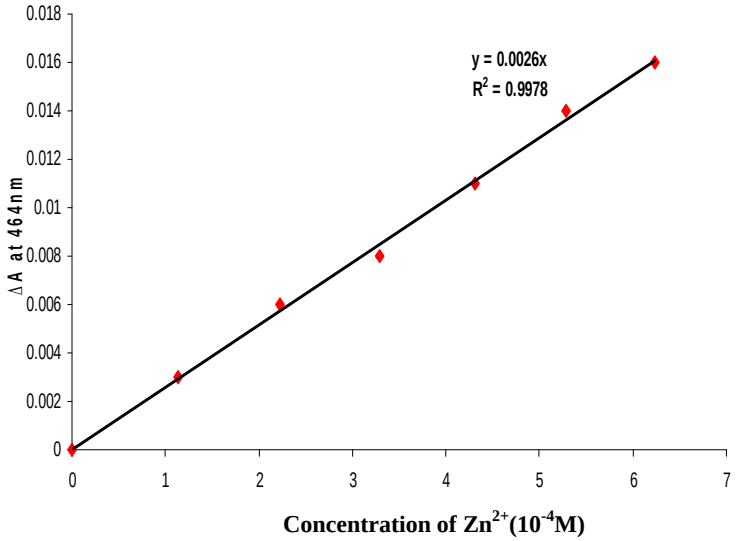

Figure 6. Standard calibration curve for Zn(II)-ELPO complex

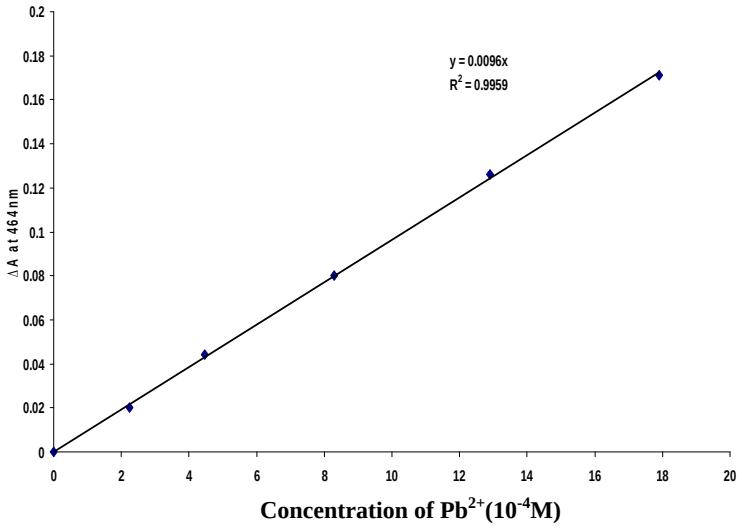

Figure 7. Standard calibration curve for Pb(II)-ELPO complex

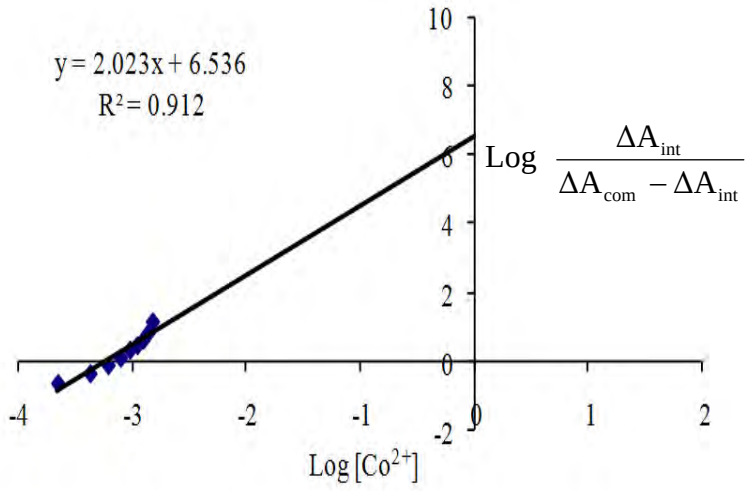

Figure 8. Plot of $\text{Log}\ \frac{\Delta A_{int}}{\Delta A_{com} - \Delta A_{int}}$ as a function of Log $[Co^{2+}]$

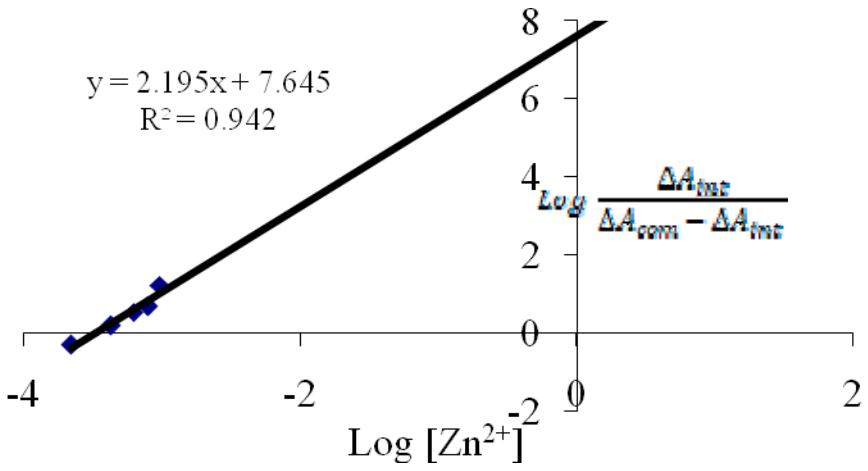

Figure 9. Plot of $\mathbf{Log}\ \frac{\Delta A_{int}}{\Delta A_{com} - \Delta A_{int}}$ as a function of Log $[Zn^{2+}]$ at 464 nm

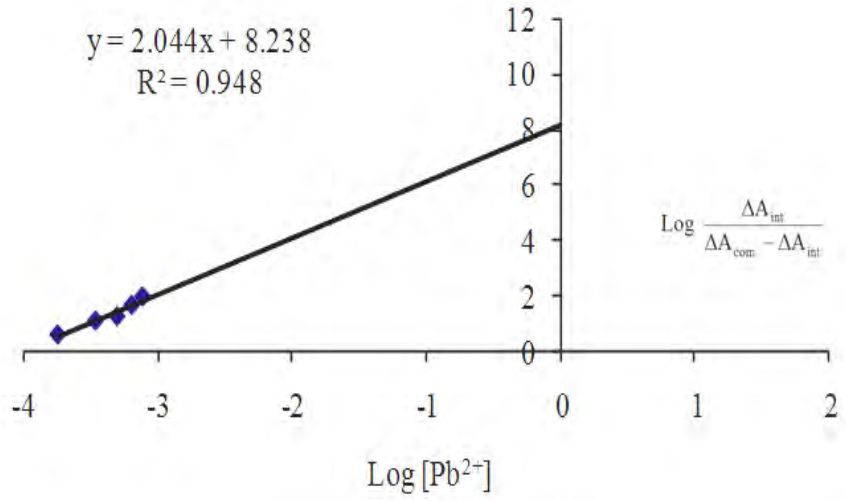

Figure 10. Plot of $\mathbf{Log}\ \frac{\Delta A_{int}}{\Delta A_{com} - \Delta A_{int}}$ as a function of Log $[Pb^{2+}]$ at 464 nm

Conclusion

The ELPO ligand was prepared by the condensation reaction between ethanolamine and acetylacetone and yield % was found to be 95.03. The visible spectrum of the prepared ligand showed two strong absorption peaks at 454nm and 390nm. The wavelengths of maximum absorption of the all complexes were found at 464 nm. Maximum complex formation for the complexes was found at 100min reaction time. Standard calibration curves of the complexes were linear and passed the origin. Therefore Beer's law was obeyed. By applying the Bunton's equation, the stoichiometric composition for all complexes were found to be 1:2 (M:ELPO) and the stability constants for the ELPO complexes of Co(II), Zn(II), and Pb(II) were determined to be 3.43×10^6, 44.1×10^6, and 172×10^6 respectively. Among the complexes studied, the highest stability constant was obtained for Pb^{2+} and the lowest one was Co^{2+} complex. Therefore, the prepared ELPO ligand can be used for the selected separation of Pb^{2+} from the mixture of metal ions in aqueous solutions.

Acknowledgements

The authors are thankful to Rector U Kyaw Ye` Tun, Pro-Rectors Dr. Kyaw Kyaw Khaung and Dr. Marlar Aun, East Yangon University, and Professor Daw Phyu Phyu Thein Head of Department, Department of Chemistry, East Yangon University, for their kind encouragement.

References

Cox, P.A, (2000), "Instant Notes of Inorganic Chemistry", Viva Books Private Ltd., New Delhi

Fiedler, H.D., Westrup, J.L., Souza, A.J., Pavei, A.D., Chagas, C.U., and Nome, F., (2004), "Cd(II) Determination in the Presence of Aqueous Micellar Solutions", *Talanta*, **64**, 190-195

Graddon, D.P, (1968), "An Introduction to Co-ordination Chemistry", Pergamon Press, New York

Hamilton, L.F., Simpson, S.G., and Ellis, D.W., (1969), "Calculation of Analytical Chemistry", Mc Graw-Hill Book Co., Inc., New York

Jolly, L.W., (1991), "Modern Inorganic Chemistry", 2nd edition, Mc Graw-Hill Book Co.Ltd., New York

Oxtoby, W.D., Gillis, H.P., and Nachtrieb, H.N., (1999), "Modern Chemistry", Saunders Golden Sunburst Series, New York

Prakash, S., Basu, S.K., Tuli, D., and Madan, R.D., (1983), "Advanced Inorganic Chemistry", S.Chand and Company Ltd., New Delhi

Vogel, A.I., (1968), "A Textbook of Quantitative Inorganic Analysis", Prentice-Hall, Inc., Englewood Clifts, New Jersay

Chemical Investigation of *Ipomoea batatas* (L.) Lam. (Sweet Potato) Leaves and Study of its Antihyperglycemic Activity

Myint Myint Khine[1], May Thu Aung[2], Mon Mon Thu[3] and Saw Hla Myint[4]

Abstract

The main aim of this research work is to study some biological activities of *Ipomoea batatas* (L.) Lam. (Sweet potato) leaves and to investigate some bioactive compounds. Compounds-1 (0.001 %), compound-2 (0.003 %), compound-3 (0.004 %) and compound-4 (0.005 %) were isolated from petroleum ether extract and ethyl acetate extract by using liquid-liquid extraction and column chromatographic method. The isolated compounds were identified by UV, FTIR, ^{1}H NMR and ^{13}C NMR spectroscopy. Compounds 1 and 2 were deduced as β-sitosterol and stigmasterol glucoside. Remaining two compounds, compound 3 and 4 were partially identified as phenolic acids such as gentisic and protocatechuic acids respectively by colour reaction and UV spectroscopy. The percent inhibition of hyperglycemic effect (peak effect) of aqueous extract were 1.88 % , 10.24 % and 29.22 % at the dose of 1.5 g/kg, 3 g/kg and 6 g/kg after 4 hours administration of adrenaline respectively. The percent inhibition of hyperglycemic effect of 70 % ethanolic extract were 11.64 %, 26.49 % and 40.56 % at the dose of 1.5 g/kg, 3 g/kg and 6 g/kg respectively after 4 hours administration of adrenaline. The percent inhibition of hyperglycemic effect of standard glibenclamide was 63.11 % at 4 hours after administration of adrenaline. From above data, 70 % ethanolic extract exhibited more significant antihyperglycemic activity than aqueous extract at the dose of 1.5 g/kg, 3 g/kg and 6g/kg after 4 hours administration of adrenaline.

Key words: *Ipomoea batatas* (L.) Lam, sweet potato leaves, β-sitosterol, stigmasterol glucoside, adrenaline, antihyperglycemic activity

Introduction

The sweet potato (*Ipomoea batatas*) is a dicotyledonous plant which belongs to the family Convolvulaceae. *Ipomoea batatas* is a crop plant whose large, starchy, sweet tasting tuberous roots are an important root

1. Lecturer,Dr, Department of Chemistry, Sittwe University
2. Demonstrator,Dr, Department of Chemistry, University of Yangon
3. Lecturer,Dr, Department of Chemistry, Taungoo University
4. Professor,Dr, Department of Chemistry, University of Yangon

vegetable (Purseglove, 1991; Woolfe, 1992). The young leaves and shoots are sometimes eaten green. The genus *Ipomoea* that contains the sweet potato also includes several garden flowers called morning glories, though that term is not usually extended to *Ipomoea batatas*. Some cultivars of *Ipomoea batatas* are grown as ornamental plants.

Ellagic acid, 3,5-dicaffeoylquinic acid, boehmeryl acetate, cyanidin glycosides, peonidin, p-hydroxybenzoylcyanidin, p-hydroxybenzoyl-peonidin, caffeoyl-p-hydroxybenzoylcyanidin, caffeoyl-p-hydroxybenzoyl-peonidin and caffeoylpeonidin were identified from roots.

The root is considered laxative. In Malaya, a drink prepared from the root is given to allay thirst in fever. Tops and tender shoots are used in poultices. A paste of roots or leaves is used as an application to scorpion bites (The Wealth of India, 1959). According to Hartwell (1967–1971), the leaf decoction is used in folk remedies for tumors of the mouth and throat. Reported to be alterative, aphrodisiac, astringent, bactericide, demulcent, fungicide, laxative and tonic, sweet potato is a folk remedy for asthma, bugbites, burns, catarrh, ciguatera, convalescence, diarrhea, dyslactea, fever, nausea, renosis, splenosis, stomach distress, tumors and whitlows (Duke and Wain, 1981).

Materials and Methods

Leaves of *I. batatas* (L.) Lam.were collected in September 2006 from Yangon Region and identified by authorized botanists at Botany Department, University of Yangon. UV-vis (MeOH), FT-IR (KBr), ^{1}H NMR (DMSO, 300 MHz, Bruker Avance 600 Spectrometer), ^{13}C NMR (DMSO, Varian 100 MHz Spectrometer) were recorded in the different modes. Column Chromatography was performed by using silica gel (70-230, 230-400 mesh, Merck, Germany), Sephadex LH-20 (25-100 µm, Fluka, Switzerland) and Thin Layer Chromatography by precoated TLC plates (60 F_{254} Aluminium plates, Merck, Germany).

Extraction and Isolation of Phytochemical Constituents from *I. batatas* (L.) Lam. Leaves

The dried powdered leaves sample of *I. batatas* (L.) Lam. (700 g) was percolated in methanol (1 L) with occasional shaking for two weeks and filtered.The methanol crude extract was shaken by petroleum ether to remove the fat. Petroleum ether soluble portion was evaporated to obtain

petroleum ether extract. The residue portion was hydrolysed with 2 M HCl extracted with ethyl acetate, upper ethyl acetate layer and lower acid layer were obtained. Ethyl acetate layer was concentrated to obtain ethyl acetate extract.

Petroleum ether extract (1.5 g) was carried out by column chromatography method by using silica gel (70-230 mesh) various solvent systems of petroleum ether only, petroleum ether : ethyl acetate (9:1, 7:1, 5:1, 3:1, 2:1, 1:1) and ethyl acetate only were used. The fractions obtained were checked under UV lamp and spraying reagents on thin layer chromatogram. Seven fractions were obtained after combining the similar fractions. Fraction number F_3 gave compound-1 (0.001 %) as colourless crystals. Ethyl acetate extract 0.3 g (0.3 g × 4 times) was separated by column chromatography on Sephadex LH-20 (25-100 µm) using methanol only as solvent system. Four fractions (F_I to F_{IV}) were obtained. Fraction number II was separated on a silica gel (230-400 mesh) column using gradient solvent system of petroleum ether : acetone (5:1, 3:1, 2:1, 1:1 v/v), acetone only, acetone : methanol (1:1, 1:2 v/v) and methanol only. Six combined fractions were collected. Fraction F_4 was chromatographed over Sephadex LH-20 (25-100 µm) using a stepwise gradient of acetone : methanol (2:1 v/v) and methanol only as solvent system. Isolated compound-3 (0.004 %) was obtained. Fraction number III was separated on a silica gel (230-400 mesh) column using gradient elution with petroleum ether : acetone (9:1, 7:1, 5:1, 3:1, 2:1, 1:1 v/v), acetone only, acetone : methanol (1:1, 1:2 v/v) and methanol only as solvent system to afford ten combined fractions. Fraction F_5 using petroleum ether : acetone (2:1 v/v) solvent system gave pure compound-2 (0.003%) as colourless. Fraction F_{10} was chromatographed on Sephadex LH-20 (25-100 µm) using methanol only as the gradient elution system. Isolated compound-4 (0.005%) was obtained.

Pharmacological Activities of *I. batatas* (L.) Lam Leaves

Antihyperglycemic activity of leaves of *I. batatas* (L.) Lam. was screened by Pharmacology Research Division, Department of Medical Research (Lower Myanmar), Yangon.

Antihyperglycemic activity was carried out by using *I. batatas* (L.) Lam. (leaves) extract according to the method of Gupta *et al.*, (1967). Seven adult healthy rats of Wister strain weighing 180-230 g were used in this experiment. The animals were kept on a standard laboratory diet. For experimental purpose, the animals were kept fasting overnight for 18 hr but

were allowed free access to water. Fasting blood glucose level (0 hr) was taken from venous blood obtained by cutting of 1 mm of tail and measured by glucometer.

Results and Discussion

Characterization and Identification of Isolated compounds

β-sitosterol (Compound-1): colourless needle shape crystals, 0.001% yield, mp (138 ºC), R_f =0.38 (PE:EtOAc, 7:1); FTIR (KBr) cm^{-1}: 3448 (υ_{O-H}), 2952, 2864 (υ_{C-H}), 1654 ($\upsilon_{C=C}$), 1460, 1379 (δ_{C-H}), 1053 (υ_{C-O}).

Stigmasterol glucoside (Compound-2): White powder, 0.003% yield, mp (202 ºC), R_f =0.45 (PE: CH_3COCH_3, 2:1); FTIR (KBr) cm^{-1}: 3429 (υ_{O-H}), 2923, 2862 ($\upsilon_{asy\ sy-CH}$), 1623 ($\upsilon_{C=C}$), 1458, 1384 (δ_{C-H}), 1064 (υ_{C-O}); ^{13}C NMR (100 MHz, MeOH-d_4) δ_C ppm: 140.1 (C-5), 122.0 (C-6), 137.0 (C-22), 129.5 (C-23), 100.8 (C-12), 69.8 - 76.8 (C-22 - 52), 61.1 (C-62).

Gentisic acid (Compound-3): Amorphous pale yellow colour, 0.004% yield, R_f =0.53 (Toluene: MeOH: A/A, 1:2:0.01); UV λ_{max} (nm) MeOH, NaOH: 280 (296); FTIR (KBr) cm^{-1}: 3417 (υ_{O-H}), 1701 ($\upsilon_{C=O}$), 1643, 1596 ($\upsilon_{C=C}$), 1396, 1199, 1045 (υ_{C-O}); ^1H NMR (300 MHz, DMSO-d_6) δ_H ppm: 6.65 (H-3, *d*, *J* = 8.8 Hz), 7.07 (H-4, *d*, *J* = 8.8 Hz), 7.69 (H-6, *d*, *J* = 3 Hz).

Protocatechuic acid (Compound-4): Amorphous pale yellow colour, 0.005% yield, R_f =0.23 (Toluene: MeOH: A/A, 1:2:0.01); UV λ_{max} (nm) MeOH, NaOH: 280 (286, 340); FTIR (KBr) cm^{-1}: 3406 (υ_{O-H}), 1700 ($\upsilon_{C=O}$), 1650, 1573 ($\upsilon_{C=C}$), 1269, 1045 (υ_{C-O}); ^1H NMR (300 MHz, DMSO-d_6) δ_H ppm: 7.69 (H-2, *d*, *J* = 3 Hz), 7.08 (H-5, *d*, *J* = 8.8 Hz), 7.50 (H-6, *dd*, *J* = 8.8, 3 Hz).

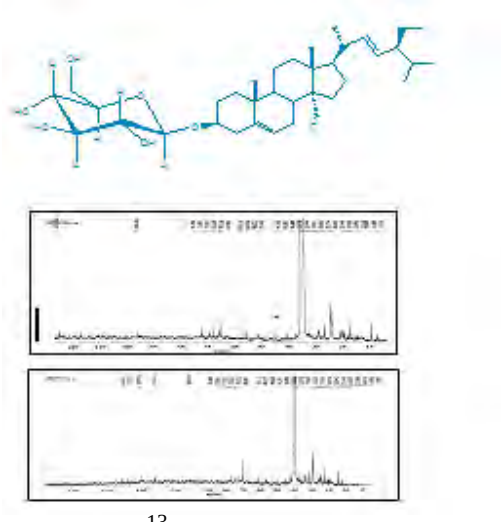

Figure 1 ^{13}C NMR spectrum (100 MHz, MeOH-d_4) of compound-2

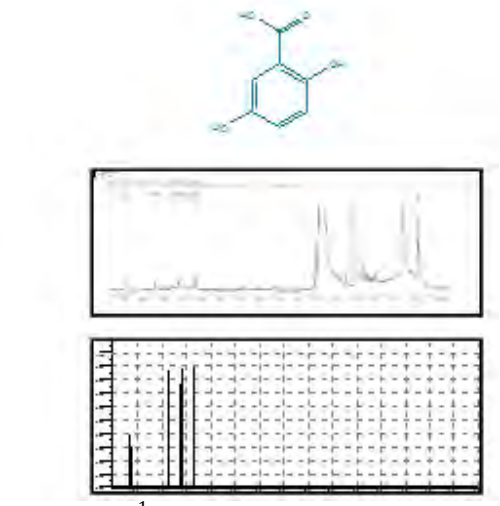

Figure 2 ^{1}H NMR spectrum (300 MHz, DMSO-d_6) of compound-3 compared with predicted spectrum of gentisic acid by ACD Lab's software

Table 1 Comparison of ^{13}C NMR Spectral Data of Compound-2 with Reported Stigmasterol Skeleton (Harborne, 1989)

Position	$^{\delta}c$(ppm)		Interpretation
	Compound-2*	Ref. Stigmasterol skeleton	
1	37.3	37.3	Methylene
2	31.3	31.7	Methylene
3	72.3	71.8	Oxymethine
4	41.9	42.4	'q' carbon
5	140.1	140.8	Olefinic 'q'
6	122.0	121.7	Olefinic methine
7	31.3	31.9	Methylene

Position	$^{\delta}$c(ppm)		Interpretation
	Compound-2*	Ref. Stigmasterol skeleton	
8	31.3	31.9	Methine
9	49.6	50.2	Methine
10	36.8	36.6	‘q’ carbon
11	22.1	21.1	Methylene
12	39.7	39.7	Methylene
13	41.9	42.4	‘q’ carbon
14	56.2	56.9	Methine
15	24.5	24.4	Methylene
16	29.0	29.0	Methylene
17	56.2	56.1	Methine
18	11.8	11.1	Methyl
19	19.4	19.4	Methyl
20	40.5	40.5	Methine
21	21.1	21.1	Methyl
22	137.0	138.4	Olefinic methine
23	129.5	129.3	Olefinic methine
24	51.3	51.3	Methine
25	31.3	31.9	Methine
26	21.3	21.3	Methyl
27	19.0	19.0	Methyl
28	25.4	25.4	Methylene
29	11.7	12.3	Methyl

* 100 MHz, MeOH-d_4

Table 2 ^{1}H NMR (300 MHz, DMSO-d_6) Spectral Data of Compound -3

Position	$^{\delta}$µ(ppm)		Interpretation
	Compound-3	Predicted Gentistic acid by ACD Lab's software	
H-6	7.69 (*d*, *J* = 3 Hz)	7.38 (*d*, *J* = 3 Hz)	Aromatic methine with ortho carboxyl gp and OH gp
H-4	7.07 (*d*, *J* = 8.8 Hz)	7.10 (*d*, *J* = 9 Hz)	Aromatic methine with ortho OH gp
H-3	6.65 (*d*, *J* = 8.8 Hz)	6.85 (*d*, *J* = 9 Hz)	Aromatic methine with ortho OH gp

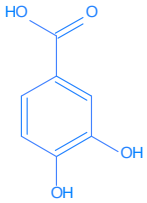

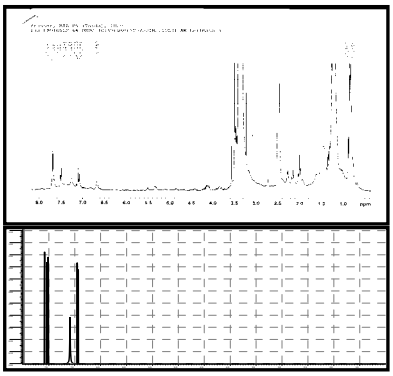

Figure 3 ^{1}H NMR spectrum (300 MHz, DMSO-d_6) of compound-4 compared with predicted spectrum of protocatechuic acid by ACD Lab's software

Table 3 ^{1}H NMR (300 MHz, DMSO-d6) Spectral Data of Compound-4

H-atom	δ_H[ppm] Compound-4 (DMSO-d_6)	Ref.[a] Protocate-chuic acid (MeOH-d_4)	Ref.[b] Protocate-chuic acid ($CDCl_3$)	Predicted Protocatechuic acid by ACD Lab's softw are	Assign-ment
2	7.69 *d* (*J* = 3 Hz)	7.54 *bd s*	7.50 *d* (*J* = 1.9 Hz)	7.58 *d* (*J*=3Hz)	aromatic – CH
5	7.08 *d* (*J* = 8.8 Hz)	6.85 *d* (*J* = 8.8 Hz)	6.80 *d* (*J* = 8.8 Hz)	6.94 *d* (*J* = 8.2 Hz)	aromatic – CH
6	7.50 *dd* (*J* = 8.8, 3 Hz)	7.54 *bd s*	7.52 *dd* (*J* = 1.9, 8.8 Hz)	7.52 *d* (*J* = 8.2 Hz)	aromatic – CH

a = Hnin Yu Win, 2009

b = Myint Myint Than, 2003 ; Beistel and Edwarts , 1976

Bioactivities of *I. batatas* (L.) Lam.

In vivo antihyperglycemic activity on crude extracts of *I. batatas* (L.) Lam. leaves were tested on adrenaline-induced hyperglycemic rat model. The mean blood glucose levels of control and treated animals after oral administration of different dosage of aqueous extracts, 70% ethanolic extracts and standard glibenclamide at various time intervals were shown in Table 4 and Figure 4.

Table 4. Percent Inhibition Effect (Mean ± SEM) of Aqueous Extract and Ethanolic Extract of *I. batatas* (L.) Lam. (Leaves) on Adrenaline-Induced Hyperglycemic Rat Model

Group of rats	Percent inhibition of hyperglycemia			
	1 hr	2 hr	3 hr	4 hr
Ethanolic extract 6g/kg (n=6)	30.73 ± 7.49	24.76 ± 4.09	32.19 ± 5.26	40.56 ± 6.24

Group of rats	Percent inhibition of hyperglycemia			
	1 hr	2 hr	3 hr	4 hr
Aqueous extract 6g/kg (n=6)	35.2 ± 4.21	16.34 ± 3.14	24.77 ± 5.19	29.22 ± 4.99
Glibenclamide 4mg/kg(n=6)	54.19 ± 8.99	69.04 ± 19.39	51.70 ± 11.15	63.11 ± 10.94

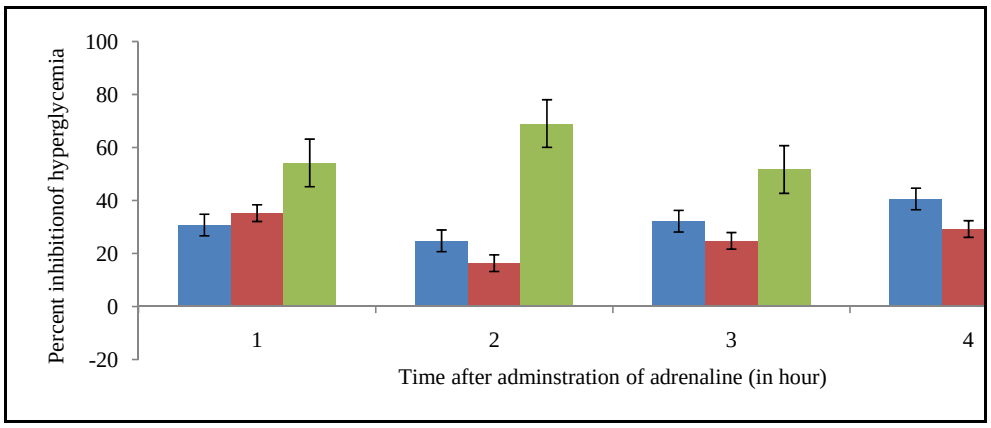

Figure 4. Percent inhibition effect of aqueous extract and ethanolic extract of *I. batatas* (L.) Lam. (leaves) on adrenaline-induced hyperglycemic rat model

Conclusion

From the overall assessment of the present work concerning the chemical and some biological investigations on the leaves of *I. batatas* (L.) Lam., the following inferences could be deduced. It was found that β-sitosterol, stigmasterol glucoside, and two phenolic acids, gentisic and protocatechuic acids were isolated from petroleum ether and ethyl acetate extracts after hydrolysis. Aqueous and 70 % ethanolic extracts of leaves showed blood glucose lowering effects at the dose of 1.5 g/kg, 3 g/kg and 6 g/kg after 4 hours administration of adrenaline with dose

dependent manner. According to the data, 70 % ethanolic extract exhibited more significant antihyperglycemic activity than aqueous extract at the dose of 1.5 g/kg, 3 g/kg and 6 g/kg after 4 hours administration of adrenaline. Based on above investigation, it can be concluded that the aerial parts of *I. batatas* (L.) Lam. (Sweet potato) leaves should be useful in traditional medicine due to their antihyperglycemic and antioxidant actions (the tests for the latter activity being not reported here).

Acknowledgements

The authors wish to thank the Department of Higher Education (Lower Myanmar), Ministry of Education, Yangon, Myanmar, for the financial support of this research programme, and to Dr Ni Lar (Professor and Head), Department of Chemistry, University of Yangon, for the kind provision of the research facilities.

References

Beistel, D.W. and Edwards, W.D., (1976), "The Internal Chemical Shift-A Key to Bonding in Aromatic Molecules. 2. Substituent Effects on the Carbon-13 Magnetic Resonance Spectra of the 1,4-disubstituent Benzenes", *J. Phys. Chem.*, **80**, 2023-2027

Duke, J.A., and Wain, K.K., (1981), "Medicinal Plants of the World", Computer Index With More Than 85,000 Entries, 3 vols

Gupta, S.S., Verma, S.G.L., Gang, V.P. and Mehesh, Ral., (1967), "Antidiabetes Effects of Tinospora Cordifolia", *J. Med. Res., India*, **55**(7), 733-745

Harborne, J.B., (1989), "Methods in Plant Biochemistry", Academic Press, Tokyo, 1, 64

Hartwell, J.L., (1967-1971), "Plants Used Against Cancer", A Survey, *Lloydia*, 30-34

Hnin Yu Win, (2009), "Bioactive Mandalarpyrones, their Derivatives and Further Novel Secondary Metabolites from Marine and Terrestrial Bacteria", PhD (Dissertation), Institute of Organic and Biomolecular Chemistry, Georg-August University of Goettingen, Germany

Myint Myint Than, (2003), "Chemical Constituents of Brazilian Propolis and Myanmar Medicinal Plants", M.Sc (Thesis), Department of Natural Products Chemistry, Institute of Natural Medicine, Toyama Medical and Pharmaceutical University, Japan

Purseglove, J.W., (1991), "Tropical Crops Dicotyledons", Longman Scientific and Technical, John Wiley and Sons, Inc., New York

Wealth of India, (1959), "A Dictionary of Indian Raw Materials and Industrial Products", Council of Scientific and Industrial Research, New Delhi, **V**(H-K), 238, 240, 247-248

Woolfe, J.A., (1992), "Sweet Potato: An Untapped Food Resource",Cambridge Univ. Press and the International Potato Center (CIP), Cambridge, UK

Chitosan-g-Poly (Acrylic Acid) Hydrogel as Superabsorbent

Mi Mi Lay[1], Tun Aung[2] and Kyaw Myo Naing[3]

Abstract

This research work is concerned with the copolymerization of acrylic acid on chitosan in a homogeneous phase by using potassium persulphate (KPS) as a redox system in the presence of N,N-methylene-bis-acrylamide (MBA) as a cross linking agent. Commercial chitosan was obtained from United Network Co.,Ltd., Yangon, which was purified with sodium carbonate. The purified chitosan was characterized by spectroscopic method such as SEM, FT IR and TG-DTA. Optimal conditions as regard to reaction parameters such as polymerization time, reaction temperature, initiator concentration and amount of solvent were found out. Water absorbency and water content percentage of prepared chitosan-g-poly (acrylic acid) hydrogel were initially checked in deionized water. The grafted and cross-linking characteristics of cross-linked hydrogel (CGC) compared to uncross-linked hydrogel (UGC) were confirmed by FT IR, TG-DTA and SEM. Then, the swelling behaviour of cross-linked hydrogel (CGC) was investigated in salt solutions and different pHs. On the basis of the swelling nature, the cross-linked hydrogel (CGC) was utilized in selective absorption of water from different oil-water emulsions, such as petrol-water, diesel-water and petroleum ether-water. The factors affecting the oil-water emulsions were the time, pH and NaCl concentration.

Key words: chitosan, acrylic acid, cross-linked hydrogel, swelling behavior, pH-sensitivity, oil-water emulsion

Introduction

Hydrogels are loosely cross-linked, three-dimensional networks of flexible polymer chains that carry dissociated, ionic functional groups. Hydrogels are polymeric networks that absorb fluids such as water, electrolyte solution, synthetic urine, brines, biological fluids such as urine sweat and blood. They are polymers which are characterized by

1. Lecturer, Dr, Department of Chemistry, University of Yangon
2. Lecturer, Dr, Department of Chemistry, University of Yangon
3. Professor, Dr, Department of Chemistry, University of Yangon

hydrophilicity containing carboxylic acid, carboxamide, hydroxyl, amine, imide groups and so on. Because of their ionic nature and interconnected structure, they absorb large quantities of water and other aqueous solutions. In polymeric network, there are hydrophilic groups or domains that are hydrated in an aqueous environmental, thereby creating a hydrogel structure (Kim *et al.*, 2002). Graft copolymerization of vinyl monomers onto polysaccharides is an efficient route for the preparation of hydrogels. The hydrogel forming ability through graft copolymerization of vinyl monomers onto polysaccharides such as starch, chitosan, sodium alginate, carrageenan, and cellulose has been well documented (Castel *et al.*, 1990). Because of the presence of certain functional groups along the polymer chains, hydrogels are often sensitive to the conditions of the surrounding environment, which are referred to as "intelligent materials" or "smart materials". For example, the water uptake of these materials may be sensitive to temperature, pH, or ionic strength of the swelling solutions, or even to the presence of a magnetic field or ultraviolet light (Qiu and Park, 2001). These smart hydrogels are of general interest for biomedical applications such as artificial muscles or switches, biomedical separation system, and controlled release systems.

In the present study, chitosan-g-poly (acrylic acid) hydrogel, *i.e*., grafting of chitosan with poly (acrylic acid) was prepared. Regarding the water absorbency of the prepared hydrogel, the optimization parameters on preparing desired hydrogel were determined. The water absorbencies of cross-linked hydrogels in different pH media and in different electrolyte solutions were determined. The separation of water from oil-water emulsion (petrol-water, diesel-water, petroleum ether-water) was carried out.

Materials and Methods

Chitosan was obtained from United Network Co. Ltd. (Yangon). The degree of deacetylation was found to be about 83 % by using titrimetric analysis and the viscosity average molecular weight(Ravi Kumar,2000) is found to be 0.8013×10^5 Da by a viscometric method. The chemicals used in the experimental work were from the British Drug House Chemical Ltd., Poole, England, and Wako Chemicals Co. Inc., Tokyo, Japan. All chemicals were of reagent grade and were used as received. In all the investigations

the recommended methods and standard procedure involving both conventional and modern techniques were employed.

Synthesis of Chitosan-g-poly (Acrylic acid) Hydrogels

Chitosan solution (0.5 g of chitosan in 20 mL of 2 % v/v acetic acid) was placed in the polymerization reactor. Following this, monomer, acrylic acid (AA), (2.0 g, 0.69 mol L^{-1} in 20 mL of 2 % v/v acetic acid solution) was added to the reactor. The solution mixture was stirred well by magnetic stirrer for 10 minutes. 0.0015 M of methylene bis acrylamide was added into the mixture. Then potassium persulphate (KPS) initiator (0.2162 g, 0.02 mol L^{-1} in solution) was added into the reactor. Then the flask was placed in a thermostated oil bath at 60 ºC. Polymerization was started and continued for 60 minutes. After 60 minutes, the reaction was stopped by rapidly cooling down the reaction. The product was precipitated by pouring the polymerization mixture into a large amount of acetone. The precipitate was filtered, washed thoroughly with acetone and dried under vacuum at 60 ºC to get constant weight. Unreacted monomer, initiator and poly (acrylic acid) as homopolymer were allowed to remove by soxhlet extraction method. In this extraction, water was used as solvent for 8 hr. After drying under reduced pressure, the remaining product was obtained as a graft copolymer.

Characterization of Chitosan-g-poly (Acrylic acid) Hydrogels

Chitosan-g-poly (acrylic acid) hydrogel was characterized by SEM, FT IR(Baxter *et al*.,1997) and TG-DTA.

Determination of the Water Absorbency

For determination of water absorbency, the particles were used 60 mesh size of amorphous shape. Hydrogels weighing 0.01 g was put into a weighed teabag and immersed in 100 mL of distilled water at room temperature. It was confirmed that 24 hr equilibrium was long enough to reach equilibrium swelling of the gel.

The equilibrated swollen gel was allowed to drain by removing the teabag from water about 20 minutes. Then the bag was weighed to determine the weight of the swollen gel. Dry weight was determined after drying gel in vacuum desiccators about 3 hr.

Based on these two values, the water absorbency and water content percentage were calculated.

Determination of Water Absorbency of Prepared Hydrogels (CGC) at Salt Solutions

The swelling behavior of hydrogel was determined in aqueous solutions of 0.15 M NaCl, $CaCl_2$ and $AlCl_3$. The same procedure is mentioned above.

Determination of Water Absorbency of Prepared Hydrogels (CGC) at Various pH

In this experiment, the equilibrium swelling of the hydrogel (CGC) was studied at various pHs ranging from 1.0 to 13.0. Therefore, stock NaOH (pH 13.0) and HCl (pH 1.0) solutions were diluted with distilled water to reach the desired basic and acidic pH, respectively.

Application of Cross-linked Chitosan-g-Poly (Acrylic acid) Hydrogels Selective Absorption of Water from Different Oil-water Emulsions

Water absorption studies from different oil-water emulsions (petrol-water, diesel-water, petroleum ether water) were carried out at different time intervals, pH and NaCl concentration.

Results and Discussion

The highly purified chitosan with the 75 % yield was achieved. Optimization of different reaction parameters indicates that initiator concentration was (20×10^{-3} mol L^{-1}), the amount of solvent was 40 mL, the polymerization time was 60 min, concentration of acrylic acid was 0.6938 M, concentration of methylene bis acrylamide was 0.0015 M and the reaction temperature was 60 ± 2 ºC.

Table 1. Effect of polymerization time on the grafting percentage

Polymerization time (min)	Grafting percentage (%)
15	94
30	138
45	160
60	215
75	150

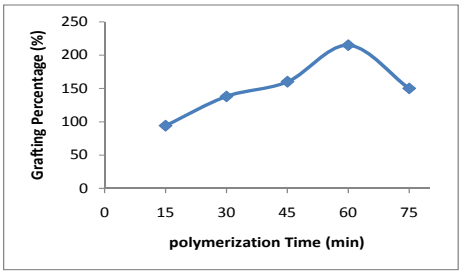

Figure 1. Effect of polymerization time on the grafting percentage

Table 2. Effect of reaction temperature on the grafting percentage

Reaction temperature (ºC)	Grafting percentage (%)
40	90
50	105
60	210
70	120
80	81

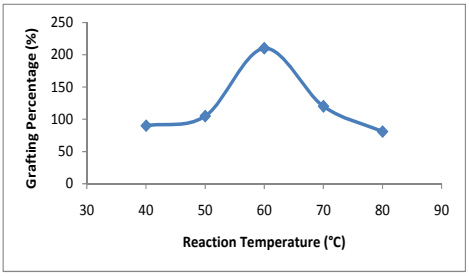

Figure 2. Effect of reaction temperature on the grafting percentage

Table 3. Effect of initiator concentration on the grafting percentage

[KPS] (× 10^{-3} M)	Grafting percentage (%)
5	110
10	129
15	140
20	219
25	195

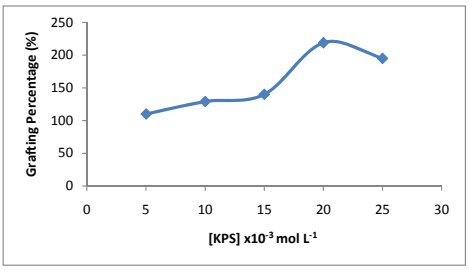

Figure 3. Effect of initiator concentration on the grafting percentage

Table 4. Effect of the amount of solvent on the grafting percentage

Amount of solvent (mL)	Grafting percentage (%)
30	180
40	250
50	215
60	165
70	120

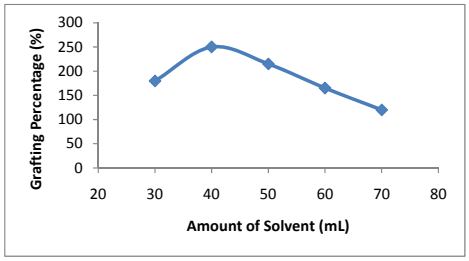

Figure 4. Effect of the amount of solvent on the grafting percentage

The SEM micrographs of chitosan and cross-linked hydrogel were shown in Figures 5(a) and (b). From SEM analysis, several branching in the macrofibrils and meshy frameworks were observed in chitosan. Lamellae folded structure was observed in cross-linked hydrogel.

(a) (b)

Figure 5. SEM micrographs of (a) chitosan and (b) cross-linked chitosan-g-poly (acrylic acid) hydrogels

The FT IR spectra of chitosan and cross-linked chitosan-g-poly (acrylic acid) hydrogels were shown in Figures 6 (a) and (b). From FT IR spectra, the effect of cross-linker concentration on hydrogel was observed distinctly. In the FT IR spectrum of cross-linked hydrogel, the amide I band was observed at 1658 cm^{-1} as sharp and intense band due to the cross-linker effect. Then the very intense characteristic band 1541 cm^{-1} is due to C=O asymmetric stretching in the carboxylate anion that is reconfirmed by another sharp peak at 1404 cm^{-1}, which is related to a symmetric stretching mode of the carboxylate anion. In fingerprint region, three new weak bands were observed at 1313 cm^{-1}, 1250 cm^{-1} and 1170 cm^{-1}. The absorption band at 1313 / 1250 cm^{-1} was appeared due to the interaction between δ_{NH} and ν_{CN}. Similarly, the absorption band at 1250/1170 cm^{-1} was due to

interaction between δ_{CN} and ν_{CO}. The above absorption bands between 1100 cm^{-1} and 1200 cm^{-1} were not observed in chitosan.

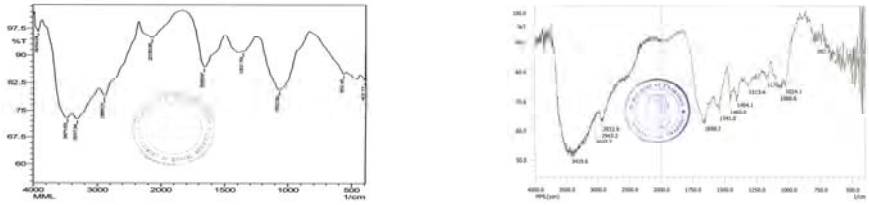

(a) (b)

Figure 6. FT IR spectra of (a) chitosan and (b) cross-linked chitosan-g-poly (acrylic acid) hydrogels

Table 5. FT IR spectra band assignments for chitosan and cross-linked chitosan-g-poly (acrylic acid) hydrogels

Observed frequency (cm^{-1})		General range (cm^{-1})	Band assignments
Chitosan	Cross-linked CHI-g- PAA		
3471 3317	3419 3037	3200-3600 3060-3330	υ_{O-H} υ_{N-H}
2885	2923	2850-2990	υ_{C-H}
1659 - 1563	1658 1541 -	1600-1950 1550-1650 1515-1570	$\upsilon_{C=O}$ (amide I) $\upsilon_{asC=O}$ ($-COO^{\Theta}$) δ_{N-H} (amide II)
-	1404	1375-1450	$\upsilon_{sC=O}$ ($-COO^{\Theta}$)
-	1313/1250	~1250	weak band interaction between δ_{NH} & υ_{C-N}
-	1250/1170	1100-1200	weak band interaction between δ_{C-N} & υ_{C-O}
1072	1066	1050-1200	υ_{C-O-C}

Chitosan and prepared hydrogel (CGC) having a weight loss in stages were shown in Figure 7 (a), (b) and Table 6. In the TG-DTA thermograms, the early stage both of TG profiles below 140 ºC it is very possible that surface water, adsorbed water and bound water were removed. Above 140 ºC, the TG profile for chitosan depicts in weight loss due to decomposition of some fraction of chitosan chain whereas due to decarboxylation from PAA and degradation in cross-linking point (unzipping). Above 330ºC, the TG profiles for the last stage are probably due to chain scissions both in PAA and chitosan backbone.

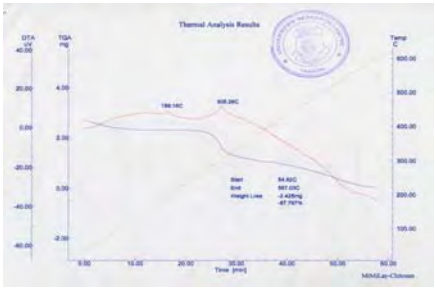

(a)

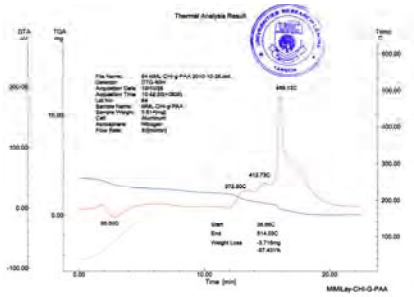

(b)

Figure 7. TG-DTA thermograms of (a) chitosan and (b) cross-linked hydrogel

Table 6 Thermal analysis of chitosan and cross-linked chitosan-g-poly (acrylic acid) hydrogels

Sample	TG			DTA	TG & DTA remark
	Temperature range (ºC)	Break in temperature (ºC)	Weight loss (%)		
Chitosan	55-140	90	12.67	-	Loss of adsorbed water and bound water
	140-250	-	-	199.16 (exo)	Thermally stable
	250-335	290	31.44	305.28 (exo)	Decomposition of some fraction of chitosan chain
	335-565	355	40.72	-	Degradation of chitosan backbone
Cross-linked CHI-g-PAA	38-140	100	24.84	86.6 (endo)	Loss of adsorbed water and bound water

Sample	TG			DTA	TG & DTA remark
	Temperature range (ºC)	Break in temperature (ºC)	Weight loss (%)		
	140-380	340	33.12	372.5 (exo)	decarboxylation of PAA chains and degradation in cross-linking point (unzipping)
	380-520	460	38.64	412.73 (exo) 456.12 (exo)	Chain scissions both in PAA and chitosan backbone
	520-600	-	-	-	Graphitization

The swelling behavior of cross-linked hydrogel (CGC) in aqueous solutions of 0.15 mol L^{-1} NaCl, $CaCl_2$ and $AlCl_3$ is shown in Table 7 and Figure 8. The swelling of the absorbent in salt solutions was appreciably decreased compared to the values measured in deionized water. This well-known phenomenon commonly observed in the swelling of ionic hydrogel, is often attributed to a screening effect of the additional cations causing a non-perfect anion-anion electrostatic repulsion, leading to a decreased osmotic pressure (ionic pressure) difference between the hydrogel network and the external solution. The swelling capacity increases with a decrease in the charge of the metal cation ($Al^{3+} < Ca^{2+} < Na^{+}$). This may be explained by complexing ability arising from the coordination of the multivalent cations with carboxylate groups present in cross-linked hydrogel (CGC). In the cross-linked hydrogel (CGC), the carboxylated groups cause complexing between ionic groups, so that the crosslink density increases and swelling capacity decreases.

Table 7 Water absorbencies of cross-linked hydrogel (CGC) at salt solutions

Sample	Water absorbency (g/g)		
	NaCl (0.15 M)	$CaCl_2$ (0.15 M)	$AlCl_3$ (0.15 M)
CGC	51.5	7.49	6.52

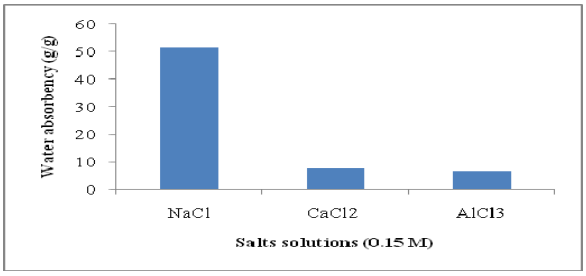

Figure 8. Water absorbencies of cross-linked hydrogel (CGC) in salt solutions (0.15 M)

The dependence of the equilibrium swelling of the cross-linked hydrogel (CGC) was characterized by a curve with 2 maxima at pH 3 and 8 as shown in Figure 9. The remarkable swelling changes are due to the presence of different interacting species depending on the pH of the swelling medium. Under acidic condition, the swelling was controlled mainly by the amino group ($-NH_2$) on the C-2 carbon of the chitosan component. ($-NH_2$) group accepted protons and increased charge density on the polymer should enhance the osmotic pressure inside the gel particles because of the N^+H_3-N^+H_3 electrostatic repulsion. The osmotic pressure difference between the internal and external solution of the network is balanced by the swelling of the gel. However, under very acidic conditions (pH <3), a screening effect of the counter ion, *i.e.*, Cl^-, shields the charge of the ammonium cations and prevents an efficient repulsion. As a result, a remarkable decrease in equilibrium swelling was observed.

In the pH range 4 to 7, the majority of the base and acid groups are as N^+H_3 and COO^- or NH_2 and COOH forms and therefore ionic interaction of N^+H_3 and COO^- species (ionic cross-linking) or hydrogen bonding between amine and carboxylic acid may lead to a kind of cross-linking followed by decreased swelling.

At pH 8, the carboxylic acid groups become ionized and the electrostatic repulsive force between the charge sites (COO^-) causes an increase in swelling. Again, a screening effect of the counter ions (Na^+) limits the swelling at pH 9-13. In fact, at high and low pHs, the presence of high concentrations of the ions results in high ionic strength. When the ionic strength of the solution is increased, the difference in osmotic pressure between the hydrogel and the medium is decreased. Thus the swelling capacity of the hydrogel is decreased.

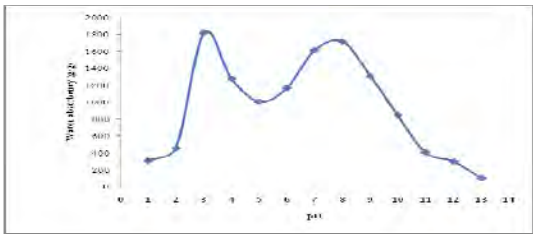

Figure 9. Water absorbencies of cross-linked hydrogel (CGC) at various pHs

Application of Cross-linked Chitosan-g-Poly (Acrylic acid) Hydrogels

The cross-linked hydrogel (CGC) was utilized in selective absorption of water from different oil-water emulsions, such as petrol-water, diesel-water and petroleum ether-water. The factors affecting the oil-water emulsions were the time, pH and NaCl concentration

Effect of Time

Water absorbency increased with increase in time but the rate of water absorbency started decreasing after 30 min and attained a constant value at 1 hr. The reason behind these observations is that the porous network of the gel becomes saturated and afterwards the absorption is almost ceased. The resulting data are presented in Table 8 and Figure 10.

Effect of pH

It was found that the polymer possesses more swelling behaviour in acidic medium than that of in alkaline medium. The implication of swelling and deswelling at low pH and high pH is that at low pH, $–NH_2$ groups attached to polymer backbone are protonated and these (NH_3^+) groups repel each other so, the polymer can able to swell at low pH, and the reverse happen at high pH. The results regarding to the effect of pH are shown in Table 9 and Figure 11.

Effect of NaCl Concentration

It has been found that water absorbency of the gel showed a gradual decrease with increase in NaCl concentration. The effects are shown in Table 10 and Figure 12. It can be interpreted that the swelling behaviour depends upon the osmotic pressure (ionic pressure) of the system. When the ionic strength of the solution is increased, the difference in osmotic pressure between the hydrogel and the medium is decreased. Thus, the swelling capacity of the hydrogel is decreased.

Table 8. Effect of time on water absorbency of cross-linked hydrogel (CGC) in different oil-water emulsion

Time (min)	Water absorbency (g / g)		
	Petrol – water	Diesel – water	Petether – water
10	87.01	58.30	33.02
20	188.10	159.50	130.30
30	373.02	344.50	255.10
40	341.32	316.28	226.00
50	331.10	302.90	210.70
60	330.90	302.10	209.90

Table 9. Effect of pH on water absorbency of cross-linked hydrogel (CGC) in different oil-water emulsion

pH	Water absorbency (g / g)		
	Petrol – water	Diesel – water	Petether – water
4	350.11	319.21	229.10
7	377.93	349.91	257.72
9	338.12	310.90	218.01

Table 10. Effect of NaCl concentration on water absorbency of cross-linked hydrogel (CGC) in different oil-water emulsion

[NaCl] (w / v %)	Water absorbency (g / g)		
	Petrol – water	Diesel – water	Petether – water
1	40.11	37.90	28.90
2	32.01	28.15	20.01
3	21.20	17.95	9.91
4	10.99	7.87	0.98
5	1.02	0.92	0.05

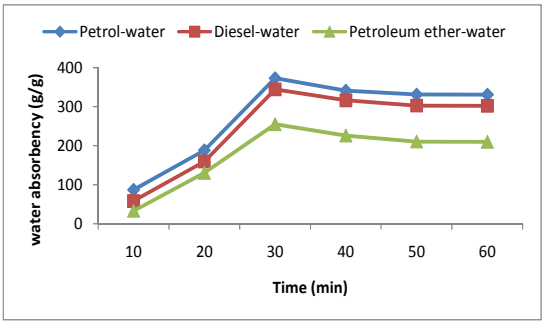

Figure 10. Effect of time on water absorbency of cross-linked hydrogel in different oil-water emulsions (CGC)

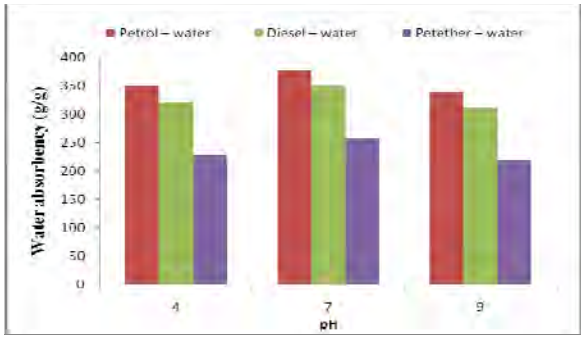

Figure 11. Effect of pH on water absorbency of cross-linked hydrogel in different oil-water emulsions (CGC)

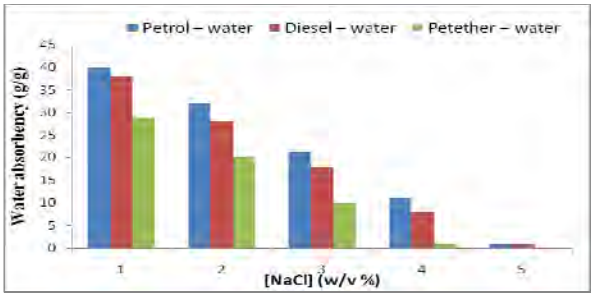

Figure 12 Effect of NaCl concentration on water absorbency of cross-linked hydrogel in different oil-water emulsion (CGC)

Conclusion

The swelling behaviors of cross-linked hydrogel (CGC) were affected by electrolytes, such as NaCl, $CaCl_2$ and $AlCl_3$. The swelling of the hydrogel in saline solutions was appreciably decreased compared to the values measured in deionized water. The order of swelling capacity increases as charge of the metal cations decreases (*i.e.*, $Al^{3+} < Ca^{2+} < Na^{+}$).

The equilibrium swelling behaviour of cross-linked hydrogel at various pHs was shown by a curve with two maxima at pH 3 and pH 8. The remarkable swelling changes are due to the presence of different interacting species ($-NH_2$ and –COOH) depending on the pH of the swelling medium.

On a comparative basis, from the resulting data of oil/water emulsions; the order of selective absorption was found to be petrol-water > diesel-water > petroleum ether-water. This hydrogel can be used for the removal of metal ions from polluted water.

Acknowledgements

The authors wish to thank Professor and Head, Dr Nilar, Department of Chemistry, University of Yangon, for her kind guidance, invaluable suggestions and for providing the research facilities.

References

Baxter,A.,Dillin,M., Taylor,K.D.A., and Roberts, G.A.G.,(1997) ,"Improved Method for IR Determinationof the Degree of N-Acetylation of Chitosan *", Intl. J.Biol. Macromol*.,**14**:166-169

Castel, D., Ricard, A. and Audebert, R., (1990), "Swelling of Anionic and Cationic Starch-Based Super Absorbents in Water and Saline Solution", *J.Appl. Poly.Sci*.,**39**:11-29

Kim, S.J., Lee, K.J., Lee, K.B. and Park, Y.D., (2002), "Sorption Characterization of Poly (Vinyl Alcohol)/Chitosan Interpenetrating Polymer Network Hydrogels", *J. App. Polymer Sci.*, **90**, 86-90

Qiu, Y. and Park, K., (2001), "Environment Sensitive Hydrogels for Drug Delivery", *Adv. Drug Deliv. Rev.*, **53**, 321-339

Ravi Kumar,M.N.V.,(2000), "Chitin and Chitosan Fibres:An Overview on Chitin and Chitosan Applications",*Reactive and Funct.Polyl*.An Internet Chitin and Chitosan Applied Research Resource

Removal of Cu^{2+}, Cd^{2+}, Hg^{2+}, and Ag^{+} from Industrial Wastewater by Using Thiol-Loaded Silica Gel

Aye Aye Myat[1], Kyaw Naing[2] and San San Myint[1]

Abstract

In this research, the preparation of modified silica gel with 3-trimethoxysilyl-1-propane-thiol ligand as solid phase extractor was carried out. In the TG-DTA thermogram of silica gel, weight-loss percent was found to be 11.76 %. This is related to the evolution of physically absorbed water and condensation of the silinol groups on the silica surface. In the case of thiol-modified silica, about 16 % was observed and that is 4% higher than silica gel. This is related to mass losses due to combustion of carbon and sulphur in thiol-modified silica. The sorption capacity of thiol-modified silica clearly depends on pH. At 60 min of contact time, the optimum pH was observed at pH 7.0 with 96.85% Cu (II) sorbed, at pH 4.0 with 92.13% Cd (II) sorbed, at pH 3.0 with 96.33% Ag (I) sorbed and at pH 5.0 with 97.32% Hg (II) sorbed. The sorption isotherms followed the Langmuir equation. The sorption coefficients (K_L) of Cu (II), Cd (II), Ag (I) and Hg (II) were found to be 0.252, 0.049, 0.265 and 0.290 g L^{-1}, respectively. The sorption capacities (X_m) of Cu (II), Cd (II), Ag (I) and Hg (II) were found to be 384.62, 416.67, 369.86 and 369.86 mg g^{-1}, respectively. The sorption isotherms followed the Freundlich equation. The sorption capacities (K) of Cu (II), Cd (II), Ag (I) and Hg (II) were found to be 6.219 x 10^3, 2.823 x 10^3, 6.770 x 10^3 and 6.862 x 10^3, respectively. Then sorption intensities (1/n) of Cu (II), Cd (II), Ag (I) and Hg (II) were found to be 0.215, 0.360, 0.175 and 0.180, respectively. The metal ions were recovered from the metal-loaded thiol-modified silica by using 8 M HCl solution. Therefore thiol-modified silica can be used to remove the Cu^{2+}, Cd^{2+}, Ag^{+} and Hg^{2+} ions from wastewater and then preconcentrated into solution of smaller volume. Application of thiol-modified silica was used for the removal of trace metals in wastewater from a paint factory, Bahan Township, Yangon Region, Myanmar. The order of sorbed percent of metal ions are $Hg^{2+} > Cu^{2+} > Cd^{2+}$.

Key words: Thiol loaded silica gel, 3-(trimethoxysilyl)-1-propane-thiol, sorption isotherms, Langmuir equation, Freundlich equation

1. Lecturers, Dr, Department of Chemistry, University of Yangon
2. Professor, Dr, Department of Chemistry, University of Yangon

Introduction

Heavy metal in trace concentration is extremely needed by life process, for instance, the human body needs some minerals to support the metabolic process. However, heavy metal in high concentration can cause illness or poison in human nerve system, blood composition heart and lung diseases. Therefore, analytical methods of separation technology have been developed to identify the heavy metal pollution (Budiman *et al.*, 2009).

An analysis of metal ions at trace levels poses unique problem to analysts, because it involves the requirements of versatility, specificity, sensitivity, and accuracy in the analysis (Sharma *et al.*, 2003). For determination of trace metal ions present in various samples like natural and wastewater, biological and alloy samples, direct determination using various instrumental methods is not possible owing to matrix effects and low concentration of metal ions in these samples. Thus, the need of separation and preconcentration arises (Sharma, 2001). Solid phase extraction is the most frequently used technique for separation and preconcentration of heavy metals because it is unnecessary to use the dangerous solvent. In this technique, many materials are used as adsorbent such as glass silica, and silica modified by grafting or sol gel method. For analytical purpose, silica modified by organic functional group is commonly used since the material silica provides many advantages such as inert, good adsorption and cation exchange capacity, easy to prepare with chemical compound and particular impregnate medium to create several of modified silica surface, high mechanic and thermal stability (Poole, 2003).

Silica gel, because of its ion-exchange porperty, can be directly used as an adsorbent as well as a supporting material for various chelating agents. It is good selectivity, rapid sorption of metal ions, and no swelling. It has good mechanical strength and thermal stability. Chelating silica gel may be prepared by two methods: by chemical immobilization of chelating agent on the surface of silica gel and by adsorption of chelating agent on silica surface.

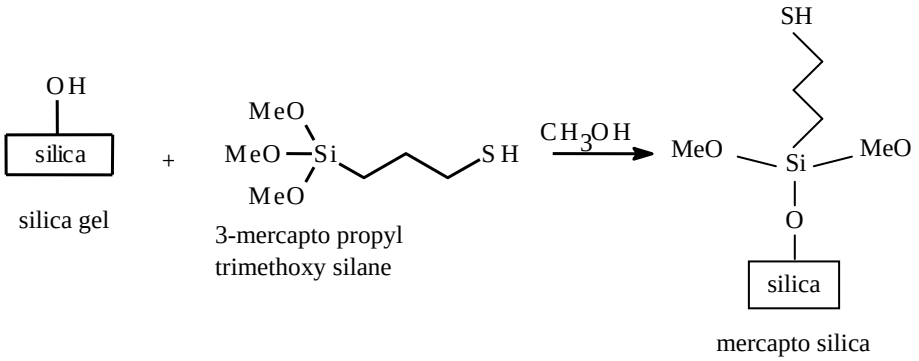

Materials and Methods

All the chemicals used in this work of reagent grade (BDH) were used as received. The apparatus and instruments used were Energy Dispersive X-ray Fluorescence Spectrometer (Shimadzu-EDX-700), FT IR Spectrophotometer (Perkin Elmer 1600 Fourier Transform Infrared Spectrometer with a scan speed of 16 scans/sec from 600 to 4000 cm^{-1}), Magnetic stirrer (Made in UK by Bibby Sterilin LTD, Stone, Staffordshire, England, ST 15 OSA, UK), pH meter (Cole, Parmer), Atomic Absorption Spectrophotometer.

Preparation of Thiol-modified Silica

In this research, thiol-modified silica was used as adsorbent. At first, silica gel was digested with hydrochloric acid (1:1) for one day and washed with distilled water until pH of the filtrate becames neutral. The clean silica gel was dried at 150˚C for one day. The 6 g of dried silica gel, 4 mL of 3-(trimethoxy silyl)-1-propane thiol and 50 mL of methanol were added into a 100 mL round bottom flask and refluxed at 50˚C for 5 hr. The residual solvent was removed by decantation and repeatedly washed with methanol. By air drying, 6.22 g of thiol-modified silica was obtained.

Determination of Thiol Content in Thiol-Modified Silica Sample

The degree of thiolation in the thiol-modified silica was determined by the titrimetric method (Website).

Sorption Studies

In this research, Cu^{2+}, Cd^{2+}, Hg^{2+} and Ag^{+} ions model solutions were used to study the sorption properties of thiol loaded silica gel. Investigations were carried out by changing the parameters such as solution pH, contact time, dosage of thiol loaded silica gel, etc.

Desorption of Metal Ions from Metal-loaded Thiol-Modified Silica Sample

Various concentrations (2, 4, 6 and 8 M) of hydrochloric acid solutions were applied to release the Cu^{2+}, Cd^{2+}, Ag^{+} and Hg^{2+} ions from the metal-loaded thiol-modified silica. The maximum concentration of metal ion was obtained in 8 M HCl solution.

Application of Thiol-Modified Silica Sample for the Removal of Cu, Cd and Hg in Wastewater Sample

Applications of thiol-modified silica were used for the removal of trace metals in wastewater from a paint factory, Bahan Township, Yangon Region, Myanmar.

Results and Discussion

Characterization of Thiol-modified Silica

Characterization of the prepared thiol-modified silica was carried out by using FT IR. In the FT IR data, the functional group Si-SH (2862 cm^{-1}) and propyl group (2913 cm^{-1}) were observed (Nakamoto, 1986).

TG-DTA measurements were carried out on silica gel and thiol-modified silica (Figures 1 and 2). The TG-DTA data were shown in Table 1. The significant differences were observed between the thermograms of silica gel and thiol-modified silica. In the TG-DTA thermogram of silica gel, weight-loss percent was found to be 11.76 %. This is related to the evolution of physically absorbed water and condensation of the silinol groups on the silica surface.

In the case of thiol-modified silica, about 16 % of weight loss was observed and that is 4% higher than silica gel. This is related to mass losses due to combustion of carbon and sulphur in thiol-modified silica. The

exothermic peak at 379˚C is concerned with the combustion of organic matter. The degree of thiolation was calculated to be 24.1%.

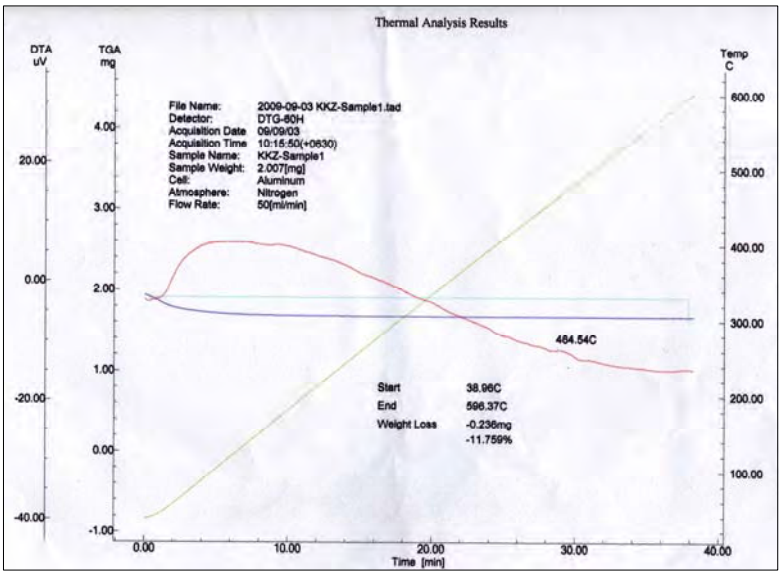

Figure 1 TG-DTA thermogram of silica gel

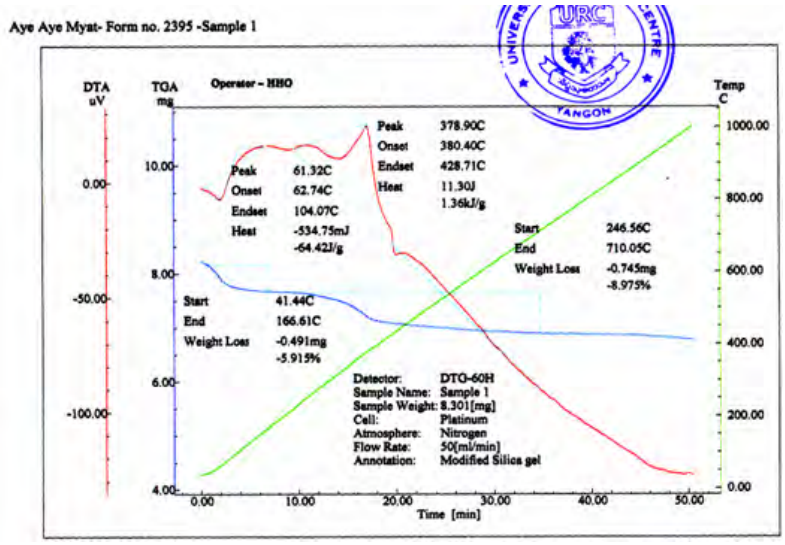

Figure 2 TG-DTA thermogram of thiol-modified silica

Table 1 TG-DTA data of silica gel and thiol-modified silica

No	Decomposition temperature of DTA thermogram (˚C)		Interpretation
	silica gel	thiol-modified silica	
1	40	60	condensation of the silinol group on the surface of the silica
2	-	265	Organic matter losses (due to the combustion of carbon and sulphur in propyl thiol group)
3	-	345	

Sorption of Cu (II), Cd (II), Ag (I) and Hg (II) ions onto Modified Silica

It was observed that 96.85% of Cu (II) ion at pH 7, 92.13% of Cd (II) ion at pH 4, 96.33% of Ag (I) ion at pH 3 and 97.32% of Hg (II) ion at pH 5 were sorbed by 0.3 g of thiol-modified silica (Table 2). Figure 3 indicated the effect of pH on sorption of Cu (II) and Cd (II) ions. Sorption percent of Cu (II) was maximum at pH 7 whereas that of Cd (II) was found at pH 4 (Stavin, 1968).

The effect of contact time on the sorption of Cu (II) and Cd (II) were studied by plotting percent Cu (II) and Cd (II) sorbed as a function of contact time (min). In Table 3 and Figure 4, sorption was rapid during the first 15 min of contact time. Then, Cu (II) sorption increased steadily. After 60 min of contact time, about 96.85% of Cu (II) was sorbed. During 5 min, 54.11% of Cd (II) was sorbed and at 60 min, 92.13% of Cd (II) was sorbed. It was also observed that during 5 min, 84.37% of Ag (I) was sorbed and at 60 min, 97.24% of Ag (I) was sorbed. Moreover 87.05% of Hg (II) was sorbed during 5min, and 98.44% of Hg (II) was sorbed after 60 min. (Table 3).

Table 4 showed the percent Cu (II), Cd (II), Ag (I) and Hg (II) sorbed increased with increase in weight of thiol-modified silica. The effect of dosage on percent Cu (II) and Cd (II) sorbed was shown in Figure 5.

Finally, the sorptions of Cu (II) and Cd (II) ions on thiol-modified silica were studied by construction of the Langmuir and Freundlich adsorption isotherms (Table 5 and Table 6). The Langmuir isotherm

parameters, X_m and K_L of Cu (II) ion were found to be 384.62 mg g^{-1} and 0.252 g L^{-1}, respectively (Table 7 and Figure 6). The Langmuir isotherm parameters (Table 7 and Figure 7) X_m and K_L of Cd (II) ion were found to be 416.66 mg g^{-1} and 0.049 g L^{-1}, respectively.

The Freundlich isotherm parameters K and n of Cu (II) ion were found to be 6.219 x 10^3 and 4.651, respectively (Table 8 and Figure 8). The Freundlich isotherm parameters (Table 8 and Figure 9) K and n of Cd (II) ion were found to be 2.823x 10^3 and 2.777, respectively.

Recovery of metal ions from metal-loaded thiol-modified silica was carried out by using 8 M HCl solution. Table 9 showed the contents of metal ions in filtrate. The metal ions were recovered from the metal-loaded thiol-modified silica. Therefore thiol-modified silica can be used to remove the Cu^{2+}, Cd^{2+}, Ag^{+} and Hg^{2+} ions from wastewater and then preconcentrated into solution of smaller volume.

In this work, application of thiol-modified silica (TMS) was used for the removal and recovery of some heavy metal ions from industrial wastewater. Table 10 showed the sorbed percent of copper, cadmium and mercury by thiol-modified silica. The order of sorbed percent of metal ions are $Hg^{2+} > Cu^{2+} > Cd^{2+}$.

Table 2 Maximum sorption percents of metal ions

No.	metal ions	pH	Maximum sorbed (%)
1	Cu^{2+}	7.0	96.85
2	Cd^{2+}	4.0	92.13
3	Ag^{+}	3.0	96.33
4	Hg^{2+}	5.0	97.32

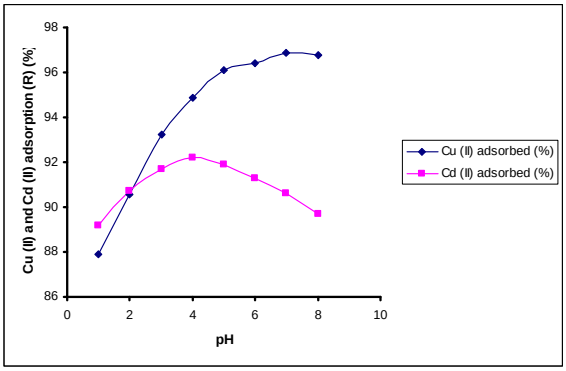

Figure 3 Effect of pH on sorption percent of Cu (II) and Cd (II) ions

Table 3 Effect of contact time on sorption of Cu (II), Cd (II), Ag (I) and Hg (II) ions onto thiol-modified silica

No.	Contact Time (min)	Cu (II) sorbed (%)	Cd (II) sorbed (%)	Ag (I) sorbed (%)	Hg (II) sorbed (%)
1	5	67.90	54.11	84.37	87.05
2	15	76.47	68.53	90.75	92.63
3	30	88.23	81.67	94.76	95.48
4	45	93.50	92.12	95.60	96.80
5	60	96.85	92.13	96.34	97.32
6	90	96.08	92.13	97.24	98.37
7	120	96.43	92.18	97.73	98.44

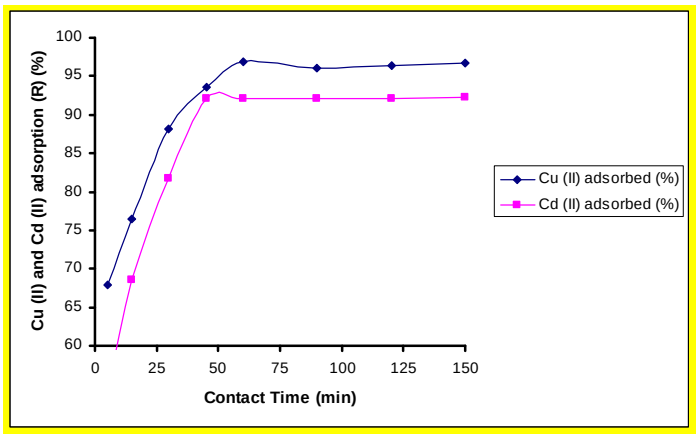

Figure 4 Effect of contact time on sorption percent of Cu(II) and Cd(II) ions

Table 4 Effect of dosage on sorption of Cu (II), Cd (II), Ag (I) and Hg (II) onto thiol-modified silica

No.	Weight of thiol-modified silica (g)	Cu(II) sorbed (%)	Cd(II) sorbed (%)	Ag (I) sorbed (%)	Hg (II) sorbed (%)
1	0.100	85.65	82.95	92.34	92.53
2	0.200	92.82	90.38	96.03	96.41
3	0.300	96.85	92.13	96.33	97.32
4	0.400	96.41	93.30	97.29	98.04
5	0.500	96.58	93.90	98.02	98.29

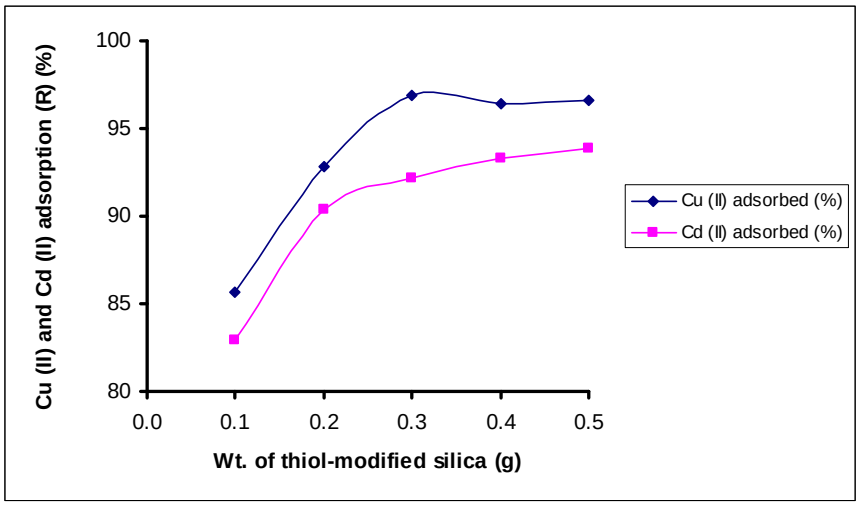

Figure 5 Effect of dosage on percent Cu (II) and Cd (II) ions sorbed

Table 5 Equilibrium data of Cu (II) sorption onto thiol-modified silica

No	C_o (ppm)	C_e (ppm)	q_e (mg g^{-1})	$1/q_e$ (g mg^{-1})	$1/C_e$ (Lmg^{-1})	Log C_e	N (mg L^{-1} g^{-1})	Log N
1	450	80.30	369.70	0.0027	0.0125	1.9047	14788.00	4.1699
2	400	40.51	358.49	0.0028	0.0241	1.6182	14339.60	4.1565
3	350	17.67	332.33	0.0030	0.0566	1.2472	13293.20	4.1236
4	300	12.03	287.97	0.0035	0.0831	1.0803	11518.80	4.0614
5	250	8.74	241.26	0.0041	0.1144	0.9415	9650.40	3.9845
6	200	3.94	196.06	0.0051	0.2538	0.5955	7842.40	3.8944

Table 6 Equilibrium data of Cd (II) sorption onto thiol-modified silica

No	C_o (ppm)	C_e (ppm)	q_e (mgg^{-1})	$1/q_e$ ($g\ mg^{-1}$)	$1/_{Ce}$ ($L\ mg^{-1}$)	Log C_e	N ($mg\ L^{-1}\ g^{-1}$)	Log N
1	450	99.25	350.75	0.0029	0.0101	1.9967	14030.00	4.1471
2	400	71.52	328.48	0.0030	0.0140	1.8544	13139.20	4.1186
3	350	45.25	304.75	0.0033	0.0221	1.6556	12190.00	4.0860
4	300	33.34	266.66	0.0038	0.0300	1.5230	10666.40	4.0280
5	250	29.34	220.66	0.0045	0.0341	1.4675	8826.40	3.9458
6	200	15.50	184.50	0.0054	0.0645	1.1903	7380.00	3.8681

C_o=initial metal ion concentration, C_e=equilibrium metal ion concentration

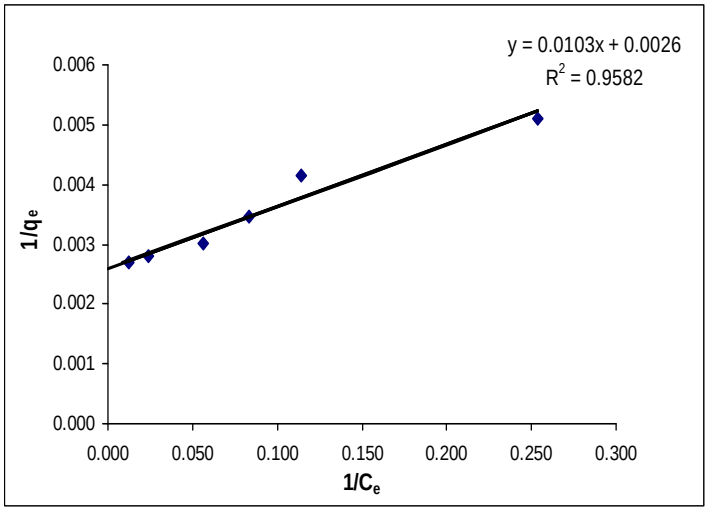

Figure 6 Langmuir isotherm plot for Cu (II) sorption onto thiol-modified silica

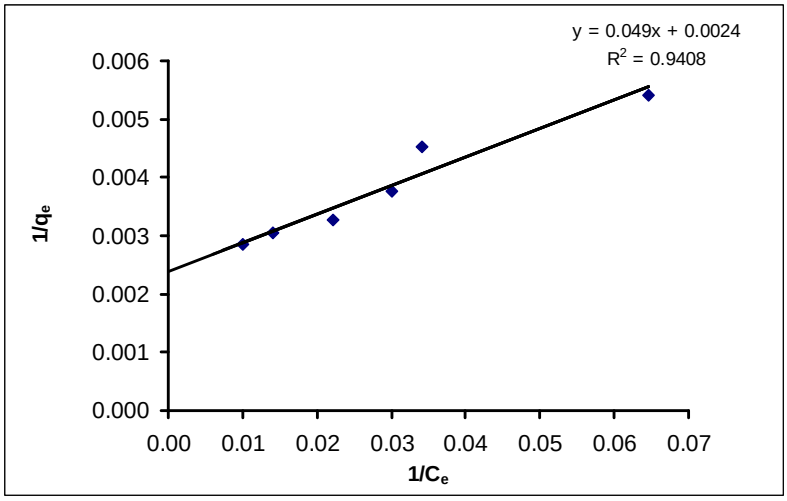

Figure 7 Langmuir isotherm plot for Cd (II) sorption onto thiol-modified silica

Table 7 Langmuir isotherm parameters for Cu (II), Cd (II), Ag (I) and Hg (II) ions

Metal ions	X_m(mg g^{-1})	K_L (g L^{-1})	R^2
Cu^{2+}	384.62	0.252	0.9582
Cd^{2+}	416.67	0.049	0.9410
Ag^{+}	369.86	0.265	0.9851
Hg^{2+}	369.86	0.290	0.9949

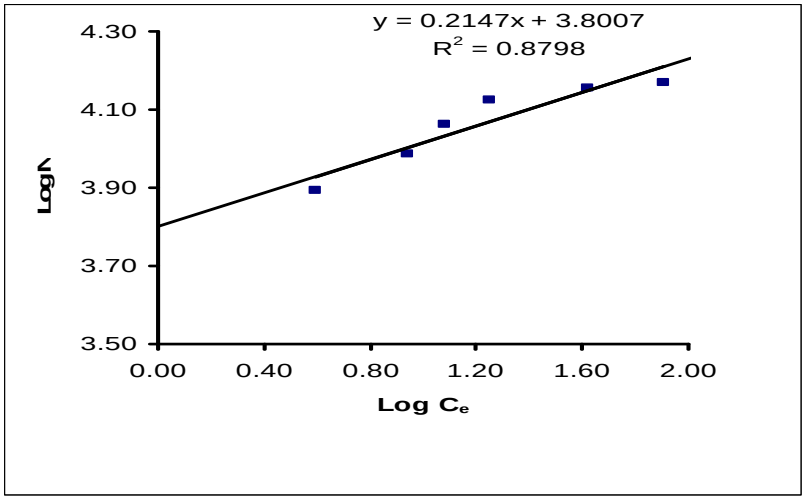

Figure 8 Freundlich isotherm plot for Cu (II) sorption onto thiol-modified silica

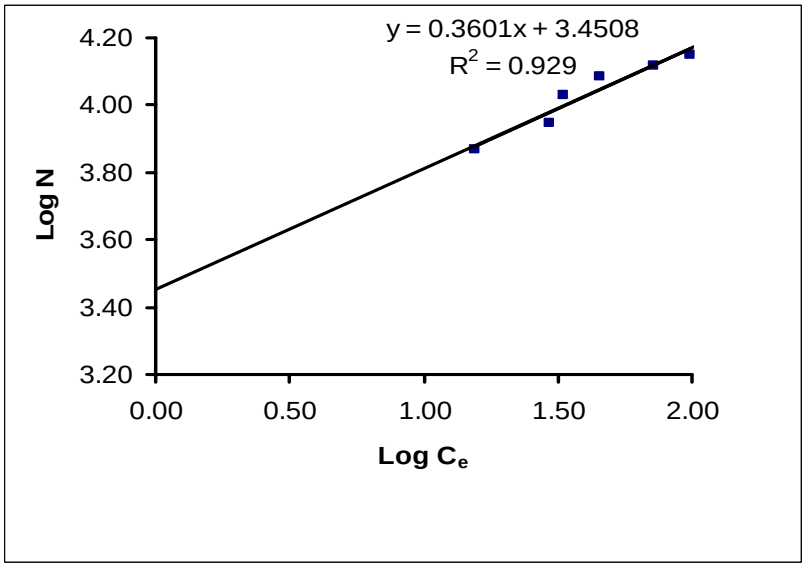

Figure 9 Freundlich isotherm plot for Cd (II) sorption onto thiol-modified silica

Table 8 Freundlich isotherm parameters for Cu(II), Cd(II), Ag (I) and Hg (II) ions

Metal ions	1/n	n	K	R^2
Cu^{2+}	0.215	4.651	$6.219x10^3$	0.8798
Cd^{2+}	0.360	2.777	$2.823x10^3$	0.9290
Ag^{+}	0.175	5.7077	$6.770x10^3$	0.8612
Hg^{2+}	0.180	5.5430	$6.862x10^3$	0.8778

Table 9 Content of metal ion in the filtrate obtained from desorption experiments

No	Metal ions	Concentration in filtrate* (ppm)
1	Cu^{2+}	50.34
2	Cd^{2+}	44.87
3	Ag^{+}	47.21
4	Hg^{2+}	52.36

***** as determined by AAS, metal-loaded thiol-modified silica

Table 10 Sorbed percent of Cu (II) , Cd (II) and Hg (II) from wastewater sample

Metal ions	Before treatment (ppm)	After treatment with TMS* (ppm)	Sorbed by TMS* (%)
Cu^{2+}	2.628	1.070	59.28
Cd^{2+}	0.127	0.068	46.45
Hg^{2+}	0.946	0.341	63.95

* TMS - Thiol-Modified Silica

Conclusion

In this research, thiol-modified silica was prepared by using the reaction between silica gel and 3-trimethoxysilyl-1-propane-thiol ligand. Both FT IR spectra indicated the presence of Si-OH and Si-O-Si groups. The strong evidence for the presence of propyl thiol group in thiol-modified silica was indicated by peaks at 2913 cm^{-1} (propyl group), 2862 cm^{-1} (SH group).

TG-DTA measurement were carried out on silica gel and thiol-modified silica. The significant differences were observed between the thermograms of silica gel and thiol-modified silica. In the TG-DTA thermogram of silica gel, weight-loss percent was found to be 11.76 %. This is related to the evolution of physically absorbed water and condensation of the silinol groups on the silica surface. In the case of thiol-modified silica, about 16 % was observed, that is, 4% higher than silica gel. This is related to mass losses due to combustion of carbon and sulphur in thiol-modified silica.

Similar observations were observed in the DTA thermogram. Exothermic peak at 40˚C was observed for silica gel, whereas exothermic peaks were observed at 60, 265 and 345˚C for thiol-modified silica. The latter two peaks were related with organic matter losses due to the combustion of carbon and sulphur in propyl thiol group. The degree of thiolation in the thiol-modified silica was calculated to be 24.1%.

The optimum pH was observed at pH 7.0 with 96.85% Cu (II) sorbed; at pH 4.0 with 92.13% Cd (II) sorbed; at pH 3.0 with 96.33% Ag (I) sorbed and at pH 5.0 with 97.32% Hg (II) sorbed.

The 96.85% of Cu (II), 92.13% of Cd (II), 96.34% of Ag (I) and 97.32% of Hg (II) at 60 min of contact time were observed.

The sorption isotherm followed the Langmuir equation. The sorption coefficients (K_L) of Cu (II), Cd (II), Ag (I) and Hg (II) were found to be 0.252, 0.049,0.265 and 0.290 g L^{-1}, respectively. The sorption capacities (X_m) of Cu (II), Cd (II), Ag (I) and Hg (II) were found to be 384.62, 416.67, 369.86 and 369.86 mg g^{-1}, respectively.

The sorption isotherm followed the Freundlich equation. The sorption capacities (K) of Cu (II), Cd (II), Ag (I) and Hg (II) were found to be 6.319×10^3, 2.823×10^3, 6.770×10^3 and 6.862×10^3, respectively.

Then sorption intensities (1/n) of Cu (II), Cd (II), Ag (I) and Hg (II) were found to be 0.215, 0.360, 0.175 and 0.180, respectively.

The metal ions were recovered from the metal-loaded thiol-modified silica by using 8 M HCl solution. Therefore thiol-modified silica can be used to remove the Cu^{2+}, Cd^{2+}, Ag^{+} and Hg^{2+} ions from wastewater and then preconcentrated into solution of smaller volume.

In this research, applications of thiol-modified silica was used for the removal of trace metals in wastewater from a paint factory, Bahan Township, Yangon Region, Myanmar. The order of sorbed percent of metal ions are $Hg^{2+} > Cu^{2+} > Cd^{2+}$.

Acknowledgements

The authors would like to express sincere gratitude to Professor Dr Nilar, Head of Department of Chemistry, University of Yangon, for providing all of the departmental facilities and constant encouragement.

References

Budiman, H., Fransiska, S.H.K. and Setiawanp, A.H., (2009), "Preparation of Silica Modified with 2-Mercaptoimidazole and its Sorption Properties of Chromium (III)", *E-Journal of Chemistry*, **6**, 141-150

Nakamoto, K.,(1986), "Infrared and Raman Spectra of Inorganic and Coordination Compounds", John Wiley & Sons Inc., New York, 375-403

Poole, C.F., (2003), "New Trends in Solid-phase Extraction", *Trends Anal. Chem* , **22**, 362-373

Sharma, R.K., (2001), "Design, Synthesis, and Application of Chelation Polymers for Separation and Determination of Trace and Toxic Metal Ions", *Pure Appl. Chem.*, **73**, 181-186

Sharma, R.K., Mittal, S., and Koel, M. (2003), "Analysis of Trace Amounts of Metal Ions Using Silica-Based Chelating Resins: A Green Analytical method", *Anal. Chem.*, **33**, 183-197

Stavin, W., (1968), "Atomic Absorption Spectroscopy", John Wiley & Sons Inc., New York, 183-184

Online Materials

http://jbcs,sbq,org.br/jbcs/JBCS/201995/vol.6/V6n3/v6n3-13,pdf (1995)

Preparation of Banana Oil from By-Products of Alcoholic Fermentation and Fractional Distillation

Malar Yi

Abstract

The methods of recovering fusel oil and isoamyl alcohol from low oil, by-products of alcoholic fermentation and fractional distillation, followed by preparation of banana oil (isoamyl acetate) have been investigated. Five types of low oil containing less than 95 % v/v alcohol were collected from the alcoholic distillery plant no. 2 at Mupon, Mawlamyine. Fusel oil was extracted from low oil which is mainly 55 % alcohol. Isoamyl alcohol was obtained in high yield (54 %) from pure fusel oil. Banana oil was prepared by esterification of recovered isoamyl alcohol and glacial acetic acid in the presence of sulphuric acid catalyst in various reflux times and catalyst amounts. Fractional distillation technique was employed principally at all appropriate stages in regaining alcohol and related compounds. Identification and purity of recovered alcohol and prepared banana oil were examined by infrared spectrophotometric and gas chromatographic methods.

Key words: fusel oil, banana oil, fractional distillation, isoamyl alcohol, isoamyl acetate

Introduction

The nature of by-products of alcoholic fermentation and fractional distillation is complex, and varies sensibly according to the raw materials employed and the methods of fermentation and distillation. They may be classified as (a) higher alcohols (fusel oil), (b) esters, (c) fatty acids, (d) fatty aldehydes and acetal, (e) furfural, (f) terpene, terpene hydrate and ethereal oils and (g) volatile bases (Website 1).

Fusel oil is a by-product of the distillation of alcohol produced by fermentation of molasses, corn, wheat, rye, and potatoes. Fusel in German means inferior liquor. It is a colorless or yellowish oily liquid. It has a disagreeable odor, nauseating taste and considerable toxicity (Website 2). Having 20 cm^3 of fusel oil can cause death and smaller amounts cause such kidney disorders as methemoglobinuria, glycosuria and nephritis. It is used as a solvent in the production of lacquers, enamels, varnishes,

Lecturer, Department of Chemistry, Mawlamyine University

pharmaceutical, resins, oil and waxes.The composition of it depends on the sources of fusel oil (Website 3). It is composed of approximately 80% amyl alcohols, 15% butyl alcohols and 5% other alcohols.

Isoamyl alcohol is used as a solvent for fats, resins, alkaloids, etc. It is used in the manufacture of isoamyl compounds, isovaleric acid, mercury fulminate, pyroxylin, artificial silk, lacquers and smokeless powders. It is also used for dehydrating celloidin solutions and determining fat in milk (Merck, 2001).

Isoamyl acetate or isopentyl acetate known as banana oil (Website 4), is prepared by the acid catalysed reaction (Fischer esterification) between isoamyl alcohol and glacial acetic acid as shown in the reaction below.

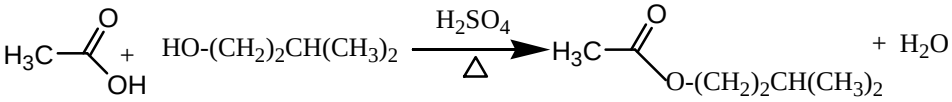

Acetic acid Isoamyl alcohol Isoamyl acetate

It is used in soft drinks because of having apple flavour and banana odour. It is used as a solvent for lacquers, bronzing mixtures, metallic paints, nitrocellulose, and celluloid cements. It is used as an extractant in penicillin manufacture, and in the production of photographic film, leather polishers, dry cleaning preparations, and flavouring agents and perfumes (Website 5).

Materials and Methods

Samples Collection

Five types of low oil (65% alcohol, 55% alcohol, 50% alcohol, 46% alcohol and 36% alcohol v/v) were collected from the alcoholic distillery plant no. 2 at Mupon, Mawlamyine, Myanmar.Low oil was obtained from the fraction, where the alcohol concentration is less than 95 % v/v. This fraction was collected as the distillate when the under proof spirit containing less than 57 % v/v alcohol was subjected to fractional distillation using over proof bubble cap column (Pe Thein, 1982).

Recovery of Crude Fusel Oil from Low Oil

In order to recover alcohol and fusel oil, five types of low oil were separately subjected to fractional distillation. 1435 cm^3 of low oil (65 % alcohol, sp. gr. 0.9000), was added to a two litre capacity round-bottomed

flask followed by a few pieces of pumice stones. Fractional distillation was performed till the residue indicated 0 % alcohol concentration. The distillate so obtained was distilled again until the fusel oil separated out from the residue as white oily liquid. Then the mixture containing fusel oil and residue was transferred to a separating funnel and shaken 20 times. When the two layers were distinctly separated, the lower layer was run off and the upper layer containing fusel oil was collected. Distillation was repeated till no fusel oil separated out from the residue. Similarly, low oils (55 % alcohol, sp. gr. 0.922); (50 % alcohol, sp. gr. 0930); (46 % alcohol, sp. gr. 0.938) and (36 % alcohol, sp. gr. 0.950) were fractionally distilled. The results were listed in Table 1. Isoamyl alcohol was obtained from crude fusel oil and pure fusel oil.

Isolation of Isoamyl Alcohol from Crude Fusel Oil

Crude fusel oil (sp. gr. 0.839, pH 4.1) (300 cm^3)was transferred to a 500 mL round-bottomed flask. After adding a few pieces of pumice stones, fractional distillation was carried out. The fraction boiling between 128º C and 132º C was collected and the specific gravity was determined by using a hydrometer. The results were depicted in Table 2.

Isolation of Isoamyl Alcohol from Pure Fusel Oil

Sodium chloride (35.7 g) was added to a 100 cm^3 volumetric flask containing a moderate amount of distilled water. The contents were shaken and distilled water was added to the mark. The saturated sodium chloride solution so obtained was added to the crude fusel oil (100 cm^3) in a separating funnel. The mixture was shaken for a few minutes and the separated upper layer was collected. The yield of pure fusel oil was 85 cm^3.

Pure fusel oil (sp. gr. 0.817, pH 4.45) (255 cm^3) which was obtained from 300 cm^3 of crude fusel oil, separated from the saturated sodium chloride solution, was fractionally distilled as described above. The results were shown in Table 2.

Preparation of Isoamyl Acetate

Isoamyl acetate was prepared by reacting recovered isoamyl alcohol with glacial acetic acid, using concentrated sulphuric acid as a catalyst. The reaction was carried out by variation in reaction time and the amount of sulphuric acid. 10 % v/v excess of recovered isoamyl alcohol (100 cm^3) and glacial acetic acid (47.4 cm^3) in the mole ratio of 1:1 were added to a 250 cm^3 round-bottomed flask. Then concentrated suphuric acid (8 cm^3)

in constant amount as a catalyst was added. The mixture was refluxed for 15 min and cooled to room temperature.. If the two layers were developed, the upper layer was collected. It was then transferred to a separating funnel and treated with saturated sodium chloride solution in equal volumes. The two layers were developed and the upper layer was collected. It was then neutralized with sodium hydroxide solution (0.5 M) by using phenolphthalein indicator. The two layers were developed and the lower layer was run off and the upper layer was transferred to a 250 cm^3 round-bottomed flask and distilled fractionally using a fractionating column. The three fractions were collected in various ranges of temperature such as 30ºC to 120ºC, 120ºC to 137ºC and 137ºC to 142ºC.Similarly, the reactions were carried out by variation in reflux time of 30 min, 60 min, 120 min and 180 min. The fractions were collected respectively.The results were tabulated (Table 3). Again, the reactions were carried out by variation in sulphuric acid amount of 0 cm^3, 1 cm^3, 2 cm^3, 4 cm^3, 6 cm^3, 8 cm^3, and 10 cm^3 in constant reflux time (60 min). The fractions were collected respectively. The results were shown in Table 4.

Identification of Recovered Isoamyl Alcohol and Prepared Isoamyl Acetate by Infrared Spectrophotometric and Gas Chromatographic Methods

A small drop of standard isoamyl alcohol was placed on a NaCl plate and covered with a second NaCl plate which was pressed to spread as a thin film. The plates were then placed in the holder of the beam path. The IR spectrum of the compound was recorded by Recording Infrared Spectrophotometer, Shimadzu, Japan.

Similarly, the IR spectra of the compounds, viz, standard isoamyl acetate, recovered isoamyl alcohol and prepared isoamyl acetate were taken as mentioned above.

The gas chromatograms of standard mixture, crude fusel oil, pure fusel oil, standard isoamyl alcohol, recovered isoamyl alcohol, standard isoamyl acetate and prepared isoamyl acetate were successively taken by 6C-9, gas chromatography instrument, Shimadzu, Japan.

Results and Discussion

Fusel oil in crude alcohol separates as an oil on dilution with water because amyl alcohols, unlike the lower members of the series, are only sparingly soluble in water (Amerine, 1980). Data for the recovery of fusel oil from low oils (65 %, 50 %, 55 %, 46 % and 36 % alcohol) are shown in Table 1. The concentrations of fusel oil were determined to be (0.65 %, 6.27 %, 5.4 %, 5.02 % and 2.16 % v/v) in (65 % alcohol, 55 % alcohol, 50 % alcohol, 46 % alcohol and 36 % alcohol) respectively. It can be inferred that among the five types of low oil, fusel oil was obtained in good yield (6.27 %) from low oil which contained moderately high concentration of alcohol (55 % alcohol). It was also observed that the maximum separation of fusel oil from alcohol solution was mostly from 86–90 % alcohol solution at the optimum temperature range of 85–87.5ºC.

Table 1. Fractional distillation of low oil (65 %, 55 %, 50 %, 46 % and 36 % alcohol)

Low oil 1435 cm^3	First distillation				Second Distillation				Third distillation				Fourth distillation				Fifth distillation				Total F cm^3	Yield %
	D		T °C	F cm^3	D		T °C	F cm^3	D		T °C	F cm^3	D		T °C	F cm^3	D		T °C	F cm^3		
	A %	V cm^3			A %	V cm^3			A %	V cm^3			A %	V cm^3			A %	V cm^3				
65% alcohol Sp. gr. 0.900	85.1	1078	82	0	91	966	85	1.3	92	917	85.5	5	93.6	891	85	3	-	-	-	-	9.3	0.65
55% alcohol Sp. gr. 0.922	81	885	85-96	0	87	784	87	30	90	726	86.5	36	91	679	85	19	93.2	658	85.6	5	90	6.27
50% alcohol Sp. gr. 0.930	80	861	96	0	87	724	86	27.5	90	663	86.7	28	91	626	86	12	92.1	627	86	10	77.5	5.40
46% alcohol Sp. gr. 0.938	79.5	782	85-96	0	88	643	87	25.5	90	593	86.5	24	90.1	557	86	10.5	92.2	552	85	12	72	5.02
36% alcohol Sp. gr. 0.950	79	630	84-95	0	88	543	85	1	91	499	86.5	16	91	499	86	9	92	475	85	5	31	2.16

D Distillate, A Alcohol, V Volume, F Fusel Oil

Results for the isolation of isoamyl alcohol from fusel oil can be seen in Table 2. From this table it can be observed significantly that isoamyl alcohol was recovered in good yield from pure fusel oil than from crude fusel oil. This value is consistent with published result (Alexander, 1978).

Table 2. Comparison between crude fusel oil and pure fusel oil in terms of boiling fraction range

Boiling fraction range	300 cm^3 of crude fusel oil with sp. gr. 0.839 and pH 4.1		255 cm^3 of pure fusel oil with sp. gr. 0.817 and pH 4.45		Specific gravity
	cm^3	%	cm^3	%	
30°C – 128°C	144	48	82	27.33	-
128°C-132°C Isoamyl alcohol	145	48.33	162	54	0.805
Above 132°C Residue	8	5.33	8	5.33	-

The yields of isoamyl acetate in various reflux times and various amounts of H_2SO_4 catalyst were described in Tables 3 and 4.

Table 3. Yield of isoamyl acetate in various reflux time

Sr. no.	H_2SO_4 (cm^3)	Reflux time (min)	Separate lower layer (cm^3)	30-120ºC (cm^3)	120-137ºC (cm^3)	137-142ºC (cm^3)	Yield %
1	8	15	21	16.5	26	96	76.86
2	8	30	21	15	19	104.5	83.66
3	8	60	22	12	19	107.5	86.08
4	8	120	22	13	20	105.5	84.47
5	8	180	22	14	20.5	104	83.26

Table 4. Yield of isoamyl acetate in various amount of sulphuric acid

Sr. no.	H_2SO_4 (cm^3)	Reflux time (min)	Separate lower layer (cm^3)	30-120ºC (cm^3)	120-37ºC (cm^3)	137-142ºC (cm^3)	Yield %
1	0	60	-	7.5	76	2	1.6
2	1	60	6.5	20.5	51.3	51.5	41.2
3	2	60	12	18.0	26.6	75	60.03
4	4	60	15	14.0	14.1	98.5	78.8
5	6	60	17	12.0	11.6	104.0	83.26
6	8	60	22	12.0	4.6	107.5	86.08
7	10	60	23	12.0	8.6	105.0	84.07

From the above data, it can be concluded that the yield of isoamyl acetate was the highest (86.08 %) by using sulphuric acid (8 cm^3) in 60 minutes of reflux time when 10 % excess of isoamyl alcohol (100 cm^3) was esterified with glacial acetic acid (47.4 cm^3) in the molar ratio of 1:1.

Identification of Recovered Isoamyl Alcohol and Prepared Isoamyl Acetate by Infrared Spectrophotometric and Gas Chromatographic Methods

Different types of chemical bonds absorb radiation of different frequencies or wavelengths. Certain types of bonds are known to be present in the molecule by looking at the absorption bands at characteristic frequencies(Malcoln,1985).

The Infrared Spectra of recovered isoamyl alcohol and prepared isoamyl acetate were indicated in Figures 1 and 2.

Figure 1. IR spectrum of recovered isoamyl alcohol

According to IR spectrum of recovered isoamylalcohol, it could be assigned from the absorption bands as 3300 cm^{-1}(ν_{O-H}) , 2950 cm^{-1}($\nu_{asymC-H)}$, 2875 cm^{-1} ($\nu_{symC-H)}$, 1460 cm^{-1} (δ_{C-H}), 1380 and 1364 cm^{-1} for bending of gem dimethyl groups, 1115 and 1050 cm^{-1} for C-O stretching and 963cm^{-1} appeared due to CH_2 bending.

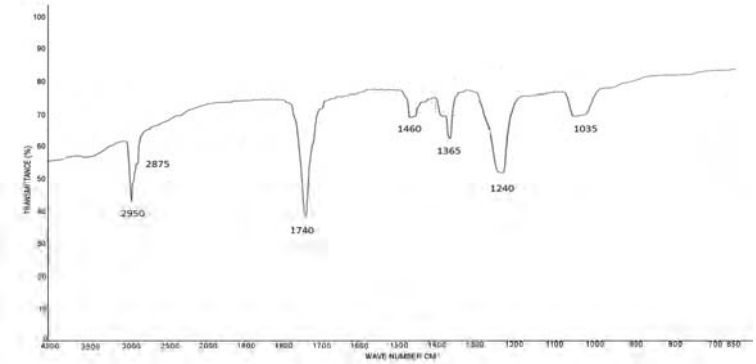

Figure 2. IR spectrum of prepared isoamyl acetate

From the IR spectrum of prepared isoamyl acetate, the absorption bands occurred at wave numbers of 2950 and 2875 cm^{-1} appeared due to asymmetric and symmetric C-Hstretching vibrations, 1740cm^{-1} corresponding to C = O stretching vibration, 1460 and 1365 cm^{-1} due to C-H bending, 1240 and 1035 cm^{-1} attributed to C-O-C and C-O stretching vibrations.

By comparing the infrared spectra of isolated samples with those of standard samples respectively taken under the same conditions, it was found that characteristic absorption bands were identical. Therefore, it can be inferred that the samples assigned by spectra shown in Figures 1 and 2 are authentically isoamyl alcohol and isoamyl acetate respectively.

The compositions of crude and pure fusel oil comparing with standard mixture were investigated by gas chromatographic technique (chromatograms 1 to 3, and Tables 5 and 6).

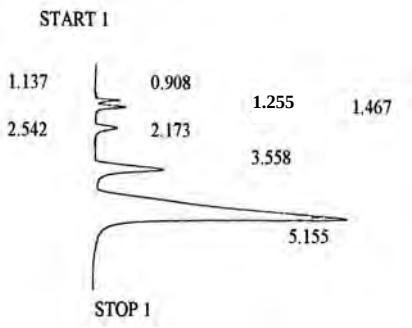

PKNO	TIME	AREA	IDNO	CONC	NAME
1	0.908	34		0.0035	
2	1.137	2014		0.2099	
3	1.255	13747	1	1.4321	ETAC
4	1.467	24301	2	2.5316	IPOH
5	2.173	27411	3	2.5856	NPOH
6	2.542	131		0.0136	
7	3.558	120143	4	12.5161	NBOH
8	5.155	772126	5	80.4376	AMOH
	TOTAL	959907		100	

PKNO	NAME	TIME	FACTOR	CONC
1	ETAC	1.25	1.40976	0.01938
2	IPOH	1.46	1.34152	0.0326
3	NPOH	2.17	8.39081	0.023
4	NBOH	3.55	9.88822	0.1188
5	AMOH	5.15	7.90807	0.6106

Chromatogram 1. Standard mixture

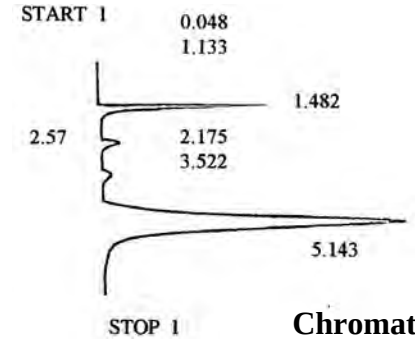

PKNO	TIME	AREA	IDNO	CONC	NAME
1	0.048	13			
2	1.138	2721			
3	1.482	98199	2	0.1317	IPOH
4	2.175	2748	3	0.0023	NPOH
5	2.57	22446			
6	3.522	18009	4	0.0178	NBOH
7	5.143	685394	5	0.542	AMOH
	TOTAL	829529		0.6939	

Chromatogram 2. Crude fusel oil

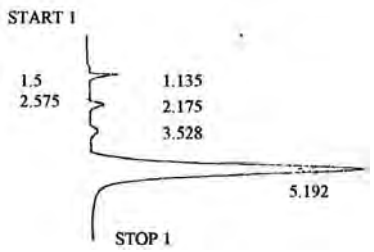

PKNO	TIME	AREA	IDNO	CONC	NAME
1	1.135	1948			
2	1.5	23716	2	0.0318	IPOH
3	2.175	2655	3	0.0022	NPOH
4	2.575	22561			
5	3.528	19832	4	0.0196	NBOH
6	5.192	827920	5	0.6547	AMOH
	TOTAL	898632		0.7084	

Chromatogram 3. Pure fusel oil

Table 5. The composition of crude fusel oil (Chromatogram 2)

Sr. No.	Components	% w/v	% v/v
1	isopropyl alcohol	13.17	16.76
2	n-propyl alcohol	0.23	0.28
3	n-butyl alcohol	1.78	2.20
4	isoamyl alcohol	54.2	66.98

Table 6. The composition of pure fusel oil (Chromatogram 3)

Sr. No.	Components	% w/v	% v/v
1	isopropyl alcohol	3.18	4.03
2	n-propyl alcohol	0.22	0.27
3	n-butyl alcohol	1.91	2.42
4	isoamyl alcohol	65.47	80.41

In the present case, it is observed that the presence of isoamyl alcohol (80.41 % v/v) in pure fusel oil fraction is higher than the amount of isoamyl alcohol (66.98 % v/v) in crude fusel oil. This observation illustrates the validity of the phenomenon of salting out of organic compounds, i.e., the decrease of solubility of organic compounds in water when the solution is saturated with an inorganic compound. In addition, the composition of pure fusel oil is consistent with the published data (fusel oil compositions: 80 % amyl alcohols, 15 % butanols and 5 % other alcohols).

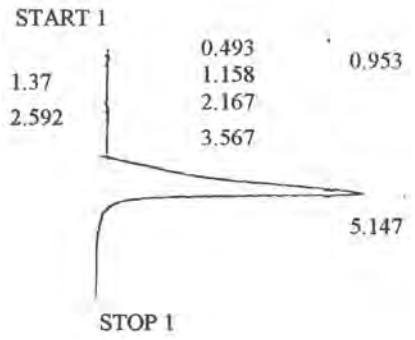

PKNO	TIME	AREA	IDNO	CONC	NAME
1	0.493	624	1	0.1054	A
2	0.953	60	2	0.0101	B
3	1.158	122	3	0.0207	C
4	1.37	2430	4	0.4103	D
5	2.167	68	5	0.0115	E
6	2.592	5199	6	0.8777	F
7	3.567	1168	7	0.1973	G
8	5.147	182626	8	98.367	IAOH
	TOTAL	592298		100	

NAME	TIME	FACTOR	CONC
A	0.49	0.00016889	0.1054
B	0.95	0.000168736	0.0101
C	1.15	0.000169145	0.0207
D	1.37	0.000168821	0.4103
E	2.16	0.000168415	0.0115
F	2.59	0.000168832	0.8777
G	3.56	0.000168852	0.1973
IAOH	5.14	0.000168834	98.367

Chromatogram 4. Standard isoamyl alcohol

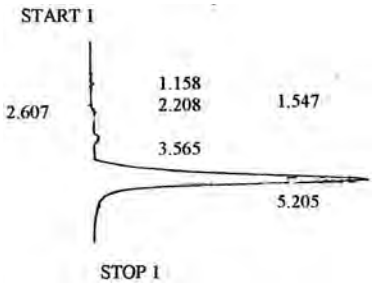

TIME	AREA	IDNO	CONC	NAME
1.158	79	3	0.0113	C
1.574	191			
2.208	376	5	0.0532	E
2.607	7005	6	0.9947	F
3.565	12677	7	1.8003	G
5.205	684114	8	97.1405	IAOH
TOTAL	7044443		100	

Chromatogram 5. Recovered isoamyl alcohol

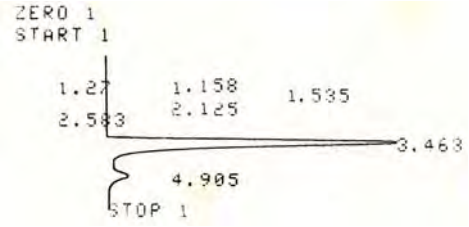

PKNO	TIME	AREA	IDNO	CONC	NAME
1	1.158	66	1		A
2	1.27	981			
3	1.535	147			
4	2.125	511	3		C
5	2.583	2908			
6	3.463	532448	5		ISAA
7	4.905	61204	6		E
	TOTAL	598266			

IDNO	NAME	TIME	FACTOR	CONC
1	A	1.15	0.00200738	0.1334
2	B	1.85	0	0.1635
3	C	2.1 0	0.0146575	7.4924
4	D	2.73	0	1.3235
5	ISAA	3.44	0.000156074	83.1012
6	E	4.88	0.000127214	7.786

Chromatogram 6. Standard isoamyl acetate

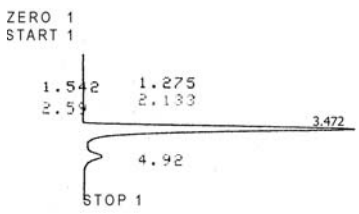

PKNO	TIME	AREA	IDNO	CONC	NAME
1	1.275	1025			
2	1.542	152			
3	2.133	539	3	7.515	C
4	2.59	3106	4		D
5	3.472	567903	5	84.3476	ISAA
6	4.92	67218	6	8.1375	E
	TOTAL	639943		100	

Chromatogram 7. Prepared isoamyl acetate

Examination of the chromatograms 4 and 5 indicated that the purity of the standard isoamyl alcohol was 98.367 % and the purity of the recovered isoamyl alcohol was 97.14 %. In addition, it was found that the purity of the standard isoamyl acetate was 83.10 % from analyzing chromatogram 6 and the purity of prepared isoamyl acetate was found to be 84.3476 % from the analysis of chromatogram 7. Therefore, it could be inferred that the purity of prepared isoamyl acetate was comparable to that of standard isoamyl acetate.

Conclusion

From the present research work, 10.0134 gallons of fusel oil can be obtained from 180 gallons of low oil.The extracted amount of isoamyl alcohol from pure fusel oil is 54 % v/v.The yield of isoamyl alcohol 66.98 % v/v is the highest, followed by isopropyl alcohol (16.76 %), n-butyl alcohol (2.20 %) and n-propyl alcohol (0.28 %) in the crude fusel oil fraction.By treating crude fusel oil with saturated sodium chloride solution followed by fractional distillation of the organic layer, isoamyl alcohol was quantitatively extracted (approx: 80.65 % v/v) from crude fusel oil.In the pure fusel oil fraction, the concentration of isoamyl alcohol (80.41 % v/v) is the highest and is much higher than the amount of isoamyl alcohol (66.98 %) present in the crude fusel oil fraction.The yield of isoamyl acetate is 86.08 % by using sulphuric acid as catalyst (8 cm^3) in 60 minutes of reflux time when 10 % volume excess of recovered isoamyl alcohol (100 cm^3) is esterified with glacial acetic acid (47.4 cm^3) in the molar ratio of 1:1. The recovered isoamyl alcohol and prepared isoamyl acetate are proved to be authentic by IR spectrophotometric method. The purity of the recovered isoamyl alcohol and the prepared isoamyl acetate are found to be 97.14 % and 84.35 % respectively. Thus, the chemical compounds are graded as high quality.

Acknowledgements

The author would like to express sincere thanks to Rector Dr Htay Aung, Professor and Head Dr Than Than Htay and Professor Dr Hnin Hnin Aye, Department of Chemistry, Mawlamyine University for giving the opportunity to present this paper. Special thanks are due to Dr Maung Maung Htay, Retired Professor and Head, Department of Chemistry, University of Yangon for his numerous invaluable suggestions in this research work. Sincere thanks are extended to Dr Than Than Htay for her kind help, reviewing and editing this manuscript enthusiastically.

References

Alexander, M.,(1978), "Industrial Organic Chemistry",1st edition, Mc Graw Hill Ltd., New York, 167

Amerine, A.M.,(1980),"Methods for Analysis of Wines", John Wiley and Sons, New York, 73

Malcoln, D.H.,(1985), "Success in Organic Chemistry", 1st edition, John Murray Ltd., London, 24-27

Merck, I., (2001), "An Encyclopedia of Chemicals, Drugs" , 13 rd edition, Merck & Co., Inc, USA, 588

Pe Thein, (1982), " Quality Control of Finished Products", Myanmar Food Enterprise, Ministry of Industry", 2

Online Materials

1. Kuhn, E.R., (2003), " Complete Separation and Quantitation of Fusel Oil by GC" (www.agilent.com)
2. Hazelwood, L.A., (2008), " The Ehrlich Pathway for Fusel Alcohol Production" (www.pubmedcentral.gov)
3. Ceylan,K., (1998), " Potential Utilization of Fusel Oil" (www.tubitak.gov)
4. Williamson, K.L.,(1999), " Preparation of Banana Oil" (www.thepurple.com)
5. Fahlbusch, K.G., (2002), " Flavors and Fragrances " (www.en.wikipedia.org)

Structural Elucidation of an Unknown Bioactive Organic Compound Isolated from Myanmar Traditional Indigenous Medicinal Plant *Leonotis nepetifolia* (L.) R.Br. (Ame da zoe pin)

Aye Aye Maw

Abstract

Myanmar indigenous medicinal plant *Leonotis nepetifolia* (L.) R.Br. (Ame da zoe pin) was chemically analysed in this research work. A pure unknown bioactive organic compound could be isolated from ethyl acetate extract of *Leonotis nepetifolia* (L.) R.Br. by Thin Layer and Column Chromatographic separation techniques. The pure pale green crystal (18.5 mg) was obtained and its melting point is 164-166 °C. Total yield percent of this compound was 0.74% based upon the ethyl acetate extract. The antimicrobial activity of pure compound was also tested by agar well diffusion method on six organisms and it gave high activity on *Candida albicans* and medium activity on *Bacillus pumalis*. By using some spectroscopic techniques, the molecular formula of pure unknown bioactive organic compound could be determined as $C_{23}H_{34}N_2O_3$ and the complete structure of this compound could be elucidated. This elucidated structure was confirmed and the unknown compound was named as 2_a-S, 4-S, 5_a-S, 8_a-S, 10-S, 12_a-R-4,10-dihydroxy- 2_a, 5, 5, 9, 9,12_a-hexamethyl -2_a, 2, 3, 4, 5, 5_a, 8_a, 9, 10, 11, 12, 12_a-dodecahydro-imidazo-bis [1,5_a] indole -7-one.

Key words: *Leonotis nepetifolia* (L.) R.Br., antimicrobial activity, spectroscopic techniques,

Introduction

This research has been done on the interesting upgrade level of Myanmar medicine isolated from the Myanmar indigenous medicinal plants. In this research work, indigenous medicinal plant, *Leonotis nepetifolia* (L.) R.Br. which is locally known as Ame da zoe pin was studied chemically(Hooker, 1885). This plant is one of the well-known indigenous medicinal plants and widely distributed in tropical countries, such as Myanmar, India, Thailand, Malaysia, Southern Africa and America, etc. (Lemmens and Bogor, 2003). In Myanmar, this plant is

Lecturer, Dr, Department of Chemistry, Magway University

found in road-sides of tropical area, fallow fields and along ponds and lakes.

Preliminary phytochemical screening and antimicrobial activity of crude extract of Ame da zoe pin were carried out. As an experimental work, a pure unknown bioactive organic compound could be isolated from this plant by using sophisticated separation techniques such as Thin Layer and Column Chromatographic methods. Its structure could be elucidated by using advanced spectroscopic methods, such as FT IR, ^{1}H NMR (500 MHz), ^{13}C NMR (125 MHz), ^{1}H-^{1}H DQF-COSY, HMQC, HMBC and EI-MS.

Botanical Description and Medicinal Uses

Family	:	Labiatae (Lamiaceae)
Botanical Name	:	*Leonotis nepetifolia* (L.) R.Br.
Local Name	:	Ame da zoe pin
English Name	:	Lion's ear
Medicinal Uses	:	Rheumatism, Rickets, Taenifuge, Piles, Swelling Gastro-intestinal troubles, Skin infections, Diuretic, Dysmenorrhoea
		(Ah Shin Nagathein, 1976)

Materials and Methods

Commercial and analytical grade reagents from BDH, Merck were used in this research work. Analytical and preparative Thin Layer Chromatography was performed by using precoated silica gel plates

(Merck. Co. Inc, Kiesel gel 60 F_{254}). Silica gel (70-230 mesch ASTM) was applied for Column Chromatography.

Sample Collection

The plants to be analysed were collected from Nga-Phe area, Minbu Township, Magway Region. The collected samples were cut into small pieces and were dried in the shade. Then the raw materials were stored in the well-stoppered bottle and used throughout the experiment.

These plant materials were screened and identified by authorized Botanist from Department of Botany, University of Mandalay.

Preliminary Phytochemical Examination

The preliminary phytochemical tests (Harborne, 1993) were done on the plant extract to determine the presence or absence of organic constituents in it.

Determination of Antimicrobial Activities on Crude Extract of *Leonotis nepetifolia* (L.)R.Br.

The plant (Ame da zoe pin) was extracted in various solvent systems and then they were sent to DCPT (Development Center for Pharmaceutical Technology), Insein, Yangon, for the measurement of antimicrobial activities. Antimicrobial activities of crude extracts of this plant were determined by using agar well diffusion method on six organisms, such as, *Bacillus subtilis, Staphylococcus aureus, Pseudomonas aeruginosa, Bacillus pumalis, Candida albicans* and *Mycobacterium* species.

Extraction and Isolation of Compound

Preparation of Crude Extract

The air dried sample of Ame da zoe pin (374) g was percolated with 95% ethanol (3 L) for two months. Percolated solution was filtered and concentrated by using rotary evaporator. The residue was dissolved in 350 ml of ethyl acetate and ethyl acetate extract was washed with 0.1 M HCl and 0.1 M NaOH Solution to remove acid soluble and alkali soluble materials. And then, it was washed with distilled water for two times. The obtained neutral ethyl acetate extracted solution was dried with anhydrous sodium sulphate to remove water moisture. Concentrated ethyl acetate crude extract (2.5) g was obtained.

Isolation of Pure Unknown Compound

Ethyl acetate crude extract (2.5 g) was chromatographed on a silica gel (70-230 Mesh) column, using n-Hexane and ethyl acetate as eluent with various ratios from nonpolar to polar. Total 155 fractions were obtained. Each and every fractions were checked by TLC and UV detector. The fractions with the same R_f value were combined and seven combined fractions were obtained. The major combined fraction (D) was further rechromatographed by using silica gel, EtOAc and n-Hexane with suitable solvent system. All fractions were again checked by TLC. The fractions which shown only one spot on TLC with the same R_f value were combined and the combined fraction was recrystallized by using n-hexane and ethyl acetate. Total yield percent of pure compound is 0.74 % based upon the ethyl acetate crude extract. Its melting point was measured applying Gallenkamp melting point apparatus.

Antimicrobial Activities of Pure Unknown Compound

The antimicrobial activities of pure unknown compound were rechecked by agar well diffusion method on six organisms.

Table-1. Antimicrobial Activities of Pure Unknown Compound

Sample	Microorganisms					
	A	B	C	D	E	F
Pure compound	-	-	-	10mm (++)	15mm (+++)	-

Agar well-5mm:
5mm ~ 9mm (+); 10mm ~ 14mm (++);15mm ~ above (+++)
Microorganisms

A= *Bacillus subtilis;* B = *Staphylococcus aureus;* C = *Pseudomonas aeruginosa;* D = *Bacillus pumalis;* E = *Candida albicans;* F=*E. Coli*

Spectroscopic Studies on Isolated Pure Bioactive Compound

Analysis of pure bioactive compound was done by FT IR spectrophotometer (Hyper-IR), Shimadzu), Mass spectrometer (JEOL, JMS 500 MHz) and ^{13}C Nuclear Magnetic Resonance (JEOL, 125 MHz).

Results and Discussion

The results of phytochemical tests show that alkaloid, sugar, glycoside, lipophilic and polyphenol are present in this plant. From the results of antimicrobial activity test, EtOAc extract of *Leonotis nepetifolia* (L.) R.Br. (Ame da zoe pin) responds high activity on five tested rganisms, but medium activity on *Pseudomonas aeruginosa*. The isolated pure organic compound has high activity on *Candida albican* and medium activity on *Bacillus pumalis.*

Molecular Formula Determination

The molecular formula of isolated pure organic compound could be determined by some spectroscopic methods such as FT TR, ^{1}HNMR (500 MHz), ^{13}C NMR (125 MHz), DEPT, HMQC and EI-MS, respectively.

According to FT IR spectrum (Figure 1), -OH group, sp^2 hydrocarbons, sp^3 hydrocarbons, C=O group, C-N group and cis or Z alkenic group were observed. (Silverstein *et al.*, 2005)

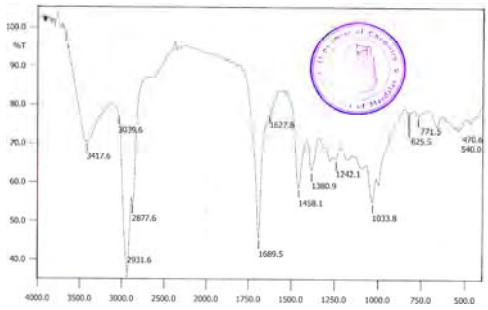

Figure 1. FT IR Spectrum of an unknown compound

According to ^{1}H NMR (500 MHz) spectrum (Figure 2), this compound contains 34 protons (Nelson,2003; Claridge, 1993).

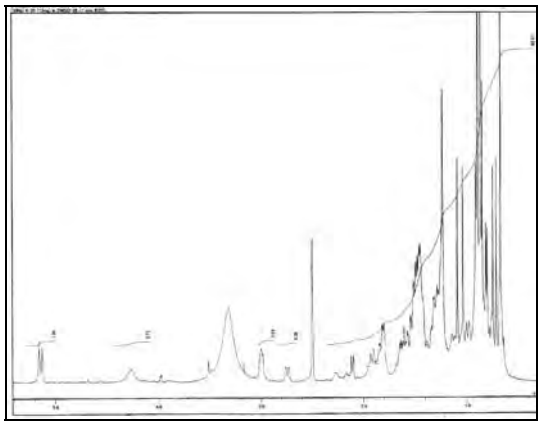

Figure 2. ^{1}H NMR (500 MHz) spectrum

The ^{13}C NMR (125 MHz) spectrum (Figure 3) indicates the total number of carbons (23 carbons) in this compound.

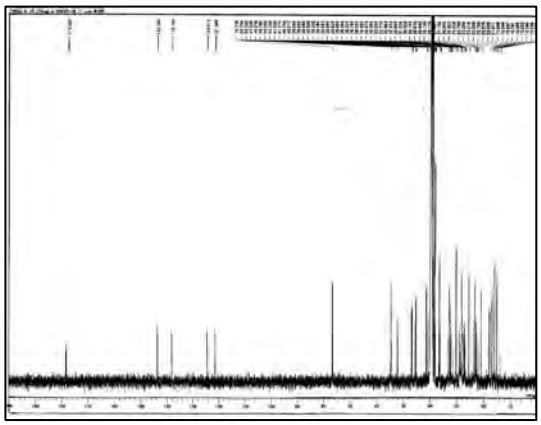

Figure 3. ^{13}C NMR (125 MHz) spectrum

The HMQC spectrum (Figure 4) gives rise to the directly attached proton-carbon coupling which produces varieties of hydrocarbons.

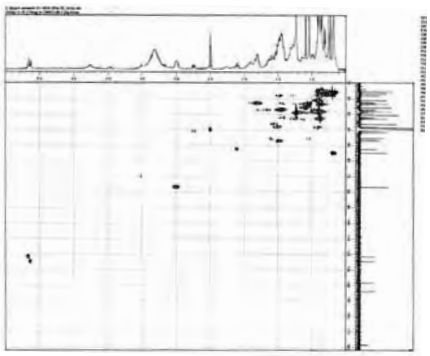

Figure 4. HMQC spectrum of an unknown compound

The DEPT spectrum (Figure 5) also implies the number of protons, carbons and the kinds of hydrocarbons.

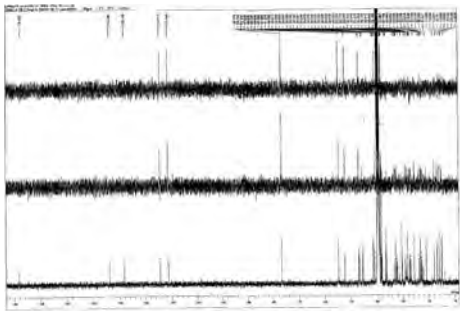

Figure 5. DEPT spectrum of an unknown compound

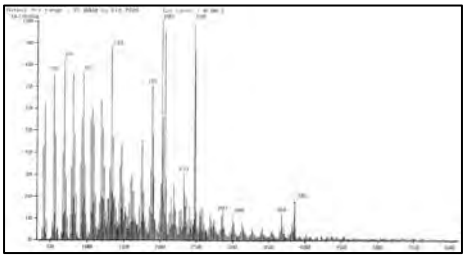

Figure 6. EI-Mass spectrum of an unknown compound

According to the FT IR, ^{1}H NMR and ^{13}C NMR spectral data, this compound should consist of two –OH groups and one carbonyl group. Hence, the partial molecular formula could be determined as $C_{23}H_{34}O_3$. Therefore, partial molecular mass is 358.

In EI-Mass spectrum (Figure 6), molecular ion peak, m/z 386 indicates the molecular mass of this compound (Porter and Baldas, 1971). Thus, the remaining partial molecular mass is 28. Consequently the real molecular formula of this compound could be determined as $C_{23}H_{34}N_2O_3$ which agrees with the "Nitrogen Rule".

$$\text{Hydrogen deficiency index} = 23 - \frac{34}{2} + \frac{2}{2} + 1 = 8$$

Structure Elucidation of Isolated Pure Compound

The structure of isolated pure compound was elucidated by DQF-COSY (Figure 7) and HMBC (Figure 8) spectra. DQF-COSY spectrum implies the proton-proton correlation of germinal and vicinal coupling protons by their graphic area. HMBC spectrum represents the α, β and γ proton-carbon long range coupling with protons and their relative carbons. The structure assignment of isolated pure compound is described as follows.

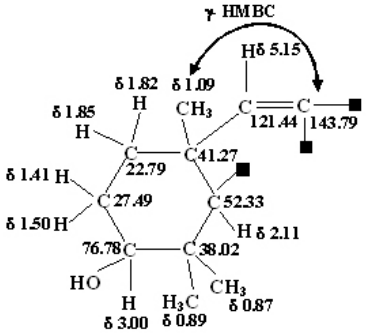

Fragment (1)

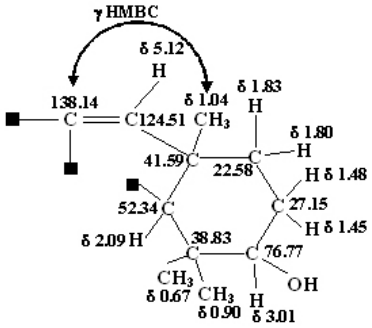

Fragment (2)

The logical connection between the sp^2 quaternary carbon (δ 143.79 ppm) in fragment (1) and another sp^2 quaternary carbon (δ 138.14 ppm) in fragment (2) could be done by DQF-COSY spectrum.

In this DQF-COSY spectrum (Figure 7), the observation of long range coupling between the sp^2 methine protons (δ 5.12 and δ 5.15 ppm) reveals the following fragment (3).

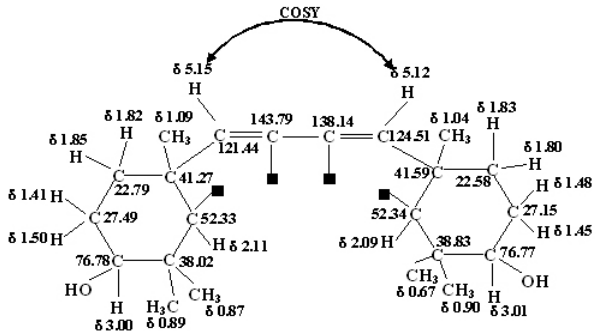

Fragment (3)

The partial molecular formula of this fragment (3) could be assigned as $C_{22}H_{34}O_2$ and the remaining still unassigned fragment is ($C_{23}H_{34}N_2O_3 – C_{22}H_{34}O_2 = N_2CO$).

Hence, it should be two nitrogen atoms and one carbonyl group.

On the other hand, the observation of the medium down field chemical shift of the two sp^2 quaternary carbons (δ 138.14 and δ 143.79 ppm) and the two sp^3 methine carbons (δ 52.33 and δ 52.34 ppm) reveals the attachment of these carbons to two trivalent nitrogen atoms.

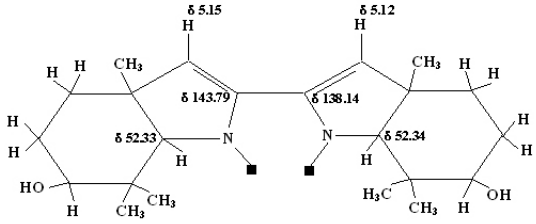

Moreover, according to the literature (Silverstein *et al.*,, 2005), the appearance of 1689 cm^{-1} of C = O stretching vibration of this compound in FT IR spectrum should be due to the substitution on the amide nitrogen of unsaturated groups that are capable of lowering the degree of lone pair delocalization cause an increase in the carbonyl stretching frequency. This evidence agrees with the attachment of the two nitrogen atoms to the carbonyl group which accomplishes the complete structure of compound as follows.

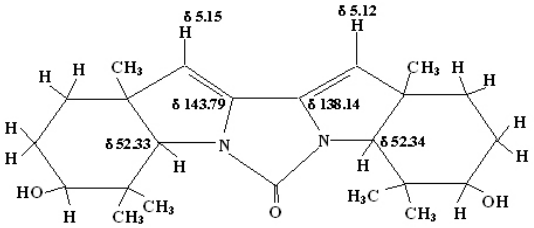

It was confirmed by the occurrence of γ ^{1}H–C long range coupling between the sp^{3} methine proton (δ 2.11 ppm) and sp^{2} quaternary carbon (δ 138.14 ppm) as depicted in HMBC spectrum (Figure 8).

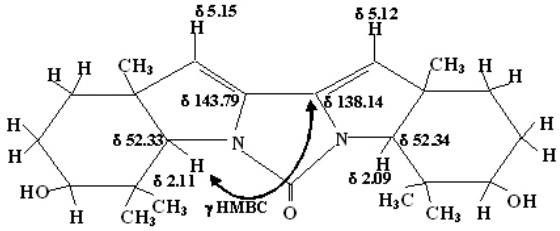

Hydrogen deficiency index (HDI-8) of this elucidated structure agrees with the calculated value (8) from the molecular formula ($C_{23}H_{34}N_2O_3$).

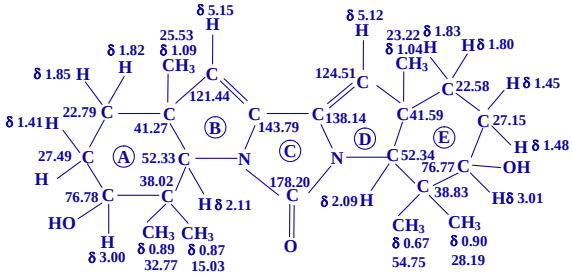

Complete Structure of Isolated Pure Compound

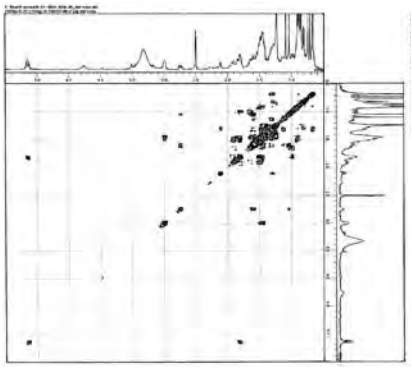

Figure 7. DQF-COSY spectrum of an unknown compound

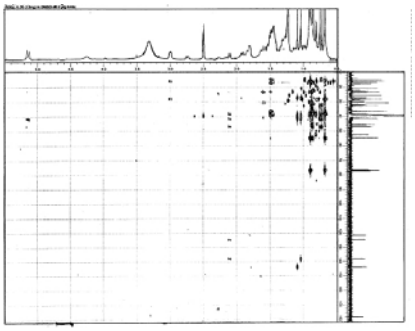

Figure 8. HMBC spectrum of an unknown compound

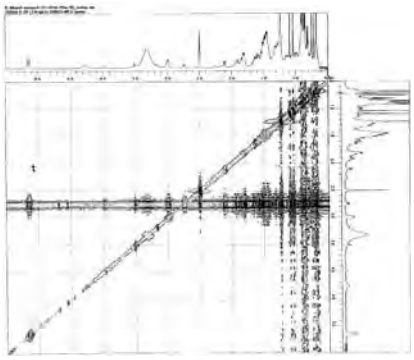

Figure 9. NOESY spectrum of an unknown compound

Furthermore, conformational structure of this compound could be assigned by using NOESY spectrum (Figure 9) and absolute configuration of six chiral centers could be determined.

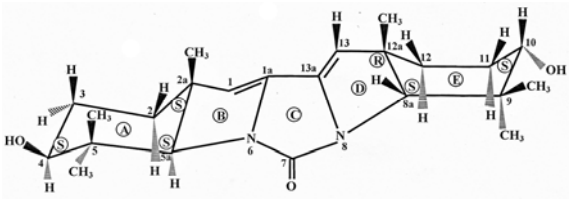

I.U. P.A.C name of this imidazole compound is 2_a -S, 4 -S, 5_a-S, 8_a -S, 10 -S, 12_a – R -4,10-dihydroxy- 2_a, 5, 5, 9, 9, 12_a- hexamethyl- 2_a, 2, 3, 4, 5, 5_a, 8_a, 9, 10, 11, 12, 12a-dodecahydro - imidazo-bis [1, 5_a] indole - 7-one.

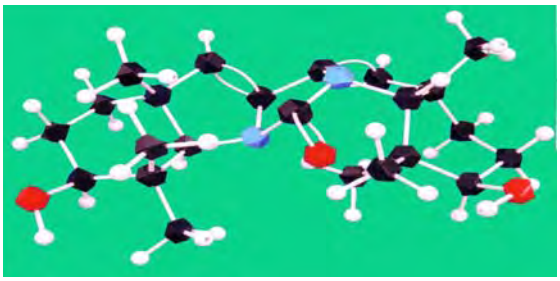

Conclusion

In this research work, a Myanmar indigenous medicinal plant namely *Leonotis nepetifolia* (L.) R.Br (Ame da zoe pin) was selected for detailed chemical analysis and focused on the complete structural elucidation of unknown compound isolated from this plant. A pure bioactive imidazole compound was isolated. The molecular formula and the complete structure elucidation of this compound were determined by some spectroscopic methods. This elucidated structure was then confirmed by mass fragmentation behaviors in EI-mass spectral data. Finally, the absolute configuration of six chiral centers of this imidazole compound was assigned as C_{2a} – S, C_4 – S, C_{5a} – S, C_{8a} – S, C_{10}-S and C_{12a} – R, respectively.

Acknowledgements

The author would like to express gratitude to Professor Dr Mya Aye, for his supervision, invaluable advice, helpful criticism, comments and constant encouragement in this research work. Special thanks are due to Dr Aye Kyaw, Rector, Magway University and Dr Aye Aye Wai, Professor and Head, Department of Chemistry, Magway University, for their encouragement. The author would like to convey sincere thanks to Dr Yoshiaki Takaya, Professor, Faculty of Pharmacy, Meijo University, Tempaku, Nagoya, Japan, for the measurements of valuable spectra and Dr Myo Myint, Deputy Director, Fermentation Department, Development Centre for Pharmaceutical Technology, Ministry of Industry (I), for his kind support in the test of the antimicrobial activities and Dr Soe Myint Aye, Associate Professor, Department of Botany, Myitkyina University, for his kind help in ascertaining the plant species for this research work.

References

Ah Shin Nagathein, (1976), "Pon Pya Say Abidan", 3rd Ed., Mingala Printing Press, Yangon.

Claridge, D. W. T., (1999), "High-Resolution NMR Techniques in Organic Chemistry", Oxford.

Harbonne, J.B., (1993), "Phytochemical Methods: A Guide to Modern Techniques of Plant Analysis", Chapman and Hall Ltd, U. S. A.

Hooker, J.D. (1885)" Flora of British India", Vol. IV. pg. 691 .L. Reeve & Co. Ltd. The Oast House, Brook, Ashford, Kent.

Lemmens, R. H. M. J. and Bogor, N. B., Indonesia, (2003), "Medicinal and Poisonous Plants 3 ", *Plant Resources of South-East Asia*, No **12** (3) .

Nelson, J. H., (2003), "Nuclear Magnetic Resonance Spectroscopic", Person Education, Inc.,Upper Saddle River, NJ 07458.

Porter, Q.N., and Baldas, J.,(1971), "Mass Spectrometry of Heterocyclic Compounds ", Wiley- Inter Science, A Division of John Wiley and Sons, Inc. New York. Landon. Sydney. Toronto.

Silverstein, R.M., *et al*, (2005), "Spectrometric Identification of Organic Compounds", 7th Ed., John Willy and Sons, Inc., New York.

Purification and Application of β-Galactosidase from Jack Bean (*Canavalia ensiformis L.*)

Yee Yee Myint

Abstract

In this research, β-galactosidase (E.C 3.2.1.23) was isolated from jack bean (*Canavalia ensiformis* L.) seed using successive ammonium sulphate precipitation method. Further purification was carried out using Sephacryl S-200 gel chromatography. The product glucose liberated from enzymic hydrolysis on lactose substrate was determined by using glucose oxidase enzyme reagent method.The fractional numbers from Sephacryl S-200 gel column were analyzed for the determination of β-galactosidase activity and protein content (absorbance at 280 nm). The fraction numbers (20-30) showing the highest β-galactosidase activity were pooled and further experiments were carried out using the pooled fraction. The relative purity of the β-galactosidase enzyme increased about 8 folds from crude to final purification step. The β-galactosidase activity was found to be 45.8 EU per gram of jack bean seeds at final purification step. The purity of the enzyme was confirmed by non SDS-PAGE electrophoresis as a single band. The molecular weight of the purified enzyme was determined to be 75,850 dalton.

Key words*:* β-galactosidase, jack bean, Sephacryl S-200, non SDS-PAGE, molecular weight

Introduction

Every organism contains thousands of different proteins with a variety functions. One of the functions is as catalysts. Nearly all chemical reactions in biological systems are catalyzed by specific macromolecules called enzyme(Garrett and Grisham, 1992).Enzymes are proteins which may consist of more than 20 types of amino acids with wide-ranging compositions and structural complexities (Gemeiner, 1992).

The ability of β -galactosidase to hydrolyse lactose into galactose is applied in food industry, particularly in the field of dairy products because of the nutritional (lactose intolerance), technological (crystallization) and environmental (pollution) problems associated with lactose (Blakebrough,

Lecturer,Dr, Department of Chemistry, Pathein University

1981). The added value gained by the hydrolysis of lactose to its constituent monosaccharides glucose and galactose, lies in the increased usefulness of hydrolysed lactose as a food carbohydrate.

The botanical aspect of jack bean(Figure 1) is as follows:

Family	- Fabaceae
Genus	- *Canavalia*
Species	- *ensiformis*
Botanical Name	- *Canavalia ensiformis (*Linn) Do
English Name	- Jack bean
Myanmar Name	- Pe-dalet

Figure 1. Photograph of Jack Bean (*Canavalia ensiformis* L.) plant

It is an annual, upright and bushy plant, growing to the height of 2 to 5 ft and bearing sword-shaped pods, 8-5 in long and about 1 in broad. The pod contains 10-12 white seeds each having a brown hilum extending to half the length of the seed (Bhatnager,1950).

The β-galactosidases are mainly used in the applications of biochemistry and biotechnology (Blakebrough ,1981). These are in the production of low lactose milk and utilization of whey lactose and the synthesis of disaccharides by reversal of hydrolysis. The ability of β - galactosidase to hydrolyse lactose into galactose is applied in food industry, particulary in the field of dairy products.

It can also be used to study the structure of complex carbohydrate chains and as a reagent to determine the lactose in the blood and other biological fluids (Byme and Johnson, 1975).

Materials and Methods

Isolation of β-Galactosidase from Jack Bean

Jack bean seeds (*Canavalia ensiformis*)were purchased from Nay Pyi Taw Pyinmana Township. Jack bean seeds (200 g) were blended in the blender (Li *et al*., 1975). A 100 g of jack bean meal was suspended in 600 mL of distilled water and stirred for 2 hours at room temperature. The suspension was filtered through cheesecloth. The turbid filtrate was adjusted to pH 5.5 at room temperature with 1.5 M sodium citrate (pH 2.7) and centrifuged to obtain 450 mLof extract. Solid ammonium sulphate (79.07g) was added to this extract to obtain 30% saturation (Rosenberg, 1996).

After standing for 2 hr, the precipitate was removed by centrifugation for 20 min at 5000 rpm and was discarded. β-Galactosidase in the supernatant (400 mL) was precipitated by adding solid ammonium sulphate (76.05 g) to 60% saturation. After standing overnight, the precipitated protein containing β-galactosidase was collected by centrifugation for 20 min at 5000 rpm and dissolved in 50 mL of 0.1 M sodium phosphate buffer (pH 7.0) to obtain an opaque solution.

Determination of β-Galactosidase Activity

The reaction mixture consisted of the 0.1 mL of enzyme fraction solution and 0.25 mL of lactose (substrate). The mixture was shaken well and incubated at 37 °C for 30 min. After incubation time, the mixture was heated on a boiling water bath for 10 min in order to stop the enzyme reaction. Then this solution was cooled under tap water for 10 min.

Finally, 0.5 mL of glucose oxidase enzyme reagent was added to the reaction mixture. The mixture was incubated at 37°C for 10 min. The filtrate was measured for absorbance at 500 nm by using UV-visible spectrophotometer. The amount of glucose liberated was calculated from a calibration curve, which relates the measured absorbance to an equimolar mixture of glucose and galactose.

Purification of β-Galactosidase Enzyme Using Gel Chromatography

Gel filtration was carried out in a column (2.5x27 cm) packed with pre-swollen Sephacryl S-200 using 0.1 M phosphate buffer (pH 7) and equilibrated with the same buffer (500 mL). The enzyme was eluted from the column with the same equilibrated buffer.

Crude β-galactosidase (0.04 g) was dissolved with 2 mL of pH 7.0 phosphate buffer. This solution was applied to a Sephacryl S-200 gel filtration column previously equilibrated with the same buffer. The flow rate was adjusted to 15 mL/hr by a mini pump and 2.5 mL fractions were collected per tube using a fraction collector. After collection, the protein content of each tube was checked by measuring the absorbance at 280 nm wavelength using a UV-visible spectrophotometer. Each tube was also measured for β-galactosidase activity. The fractions that had the highest β-galactosidase activity were pooled. The pooled β-galactosidase fraction was measured for protein content by the modified Lowry's method and β -Galactosidase activity. The pooled highest β-Galactosidase fraction was concentrated with acetone, 1:9 ratio (Rosenberg, 1996).

Purification by Ion Exchange Chromatography

The ion exchange chromatography was packed in a column with DEAE Sephadex A-50 using 0.02 M sodium phosphate buffer (pH 8.0) and equilibrated with the same buffer.

The concentrated β-galactosidase fraction obtained by Sephacryl S-200 gel filtration column was applied to a DEAE Sephadex A-50. The flow rate was adjusted to 15 mL /hr using a mini-pump and 2.5 ml fraction was collected per tube using a mini-collector. During collection, the protein content of each tube was continuously monitored at 280 nm wavelength by a bio-mini UV-monitor.

Detemination of Molecular Weight of the Purified β-Galactosidase Sample

The procedure is according to the method of Halim and Smith (Smith, 1975).

Determination of Lactose Content

A 1 mL of the clear milk solution was mixed with 1 mL of phosphate buffer (pH 5.6) and enzyme reaction was started by adding 3 beads of immobilized β-galactosidase. After 30 min the solution was filtered and determination of glucose content was carried out by using glucose oxidase enzyme reagent method.

Results and Discussion

Isolation of β-Galactosidase from Jack Bean

In this research, the jack bean meal was suspended in water (Li, 1975). After being stirred for 2 hr at room temperature, filtering with cheese cloth, ultracentrifuging the suspension was filtered and finally the crude extract was obtained. Extraction steps involved the 30% $(NH_4)_2SO_4$ and 60% $(NH_4)_2SO_4$ precipitation. By adding the appropriate solid ammonium sulphate, the enzyme protein was obtained. Since ammonium sulphate has little effect on enzyme activity and in some cases stabilizes the enzymes, it is useful as salt of choice in most cases. Thus it was employed in the present work.

β -Galactosidase Activities, Protein Contents and Specific Activities of the Enzyme Solutions at Different Purification Steps

The purification step involved ammonium sulphate fractionation followed by gel filtration on Sephacryl S-200. Sephacryl S-200, superfine is a new kind of gel filtration medium which combines a highly porous gel structure with excellent chemical and physical stability (Wiseman, 1985). Sephacryl is preswollen and ready to use in both analytical and preparation applications.

In the present research, Sephacryl S-200 was used in glass column 2x40 cm, that will fractionate proteins in the molecular weight range of 5 kDa to 250 k Da (Wiseman, 1985). Figure 2 shows the fractions of highest specific activity 20-30 and these were pooled and concentrated with acetone (cold acetone: enzyme solution = 1:9).It was kept at 4 °C for 15 min, centrifuged 2000 rpm for 20 min, the enzyme precipitate was obtained. The specific activity of the β-galactosidase was increased by 8.345 fold over crude extract in Table 1. The β-galactosidase enzyme activity can be defined as micromole of glucose liberated from lactose substrate per minute of enzyme solution. The EU of β-galactosidase from jack bean was determined as 45.8 EU per gram of jack bean seeds.

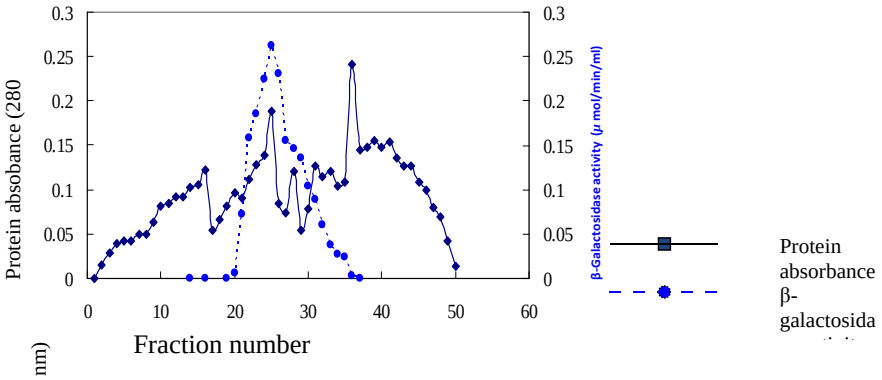

Figure 2 Purification of crude β-galactosidase enzyme by Gel (Sephacryl S-200) filtration chromatography

Table 1. β -Galactosidase enzyme activities, protein contents and specific activities of the enzyme solution at different purification steps

No	Fractions	Enzyme activity (μ mol $ml^{-1}min^{-1}$)	Protein (mg)	Specific Activities	Degree of Purification (fold)
1	Supernantant I	29.80	3.841	7.758	1.000
2	Supernantant II	24.59	2.342	10.500	1.353
3	Crude enzyme solution	19.40	0.698	27.790	3.582
4	After passing S-200Sephacryl gel	13.66	0.211	64.740	8.345

Molecular Weight of Purified β-Galactosidase

In this work, proteins from the pharmacia high molecular weight (HMW) calibration kit: thyroglobulin (669,000), ferritin (440,000), catalase (232,000), lactate dehydrogenase (140,000) and bovine serum albumin (67,000) were used for molecular weight determined by non SDS-PAGE. The homogeneity of the purified β-galactosidase was confirmed by non-sodium dodecyl sulphate-poly acrylamide gel electrophoresis (non SDS-

PAGE).The purified β-galctosidase enzyme showed a single band on non SDS-PAGE where the molecular weight of purified β -galactosidase was located near the standard protein (mol wt. 67,000) (Figure 3) after the final step purification (Table 1).

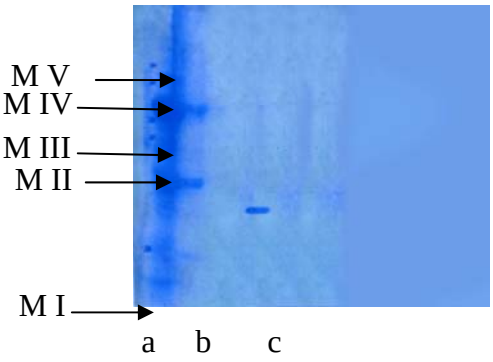

Figure 3 Photograph of non sodium dodecyl sulphate polyacrylamide gel electrophoresis*

*Lane (a) High molecular weight marker proteins

M I = Bovine Serum Albumin, M II = Lactate Dehydrogenase

M III = Catalase, M IV = Ferritin, M V = Thyroglobulin

(b) Crude enzyme solution

(c) Purified β-galactosidase fraction obtained from sephacryl S-200 gel

An estimated molecular weight of purified β-galactosidase from jack bean sample was 75,850 dalton from the log of known HMW marker proteins vs. R_f values for non SDS-PAGE.

Lactose Content in Commercial Milk Powder Products Using Immobilized β-Galactosidase Enzyme

In this research, the rapid analytical method was developed for the determination of lactose in milk powder sample. After enzymic hydrolysis on lactose in the solution by immobilized β-galactosidase, lactose content was calculated (Table 2). The glucose content in deproteinized milk powder sample was determined using glucose oxidase enzyme reagent methods.

The precision and accuracy (error percent) of the lactose determination in PEP milk powder samples were 1.06% and 2.16%. The

precision and accuracy (error percent) of the lactose determination in Dumex milk powder sample were 0.39% and 4.30% .

Table 2. Lactose Contents in Milk Powder Samples

No.	Sample	Absorbance at 500 nm	Lactose Content(%)	Average	Precision
1	PEP^+	0.816 0.847 0.840	27.83 28.91 28.67	28.47 ±0.3216	1.1296
2	Deng Chuan Instant Whole Sweet Milk Powder	0.570 0.561 0.551	19.46 19.14 18.79	19.13 ±0.1123	0.5870
3	Dumex*	1.143 1.135 1.129	39.01 38.73 38.53	38.76 ±0.0582	0.1502

PEP^+ certified value = 29.1%, Dumex* certified value = 40.5%

Conclusion

In this research, β –galactosidase (EC 3.2.1.23) was isolated from jack bean (*Canavalia ensiformis* L.) seed using successive ammonium sulphate precipitation method. Further purification was carried out using Sephacryl S-200 gel chromatography. The product glucose liberated from enzymic hydrolysis on lactose substrate was determined by using glucose oxidase enzyme reagent method.

The fractional numbers were analyzed for the determination of β-galactosidase activity and protein content (absorbance at 280 nm). The fraction numbers (20-30) showing the highest β -galactosidase activity were pooled and further experiments were carried out using the pooled fraction. The relative purity of the β -galactosidase enzyme increased about 8 folds from crude to final purification step.The purity of the enzyme was confirmed by Sephacryl S-200 gel as a single band. The molecular weight of the purified enzyme was determined to be 75,850 dalton.

In this research, a rapid determination of lactose in milk powder samples were carried out using immobilized β-galactosidase.The results obtained were not much differed from the certified values.

Acknowledgements

The author would like to thank the Department of Higher Education (Lower Myanmar), Ministry of Education, Myanmar, for allowing to carry out this research programme. Sincere thanks are due to Dr Nyunt Pe, Rector, Dr Than Soe Pro-Rector and Professor and Head Dr Khin Aye Kyu, Department of Chemistry, Pathein University for giving the opportunity to present this paper. Grateful thanks are due to Dr Kyaw Naing, Professor, and Dr San San Myint, Lecturer, Department of Chemistry, University of Yangon for their close supervision.

References

Bhatnager,S.S.,(1950), 'The Wealthy of India', Raw Material Government of India Press, New Delhi**,2,**55-58

Blakebrough,G.,(1981), 'Enzyme and Food Processing', Applied Science Pub.,Ltd., London,56-60

Byme,M.,and Johison,D.,(1975), 'Studies on the Immobilization of beta Galactosidase, *J., Biochem.Soc.,Trans*,2,96-102

Garrett, R.H., and Grisham,C.M.,(1992),'Biochemistry', Saunders College Pub., New York,428.429

Gemeiner, P.,(1992) ,'In Enzyme Engineering': Immobilized Biosystem, Eills Horwood Limited,167-169

Li,S., and Mazzota,M., Chien.S., and Li.T.,(1975),' Isolation and Characterization of Jack Bean β-Galactosidase',*J.Biol.Chem*.,**250**,6786-6790

Rosenberg,I.M.,(1996), 'Protein Analysis and Purification', Birkhauser, Boston,127-138

Smith,I.,(1975), "Chromatographic and Electrophoresis Techniques",Willams Helnmann Medical Books Ltd.,London,153-160

Wiseman,A.,(1985), 'Hand Book of Enzyme T echnology', Ellis Horwood Ltd., New York,95-103

Characterization and Determination of Physicochemical Properties of EM Compost and Vermicompost Fertilizers

Mi Mi Hlaing

Abstract

In this research work, various kinds of organic fertilizers were prepared from organic waste materials such as rice straw, cow dung and kokko (*Samanea saman* (Jacq.) Merr.) leaves. The waste materials were qualitatively and quantitatively determined by ED-XRF, AAS and other modern and conventional methods. Preparation of EM compost fertilizers (EMC) based on effective microorganisms (EM) and wastes, and preparation of various kinds of vermicompost fertilizers (VE and VP) based on two species of earthworms (*Eudrilus egeniae* and *Pheretima andamanensis*) and wastes were made. Analytical assay of EM compost and vermicompost fertilizers were also carried out. It is feasible to prepare vermicompost fertilizers based on rice straw, cow dung and two species of earthworms. The vermicompost produced by two species of earthworms differed in their nutrient concentrations, but possessed higher concentration of N, P and K than that of EM compost fertilizers. *Bacillus* spp, *Trichoderma spp*, and *Aspergillus niger* were the common genera observed in both samples. *Chrysosponium* spp were isolated from compost and *Pseudomonas aeruginosa* and *Rhizopus spp* were recorded in vermicompost.

Key words: Waste materials, earthworms, effective microorganisms (EM), EM compost fertilizers, vermicompost fertilizers

Introduction

Myanmar is an agricultural country and it has to develop its agriculture sector by means of expanding agricultural land, tapping of water resources to be able to feed its growing people. Intensive agricultural systems demand the use of large quantities of mineral fertilizers in order to supply plant nutrients. It leads to loss of soil fertility due to continuous and imbalanced use of fertilizers that has adversely affected agricultural productivity and causes soil degradation. Nowadays gradual deficiencies in soil organic matter and reduced yield of crop are alarming problem in Myanmar.

On one hand, tropical soils are deficient in all necessary plant nutrients and on the other hand large quantities of such nutrients contained

Lecturer, Department of Chemistry, East Yangon University.

in agricultural by-products are wastes. Most of these organic residues are burned currently or used as land fillings (Nagavallemma, *et al*., 2004). Properly recycled, a suitable composting process is used. One method of composting farm wastes is by vermicomposting with uses earthworms to eat and break up the organic wastes.

The use of earthworms for recycling of organic wastes known as vermicomposting becomes the focus of attention by the scientific community in mid 1990's. The vermicomposting technology also enables the utilization/ recycling of organic wastes for which no proper disposal mechanisms are available, or that the conventional techniques such as incineration may be hazardous (Preetha *et al*., 2005). Vermicomposting is an appropriate technique for disposal of non-toxic solid and liquid organic wastes. It helps in cost effective and efficient recycling animal wastes (poultry, horse, and piggery excreta and cattle dung), agricultural residues and industrial wastes using low energy.

Vermicompost is a good source of different macro and micronutrients particularly N, P, K,and S. Use of vermicompost for vegetable production in large scale can solve the problem for disposal of wastes and solve the lack of organic matter. On the other hand, a judicious combination of organic and inorganic sources of nutrients might be helpful to obtain a good economic return with good soil health for the subsequent crop. Moreover, the utilization of residual organic materials contributes to pollution control and environment protection (Alam *et al*., 2007).

This paper presents an account on the recycling of farm wastes such as rice straw, kokko (*Samanea saman* (Jacq.) Merr.) leaves and cow dung into organic fertilizers by vermicomposting with the use of earthworms; *Eudrilus egeniae* (Kinberg, 1867) and *Pheretima andamanesis* Michaelsen, 1907. The later is native to Myanmar and the former is introduced from India for the purpose of vermicompost production. The comparison of the composting efficiency can be performed by using a common substrate for both species.

Materials and Methods

Sample Collection

The rice straw, kokko(*Samanea saman* (Jacq.) Merr.) leaves and cow dung used in this work were collected from Thanlyin Township,

Yangon Region. The rice straw was chopped into 1 inch in length. The earthworms, *Eudrilus eugeniae* (Kinberg, 1867) and *Pheretima andamanensis* (Michaelsen, 1907), were collected from Vegetable and Fruit Research and Development Centre (VFRDC) at Hlegu Township, Yangon Region.

The eight worm bins (3.8 cm height and 5.0 cm diameter) made of plastic were used. Selected raw materials were separately placed in each bin and then mixed with cow dung. Sprinkling of water was done onto the bin to moisten the raw materials. When the partial decomposition of the materials started, the selected earthworms (300 nos.) were released into each bin. Simultaneously, rice straw (5 kg) was composted with EM solution in another bin. After about six weeks, vermicompost and vermicasting were ready for harvesting. Then the EM compost and vermicompost prepared with two species of earthworms were collected in plastic bags, and stored in a cool place.

These composted materials were air-dried, sieved and used for analysis of various chemical elements. The microbial populations of bacteria present in the samples were determined by using dilution plate technique and fungi were determined direct microscopic examination method.

The physicochemical properties were determined by the following methods.

Moisture content was determined by an oven-dried method at (110 ± 5°C) (A.O.A.C. Method 1970). pH was measured by using pH meter. Total nitrogen content was measured by Kjeldahl Method. Phosphorous content was measured using the visible spectrophotometer (Spectrometer Ciba – Corning 259). The potassium content (%) in ash was determined by the Emission Flame Photometer (Jenway, PFP 7/C England).

The determination of calcium and magnesium contents was measured using their specific hollow cathode lamps (Varian AA-575, Australia) by the Atomic Absorption Spectrophotometer.Total organic carbon was measured by Walkely-Black procedure (Jackson, 1958).

Results and Discussion

Earthworms almost lived in the environment where cow dung (Farm Yard Manure) decomposed. It is the main reason of using cow dung as raw material.

The presence of potassium, calcium, chlorine, iron, sulphur, manganese, copper, zinc, strontium, and bromine in rice straw, cow dung, and kokko leaves are shown by ED-XRF spectra presented in Figure 1. It can be observed that each spectrum indicated that the relevant elements were contained in rice straw, cow dong, and kokko leaves. Rice straw and cow dung contained the highest silicon content.

Table 1 represents the total nutrient concentrations of rice straw (rs), kokko leaves (kl), and cow dung (cd). It indicated that the pH values of all waste materials are suitable to prepare natural fertilizers. Rice straw has 0.62% N, 0.26% P_2O_5, 1.13% K_2O, 0.91% Ca, and 41.37% total carbons. Kokko leaf has 4.58 % N, 0.59 % P_2O_5, 0.86 % K_2O, 1.06 % Ca, 1.35 % Mg and 35.65 % total carbons. Cow dung also has 1.30% N, 0.83% P_2O_5, 1.64% K_2O, 2.54% Ca, 0.58% Mg and 31.99 % total carbons. Kokko leaf has higher nitrogen, total P_2O_5, calcium, and magnesium than that of rice straw. Although the nutrient content of kokko leaf was found to be higher than that of rice straw, it was not selected as main raw material for vermicompost fertilizer (V) and EM compost fertilizer (EMC) because no earthworms (*E.eugeniae*) were found in the environment of kokko leaf. So, rice straw was selected as main raw material.

When preparation of vermicompost from farm wastes such as banana tree, corn stalks, grasses, etc., the raw organic wastes and earthworms were added together. However vermicomposting using rice straw or kokko leaves, they must be preliminary decomposed and after decomposition, earthworms were released. If rice straw, cow dung, and earthworms were added altogether, the earthworms run away from the composting bin and died during vermicomposting.

The rate of composting of tree leaves was very slow compared to different cereal crop wastes and vegetable crop wastes. From Table 2, the composting rate of dry kokko leaves, VP (kl), (180 days) was very slow as compared to that of rice straw, VE (rs-2) and VP (rs-2), (120 days). The rate of composting of mixed rice straw and kokko leaves, VP(rs +kl),(150 days) was slightly rapid than only kokko leaves (180 days).

Vermicomposting of dry leaves (kokko leaves) is slow as compared to that of rice straw. It was obvious due to hard and hydrophobic nature of dry leaves. The presence of different allelochemicals in rise straw and kokko leaves might be responsible for their slow rate of microbial decomposition. Although the composting rate of vermicomposting was generally more rapid than that of simple composting processes, EM composting rate was the most rapid.

The role of ingestion by the earthworm differ from each other may be due to different cellulose content among different plant materials. When kokko leaves were digested into vermicompost using earthworms, *E. Eugenia,* they died during composting process. But using locally available earthworms, *Ph. andamanensis*, vermicomposts were formed.

The plant-nutrient status of EM compost fertilizers (EMC) and vermicompost fertilizers (V) of different raw materials prepared with two species of earthworms were presented in Table 2 and the NPK contents of those fertilizers were shown in Figure 4.

The vermicompost fertilizers (VP and VE) processed by *Ph.andamanensis* and *E.eugeniae* possessed higher nitrogen content than EM compost fertilizers. The moisture contents of EMC (rs) and EMC (kl) were found to be 3.84% and 13.67% respectively. VE (rs-1) and VP (rs-1) have 44.81% and 18.04% in moisture contents. The moisture contents of VE (rs-2) and VP (rs-2) also have 30.31% and 40.37% respectively.

Among the prepared fertilizers, VP (rs-2) has the highest total nitrogen 2.74%, total P_2O_5 1.62 %, and total K_2O 1.29%. VE (rs-2) also has 2.30% total nitrogen, 1.10% total P_2O_5 and 1.40% total K_2O. These values of the prepared fertilizers were slightly higher than that of EM compost fertilizers.

The prepared EM compost fertilizers and vermicompost fertilizers have the total nitrogen values in the range of 1.08% to 2.74%. Their total nitrogen values were not obviously different. The prepared EMC, VE, and VP fertilizers have the 4.9-7.8 pH range. VP (kl) has the lowest pH value of 4.9. EM composts and the other vermicomposts have similar pH value. The variability in pH could be due to the production of carbon dioxide and organic acids during organic wastes decomposition. The lower pH in the end product (vermicompost) might have been due to the production of carbon dioxide and organic acids. In general, an organic carbon loss has

been observed during the vermicomposting process. A large fraction of organic matter in the initial substrates was lost as CO_2 (between 20% and 43 % as a total organic carbon) by the end of the vermicomposting period. The vermicomposted materials had greater nitrogen content (Suthar and Singh, 2008).

Total organic carbon (%) of VE (rs-2), (43.60%) was higher than that of the VP (rs-2), (33.65%). But EMC (kl) fertilizer has 40.69% total organic carbon. Total organic carbon plays a very important and sometimes spectacular role in the maintenance and improvement of soil properties

(Biswas and Nugherjee, 2005).

The inoculation of worms in waste material considerably enhances the amount of nitrogen due to earthworm mediated nitrogen mineralization of wastes. It also suggested that the earthworm also enhances the nitrogen levels of the substrate by adding their excretory products, mucus, body fluid, enzymes, and even through the decaying tissues of dead worms in vermicomposting sub-system (Suthar, 2007). The vermicompost prepared by both earthworm species showed a considerable difference for total nitrogen content. The nutrient content of vermicompost depends on the types of feedstock and beeding provided for the worms (Sherman, 2003).

Consequently, the C/N ratio of EMC (rs), (24.41) is higher than that of EMC (kl), (24.08). The C/N ratios of vermicompost fertilizers produced by two types of earthworms were also in the range of 10.22 – 21.39. Among the vermicomposts, VP (rs + kl), (21.39) was the highest. Thus, the C/N ratios of vermicomposts were lower than that of EM compost. The loss of carbon as carbon dioxide through microbial respiration and simultaneous addition of nitrogen by worms in the form of mucus and nitrogenous excretory material lowered the C:N ratio of the substrate (Suthar, 2007).

EDXRF spectra of prepared compost and vermicompost fertilizers were shown in Figures 2, and 3. In both EM compost samples, a total of eight elements (Ca, K, Fe, Mn, Cu, Zn, Si, and Sr) were detected. In the prepared vermicompost samples, the same elements were also detected. But in VP (rs-1), Cu was not detected. All prepared fertilizers also contained S except EMC (kl), VE (rs-2), VP (rs-1) and VP (rs + kl). According to ED-XRF spectra, essential elements for plants and no toxic elements were found in the prepared fertilizers.

Bacillus spp, *Trichoderma spp,* and *Aspergillus niger* were the common genera observed in both EM compost and vermicompost samples. *Chrysosponium spp* were isolated from compost and *Pseudomonas aeruginosa* and *Rhizopus spp* were recorded in vermicompost. This indicated that microbial diversity was more in vermicompost than EM compost.

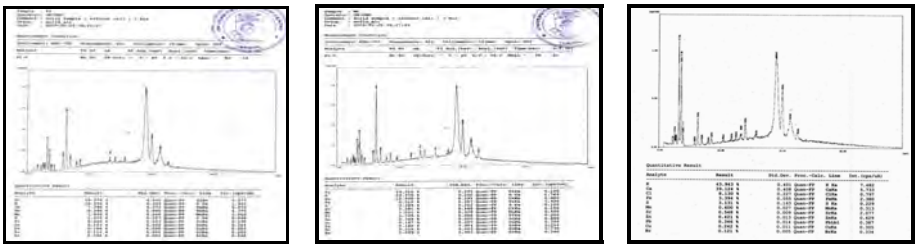

Figure 1 EDXRF spectra of rice straw, cowdung and kokko Leaves.

Table 1 Analytical assay of organic waste materials

No	Item	Rice Straw	Cowdung	Kokko Leaf
1.	pH	8.20	7.60	6.50
2.	Moisture(%)	15.59	18.66	9.36
3.	Total N (%)	0.62	1.30	4.58
4.	Total P_2O_5 (%)	0.26	0.83	0.59
5.	Total K_2O (%)	1.13	1.64	0.86
6.	Total Ca (%)	0.91	2.54	1.06
7.	Total Mg (%)	ND	0.58	1.35
8.	Total Carbon (%)	41.37	31.99	35.65

ND = Not Detected (< 0.001)

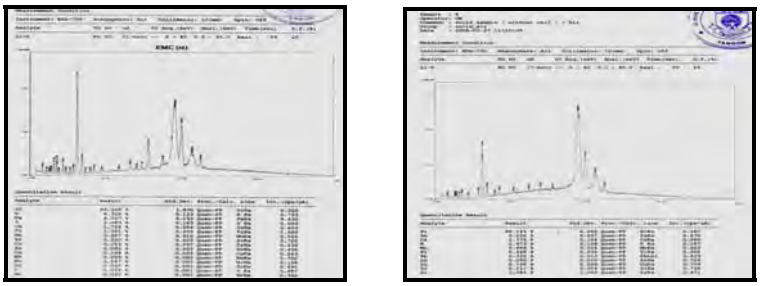

Figure 2 ED-XRF spectra of EM composts, EMC(rs) and EMC(kl)

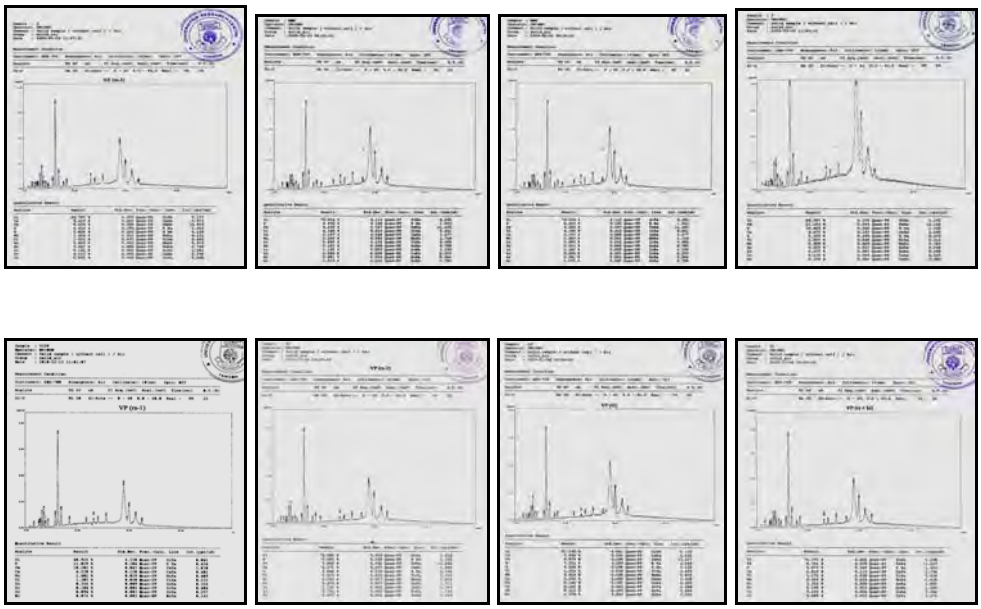

Figure 3 ED-XRF spectra of vermicompost fertilizers; VE(cd), VE(rs-1), VE(rs-2),VP(cd), VP(rs-1), VP(rs-2), VP(kl) and VP(rs + kl)

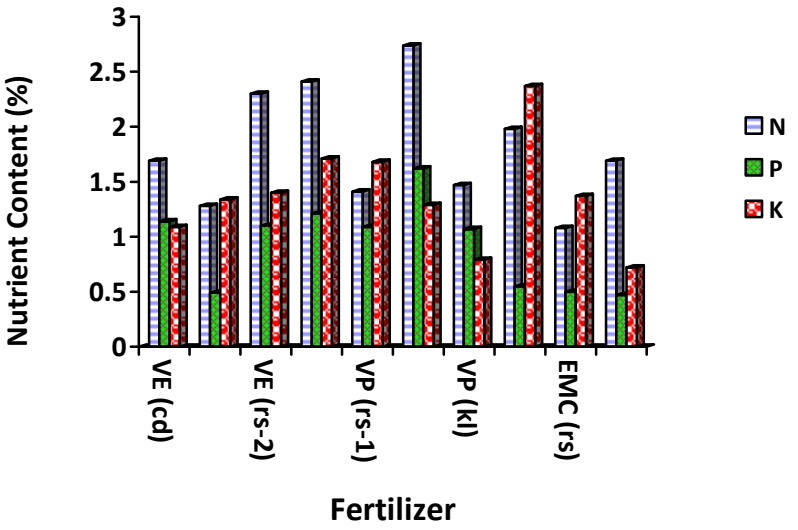

Figure 4 The nutrient contents (NPK) of various fertilizers

Table 2 Analytical assay of compost fertilizers and various vermicompost fertilizers

Item	EMC (rs)	EMC (kl)	VE (cd)	VP (cd)	VE (rs-1)	VP (rs-1)	VE (rs-2)	VP (rs-2)	VP (kl)	VP (rs+kl)
Composting period (days)	45	45	30	30	105	105	90	90	180	150
pH	7.8	7.8	7.1	6.9	6.8	7.2	7.2	7.5	4.9	7.5
Moisture (%)	3.84	13.67	15.10	27.31	44.81	18.04	30.31	40.37	11.97	12.64
Total N (%)	1.08	1.69	1.69	2.41	1.28	1.40	2.30	2.74	1.47	1.98
Total P_2O_5 (%)	0.50	0.47	1.14	1.21	0.49	1.09	1.10	1.62	1.07	0.55
Total K_2O (%)	1.27	0.72	1.09	1.71	1.34	1.68	1.40	1.29	0.79	2.37

Item	EMC (rs)	EMC (kl)	VE (cd)	VP (cd)	VE (rs-1)	VP (rs-1)	VE (rs-2)	VP (rs-2)	VP (kl)	VP (rs+kl)
Total Ca (%)	0.41	1.27	1.30	1.64	1.57	1.60	1.66	1.86	0.89	1.35
Total Mg (%)	0.24	1.28	1.26	0.31	ND	0.29	1.60	0.58	0.39	0.40
Total organic carbon (%)	26.36	40.69	22.30	24.64	24.86	23.18	43.60	33.65	23.94	42.37
C : N	24.41	24.08	13.19	10.22	19.42	16.56	18.96	12.28	16.29	21.39

ND = Not Detected (< 0.01)

EMC(rs) = rs + cd +EM (5kg : 5kg : 5L)

EMC(kl) = kl + cd +EM (5kg : 5kg : 5L)

VE(cd) = cd + *E.eugeniae* (5kg : 300 nos.)

VE(rs-1) = rs + cd + *E.eugeniae* (5kg : 5kg : 300 nos.)

VE(rs-2) = rs + cd + *E.eugeniae* (5kg : 10kg : 300 nos.)

VP(cd) = cd + *Ph.andamanensis* (5kg : 300 nos.)

VP(rs-1) = rs + cd + *Ph.andamanensis* (5kg : 5kg : 300 nos.)

VP(rs-2) = rs + cd + *Ph.andamanensis* (5kg : 10kg : 300 nos.)

VP(kl) = kl + cd + *Ph.andamanensis* (5kg : 5kg : 300 nos.)

VP (rs+kl) = rs + kl + cd + *Ph.andamanensis* (5kg : 5kg : 5kg : 300 nos.)

Conclusion

This research involved the investigation of EM compost and vermicompost fertilizers. This investigation shows that it is feasible to prepare vermicompost fertilizers based on above raw materials with two species of earthworms (*E. Eugenia* and *Ph. andamanensis*). The rice straw and cow dung can be utilized as main waste materials for both EM compost fertilizers (EMC) and vermicompost fertilizers (VE and VP).

The EM compost fertilizer, EM (rs) consisted of primary nutrients; 1.08 % N, 0.50 % P_2O_5, 1.27 % K and secondary nutrients; 0.41 % Ca, 0.24 % Mg and total organic carbon 26.36%. Its moisture content and pH were 3.841 % and 7.8, respectively.

The vermicompost fertilizer, VE (rs-2) prepared from rice straw, cow dung and earthworms (*E. Eugenia*) contained primary nutrients; 2.30 % N, 1.10 % P_2O_5, 1.40 % K and secondary nutrients; 1.66 % Ca, 1.60 % Mg and total organic carbon 43.60%. Its moisture content and pH were 30.31 % and 7.2, respectively.

The vermicompost fertilizer, VP (rs-2) prepared from rice straw, cow dung and earthworms (*Ph.andamanensis*) contained primary nutrients; 2.74 % N, 1.62 % P_2O_5, 1.29 % K and secondary nutrients; 1.86 % Ca, 0.58 % Mg and total organic carbon 33.65%. Its moisture content and pH were 40.37 % and 7.5, respectively. Therefore, these prepared fertilizers can supply primary and secondary nutrients for plant growth.

Bacillus spp, *Trichoderma spp*, and *Aspergillus niger* were the common genera observed in both samples. *Chrysosponium* spp were isolated from compost and *Pseudomonas aeruginosa* and *Rhizopus spp* were recorded in vermicompost. This indicated that microbial diversity was more in vermicompost than compost.

Use of vermicompost fertilizers for vegetable production on a large scale can solve the problem for disposal of wastes. Wastes are being recycled, and also reduced the environmental pollutions. The sustainable farming practices on vermicomposting are able to promote soil fertility and agricultural productivity.

Acknowledgements

The author wishes to acknowledge Professor Daw Phyu Phyu Thein, Head of Department of Chemistry, East Yangon University for her numerous valuable suggestions and encouragement.

References

Alam, M.N., Jahan, M.S., Ali, M.K., Islam, M.S. and Khandaker, S.M.A.T., (2007),"Effect of Vermicompost and NPKS Fertilizers on Growth, Yield and Yield Components of Red Amaranth", *Australian Journal of Basis and Applied Science (AJBAS)*, **1**(4) : 706-716.

AOAC, (1970),"Official Methods of Analysis", 11th Ed., Association of Official Analytical Chemists, Washinton, DC.

Biswas, T.D., and Mukherjee, S.K., (2005), "Text Book of Soil Science", Tata McGraw-Hill Co., Ltd., 2nd Edition, New Delhi

Jackson, M.L., (1958), "Soil Chemical Analysis", Prentice Hall of India Pvt. Ltd., New Deli, p 498

Nagavallmma, KP., Wani, SP., Lacroix, S., Padmaja,V.V., Vineela, C., Babu R.M., and Sahrawat K.L., (2004), "Vermicomposting : Recycling Wastes into Valuable Organic Fertilizer", Global Theme on Agroecosystems Report no. 8 Patancheru 502324, Andhra Pradesh, India : International Crops Research Institute for the Semi-Arid Tropics. p 1-20

Sherman, R., (2003), "Raising Earthworms Successfully", EBAE 103-83, N.C., North Carolina Cooperative Extension Service

Suthar, S., and Singh, S., (2008), "Vermicomposting of Domestic Waste by using Two Epigeic Earthworms (*Perionyx excavates* and *Perionyx sansibaricus*)", Int. *J. Environ. Sci. Tech.*, **5**(1), 99-106.

Suthar, S., (2007), " Vermicomposting Potential of *Perionyx sansibaricus* (Perrier) in different Waste Materials", *Bioresource Tech.*, **98,** 1231-1237

Antimicrobial Activity and Health Benefits of Red Wine from Grape (*Vitis vinifera* Linn.)

Nu NuYi

Abstract

The phytoconstituents in pulp, skins and seeds of grape (*Vitis vinifera* Linn.) and in red wine made from grape juice of such variety by fermentation using *Saccharomyceae cerevisiae* were investigated. Phenolic compounds, anthocyanins and tannins in red wine were also checked by general methods. The bioactivities of red wine against some pathogenic microorganisms: gram positive bacteria: *S.aureus, B.subtilis* and *B.pumalis*; gram negative bactreia: *P.aeruginosa, E.coli* and fungi, *C.albicans* were described in this paper.

Key words : *Vitis vinifera, Saccharomyceae cerevisiae,* pathogenic microorganisms, *S.aureus, B.subtilis, B.pumalis, P.aeruginosa,..*

Introduction

In this research, the fruit being focused for its phytoconstituents of biological importance is grape (*Vitis vinifera* Linn.), family Vitaceae (Figure 1). It is one of the major economic importance in wine making because of their right levels of acid, sugar, flavour and their nutritional values. Investigation of phytoconstituents in red wine and its antimicrobial activity on pathogenic microorganisms are the aims of the present study.

Health Benefits of Grape (*Vitis vinifera* Linn.) and Red Wine

Recent studies have reported that the red wine and grape juice have the same health benefits: reducing the risk of blood clots, reducing low density lipoprotein(bad cholesterol), preventing damage of blood vessels in the heart, and maintaining a healthy blood pressure.

Both red wine (Figure 2) and grape juice contain antioxidants, some flavonoids which can increase HDL (High Density Lipoprotein or " good cholesterol") and lowers the risk of clogged arteries (atherosclerosis) and thus may help lower blood pressure. Phenolic compounds in red wine inhibit oxidation of human LDL (Low Density Lipoprotein) levels (Stephanie *et al.*, 2009).

Lecturer, Department of Chemistry, Meiktila University

Figure 1. Plant of *Vitis vinifera*

Figure 2. Red wine from Grape

Antioxidants in Grape and Red Wine

Oligomeric proanthocyanidin complexes (OPCs), powerful antioxidants found in grape juice, skin, seeds and red wine from grape are useful to treat a range of health problems related to free radical damage including heart diseases, diabetes and cancers. OPCs can lower cholesterol, help to treat hypertension by protecting blood vessels from damage and can reduce the risk of developing cancer by preventing the growth of breast, stomach, colon, prostate and lung cancer cells in vitro.

Moreover, OPCs have potential benefits against the platelet aggregation and other risk factors of atherosclerosis, loss of physical performance and mental activity during ageing and hypertension in humans.

Proanthocyanidins found in red wine have antioxidant activity and these compounds play a role in the stabilization of collagen and maintenance of elastic, the two critical proteins in connective tissue that support organs, joints, blood vessels and muscle. Proanthocyanidin's antioxidant capabilities are 20-times more powerful than vitamin C and 50-times more potent than vitamin E. It causes strengthen all blood vessels and improve the delivery of oxygen to the cells.

Antioxidants in red wine are in two main forms, flavonoids and non-flavonoids. Cardioprotective effect of red wine are due to the presence of polyphenolic compounds such as flavonoids and resveratrol (non-flavonoid). Isoflavonoids and polyphenols in red wine possess the function of antioxidant, lipid lowering, immunomodulator, antiosteoporotic and anticancer properties (Stephanie *et al.*, 2009).

Some flavones have antiestrogenic effects. This may benefit people at risk of breast and prostate cancers. Thus, it possesses anticarcinogenic effects. Flavonoid intake inhibit the aggregation and adhesion of platelets in blood, which lower the risk of heart diseases. Flavonoid such as quercetin, kaempferol in grape and red wine could interfere sulfaction-induced cancer growth. Quercetin is also vasorelaxant and it showed a marked cytoprotective capacity in vitro test.

Various Medicinal Uses of Different Parts of Grape and Red Wine

Red wine enriched with resveratrol, flavonoids and other phenolic compounds possesses the beneficial effects of calories restriction in heart, skeletal muscles and brain which inhibit gene expression associated with heart and skeletal muscle aging and thus prevent age-related heart failure (Corder *et al.*, 2006).

Various medicinal uses of different parts of grape and red wine are described in Table 1.

Table 1. Medicinal uses of different parts of grape and red wine

Parts used	Medicinal values
Sap of grape vines	to treat skin, eye diseases.
Leaves	to stop bleeding , anti-inflammation, to relief pain, hermorrhoids.
Unripe grape	to treat sore throats.
Ripe grape	to treat cancer, cholera, small pox, nausea, eye infections, skin, kidney and liver diseases.
Dried grape (Raisin)	to treat constipation and thirst.
Grape skin	to prevent cancer, to protect heart and brain damage, to inhibit the degenerative nerve diseases.

Table 1. Medicinal uses of different parts of grape and red wine (Cont'd)

Parts used	Medicinal values
Grape seed extract	to treat chronic venous insufficiency, blood pools in the legs, pain, swelling, fatique, visible veins, diabetes and edema, to protect collagen and elastin in skin (i.e anti-ageing) to treat hemorrhoids, to prevent damage to human liver cells caused by chemotherapy medication.
Red wine	to reduce the risk of leukemia, breast, skin and prostate cancers, to protect heart and brain damage.

Materials and Methods

Sample Collection

Ripe and undamaged fruits of the grape plant (*Vitis vinifera*), used as raw materials for wine fermentation were collected from Tawma Village, Meiktila Township, Mandalay Region, Myanmar.

Botanical Description of Grape

Family	-	Vitaceae
Genus	-	*Vitis*
Species	-	*vinifera*
Botanical Name	-	*Vitis vinifera*
Common Name	-	Grape

Preparation of Red Wine from Grape (*Vitis vinifera*)

Ingredients for Making Red Wine

Red grape (fruits)	1 viss (680 mL grape juice)
Sugar	35 g
Yeast (*Saccharomyces cerevisiae*)	8 g
Sodium metabisulphite	0.3 g
Ammonium phosphate	0.1 g
Distilled Water	750 mL

Process of Wine Making

Wines are produced from grape by multistep process. The basic wine making steps are (1) grape processing (2) fermentation (3) clarification (4) stabilization (5) bulk aging and (6) bottling. Red Wine was prepared by the following procedure.

Before fermentation, clean, undamaged and fresh fruits of grape (*Vitis vinifera*) were pressed manually with little pressure (free run) to obtain the clearest liquid from middle of the pulp. After this, pressing was continued with heavier pressure to get the grape juice and volume of the juice was measured.

Grape juice with grape seeds and grape skins were placed in the fermenter. Brix of the juice was checked to get 22 – 24 degree. pH and temperature of the filtrate was also measured.

Sodium metabisulphite solution, prepared by dissolving 0.3 g of $Na_2S_2O_5$ crystal in 350 mL of distilled warm-water was added to the combined grape juice with stirring to inhibit the wild yeast (Wang, 2004). After being added sulphite, sugar was added to this grape juice.

Then, yeast solution (8 g yeast (*Saccharomyces cerevisiae*) was added to 200 mL of warm-water and set aside for 10 min before adding to the juice) was added to the grape juice in the fermenter. At the same time, 0.1 g of ammonium phosphate and 100 mL of distilled water were also added to the juice. The fermenter was covered with air tight stopper. Fermentation was allowed for two weeks at the dark place at room temperature in anaerobic condition.

After two weeks, decantation of turbid red wine was rapidly carried out to remove sediment including death yeast cells, grape seeds, grape skins and other impurities. Fermentation was allowed to continue. After three weeks, decantation of turbid red wine was rapidly filtered through cotton filter. Decantation was repeated at every one week to get desired clarity of red wine. After fermentation, red wine was stabilized and aging of wine was allowed for at least three months. Then, a little sodium metabisulphite solution (0.1 g in 100 mL) was added to wine just before bottling to ensure the absence of microorganisms.

Finally, clear, stable and properly aged wine with good aroma and flavor was bottled in pasteurized glass bottles of brown colour with air tight

stopper. Thus, red wine was stored in glass bottle for many years before drinking. Process of wine making from mature and undamaged grapes (*Vitis vinifera*)of good quality with grape seeds and skins by biochemical processing with careful handling, pre-treatment of juice, clarification, chemical composition of the juice, temperature and pH of the fermentation and the condition to inhibit other micro-organisms were carried out to achieve the red wine with distinctive flavor and aroma. In this processing, the original microbial population on the grape skin was eliminated by treatment with SO_2 produced from sodium metabisulphite by the following reactions.

$$Na_2S_2O_5 \longrightarrow 2SO_2 + Na_2O$$

sodium metabisulphite sulphurdioxide sodium oxide

Temperature between (20-28˚C) and pH of grape juice (4 - 4.5) are optimum condition for yeast population. So, in this research, pH of grape juice was 4 and the temperature was kept at 20 - 28˚C. This temperature is enough to extract the pigment, anthocyanin compounds from the grape skin.

Aging of wine in the dark for years is the crucial step of wine making to obtain wine of good flavor and aroma. The chemistry of the process of wine aging are

phenols + phenols---------->More complex phenols

Alcohol + Acids ---------->Aldehydes---------->Esters

Esters + Esters ---------->Delicate and more complex Esters

Results and Discussion

The flavor, aroma and quality of wine merely depend on the value of fruit juice and subsequent processing of fermentation. In this research , freshly prepared grape juice collected from ripe and undamaged fruits of grape (*Vitis vinifera*) cultivated in Tawma village , Meiktila Township, Mandalay Region were fermented by dry yeast (*S. cerevisiae*) strain for wine making. From about 1 viss of fruits, 680 mL of grape juice were obtained. Yield percentage of red wine from grape is 85%.

Some physical parameters of grape juice are control factors for wine fermentation. The optimum pH for microorganisms is near to neutral point (pH 7.0). Yeasts are usually acid tolerant and it can grow well in pH range

of 4 - 4.5. To inhibit other microorganisms except the population of *S. cerevisiae*, pH of grape juice is one of the important factors. Specific gravity and brix (the total solid content , especially sugar) of grape juice should also be measured because grape juice with 22 - 24 brix is common for wine fermentation. So, some physical parameters of grape juice were measured and data obtained were given in Table 2.

Table 2. Results of physicochemical investigation on grape juice of *Vitis vinifera* L.

No.	Parameter	Grape Juice
1	Acidity	0.65
2	pH	4
3	Specific gravity	1.08
4	Brix	23º

Phytoconstituents in the various parts of fruits (grape) and red wine made from grapes were described in Table 3.

Table 3. Results of phytochemical tests on various parts of fruits and red wine of grape

No	Tests	Extract	Observations			
			Pulp	Skin	Seed	Red Wine
1	Alkaloids	1% HCl	-	-	-	-
2	Flavonoids	95% EtOH	+	+	+	+
3	Phenolic Compounds	Distilled H_2O	+	+	+	+
4	Terpenes & Terpenoids	95% EtOH	-	-	-	-
5	Glycosides	(1) Distilled H_2O	+	+	-	+
		(2) 95%EtOH	+	+	-	+

No	Tests	Extract	Observations			
			Pulp	Skin	Seed	Red Wine
6	Tannins	Distilled H_2O	+	+	+	+
7	Steroids	95% EtOH	+	+	+	-
8	Carbohydrate	Distilled H_2O	+	+	+	-
9	Saponins	(1) Distilled H_2O	+	+	-	-
		(2) 95% EtOH	+	+	-	-

+ = present - = absent

The major constituents necessary for fermentation of grape juice to red wine are soluble sugars, monosaccharides mainly glucose, fructose and mannose. These sugars were determined qualitatively in the grape juice of *Vitis vinifera* and results obtained were stated in Tables 4 and 5.

Table 4. General tests for detection of carbohydrates in grape juice

No.	Test	Reagents	Observations	Inferences
1	Molisch	Molisch's reagent & conc: H_2SO_4	Purple colour ring at junction of two liquids	Carbohydrates are present.
2	Fehling	Fehling's A and B solution	Brick red ppt	Reducing sugars are present.
3	Benedict	Benedict's reagent	Reddish ppt	Reducing sugars are present.
4	Barfoed	Barfoed's reagent	Orange to Red ppt	Monosaccharide is present.
5	Moor	2% NaOH solution	Yellow to Reddish brown colour	Glucose is present.

No.	Test	Reagents	Observations	Inferences
6.	Seliwanoff	Seliwanoff's reagent	Red to Orange colour & Faint orange colour (>7min)	Fructose is present.
7.	rapid furfural	1% α - naphthol & conc: HCl	Purple colour	Glucose is present.

Table 5. Microchemical tests for types of monosaccharides (sugars) in grape juice (qualitative test)

Test	Observation	Inference
Osazone Test	Needle shaped Yellow Osazone Crystals (within 5 min)	Glucose, fructose and mannose are present

Physical parameters measured at Qality Cntrol Department of Development Centre of Pharmaceutical Technology (DCPT) for red wine were described in Table 6.

Table 6. Some physical parameters in red wine from grape

Parameters	(Red Wine)
Colour Description	Wine Red
Solubility	Miscible with water
Refractive Index	1.347
Specific Gravity	0.9951
Clearity of solution	satisfy

From the results of phytoconstituents in red wine mentioned above in Table 3, it can be noticed that flavonoids, phenolic compounds, glycosides and tannins are all present in red wine.

Table 7. Results from detection of phenolic compounds in red wine

No	Types of Phenols	Tests	Observations	Inferences
1.	All Phenols	Group tests	red	Phenol is present
2.	Flavin Derivatives (Anthocyanins)	H_2SO_4 tests	Red	Anthocyanins are present
		$FeCl_3$ test	Greenish blue colour	Cyanidin & Malvidin are present
		dil HCl test NaOH test	Red colour Blue colour	Pelargonidin is present Cyanidin is present
3.	Polyphenols (Tannin)	2% gelatin	Curdy white ppt	Tannin is present
		Saturated KIO_3	brown colour	Tannin is present
		HNO_2	blue colour	Ellagic tannin is present

The results obtained from the detection of phenolic compounds in red wine were given in Table 7. From this results, it can be seen that flavin derivatives, anthocyanins and polyphenol ,tannin are present in red wine fermented from grape (*Vitis vinifera*). Phenolic compounds, flavonoids, anthocyanin and anthocyanidins are all possess potential effects on human health which have already described in introduction of this research paper. So, these compounds are especially detected in red wine of grape for many medicinal values to prevent and treat such diseases as hypertension, diabetes, obesity, damage of blood vessel, damage of brain cells, leukemia, cardiovascular diseases, various types of cancers at breast, skin, stomach, colon, prostate, lung, age-related diseases.

Bioactive constituents of grape possess bioactivities which can inhibit or against the population of six microorganisms inoculated in agar-well on plate. Results given by plate diffusion tests on red wine upon such microorganisms and their inhibition zones were given in Figure 3. From such results, it can be seen that wine has potent action on many diseases which mostly occurs in daily life around the world. Types of

microorganisms and their related diseases which can be affected by red wine were given in Table 8.

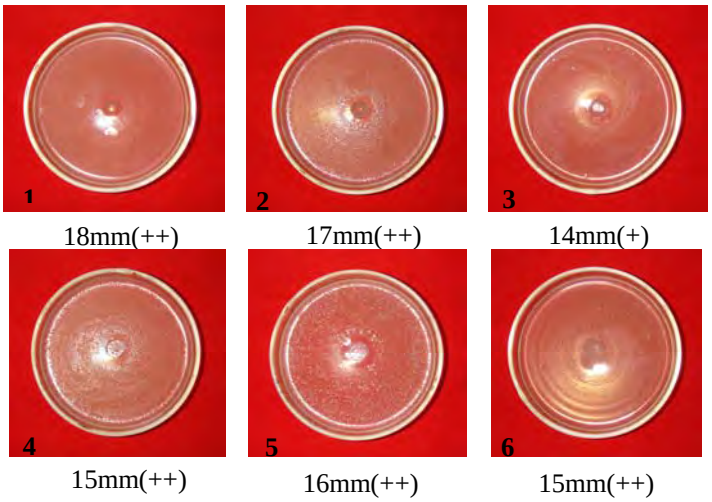

Figure 3. Inhibitory zone of six microorganisms : (1) *B. subtilis* (2) *S. aureus* (3) *P.aeruginosa* (4) *B. pumalis* (5) *C.albicans* (6) *E. coli* on Agar-well Plate affected by red wine of grape

Table 8. Bioactivity of red wine according to agar well plate diffusion test (Agar well – 10 mm)

Types of Microorganisms		Inhibitory Zone	Infection induced by such microorganisms
Gram Positive Bacteria	*Staphylococcus aureus*	17mm (++)	Skin, wound, respiratory, urinary tract, bones and joints, pneumonia, carbuncle, food poison.
	Bacillus subtilis	18mm(++)	Non- pathogenic.
	Bacillus pumalis	15mm(++)	Eye, soft tissue.
Gram Negative	*Pseudomonas aeruginosa*	14mm(++)	Skin, especially at burn sites, wounds,

Types of Microorganisms		Inhibitory Zone	Infection induced by such microorganisms
Bacteria			pressure sore and ulcers , urinary tract.
	E.coli	15mm(++)	Urinary tract, wound, bed sore , dysentery, diarrhea, haemorrhagic , pyelitis, cystitis, appendix abscess, septic wounds, gastroenteritis, peritoritis.
Fungi	*Candida albicans*	16mm(++)	mouth and skin, bloating vaginal, candidacies, poor digestion, fingernail and toenail, inflammation, invasion, vaginal mucosa.

Conclusion

Grape (*Vitis vinifera*) and 85% yield of red wine fermented from grape, cultivated in Tawma Village, Meiktila Township, Mandalay Region have good quality for commercial wine production. Flavonoids, phenolic compounds and tannins are present in the grape pulp, skins, seeds and red wine of grape juice. The occurrence of phytoconstituents and phenolic compounds including anthocyanin and resveratrol has great health benefits to prevent many diseases being encountered around the world. Especially, red wine possesses the bioactivities against some bacteria and fungi and their related diseases. So, grape and red wine made from grape cultivated in Myanmar should be consumed as medicinal foods as well as beverage of moderate drink daily.

Acknowledgements

The author would like to express sincere and profound gratitude to Rector Dr. Maung Thinn and responsible personnel of Meiktila University for giving the opportunity to do this research programme. The author wishes to convey heartfelt gratitude to Professor Dr Chaw Khin, Head of Department, Department of Chemistry, Meiktila University for kindly allowing to make use of the research facilities and for her guidance and advice in this project. Special thanks are also due to the officials from DCPT, Yangon, especially Daw Myint Myint Lwin for their help to measure bioactivity and some physical parameters of grape-wine sample for this project.

References

Corder, R., Mullen, W., Khan, N.Q., Masks, S.C., Wood, E.G., Carrier, M.J, and Crozier, A. (2006), "Red Wine Procyanidins and Vascular Health", *J-nature*, 444, 566, Nov.

Stephanie, D., Wollian, H., Peter, J. (2009), "Alcohol, Red Wine and Cardiovascular Disease", School of Dietetics and Human Nutrition, McGill University, Ste-Anne-de-Bellevue, Quebec, Canada.

Wang, N.S. (2004) "Wine Fermentation", Research Article, Dept. of Chemical Engineering, University of Maryland, College Park, MD 2074-211, EN CH 485.

Determination of Toxic Heavy Metal Contents in Freshwater Fish (Ka-Kadit and Nga-Yant) from Hinthada Township

Aye Aye Mu

Abstract

Ka-kadit (*Lates calcarifer*), and Nga-yant (*Channa striata*) are highly valued fish species and widely consumed in Myanmar. These two selected fish species were collected seasonally from Hinthada Township in Ayeyarwady Region. Seasonal variations of toxic metals (arsenic, cadmium, lead, mercury) contents in two fish species were determined. Cadmium and lead were determined by Graphite Furnace Atomic Absorption Spectrometry (GFAAS). Arsenic and mercury were determined by Flow Injection Atomic Absorption Spectrometry (FIAAS), respectively. In this research slightly higher contents of toxic metals were observed in the hot season (March) and the rainy season (August) than in the cold season (November). Lead was found to be the highest concentration in all fish species. Concentrations of lead were in the range of 0.179 to 0.289 ppm for Ka-kadit and 0.140 to 0.222 ppm for Nga-yant. The toxic metals in order of decreasing concentrations in these fish species were lead>arsenic>cadmium> mercury. In this study, all analyzed samples contained low levels of toxic metals (As, Cd, Pb, and Hg) which were much lower than the maximum permitted levels of Marine Fisheries Research Department (MFRD), Singapore. This study revealed that levels of toxic metals in two types of fish samples in Hinthada Township do not represent significant hazards to consumers from the point of view of toxic heavy metals contents.

Key words: As, Cd, Pb, Hg, *Lates calcarifer*, *Channa striata*, GFAAS, FIAAS

Introduction

Eating fish produces tremendous health benefits (Huss, 1994). It is a good source of high quality and other nutrients and is low in fat. It is often low cost and is an easy to prepare source of good nutrition. Fish is an excellent low-fat food, a great source of protein, vitamins and minerals (Dyer *et al*., 1950).

Lecturer, Dr, Department of Chemistry, Hinthada University

Order, family, scientific name, FAO name, and local name of Ka-kadit and Nga-yant fish samples are mentioned below.

Sea bass are dioecious species. Fish develops either males or females, which otherwise artificially induced, do not change sex during their life time. Sea bass feeds on fish and crustaceans. It is occurred in Ayeyarwady Region in Myanmar, and East Africa (Myint Pe *et al.,* 2005). 'Bass' also refers to a number of freshwater sport fishes (Day, 1978).

Order	Perciformes
Family	Centropomidae (snooks)
Scientific name	*Lates calcarifer*
FAO name	Giant sea perch
Local name	Ka-kadit

The most widely naturally distributed snakehead originated from Pakistan through south East Asia to Yunnan, southern China and India subcontinent to Borneo (Myint Pe *et al.,* 2005).

Order	Channiformes
Family	Channidae (Snake head)
Scientific name	*Channa striata*
FAO name	Striped snake head
Local name	Nga-yant

The term heavy metal refers to any metallic chemical element that has a relatively high density and is toxic or poisonous at low concentrations

(website 1). Heavy metals include mercury (Hg), cadmium (Cd), arsenic (As), chromium (Cr), thallium (Tl), and lead (Pb).

Heavy metals are dangerous because they tend to bioaccumulate in biological organism overtime, compared to the chemical concentration in the environment (Ministry of Agriculture, 1999).Toxic metals can negatively affect people's health (website 2) as they may build up in biological systems to become a significant health hazard.

Even trace amounts of heavy metals are harmful to human health and aquatic life (Stromgren, 1982). Since the presence of trace amounts of toxic metals cannot be directly observed, people may ingest them through drinking water or by eating contaminated fish and meat. Table 1 shows the maximum permitted level in fish and shellfish enforced by various organizations.

Table 1 Maximum permitted level in fish and shellfish enforced by various organizations

Toxic elements	Country			
	Singapore *	USA*	Canada*	Australia*
As	Not more than 1 ppm in fish, crustaceans and mollusks	Not more than 7.6 ppm for crustaceans	Not more than 3.5 ppm in fish and fish products	Not more than 2 ppm of inorganic arsenic in fish and crustaceans
Cd	Not more than 1 ppm in mollusks	Not more than 3 ppm for crustaceans	Not mentioned	Not more than 2 ppm in mollusks
Pb	Not more than 2 ppm in fish, crustaceans and mollusks	Not more than 1.5 ppm for crustaceans	Not more than 0.5 ppm in fish and fish products	Not more than 0.5 ppm in fish
Hg	No more than 0.5 ppm in fish and fish products	Not more than 1 ppm methyl mercury for all fish	Not more than 0.5 ppm of in Hg fish and fish products	Not more than a mean level of 0.5 ppm in fish and fish products

*Marine Fisheries Research Department

Fish are nutritious foods that are popular diet in Myanmar. However, environmental contamination of fish is a growing concern. As Myanmar becomes more populated and industrialized, more pollutants are

contaminated in the air, water and soil. People are exposed to toxicity if they eat the contaminated fish living in polluted water.

The aim of this study was to investigate the seasonal variations of toxic metals (arsenic, cadmium, lead and mercury) concentrations in Ka-kadit (*Lates calcarifer*) and Nga-yant (*Channa striata*) collected from Hinthada Township in Ayeyarwady Region.

Materials and Methods

Sample Collection

Two different fish species, *viz.*, Ka-kadit (*Lates calcarifer*) and Nga-yant (*Channa striata*) were collected from Eik-pyat Inn, about 20 km north of Hinthada Township in Ayeyarwady Region. Weight and length of all fish samples were measured and brought to the laboratory in ice boxes.

The five fish samples from each species were targeted and samples were collected during the hot season (March), the rainy season (August), and the cold season (November). For the analysis of toxic metals in the fish samples, the muscular tissue (flesh) of fish was used.

Methods of Analysis

Sample preparation and technique employed for chemical analysis varied with the type of toxic metal to be determined. Sample preparation included three acid methods (nitric acid, sulphuric acid, and perchloric acid) for arsenic, dry ashing method for cadmium and lead, and reflux method (nitric acid and sulphuric acid) for mercury (AOAC, 2000 and Yasui, *et al.*, 1978).

The techniques employed were Graphite Furnace Atomic Absorption Spectrometry (GFAAS) for cadmium and lead, and Flow Injection Atomic Absorption Spectrometry (FIAAS) for arsenic (hydride generation method) and mercury (Cold Vapour Technique) (Ray, 1994; Low, 2002 a, b, c and d)

Results and Discussions

Seasonal Variation of Arsenic (As) Concentrations in Ka-kadit and Nga-yant Samples

The arsenic concentration in muscular tissue for all fish samples in all seasons did not exceed the maximum permitted levels. It can be seen

from Table 2 and Figure1 that the mean values of arsenic were 0.127±0.003, 0.141±0.007, and 0.117 ±0.005ppm for the hot season, the rainy season, and the cold season. Higher arsenic concentration in Ka-kadit samples were observed in the rainy season and the hot season compared to those in the cold season. However, these values were very much less than the maximum permitted level of 1 ppm (MFRD, 2005).

The arsenic concentration in the hot season, the rainy season, and the cold season for Nga-yant ranged from 0.101 to 0.113 ppm, 0.105 to 0.115 ppm, and 0.081 to 0.096 ppm, respectively.The mean concentrations were 0.105±0.004, 0.109±0.004, and 0.089±0.006 ppm for the hot season, the rainy season, and the cold season (Table 3 and Figure 2). Higher values of arsenic concentration in Nga-yant samples were also observed in the hot season and the rainy season compared to those in the cold season.

Table 2. Seasonal variation of arsenic concentrations in Ka-kadit samples

	Arsenic concentration / ppm		
Fish Sample	Hot season	Rainy season	Cold season
Sample (1)	0.125	0.145	0.121
Sample (2)	0.121	0.149	0.120
Sample (3)	0.128	0.138	0.119
Sample (4)	0.130	0.135	0.116
Sample (5)	0.129	0.141	0.111
Mean value	0.127±0.003	0.141±0.007	0.117±0.005

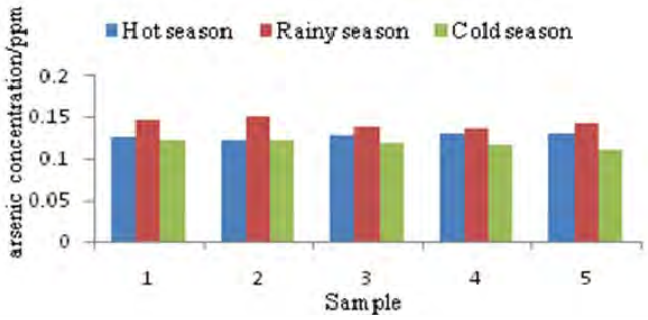

Figure 1. Arsenic concentrations in Ka-kadit samples in various seasons

Table 3. Seasonal variation of arsenic concentrations in Nga-yant samples

	Arsenic concentration / ppm		
Fish Sample	Hot season	Rainy season	Cold season
Sample (1)	0.102	0.109	0.096
Sample (2)	0.101	0.115	0.091
Sample (3)	0.113	0.107	0.083
Sample (4)	0.105	0.105	0.081
Sample (5)	0.108	0.112	0.095
Mean value	0.105±0.004	0.109±0.004	0.089±0.006

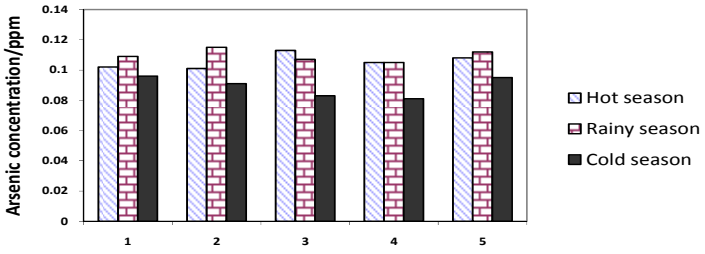

Figure 2. Arsenic concentrations in Nga-yant samples in various seasons

Seasonal Variation of Cadmium (Cd) Concentrations in Ka-kadit and Nga-yant Samples

Seasonal variations of cadmium concentration in Ka-kadit and Nga-yant samples are shown in Tables 4 and 5 and Figures 3 and 4. Mean cadmium concentrations of Ka-kadit samples were 0.094±0.026 ppm, 0.103±0.012 ppm and 0.075±0.032 ppm in hot season, rainy season and cold season respectively. Slightly higher cadmium concentration in rainy season (0.103±0.012 ppm) may be attributed to the discharge of polluted water from streams. However, in Nga-yant samples, mean cadmium concentrations were found to be not much different among three seasons, i.e., 0.075 ppm, 0.078 ppm and 0.077 ppm in hot season, rainy season and cold season respectively.

Table 4. Seasonal variation of cadmium concentrations in Ka-kadit samples

Cadmium concentration / ppm			
Fish Sample	Hot season	Rainy season	Cold season
Sample (1)	0.106	0.098	0.058
Sample (2)	0.065	0.101	0.086
Sample (3)	0.111	0.112	0.031
Sample (4)	0.107	0.108	0.098
Sample (5)	0.081	0.095	0.104
Mean value	0.094±0.026	0.103±0.012	0.075±0.032

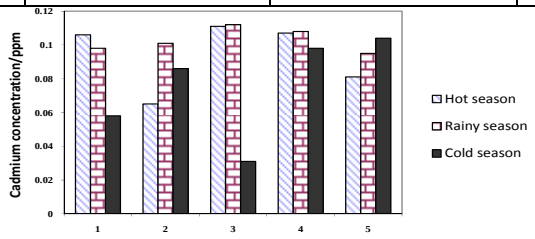

Figure 3. Cadmium concentrations in Ka-kadit samples in various seasons

Table 5. Seasonal variation of cadmium concentrations in Nga-yant samples

Cadmium concentration / ppm			
Fish Sample	Hot season	Rainy season	Cold season
Sample (1)	0.104	0.105	0.091
Sample (2)	0.031	0.061	0.113
Sample (3)	0.101	0.105	0.083
Sample (4)	0.035	0.052	0.043
Sample (5)	0.103	0.058	0.058
Mean value	0.075±0.034	0.078±0.029	0.077±0.025

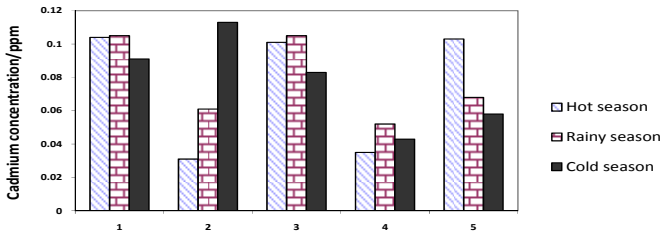

Figure 4. Cadmium concentrations in Nga-yant samples in various seasons

Seasonal Variation of Lead (Pb) Concentrations in Ka-Kadit and Nga-yant Samples

Seasonal variations of lead concentrations in Ka-kadit and Nga-yant samples are shown in Tables 6 and 7 and Figures 5 and 6.

It was noted that mean lead concentrations of Ka-kadit samples were 0.221±0.022 ppm, 0.289±0.010 ppm in the hot season and the rainy season respectively. These values are higher than cadmium concentration in cold season, i.e., 0.179±0.015 ppm. Similarly, mean lead concentration of Nga-yant samples in the rainy season (0.222±0.002 ppm) was found to be slightly higher than those in the hot season (0.179±0.015 ppm), and in the cold season (0.140±0.003 ppm).

The results of all fish samples analyzed indicated that lead concentration in the fish samples in Hinthada Township were below the maximum permitted level of 2.00 ppm (MFRD, 2005).

Table 6. Seasonal variation of lead concentrations in Ka-kadit samples

	Lead concentration / ppm		
Fish Sample	Hot season	Rainy season	Cold season
Sample (1)	0.205	0.298	0.159
Sample (2)	0.213	0.288	0.169
Sample (3)	0.254	0.276	0.183
Sample (4)	0.209	0.286	0.193
Sample (5)	0.226	0.296	0.195
Mean value	0.221±0.002	0.289±0.010	0.179±0.015

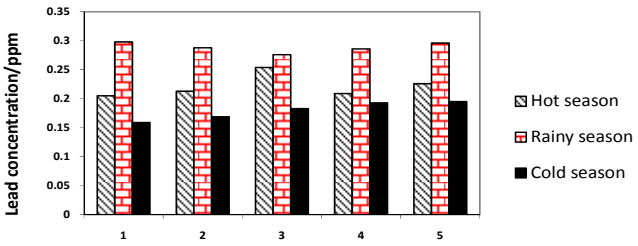

Figure 5. Lead concentrations in Ka-kadit samples in various seasons

Table 7. Seasonal variation of lead concentrations in Nga-yant samples

Lead concentration / ppm			
Fish Sample	Hot season	Rainy season	Cold season
Sample (1)	0.180	0.221	0.141
Sample (2)	0.179	0.223	0.139
Sample (3)	0.171	0.224	0.138
Sample (4)	0.181	0.223	0.144
Sample (5)	0.178	0.220	0.140
Mean value	0.179±0.004	0.222±0.002	0.140±0.003

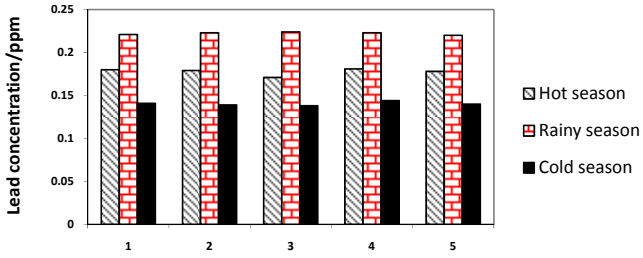

Figure 6. Lead concentrations in Nga-yant samples in various seasons

Seasonal Variation of Mercury (Hg) Concentration in Ka-kadit and Nga-yant Samples

Seasonal variation of mercury concentrations in Ka-kadit and Nga-yant samples are shown in Tables 8 and 9 and Figures 7and 8. It was found

that the mean values of mercury concentration in Ka-kadit samples were not found to be different, *i.e.*, 0.012, 0.011, and 0.010 ppm in all three seasons. It was also noted that mean mercury concentration in Nga-yant samples were 0.010, 0.011, and 0.007 ppm and thus pronounced difference was not observed in three seasons.In this study, all analyzed samples contained low level of mercury which is much lower than the maximum permitted level of 0.5 ppm (MFRD, 2005).

Table 8. Seasonal variation of mercury concentrations in Ka-kadit samples

Mercury concentration / ppm			
Fish Sample	Hot season	Rainy season	Cold season
Sample (1)	0.009	0.008	0.007
Sample (2)	0.010	0.013	0.006
Sample (3)	0.015	0.012	0.011
Sample (4)	0.011	0.011	0.010
Sample (5)	0.016	0.013	0.013
Mean value	0.012±0.003	0.011±0.002	0.010±0.003

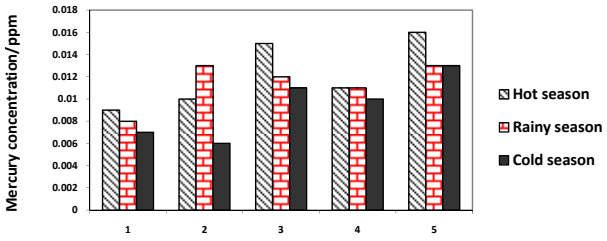

Figure 7. Mercury concentrations in Ka-kadit samples in various seasons

Table 9. Seasonal variation of mercury concentrations in Nga-yant samples

Mercury concentration / ppm			
Fish Sample	Hot season	Rainy season	Cold season
Sample (1)	0.003	0.008	0.008
Sample (2)	0.014	0.015	0.009
Sample (3)	0.010	0.011	0.005
Sample (4)	0.011	0.007	0.004
Sample (5)	0.012	0.013	0.010
Mean value	0.010±0.003	0.011±0.002	0.007±0.004

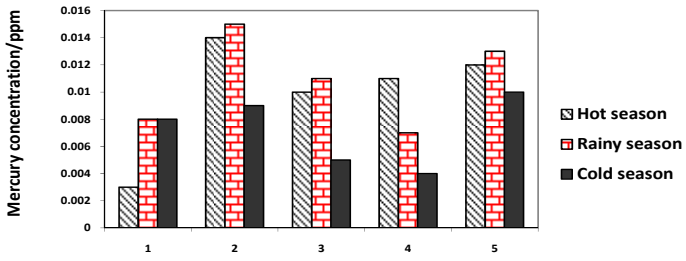

Figure 8. Mercury concentrations in Nga-yant samples in various seasons

Conclusion

Seasonal distributions of toxic metals (As, Cd, Pb, and Hg) in two different fish species, Ka-kadit (*Lates calcarifer*) and Nga-yant (*Channa striata*) collected from Hinthada Township, Ayeyarwady Region were investigated in this study.

The mean values of arsenic concentration in Ka-kadit samples were 0.127, 0.141, and 0.117 ppm for the hot season, the rainy season, and the cold season, respectively. In Nga-yant samples, the mean values of arsenic concentration were 0.105, 0.109, and 0.089 ppm for the hot season, the rainy season, and the cold season, respectively.

Mean cadmium concentrations in two different fish species during seasonal changes were 0.075 to 0.103 ppm in Ka-kadit samples and 0.075 to 0.078 ppm in Nga-yant samples. Moreover, mean values of lead concentrations for Ka-kadit and Nga-yant samples in the hot season, the rainy season and the cold season were observed as 0.221 and 0.179 ppm, 0.289 and 0.222 ppm and 0.179 and 0.140 ppm respectively. Mean values of mercury concentrations in Ka-kadit and Nga-yant samples were 0.012, 0.011 and 0.010 ppm and 0.010, 0.011, and 0.007 ppm for the hot season, the rainy season, and the cold season, respectively.

In both types of fish species analyzed, *viz.*, Ka-kadit and Nga-yant samples, lead was found to be the most dominant toxic metal. However, lead concentrations in these fish samples were lower than the acceptable limit of 2.00 ppm. Decreasing order of concentrations of toxic metals in the fish species was: Pb > As > Cd > Hg. Toxic metals were present in both

types of fish samples but higher concentrations of toxic metals were observed in the hot season and the rainy seasons.

This research findings indicate that although the toxic metals of interest were found in measurable quantities, they are still lower than the safe limits proposed by Marine Fisheries Research Department (MFRD), Singapore, and so the Ka-kadit and Nga-yant fish species from Hinthada Township, Ayeyarwady Region are health safety and suitable for consumption.

Acknowledgements

The author is grateful to Rector Dr Tin Tun Myint and Pro-Rector Dr Si Si Hla Bu, Hinthada University, Hinthada, for their permission to conduct this research work. The author also wishes to express sincere gratitude to Dr Than Htut Oo, Pro-Rector of Myeik University, for his invaluable suggestions and detailed and specific instructions on this research work.

References

AOAC, (2000), Official Methods of Analysis of International, *Association of Official Analytical Chemists* **1**, 17th ed., New York.

Day, F., (1878), "The Fish of India, being a Natural History of the Fish known to Inhibit the Sea and Freshwater of India, Burma, and Ceylon", Today and Tomorrow's Book Agency, New Delhi, 301-335.

Dyer, W. J., French, H. V., and Snow, J. M., (1950), "Proteins in Fish Muscle, I., Extraction of Protein Fractions in Fresh Fish", *J. Fisheries Research Board Can.***7**: 585-593.

Huss, H. H., (1994), "Assurance of Sea Food Quality", *FAO Fisheries Tech*., **I**: 339-401

Low, L. K., (2000a), "Method F-1, Sample Preparation by Reflux Method (Nitric Acid and Sulphuric Acid)", In "Laboratory Manual on Analytical Methods and Procedures for fish Products", 2nd Edn., MFRD, SEAFDEC: 201-203.

Low, L. K., (2000b), "Method F-4, Determination of Total Mercury in Fish Tissue by Flow Injection Cold Vapour Atomic Absorption Spectrometry", In "Laboratory Manual on Analytical Methods and Procedures for Fish and Fish Products", 2nd Edn., 2nd Edn., MFRD, SEAFDEC, Singapore.

Low, L.K., (2002c), "Method F-3, Sample Preparation by Dry Ashing Method", In "Laboratory on Analytical Methods and Procedures for Fish and Fish Products", 2ndEdn. MFRD, SEAFDEC, Singapore.

Low, L.K., (2002d), "Method F-6, Determination of Total Cadmium in Fish Tissue by Graphite Furnace Atomic Absorption Spectrometry", In "Laboratory

Manual on Analytical Method and Procedure for Fish and Fish Products", 2nd Edn., MFRD, SEAFDEC, Singapore: 209-233.

MFRD, (2005), "On-site Training on Heavy Metals Analysis", South East Asia Fisheries Development Centre (SEAFDEC), Singapore.

Ministry of Agriculture, (1999), "Fisheries and Food, Total Diet Study": "Metals and Other Elements", Food Surveillance Information Sheet **191**: 239-391.

Myint Pe, Vidthayanon, C. and Termvidchakorn, A., (2005), "Inland Fisheries of Myanmar", Department of Fisheries, Thailand. Southeast Asian Fisheries Development Center: 100-150.

Ray, S., (1994), "Cadmium-Analysis of Contaminants in Edible Aquatic Resources-General Considerations: Metals, Organo metallics, Tainting and organics", VCH Publishers, New York: 91-115.

Stromgren, T., (1982), "Effect of heavy metals (Zn, Hg, Cu, Cd, Pb, Ni) on the length growth of *Mytilus edulis", Mar Biol.***72**: 69-72.

Yasui, A., Tsutsumi, C., and Toda, S., (1978), "Selective determination of Inorganic Arsenic III, V and Organic Arsenic in Biological Materials by Solvent Extraction – Atomic Absorption Spectrophotometry", *Agric. Biol. Chem.*, **2**: 2139-2145.

Online materials

1. http:// w.w.w. luminet. net/ venonah/ hydro/ heavmet. htm

2. http: // w.w.w. fda.gov/ fdac/ reprints / mercury. htm/

Extraction of Casein and Determination of its Components from Three Kinds of Milk

Khine Zar Wynn Lae[1] and Aye Aye Cho[2]

Abstract

In this research work, cow, goat and buffalo milk were collected and the protein and sugar tests were carried out which gave rise to positive for protein and trace amount of sugar. Moreover, casein protein was extracted from each sample. It was found that cow milk contains 45.36% of casein, goat milk contains 5.47% of casein and buffalo milk contains 14.07% of casein. According to these data, cow milk contains the largest amount of casein. The elemental analysis of casein compounds were determined by using Atomic Absorption Spectroscopy (AAS). From these determinations, all three milk samples contain the sufficient amount of minerals. In other words, the three samples contain adequate amount of nutrients in suitable proportion that maintain the health of an individual.

Key words: casein protein, cow, goat, buffalo, Atomic Absorption Spectroscopy (AAS)

Introduction

Casein (from Latin causes "cheese") is the predominant phosphoprotein that accounts for nearly 80% of proteins in cow milk and cheese. Casein protein is basically the most important protein that can be found in milk(Horne, 2002).

An improved dietary supplement for mammals includes the essential dietary trace metals such as iron, copper and molybdenum. These metals are provided in a highly bioavailable state such as peptide and polypeptide chelates. This invention also includes a method for using natural proteinaceous starting materials for producing the peptide and polypeptide ligands for the chelates. The proteinaceous starting materials are obtained from a primary grown yeast, an isolated vegetable protein, dessicated tissues of animal origin and the like which, upon hydrolysis, yields the peptide and polypeptide ligands suitable for forming chelates with the iron, copper and molybdenum.

1. Assistant Lecturer, Dr, Department of Chemistry, University of Yangon
2. Professor and Head, Dr, Department of Chemistry, Myingyan Degree College

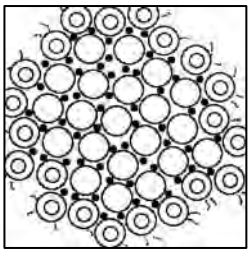

Figure 1. Casein structure

Casein protein is the majority of muscle repairing and rebuilding take place during sleep. For optimal recovery, the body needs a constant of nutrients, and most importantly, protein. When taken before bed, whey protein will be absorbed with about 45 minutes, leaving the body without a protein source for up to 8 hours. Micellar casein will provide the body with a protein source for up to 7 hours, greatly reducing muscle catabolism (Holt and Horne, 1996).

The objective of the current study is to investigate the composition of casein protein in three kinds of milk. The essential analysis of casein compounds were determined by using Atomic Absorption Spectroscopy (AAS).

Materials and Methods

The cow, goat and buffalo milk samples were collected from Mandalay area. The protein tests such as Xanthoprotein test, Biuret test and Denaturation test, of three samples were carried out. Sugar tests were also determined.

Caseins were isolated from the three kinds of milk samples which has pH of about 7. Casein will be separated as an insoluble precipitate of the milk to its isoelectric point (pH = 4.6). The fat that precipitates along with casein can be removed by dissolving it in alcohol. These precipitate milk products are protein. The identification will be achieved by performing a few important chemical test which are Biuret test, Ninhydrin test and Xanthoprotein test. The mineral contents of extracted casein protein from these three samples were determined by Atomic Absorption Spectroscopy (AAS).

Results and Discussion

The protein test for three milk samples were carried out. These data were tabulated in the following Table 1.

Table 1. Results of protein tests

No.	Protein Test	Observation	Results		
			Cow milk	Goat milk	Buffalo milk
1.	Xanthoprotein	Yellow	+	+	+
2.	Biuret	Pink	+	+	+
3.	Denaturation	Denature	+	+	+

Based on the observation, these three milk samples gave positive test for protein. Therefore, these samples may contain casein protein.

These three samples were tested the reducing sugar by using benedict solution. These were shown in the following Table 2.

Table 2. Results of Sugar Test

No.	Sample	Observation	Results
1.	Cow milk	Green	+
2.	Goat milk	Green	+
3.	Buffalo milk	Green	+

The casein content of three milk samples were described in the following Table 3.

Table 3. Casein protein from three milk samples

No.	Sample	Casein protein (%)
1.	Cow milk	45.36%
2.	Goat milk	5.47%
3.	Buffalo milk	14.07%

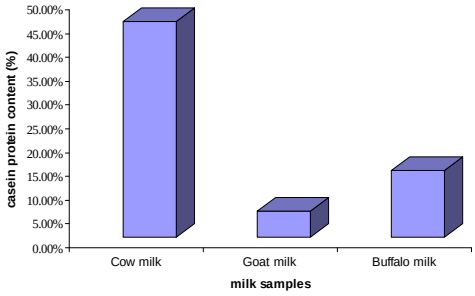

Figure 2. Casein protein from three milk samples

The elemental analyses of these three casein proteins were shown in the following Table 4.

Table 4. Elemental analyses of casein proteins from three milk samples

No.	Protein Test	Results		
		Cow milk (ppm)	Goat milk (ppm)	Buffalo milk (ppm)
1.	Calcium (Ca)	507	662	523
2.	Iron (Fe)	140	148	117
3.	Potassium (K)	348	1879	621
4.	Magnesium (Mg)	189	330	165
5.	Manganese (Mn)	12	10	16
6.	Sodium (Na)	219	767	395
7.	Zinc (Zn)	58	50	31

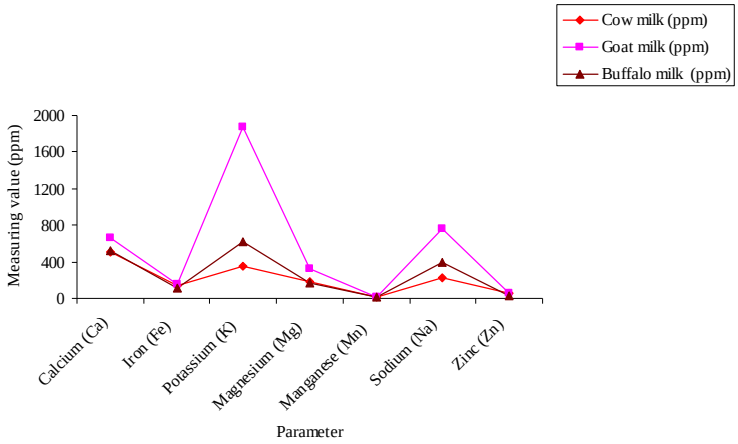

Figure 3. Elemental analyses of casein proteins from three milk samples

Calcium, magnesium, sodium and potassium are macrominerals for human that are required in amounts greater than 100 mg per day. Iron, zinc and manganese are microminerals for trace elements that are required in amounts less than 100 per day.

According to these results, all three samples contain the sufficient amount of minerals. In other words, the three samples contain adequate amount of basic nutrients in suitable proportion that maintain the health of an individuals.

Casein and lactose are found in the milk of every mammal, although in varying ratios. According to these data, cow milk contains the largest amount of casein protein. Thus, the cow milk is suitable for the best muscle growth and basic body building achievement.

Goat milk contains the small amount of the casein protein content. Goat milk protein forms a softer curd which makes the protein more easily and rapidly digestible. Theoretically, this more rapid transit through the stomach could be an advantage to infants and children who regurgitate cow's milk easily. Goat's milk may also have advantages when it comes to allergies. Goat's milk contains only trace amounts of an allergenic casein protein, alpha-S1, found in cow's milk. Goat's milk casein is more similar to human milk, yet cow's milk and goat's milk contain similar levels of the other allergenic protein, beta lactoglobulin. Some mothers are certain that their child tolerates goat's milk better than cow's milk.

So people who have an unusual milk allergy, or who are merely lactose may find goat milk more digestible other than cow's milk (Kurek *et al.*, 1992 and Millward *et al.*, 2008).

Conclusion

From this research work, it was found that three samples of milk contain casein protein. Moreover, the casein contents were observed 45.36%, 5.47% and 14.07% in cow milk, goat milk and buffalo milk respectively.

According to the research findings, cow milk contains the largest amount of casein protein. Thus, the cow milk is suitable for the best muscle growth and basic body building achievements. It was found that goat milk contains the small amount of casein protein. Although the mineral content of goat's milk and cow's milk is generally similar, goat's milk contains more calcium, potassium, iron, magnesium and sodium.

All milk has lots of casein but there are different types of casein and for someone who has casein sensitivity, goat milk may provide an alternative to which they do not react.

Acknowledgements

The authors would like to thank Rector, Dr Tin Tun, University of Yangon and Professor and Head, Dr Nilar, Department of Chemistry, University of Yangon, for their valuable advice and permission.

References

Holt C., and Horne D.S., (1996), "The hairy casein micelle: evalution of the concept and its implication for dairy technology". *Neth. Milk Dairy J*.**50**: 85-111.

Horne D.S., (2002), "Casein structure, self-assembly and gelation, current opinion in colloid and interface", *Sci*, **7**: 456-461.

Kurek M., Przybilla B., Hermann K. and Ring J., (1992), "A naturally occurring opioid peptide from cow's milk, beta-casomorphine-7, is a direct histamine releaser in man", 97.

Millward C., Ferriter M., Calver S., and Connell-Jones G., (2008), "Gluten and casein-free diets for autistic spectrum disorder", Cochrane Database of systematic Review, Issue **2**, Art. No. CD003498. DOI; 10.1002.

Study on Reaction between Se (IV) and Variamine Blue and its Application for Determination of Selenium (IV) Contents in Some Vegetables

Sandar Tun[1], Kyaw Naing[2] and San San Myint[3]

Abstract

In this research, determination of selenium is based on the reaction of Se (IV) with iodide ion to liberate iodine, which oxidizes variamine blue (light blue) to form a violet-colored product. The violet-colored products formed in the reaction were measured spectrophotometrically. The wavelength of maximum absorption of the colored product was formed at 530nm. Standard calibration curve was constructed using different concentration of Se (IV). The straight line passed through the origin and Beer's law was obeyed in the range of 0.64 to 6.99×10^{-5}M. The molar extinction coefficient and Sandell's sensitivity were determined to be 7.9×10^{3} dm^3 $mol^{-1}cm^{-1}$ and 0.0109 μg cm^{-2}, respectively. In this research, the effect of acidity (HCl molar concentration) on the reaction between selenium (IV) and variamine blue were studied under three different concentrations of KI (0.1, 0.2 and 0.3 %). The acidity of the solution was varied between 0.0125 to 0.4 M. It was found that maximum absorbance at 530 nm was attained at 0.2 M HCl and 0.2 % KI.The effect of KI concentration on the reaction was studied by changing the concentration from 0.05 to 0.9 %. At 0.2% KI solution the color development is maximum.The color of the oxidized form the variamine blue was stable up to 15 min and after that absorbance decreased slowly.In this research, effects of interfering ions (Ca^{2+}, Zn^{2+}, Ni^{2+}, Cu^{2+}, Pb^{2+}, Hg^{2+}, Na^{+}, K^{+}, Mg^{2+}, Cd^{2+}, Fe^{2+}, Fe^{3+}) on the reaction between selenium (IV) and variamine blue were studied. In this work, determination of error percents for selenium were carried out using three model solutions (lake water, tap water and Hlaing river water mixing with standard selenium (IV) solution). In this study, totally 27 vegetable samples were collected and selenium (IV) determinations were carried out. The contents of selenium in the samples were found to be lower than that of USEPA acceptable level of 2.5 ppm in vegetables.

Key words*:* Selenium,variamine blue,Sandell's sensitivity, USEPA

1. Assistant Lecturer, Department of Chemistry, West Yangon University
2. Professor, Dr, Department of Chemistry, University of Yangon
3. Lecturer, Dr, Department of Chemistry, University of Yangon

Introduction

Selenium is one of the trace element which plays an active role in many biological system as it has toxicological and physiological effects (Melwanki, and Seetharamappa, 2000). This element is an essential nutrient for humans and animals, although excesses have been known to cause toxicity. On the other hand, selenium-deficiency, syndromes have also been reported. Particularly its compounds protect the cell membrances from oxidative damage, catalyze reactions of the intermediate metabolism and inhibite the toxicity of some heavy metals. Selenium compounds can be widely spread throughout the environment as a result of the combustion of coal, as well as throughout industrial and agricultural processes (Pyrzynska, 1997).

Selenium deficiency was identified in parts of the world known for their low soil content of selenium, such as volcanic regions. Association of selenium intake and Keshan disease, a congestion cardiomyopathy in Chinese children. Some epidemiological studies revealed that there was an inverse correlation between cardiovascular disease and selenium status. A large number of different selenoproteins that carry out nutritional functions of selenium have been identified. The best known biochemical role of selenium is its function as part of the enzyme glutathione peroxidase which protects vital components of cells against oxidative damage (Sirichakwal *et.al*.,2005). It is also involved in thyroid metabolism through iodothyronine-deiodinase enzyme (Arthur *et al*., 1993).

The dietary intake of selenium depends on its concentration in food and the amount of food consumed. The selenium content of food varies depending on the content of the element in the soil where the animal was raised or the plant was grown. Food is the main source of selenium for humans. The dietary intake of selenium varies considerably across populations around the world because of the large variability of the selenium content of foods. Therefore, it is necessary to monitor the selenium content in representative and widely consumed foods in each country (Khairia, 2009)

Materials and Methods

Reagents and Solutions

All of the chemicals used were of analytical-reagent grade, and were provided by Merck and BDH, and distilled water was used throughout the

study. A stock standard selenium (IV) solution (1000μg/mL) was prepared by dissolving 1.912g of sodium hydrogen selenite in 1L distilled water. A working standard solution was prepared by a suitable dilution of the standard solution. A 0.05% of variamine blue was prepared by dissolving 50mg of viriamine blue in 25mL methanol and made up to 100mL with distilled water. A 2% of potassium iodide was prepared by dissolving 2g of potassium iodide in 100 mL distilled water. A 2 M of hydrochloric acid was prepared by dissolving 17.7mL of hydrochloric acid in 100mL distilled water (Vogel, 1968). A 1M of sodium acetate solution was prepared by dissolving 13.6g of sodium acetate trihydrate in 100mL distilled water. An Apel UV-visible spectrophotometer (PD-303)was used for absorbance measurements.

Results and Discussion

The Proposed Chemical Reaction for Se (IV) Determination

$$Se\ (IV) + 4I^- + 6H^+ \rightarrow Se^o + 2I_2 + 3H_2O$$

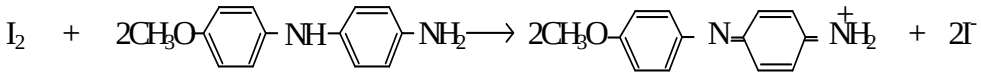

Leuco form of VB **violet-colored species**

Absorption Spectra

Figure 1 shows the reaction between Se(IV) and iodide ion was studied in the presence of variamine blue. The oxidized product iodine react with variamine and violet-coloured product was obtained. The wavelenght of maximum absorption (λ_{max}) of the violet-colored product formed the reaction between Se(IV) and variamine blue was found to be at 530nm.

Figure 2 shows the standard calibration curve is linear and passing the origin, indicating that Beer's law was well obeyed in the range of 0.64 to 6.99×10^{-5} M. The molar extinction coefficient and Sandell's sensitivity were determined to be 7.9×10^{3} dm^3 mol^{-1} cm^{-1} and 0.0109 μg cm^{-2}, respectively.

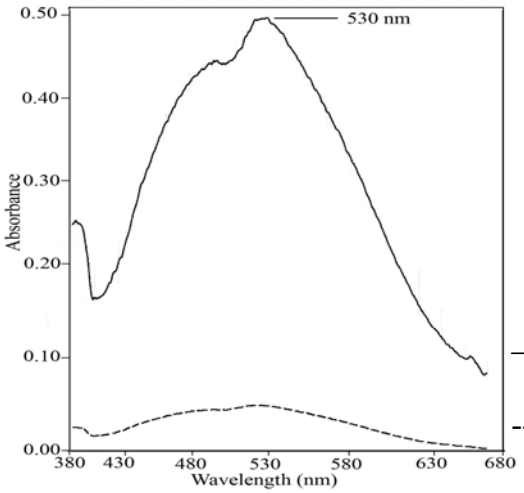

__Se (2.54×10^{-5}M) +VB (0.05%)

---VB (0.05%)

Figure 1. Absorption spectra of the product from the reaction between Se (IV) and variamine blue

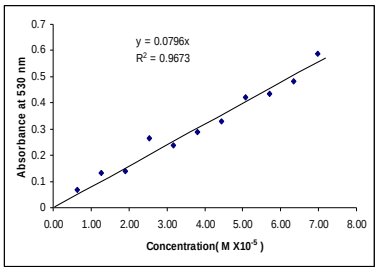

Figure 2. Standard calibration curve (A_{530} *vs* Conc: of Se(IV))

Effect of Acidity

Figure 3 shows the effects of acidity (HCl molar concentration) on the reaction between selenium (IV) and variamine blue were studied under three different concentrations of KI (0.1, 0.2 and 0.3 %). The acidity of the solution was varied between 0.0125 to 0.4 M. It was found that maximum absorbance at 530 nm was attained at 0.2 M HCl and 0.2 % KI.

Effect of Concentration of Potassium Iodide

Figure 4 shows the effect of KI concentration on the reaction was studied again by changing the concentration from 0.05 to 0.9 %. At 0.2% KI solution the color development is maximum.

Effect of Reaction Time

Figure 5 shows the reaction time required for maximum color development was determined. The color of the oxidized form the variamine blue was stable up to 15 min and after that absorbance decreased slowly.

Effect of Interfering Ions

Table 1 shows effects of interfering ions (Ca^{2+}, Zn^{2+}, Ni^{2+}, Cu^{2+}, Pb^{2+}, Hg^{2+}, Na^{+}, K^{+}, Mg^{2+}, Cd^{2+}, Fe^{2+}, Fe^{3+}) on the reaction between selenium (IV) and variamine blue were studied. The tolerance limits and tolerance ratios were calculated. All results showed the acceptable error percent < 5%.

Error Percents for Selenium Determination using Model Solutions

Error percents for selenium determinations were found to be 4.105, 1.885 and 4.884% for lake water, tap water and Hlaing river water model solutions. Error percent was the highest for Hlaing river water model solution due to the presence of large number of interfering ions in the Hlaing river water, whereas error percent was the lowest for tap water model solution (Table 2).

Determination of Selenium (IV) Contents in Some Vegetables

In this research, selenium contents of broccoli samples were found to be 1.171, 1.381 and 0.910 ppm. Selenium contents of cabbage sample were found to be 0.045, 0.096 and 0.071 ppm. Selenium contents of garlic samples were found to be 1.844, 1.951 and 1.590 ppm (Tables 3,4 and 5).

Selenium content was found to be the highest (1.951 ± 0.0276) ppm in garlic sample, whereas the lowest (0.045 ± 0.0084) ppm in cabbage sample(Table 6)

The USEPA recommended the acceptable level in vegetables is 2.5ppm.

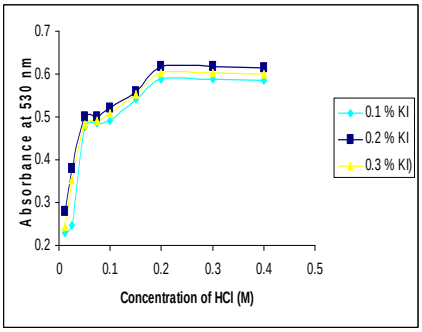

Figure 3. A plot of absorbance of selenium (IV) and variamine blue

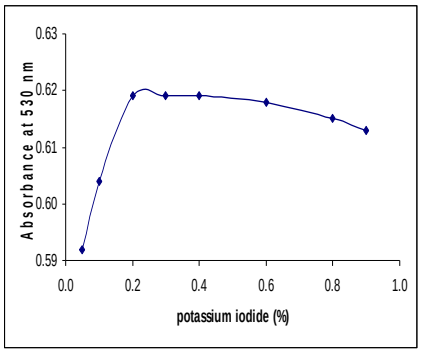

Figure 4. Variation of absorbance of selenium (IV) variamine blue adduct with concentration of potassium iodide percent

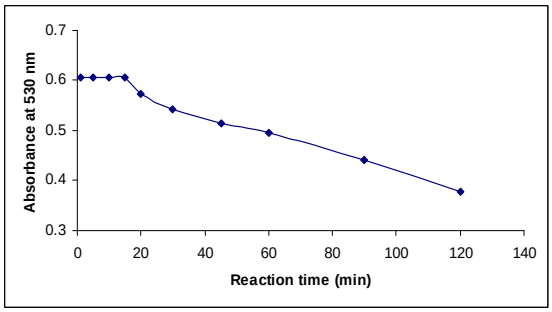

Figure 5. A plot of absorbance the oxidized product at 530nm as a function of reaction time

Table 1. Tolerance Limit[a] and tolerance ratio[b] of interfering ions on the reaction between selenium (IV) and variamine blue

No.	Interference ion	Tolerance ratio	Tolerance limit(ppm)	Error %
1	Ca^{2+}	50	100	3.00
2	Zn^{2+}	50	100	1.00
3	Ni^{2+}	50	100	1.50
4	Cu^{2+}	50	100	0.50
5	Pb^{2+}	50	100	-0.50
6	Hg^{2+}	50	100	-2.50
7	Mg^{2+}	50	100	2.00
8	Na^{+}	50	100	-2.00
9	K^{+}	50	100	-0.50
10	Fe^{2+}	25	50	3.50
11	Fe^{3+}	25	50	4.00
12	Cd^{2+}	25	50	1.00

a. tolerance limit was defined as ratio that cause less than 5% interference

b. tolerance ratio $= \frac{[\text{Interference ion}]}{[Se^{4+}]} = \frac{100}{2} = 50$

Table 2. Error percents for selenium determination using model solutions

Sr. No.	Model sample	Absorbance at 530 nm	Concentration of Se (ppm)	Error (%)
1	Lake water (WYU)	0.029	0.1144	-
2	Lake water (WYU) + standard Se solution*	0.514	2.0276	4.105
3	Tap water (WYU)	0.023	0.0907	-
4	Tap water (WYU) + standard Se solution*	0.520	2.0513	1.885
5	Hlaing river water (Insein)	0.072	0.2840	-
6	Hlaing river water (Insein) + standard Se solution*	0.551	2.1736	4.834

* Concentration of Se = 2 ppm (Absorbance at 530 nm = 0.507)

WYU = West Yangon University

Table 3. Selenium (IV) content in broccoli samples

Broccoli	Absorbance at 530 nm	Selenium content (ppm)	Mean ± SD (ppm)
Sample (1)	0.416 0.421 0.424	1.159 1.173 1.181	1.171±0.0113
Sample (2)	0.493 0.496 0.498	1.373 1.382 1.387	1.381±0.0069
Sample (3)	0.331 0.323 0.326	0.922 0.900 0.908	0.910±0.0278

Table 4. Selenium (IV) content in cabbage samples

Cabbage	Absorbance at 530 nm	Selenium content (ppm)	Mean ± SD (ppm)
Sample (4)	0.019 0.016 0.013	0.053 0.045 0.036	0.045±0.0084
Sample (5)	0.039 0.034 0.031	0.108 0.095 0.086	0.096± 0.0111
Sample (6)	0.024 0.029 0.023	0.067 0.081 0.064	0.071±0.0089

Table 5. Selenium (IV) content in garlic samples

Garlic	Absorbance at 530 nm	Selenium content (ppm)	Mean ± SD (ppm)
Sample (7)	0.643 0.684 0.659	1.791 1.905 1.836	1.844±0.0575
Sample (8)	0.693 0.706 0.718	1.930 1.967 1.981	1.951±0.0276
Sample (9)	0.571 0.575 0.566	1.591 1.601 1.577	1.590±0.0126

Table 6. Selenium (IV) contents in some vegetable samples

No.	Sample	Selenium contents (ppm)		
1	Garlic	1.951 ± 0.0276	1.844±0.0575	1.590±0.0126
2	Eggplant	1.671±0.0165	1.408±0.0070	1.299±0.0085
3	Spinach	1.421±0.0097	1.386±0.0042	1.077±0.0141
4	Broccoli	1.381±0.0069	1.171±0.0113	0.910±0.0278
5	Roselle	1.014±0.0111	0.733±0.0084	0.693±0.0153
6	Silver snow mushroom	0.646±0.0100	0.566±0.0084	0.348±0.0100
7	Okra	0.611±0.0139	0.452±0.0098	0.359±0.0128
8	Cauliflower	0.443±0.0155	0.373±0.0128	0.303±0.0152
9	Cabbage	0.096±0.0111	0.071±0.0089	0.045±0.0084

Conclusion

In this research work, the reaction between Se(IV)and iodide ion was studied in the presence of variamine blue. In this work, the effect of acidity (HCl molar concentration on the reaction between selenium (IV) and variamine blue were studied. The effect of KI concentration on the reaction was studied by changing the concentration from 0.05 to 0.9%. At 0.2% KI solution the color development is maximum. The changes of absorbance of the oxidized variamine blue with reaction time were determined. The color system was stable up to 15min. In this research, effects of interfering ions on the reaction between selenium (IV) and variamine blue were determined. The error percents for the selenium determination in model solutions were calculated. The proposed method has been applied for the determination of selenium in some vegetable samples.

Acknowledgements

The authors would like to express sincere gratitude to Professor, Dr Nilar, Head of Department of Chemistry, University of Yangon, for her kind provision of the research facilities. Grateful thanks are due to Dr Theingi Hlaing, Professor and Head, Department of Chemistry, West Yangon University for her encouragement.

References

Arthur, J. P., Nicol, F., and Beckett, G. J., (1993), "Selenium Deficiency Thyroid Hormone Metabolism and Thyroid Hormone Deiodinases", *Am. J. Clin. Nutr*., **57**, 235-239

Khairia, M. A., (2009), "Selenium Content in Selected Foods from the Saudi Arabia Market and Estimation of the Daily Intake", *Arabian Journal of Chemistry*, **2**, 95-99

Melwanki,M.B., and Seetharamappa, J., (2000), "Spectrophotometric Determination of Selenium (IV) Using Methdilazine Hydrochloride", *Turk.J. Chem.,* **24,** 287-290

Pyrzynska, K., (1997), "Spectrophotometric Determination of Selenium with 1-Napthyloamine -7- Sulfonic Acid", *Analytical Science*, **13,** 629-632

Sirichakwal, P. P., Puwastien, P., and Polngam, P., (2005), "Selenium Content of Thai Foods", *Journal of Food Composition and Analysis*, **18**, 47-59

Vogel, A.I.,(1968), "A Textbook of Quantitative Inorganic Analysis Including Elementary Instrumental Analysis", Longmans, Green and Co., Ltd., London, 315-320

Structure Elucidation of Bioactive Pure Glycosidic Diterpene Compound Isolated from the Root of *Launaea secunda* Hook (Dauk-khwa)

Myint Myint Khaine[1] and Myint Myint Sein[2]

Abstract

In this research work, one Myanmar indigenous medicinal plant, namely *Launaea secunda* Hook. (Dauk-khwa) was selected for chemical analysis. According to the phytochemical tests, the root of Dauk-khwa contains alkaloid, steroid, terpene, sugar, glycoside, phenolic compound and polyphenol. Moreover, antimicrobial activities of the crude extract of root of this plant in various solvent systems were tested by agar well diffusion method on six organisms, such as *Bacillus subtilis, Staphylococcus aureus, Bacillus pumalis, Pseudomonas aeruginosa, Candida albicans* and *Mycobacterium* species. The ethyl acetate extract of the root of Dauk-khwa responds high antimicrobial activities on all selected organisms. A bioactive organic compound (MMK-1) was isolated from the root of *Launaea secunda* Hook. (Dauk-khwa) by using Thin Layer and Column Chromatographic methods. Pure yellowish brown oily form compound (22.0 mg) was obtained and the yield percent was found to be (1.162%) based upon the ethylacetate crude extract. This pure compound gave positive for terpene and glycoside tests. The antimicrobial activities of isolated pure compound were rechecked by agar well diffusion method on six selected organisms and this pure compound gave medium activities on five tested organisms except *Bacillus subtilis.* In addition, the molecular formula ($C_{26}H_{44}O_6$) and the complete planar structure of compound (MMK-1) were elucidated by spectroscopic methods such as FT-IR, ^{1}H NMR (500 MHz), ^{13}C NMR (125 MHz), DEPT, HMQC, HMBC, DQF-COSY and FAB mass spectral data. Finally, conformational structure and absolute configuration containing (10) chiral carbons of compound (MMK-1) was determined by using ^{1}H NMR, splitting patterns, coupling constant (J-values), NOESY spectral data and model studies. The IUPAC name of elucidated pure compound is (2R, 3S, 4S, 5S, 6S)-2-((2S, 4aS, 4bS, 7S, 10aR)-7-ethyl-1, 1, 4a, 4b-tetramethyl-1, 2, 3, 4, 4a, 4b, 5, 6,7,9,10,10a-dodecahydrophenanthren-2-yloxy)-6-(hydroxymethyl) tetrahydro-2H-pyran-3, 4, 5-triol.

Key words: *Launaea secunda* Hook, FT-IR, ^{1}H NMR, ^{13}C NMR, DEPT, HMQC, HMBC, DQF-COSY, FAB mass

1. Assistant Lecturer, Dr, Department of Chemistry, University of Mandalay
2. Professor and Head, Dr, Department of Chemistry, University of Mandalay

Introduction

In Myanmar, traditional Myanmar medicinal plants have been used for many years. Even after the introduction and wide spread of modern western medicines, traditional medicinal plants are still widely used for prevention and cure. However, there is a few limited scientific knowledge on Myanmar medicines. Hence, it is necessary to look into Myanmar medicinal plants in scientific ways so that people can get access to safe and reliable Myanmar medicines.

Traditional medication involves the uses of herbal medicines, animals, plants and minerals. Herbal medicines include herbs, herbal materials, herbal preparations and finished herbal products that contain as active ingredients present in parts of plants, or other plant materials or combinations.

Medicinal plants are important sources for pharmaceutical manufacturing. Medicinal plants and herbal medicines account for a significant percentage of the pharmaceutical market. Research in natural products aimed for drug discovery may serve as leads for the development of new pharmaceuticals that address unmet therapeutic needs.

Traditional medicine is a truly inherited profession whose development has interrelations with the natural and climate conditions, thoughts and convictions and the social system of Myanmar. Traditional medicine in Myanmar is widely practised by the majority of population, partly as an alternative to modern medicine (Bodekerl and Kronenborg, 2002)

Medicinal plants have played a significant role in many ancient traditional systems of medication. These plants may save many lives if they are used correctly. The use of plants based products for disease prevention and treatment has become increasingly popular in ASEAN countries. (Bulletin, 1996)

Myanmar traditional medicine is a broad, deep and delicate branch of science covering various basic medicinal knowledge, different treaties, a diverse array of therapies and potent medicine. Local people in Yenangyaung used this species for dysentery and diabetic. Dauk-khwa is found in Meiktila District and Yenangyaung Township, Magway Region. The root of Dauk-khwa was used for the treatment of dysentery and diabetic.

In this research work, *Launaea secunda* Hook. (Dauk-khwa) was selected for chemical analysis. A pure bio-active organic compound (MMK-1) was isolated from the root of Dauk-khwa by using Thin Layer and Column Chromatographic methods.

The conformational structure of pure organic compound (MMK-1) could be determined by modern spectroscopic methods such as ^{1}H NMR (500 MHz), ^{13}C NMR (125 MHz), DEPT, DQF-COSY, HMQC, HMBC, NOESY and FAB-Mass spectroscopy, respectively (Nelson, 2003).

Botanical Description of Selected Plant

Family	:	Asteraceae
Botanical name	:	*Launaea secunda* Hook.
Myanmar name	:	Dauk-khwa
Medicinal Uses	:	Dysentery, leucoderma and diabetic

Materials and Methods

Commercial grade reagents and solvents were used with further purification. Analytical preparative thin layer chromatography was performed by using precoated silica gel (Merck. Co. Inc, Kiselgel 60 F_{254}) and silica gel 70 to 230 mesh ASTM was used for column chromatography. (Aye Mon Thida Nyo, 2004)

Common laboratory tools were used in the isolation and purification of compound (MMK-1). The advanced instruments which are used in the characterization of samples and elucidation of pure compound are UV lamp (Lambada-40, Perkin-Elmer Co. England), FT-IR spectrometer (Shimadzu, Japan), ^{1}H NMR spectrometer (500 MHz), ^{13}C NMR spectrometer (125 MHz), EI- Mass spectrometer and UV spectrometer (PD-303 UV).

Sample Collection

One Myanmar indigenous medicinal plant, Dauk-khwa, was collected from Yenangyaung Township, Magwe Region. The collected sample was cut into small pieces and the species were dried in the shade. Then the raw materials were stored in the well-stoppered glass bottle and used throughout the experiment.

Phytochemical Constituents of the Plant Extract

In order to know the type of chemical constituents consisting in selected plant, phytochemical tests were carried out. (Harbone, 1993) The root sample of Dauk-khwa gave rise to the positive for alkaloid, glycoside, phenolic, polyphenol, steroid terpene and reducing sugar respectively.

Antimicrobial Activities of Myanmar Traditional Indigenous Medicinal Plant (Dauk-khwa)

The antimicrobial activities of various solvent extracs of the selected Myanmar indigenous medicinal plant (Dauk-khwa) were tested by using agar well diffusion method. These extracts were sent to Development Centre for Pharmaceutical Technology (DCPT), Insein, Yangon. The tested organisms were *Bacillus subtilis, Staphylococcus aureus, Pseudomonas aeruginosa, Bacillus pumalis, Candida albicans* and *Mycobacterium* species. The ethylacetate extract of the root of Dauk-khwa responds high activities on all tested organisms. Hence, it was selected for chemical analysis.

Extraction and Isolation of Pure Compound (MMK-1) from the Root of *Launaea secunda* Hook.

The air dried sample (423 g) was percolated with ethanol (3000 ml) for two months. The ethanol extract was filtered and evaporated at room temperature. The residue was dissolved in 250 ml of EtOAc. When EtOAc extract was filtered and concentrated, the crude sample (2.5 g) was obtained.

Then it was chromatographed on a silica gel column, using n-hexane and ethyl acetate as eluent with various ratios from nonpolar to polar. Totally (150) fractions were obtained. Each and every fraction were checked by TLC and the same R_f values were combined. Five combined fractions were collected.

The major combined fraction (C) gives only one spot on TLC. Pure yellowish brown, oily form compound (2.2 mg) was obtained. Total yield percent of pure compound (MMK-1) was found to be 1.162% based upon the crude EtOAc extract.

Determination of Antimicrobial Activities of Pure Compound

The antimicrobial activities of pure compound (MMK-1) were tested by using agar well diffusion method on six selected organisms such as *Bacillus subtilis, Staphylococcus aureus, Pseudomonas aeruginosa, Bacillus pumalis, Candida albicans* and *E. Coli*.

Results and Discussion

According to results (Figure 1), the isolated pure compound responds medium activities on five tested organisms, such as *Staphylococcus aureus, Pseudomonas aeruginosa, Bacillus pumalis, Candida albicans, E-coli* species and no activity on remaining organism.

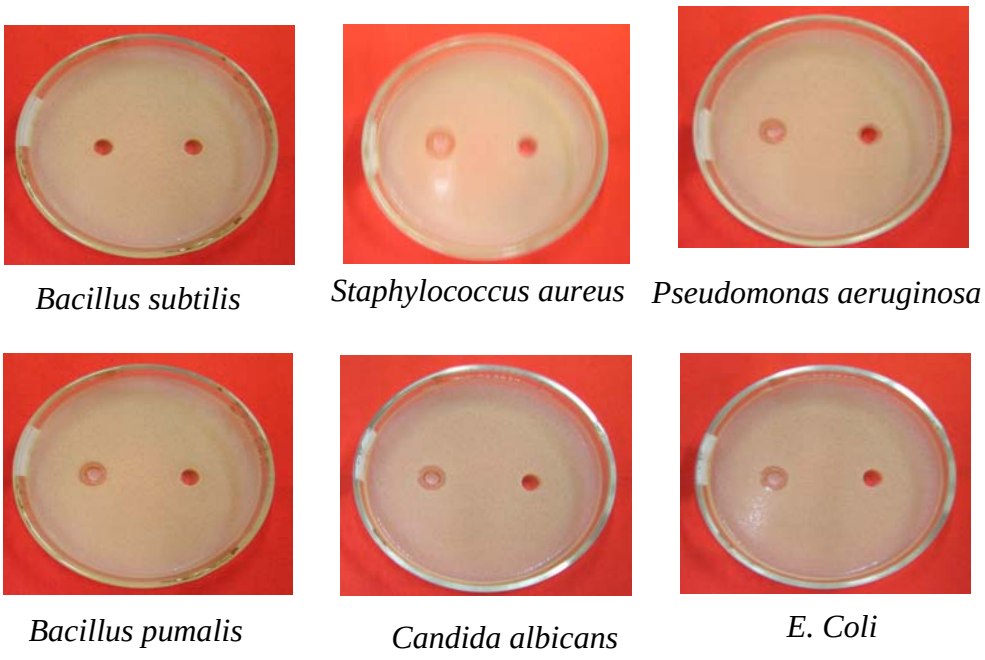

Figure 1. Antimicrobial activities of isolated pure compound (MMK-1)

Molecular Formula Determination of Pure Compound (Dolphin *et al*., 1977 ; Nakanishi, 1969**;** Silverstein, *et al*., 1989,1998)

Table 1. Results given by DEPT spectrum and FT IR spectrum

Assignment	No: of carbon	No: of proton	No: of oxygen
Five sp^3 methyl carbon	5	15	-
Seven sp^3 methylene carbon	7	14	-
One sp^3 carbinol methylene carbon (δ 62.15 ppm)	1	3	1
Five sp^3 methine carbon	5	5	-
Three sp^3 carbinol methine carbon (δ 70.14, 76.34; 74.19 ppm)	3	6	3
Three sp^3 quaternary carbon	3	-	-
One sp^2 methine carbon	1	1	-
One sp^2 quaternary carbon	1	-	-
One ether oxygen (from FT-IR)	-	-	1
Partial Molecular Formula	C_{26}	H_{44}	O_5

∴ The partial molecular formula = $C_{26}H_{44}O_5$

∴ The remaining partial molecular mass = 452 – 436 = 16

It must be one ether oxygen atom.

∴ Real molecular formula = $C_{26}\,H_{44}\,O_6$

Structure Elucidation of Pure Organic Compound (MMK-1)

In the structural assignment of this isolated compound, DQF-COSY and HMQC spectra display the following fragments a , c, d and f .

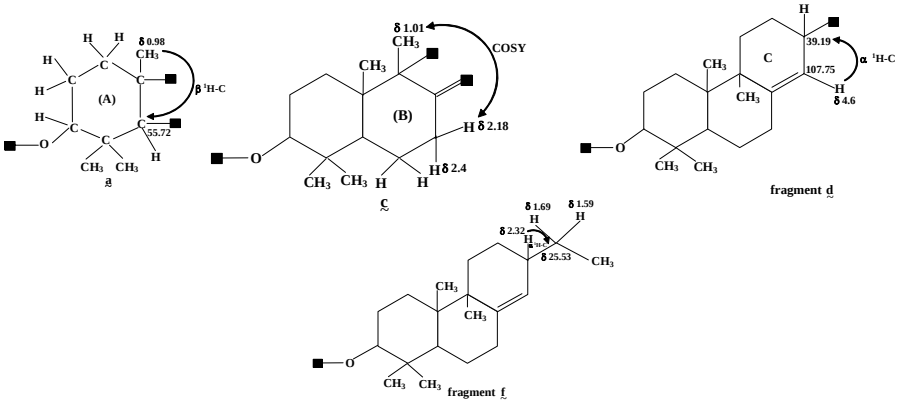

Furthermore, in DQF-COSY spectrum, the existence of medium graphic area of carbinol methine proton (δ 3.41 ppm) with acetal methine proton (δ 4.34 ppm) gives rise to the following glycoside ring fragment (h̲)(Timothy, 1999).

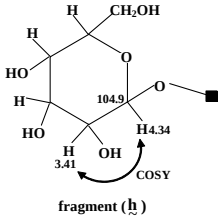

Finally, the complete planar structure of glycosidic diterpene compound (MMK-1) could be established by using the HMBC spectrum, in which acetal methine proton (δ 4.34 ppm) in glycoside fragment h̲ responds β ^{1}H-C long range coupling with ether bearing methine carbon (δ 90.06 ppm) in fragment f̲ . (Crews *et al*., 1998)

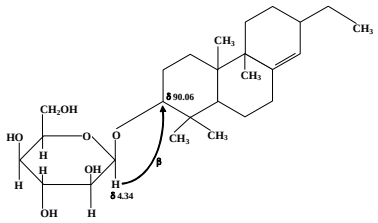

Conformational Analysis of Compound (MMK-1)

In the conformational analysis of compound (MMK-1), the splitting patterns and J-values of the proton (δ 3.14 ppm) attached to an ether bearing carbon, (dd, J = 9.2, 4.8 Hz) represents that this proton should be an axial one and the six membered ring A should be a chair conformer.

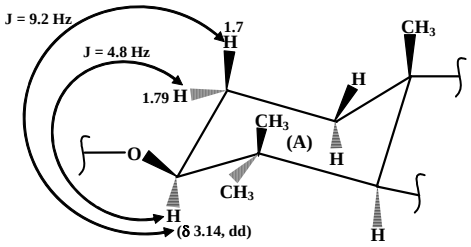

Moreover, the observation of NOESY spectrum, indicates medium NOE between ring A-B junction methyl group (δ 0.98 ppm) and an axial methylene proton (δ 1.7 ppm) implies that methyl group to be an axial one on both of ring A and B.

Inversely, the down field chemical shift proton (δ 3.14 ppm) responds medium and small NOE with ring A-B junction methine proton (δ 0.74 ppm) and ring B-C junction methyl group (δ 1.01 ppm). Hence, these three groups should be also axial one lying below the plane of their respective ring.

Therefore, the conformation of six-membered ring B could also be assigned as chair like one.

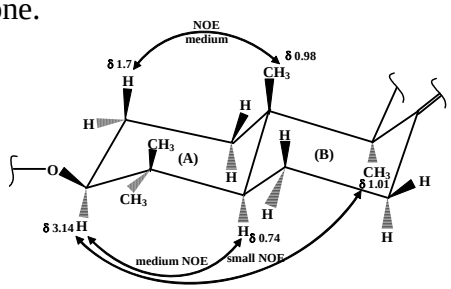

According to model study, the cyclohexene ring C containing two alkenic carbons should be the most stable boat like one.

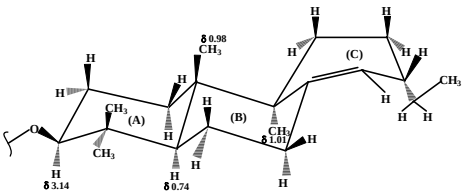

Furthermore, this NOESY spectrum displays medium NOE between ring B-C junction methyl group (δ 1.01 ppm) and side chain methylene group (δ 1.59 ppm, 1.69 ppm) which determine the allylic methine proton (δ 2.32 ppm) to be upper the plane of the ring C.

The absolute configuration of five chiral carbons should be determined as C_2 -S, C_{4a}-S, C_{4b}-S, C_7-S, and C_{10a}-R respectively.

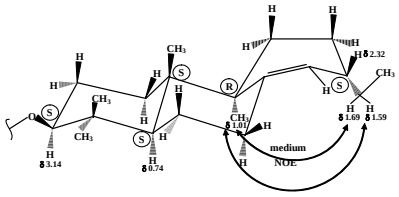

In case of glycosidic ring D, the splitting pattern and J-values of the acetal proton (δ 4.34 ppm, d, J = 7.9 Hz) indicates that it has diaxial relation with adjacent carbinol proton (δ 3.41 ppm).

In another front, there is observed medium NOE of acetal methine proton (δ 4.34 ppm) with another carbinol methine proton (δ 3.54 ppm) and another methine proton (δ 3.33 ppm) attached to the ether bearing carbon.

According to these spectral data, these three methine protons should be axial one, lying below the plane of the glycosidic ring.

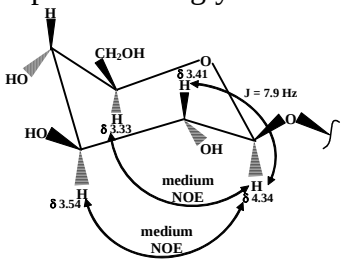

Inversely, this NOESY spectrum displays medium NOE of axial like carbinol methine proton (δ 3.41 ppm) with another carbinol methine proton

(δ 3.59 ppm) which confirms these two protons to be axial like ones, orienting upper the plane of this glycosidic ring. The absolute configuration of five chiral carbons in the glycosidic ring could be assigned as C_2-R, C_3-S, C_4-S, C_5-S, and C_6-S as shown below.

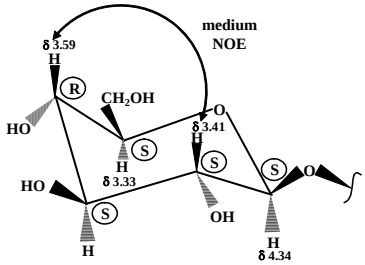

The conformational structure of this pure glycosidic diterpene compound (MMK-1) is described as follows.

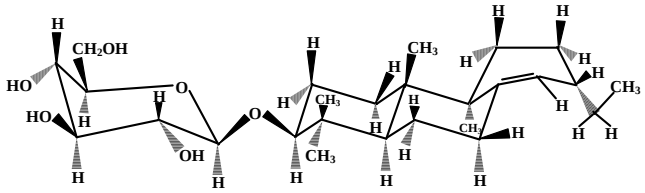

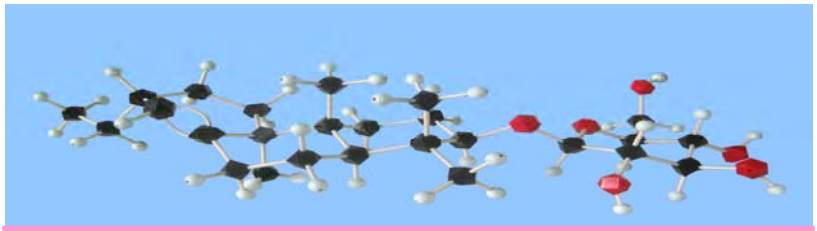

(2R, 3S, 4S, 5S, 6S)-2-((2S, 4aS, 4bS, 7S, 10aR)-7-ethyl-1, 1, 4a, 4b-tetramethyl-1, 2, 3, 4, 4a, 4b, 5, 6, 7, 9, 10, 10a-dodecahydrophenanthren-2-yloxy)-6-(hydroxymethyl) tetrahydro-2H-pyran-3, 4, 5-triol

Conclusion

In this study, one Myanmar indigenous medicinal plant *Launaea secunda* Hook., Myanmar name, Dauk-khwa (root) was collected from Meiktila Township, Mandalay Region and Yenangyaung Township, Magway Region.

Phytochemical screening and antimicrobial activities tests were done. In the result of phytochemical tests, the root of Dauk-khwa contains alkaloid, steroid, terpene, sugar, glycoside, phenolic and polyphenol compounds. Moreover, the antimicrobial activities of various solvent extracts of selected sample were tested by agar well diffusion method on six tested organisms. The ethyl acetate extract of Dauk-khwa (root) responds high antimicrobial activities on all tested organisms such as, *Bacillus subtilis, Staphylococcus aureus, Pseudomonas aeruginosa* and *Candida albicans* species. Hence, it was selected for chemical analysis. A pure compound (MMK-1) was isolated from the root of Dauk-khwa by applying Thin Layer and Column Chromatographic methods. The yellowish brown, oily form compound (0.022 g, 1.162 % yield) were collected from the column separation. This pure compound gave positive for terpene and glycoside tests. The antimicrobial activities of this pure compound has medium on five tested organisms except *Bacillus subtilis.*

The molecular formula (C_{26} $H_{44}O_6$) of isolated compound was determined by advanced spectroscopic methods such as FT-IR, ^{1}H NMR (500 MHz), ^{13}C NMR (125 MHz), DEPT, HMQC, DQF-COSY and FAB mass spectral data, respectively. Moreover, the complete planar structure of this isolated compound was assigned by DQF-COSY, HMQC and HMBC spectroscopic studies.

Furthermore, the following diterpenoid fragment and glycosidic fragment were also elucidated by DQF-COSY and HMBC spectral data as shown below.

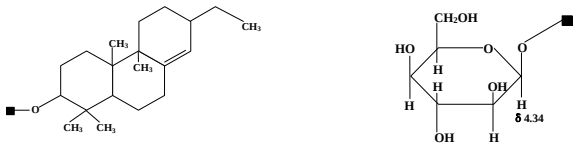

In addition, the conformational structure of gylcosidic diterpene compound could be assigned by the splitting patterns, coupling constant (J-values) of some prominent protons NOESY spectrum and model studies.

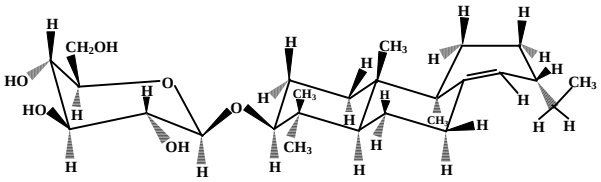

Finally, the absolute configuration of five chiral carbons in diterpene fragment could be assigned as C_2(S), C_{4a}(S) , C_{4b}(S), C_7(S), C_{10a}(R) and the absolute configuration of another five chiral carbons in glycosidic fragment could be determined as C_2(R), C_3(S), C_4(S), C_5(S) and C_6(S) respectively.

The IUPAC name of this isolated compound (MMK-1) is (2R, 3S, 4S, 5S, 6S)-2-((2S, 4aS, 4bS, 7S, 10aR)-7-ethyl-1, 1, 4a, 4b-tetramethyl-1, 2, 3, 4, 4a, 4b, 5, 6, 7, 9, 10, 10a-dodecahydrophenanthren-2-yloxy)-6-(hydroxymethyl) tetrahydro-2H-pyran-3, 4, 5-triol (Merck Index, 1983).

Since there is no research report that indicates the presence of glycosidic diterpene compound as a constituent in the root of Dauk-khwa, the finding of glycosidic diterpene compound in this plant is the pioneer result of this research.

Acknowledgements

The authors would like to express profound gratitude to Professor Dr Mya Aye for his permission, helpful advice, numerous invaluable suggestions and constant encouragement throughout this research. Sincere thanks are also due to Dr Yoshiaki Takaya, Associate Professor, Meijo University, Nagoya, Japan for giving the opportunity to have valuable spectra.

References

Aye Mon Thida Nyo, (2004), "Structural Elucidation of an unknown biologically active sterol compound isolated from selected Myanmar Indigenous Medicinal Plant *Begonia sentata* Wall (Kyauk-chin-baung)",PhD Dissertation, Department of Chemistry, University of Mandalay

Bodekerl, G. and Kronenborg, F., (2002), "Public Health Agenda for traditional, Complementary and Alternative Medicine," *American Journal of Public Health*, **92** (10).

Bulletin, DMR,(1996), "Scientific Studies on Myanmar Medicinal Plants", Vol 10.No.1.

Crews, P., Rodriguez, J. and Jaspars, M., (1998), "Organic Structure Analysis", University of California, Santa Cruz, Oxford University, New York.

Dolphin, D., et.al, (1977), "Tabulation of Infrared Spectral Data" John Wiley & Sons, Canada.

Harbone, J.B. (1993), "Phytochemical methods - A Guide to modern Techniques of Plant Analysis", Chapman and Hill Ltd, U.S.A.

Johnson, L. F. and Jankowski, W. C., (1972), "Carbon-13 NMR. Spectra, A Collective of Assigned, Coded, and Indehed Spectra", A Wiley-Inter Science Publication

Merck Index, (1983), 10th Edition, Merck & Co.,Inc., USA.

Nelson, J. H., (2003), "Nuclear Magnetic Resonance Spectroscopy", Pearson Education, Inc. Upper Saddle River. NJ07458.

Nakanishi, K., (1969), "Infrared Absorption Spectroscopy", 3rd Ed., ELBS with Macmillan

Silverstein, R.M. *et al*. (1989), "Spectrometric Identification of Organic Compound", 4th Edition, John Willy & Sons, Inc, Singapore.

Silverstein, R.M. *et al*., (1998), "Spectrometric Identification of Organic Compound", 6th Edition John Willy & Sons, Inc. Singapore.

Timothy, D.W.C., (1999), "High-resolution NMR Techniques in Organic Chemistry", Pergamon, An imprint of Elsevier Science, Amsterdam-Lausanne, New York

Study on a Bioactive Unknown Alkaloid Compound from the Root of *Mallotus philippinensis* (Lamk) Muell

Myint Myint Htay

Abstract

In this research, a potent bioactive alkaloid compound(MMH-1) was isolated from the root of *Mallotus philippinensis* (Lamk) Muell. (Taw-thidin) by using Thin-Layer and Column Chromatographic methods. The pale yellow needle shape crystal (1.6 mg, 0.08%) was obtained from ethylacetate extract by using the column separation methods. The melting point of isolated unknown compound is 198-199°C. It was reconfirmed by phytochemical test which gave rise to the positive test for alkaloid. It was screened for the antimicrobial activities employing six species of microorganism by utilizing agar well diffusion method. It was found to have medium activities on all six types of microorganism. The molecular formula of this pure bioactive alkaloid compound (MMH-1) could be elucidated by using some spectroscopic methods, such as FT IR, ^{1}H NMR (Nuclear Magnetic Resonance), ^{13}C NMR(Nuclear Magnetic Resonance), DEPT (Distortionless Enhancement by Polarization Transfer), HSQC (Heteronuclear Single Quantum Coherence), DQF-COSY (Double-Quantum Filtered Correlation Spectroscopy), HMBC (Heteronuclear Multiple Bond Coherence), NOESY (Nuclear Over Hauser Effect Spectroscopy) and EI-MS (Electron Impact Mass Spectroscopy) techniques. This compound (MMH-1) is named as 7-(3-amino-3, 4-dihydroxybutyl)-4, 4, 8- trimethyl hexahydro-1H-quinolizin-3(2H)-one.

Key words: *Mallotus philippinensis* (Lamk), Thin-Layer and Column Chromatographic methods, antimicrobial activities, ^{13}C NMR, DQF-COSY, EI-MS

Introduction

From the earliest times, herbs have been prized for their pain relieving and healing abilities. The majority of the world's population in developing countries still relies on herbal medicine to meet its health needs.

Assistant Lecturer , Dr, Department of Chemistry, Magway University

Traditional medicine is widely used and of rapidly growing health care system and economic importance. Thousands of plant species growing throughout the world have medicinal uses as they contain active constituents having direct action on the body. Since the ability of herbal medicine to affect body systems depends on the chemical constituents that it contains. Scientist first started extracting and isolating chemicals from plants.

At present, medicinal plants still play an important role in both developed and developing countries in Asia. There is world wide interest concerning the traditional medicinal plants for leading to find the new drugs because today's modern medicines are based on the information of the traditional medicines (Mnimh, 1996).

Also in Myanmar, there are many thousands of medicinal plants. Most people use the traditional medicinal plants for the treatment of diseases and to relief pain. So the study of traditional indigenous medicinal plants and their usage in therapy play a very important role.

In this research, Taw-thidin was selected for detail chemical analysis. This plant (Taw-thidin) is distributed from India and Srilanka to Myanmar, Thailand throughout South-east Asia and Malaysia, Indo-china, to Australia and the Pacific Islands. The root of *Mallotus philippinensis* (Lamk) Muell (Taw-thidin), was collected from Moe Hnyin Township, Kachin State. The root of Taw-thidin was used as medicine for skin disease, muscular inflammation and kidney diseases.

A pure bioactive alkaloid compound (MMH-1) was isolated from the root of Taw-thidin by using Thin-Layer and Column Chromatographic methods. The structure of this compound was assigned by using modern spectroscopic methods, such as FT-IR, ^{1}H NMR (500 MHz), ^{13}C NMR (125 MHz), DEPT, DQF-COSY, HMBC, HMQC, NOESY and EI mass spectral data.

Botanical Description (Lemmens and Bungapraphatsara, 2003**)**

Figure 1. Plant of *Mallotus philippinensis* (Lamk) Muell. (Taw-thidin)

Family	-	Euphorbiaceae
Botanical Name	-	*Mallotus philippinensis* (Lamk) Muell.
Myanmar Name	-	Taw-thidin
Useful Part	-	Root
Medicinal Uses	-	Skin diseases, kidney diseases and muscular inflammation

Materials and Methods

Materials

Commercial and analytical grade reagents from BDH, Merck were used in this research. Analytical and preparative thin layer chromatography was performed by using percolated silica gel plates (Merck. Co. Inc, Kieselgel 60 F_{254}). Silica gel (70-230 mesch ASTM) was applied for column chromatography.

Sample Collection

The root of *Mallotus philippinensis* (Lamk) Muell, (Taw-thidin) was collected from Moe-Hnyin Township, Kachin State. First, this sample was dried in the shade, crushed into small pieces and kept in the glass bottle with stopper.

Isolation of an Unknown Bioactive Organic Compound (MMH-1)

Air dried sample (450 g) was percolated with 2L of 95% EtOH for two months and then titrated and evaporated. The residue obtained was extracted with 250 ml of EtOAc and concentrated.

EtOAc extract (2.01 g) was run on column chromatography with silica gel, SiO_2 (70-230 mesh), using various ratios of n-hexane and EtOAc as eluents from non-polar to polar.

Totally 155 fractions were obtained and each fraction was checked by TLC for purity. The fractions with the same. R_f value were combined to give 7 combined fractions. Fraction (v) was rechromatographed by microcolumn using the same adsorbent and eluent which give rise to fractions.

Fraction B was recrystallized with n-hexane and EtOAc in the ratio of 1:1 (v/v). Pure pale yellow neddle shape crystals (1.6 g) were obtained and yield percent was found to be 0.08% based upon the crude extract. It gave the positive test for alkaloid and its melting point is found to be 198-199ºC.

Phytochemical Test for Pure Bioactive Organic Compound (MMH-1)

The pure bioactive organic compound (MMH-1) gives positive test for Dragendroff's and Mayer's reagent. Thus, this compound (MMH-1) is alkaloid **(**Harborne, 1993)

Antimicrobial Activities of Pure Bioactive Organic Compound (MMH-1)

The antimicrobial activities of pure compound (MMH-1) were tested by using Agar well diffusion method on six selected organisms. These results are shown in Table 1.

Results and Discussion

According to Table 1 and Figure 1, the pure compound (MMH-1) gave medium activity on all tested organisms.

Table 1. Antimicrobial activities of pure bioactive organic compound (MMH-1)

Sample	Organisms					
	Bacillus subtilis	*Staphylo-coccus aureus*	*Pseudo-monas aeruginosa*	*Bacillus pumalis*	*Candida albicans*	*Mycobacterium species*
Pure Compound (MMH-1)	++	++	+	++	++	++

Agar well-10 mm

(+) 10 mm ~ 14 mm

(++) 15 mm ~ 19 mm

(+++) 20 mm above

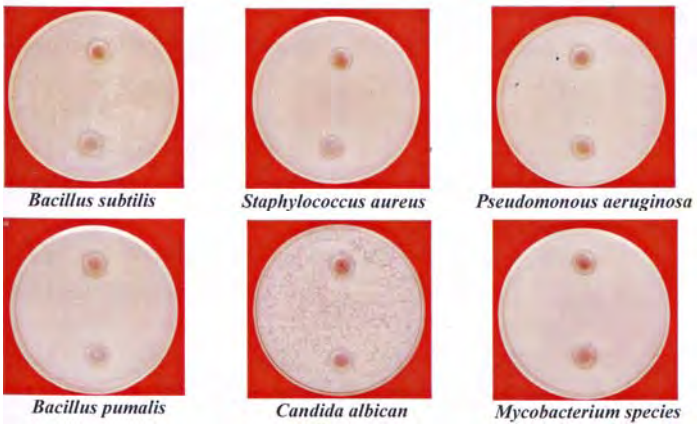

Figure 2. Antimicrobial activities of isolated pure organic compound

The functional groups observed in FT-IR spectrum are tabulated in Table 2.

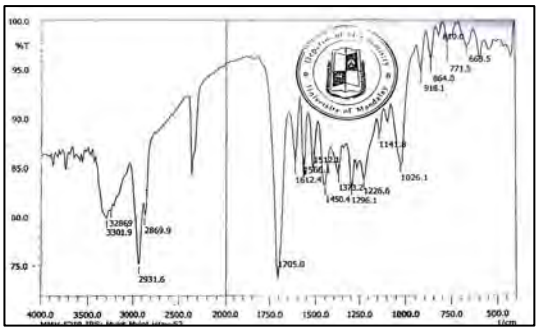

Figure 3. FT-IR Spectrum of an unknown compound

Table 2. FT-IR assignment of compound (MMH1)

Absorption bands (cm^{-1})	Assignments
3301.9	OH stretching vibration
3286.9	NH stretching vibration
2931.6, 2869.9	unsymmetrical and symmetrical – CH stretching vibration of sp^3 hydrocarbon
1705.0	C = O stretching vibration
1612.4	NH bending vibration
1450.4	CN stretching vibration
1296.1, 1373.2	C – H out of plane bending vibration of gem-dimethyl group
1226.6	C – C – O stretching vibration of alcohol group
864.0	NH wagging vibration

^{1}H NMR (500 MHz) spectrum indicates the total number of protons (26) in this unknown compound (Nelson, 2003, Silverstein *et al*., 1989 and 1998)

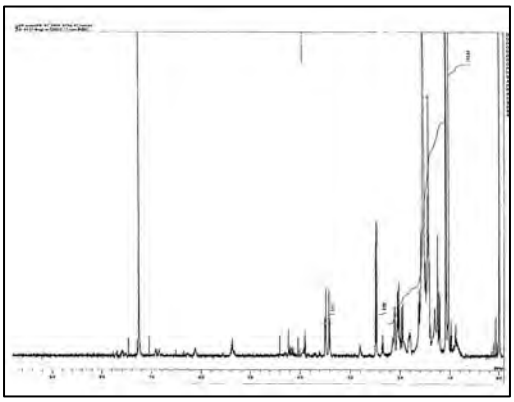

Figure 4. ^{1}H NMR (500 MHz) spectrum of an unknown compound

Moreover, ^{13}CNMR (125 MHz) spectrum showed the total number of carbons (16) in this unknown compound. (Silverstein *et al.*, 1989 and 1998)

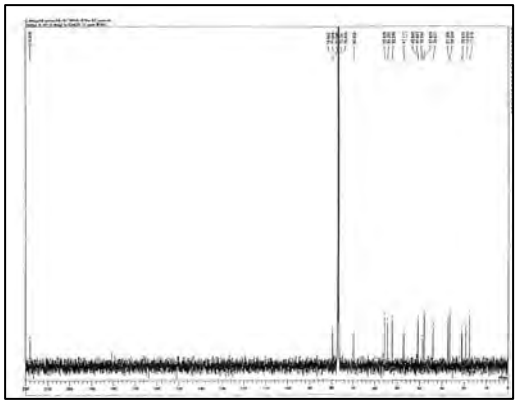

Figure 5. ^{13}C NMR (125 MHz) spectrum of an unknown compound

Hence, partial molecular formula is $C_{16}H_{26}$. According to FT-IR spectrum, this unknown compound should consist of at least one hydroxyl group, one NH group and one carbonyl group. Thus partial molecular formula could be extended to (C_{16} H_{28} O_2 N) and partial molecular mass is 266.

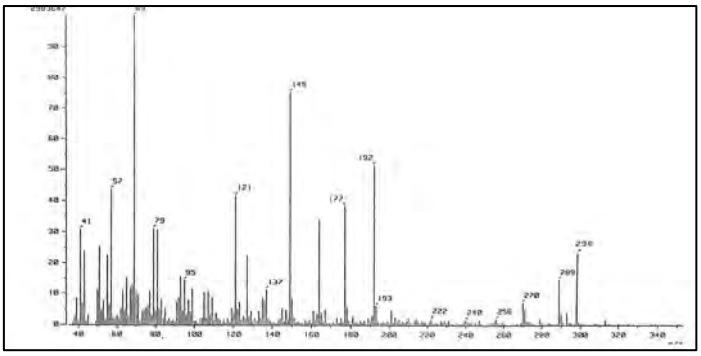

Figure 6. EI-Mass spectrum of an unknown compound

EI-mass spectrum gives rise the molecular ion peak m/z at 298 which represents the molecular mass of this compound.

According to Nitrogen rule even number molecular mass indicates the even number of nitrogen atoms in this compound. Therefore, partial molecular formula could be determined as (C_{16} H_{28} O_2 N_2) and partial molecular mass is 280.

Hence, the remaining molecular mass is 298 – 280 = 18

It should be one-OH group and one hydrogen atom. Thus, the real molecular formula is C_{16} H_{30} O_3 N_2.

Confirmation of Molecular Formula of an Unknown Compound (MMH-1) (Johnson and Jankowski, 1972 ; Merck Index, 1983**)**

Molecular formula of an unknown compound (MMH-1) could be confirmed by FT-IR and DEPT spectral data.

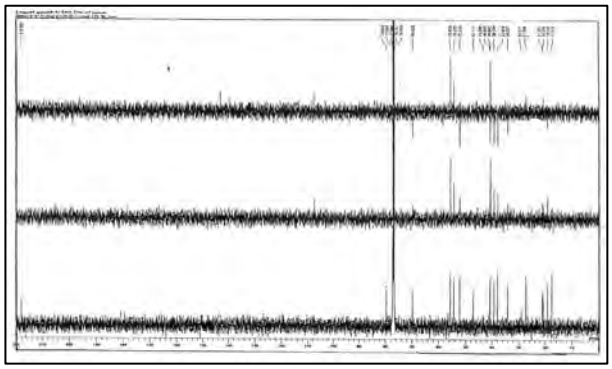

Figure 7. DEPT spectrum of an unknown compound

These data are described in Table 2.

Table 2. Confirmation of molecular formula of unknown compound (MMH-1)

Kinds of protons/ carbon	**No. of carbon**	**No. of proton**	**No. of oxygen**	**No. of nitrogen**
DEPT, 3 sp^3 methyl carbons	3	9	-	-
6 sp^3 methylene carbons	6	12	-	-
3 sp^3 methine carbons	3	3	-	-
1 sp^3 quaternary carbons	1	-	-	-
one carbinol methylene carbon	1	3	1	-
carbinol quaternary carbon	1	1	1	-
FT-IR, one amine group	-	2	-	1
one carbonyl carbon	1	-	1	-
Partial molecular formula	C_{16}	H_{30}	O_3	N

Partial molecular mass = 284

EI-mass spectrum, molecular ion peak m/z = 298

Remaining molecular mass = 298 – 284 = 14

Thus, remaining molecular mass (14) should be one nitrogen atom. Hence, the real molecular formula is (C_{16} H_{30} O_3 N_2), which agrees with Nitrogen rule.

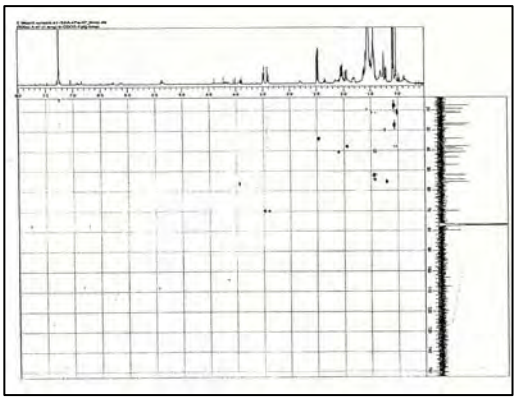

Figure 8. DQF-COSY spectrum of an unknown compound

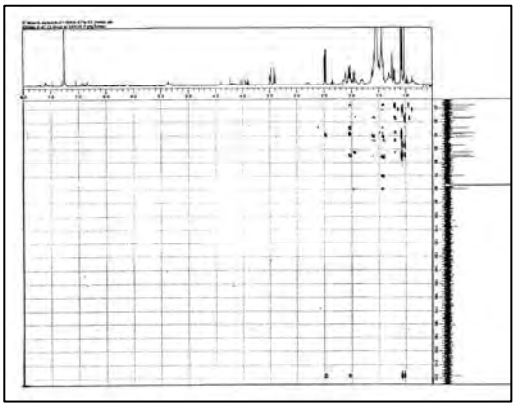

Figure 9. HMBC spectrum of an unknown compound

According to DQF-COSY spectrum and HMBC spectrum the partial fragment a could be determined.

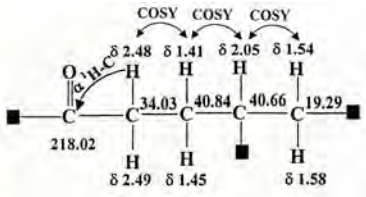

(a)

Moreover, HMBC spectrum gives information that this compound consists of gem-dimethyl group. These two methyl signals (δ 1.02, δ 1.07

ppm) gives β ^{1}H – C long range coupling with the carbonyl carbon (δ 218.02 ppm) implies the following fragment.

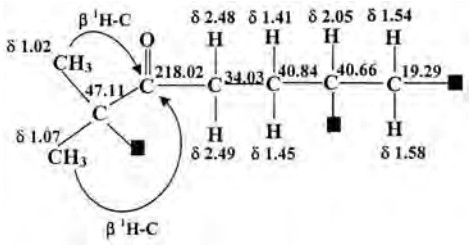

In addition, the following fragment b could be assigned by DQF-COSY spectrum.

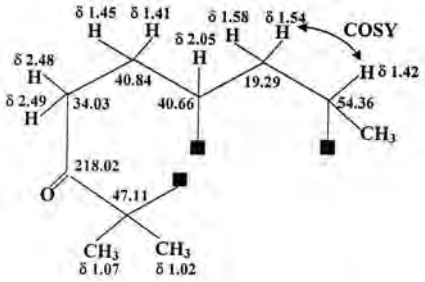

(b)

On the other hand, according to DQF-COSY and HMBC spectrums the following fragment c could be assigned.

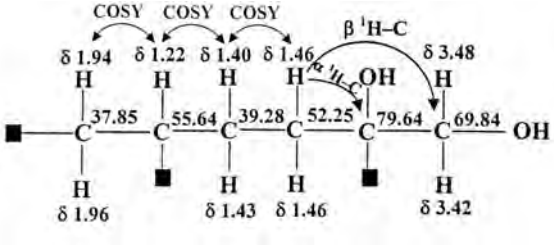

(c)

Furthermore, connection between partial fragment b and c by DQF – COSY spectrum give rise to the longer fragment d.

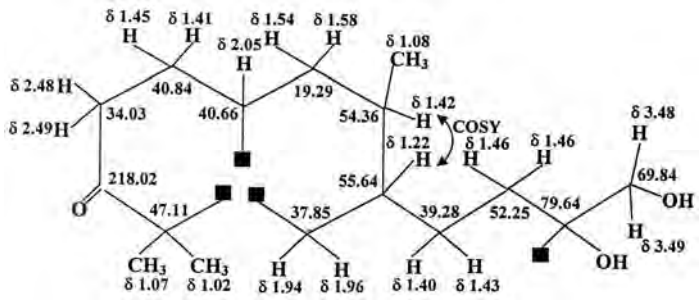

(d)

According to this fragment d̲, the partial molecular formula could be calculated as $C_{16}H_{28}O_3$ and the remaining partial molecular formula must be (C_{16} H_{30} O_3N_2 - C_{16} H_{28} O_3 = N_2H_2). It should be two NH groups or one NH_2 group and one nitrogen atom. The attachment of nitrogen atom to three unsatisfied chemical shift carbons (δ 47.11, δ 37.85 and δ 40.66 ppm) and the link of remaining primary amine group to the unusual downfield chemical shift carbinol carbon (δ 79.64 ppm) accomplish the assignment of the planar structure of this potent organic compound.

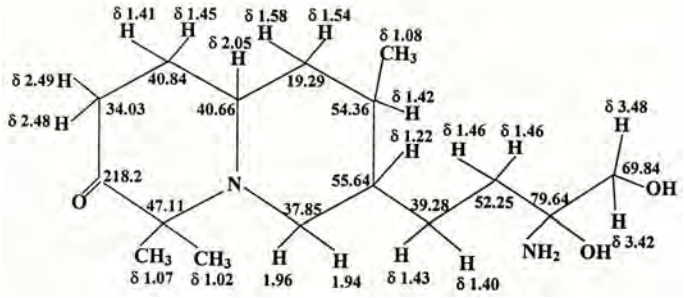

This unknown bioactive organic compound (MMH-1) is named as : 7-(3-amino-3, 4-dihydroxybutyl)-4, 4, 8- trimethyl hexahydro-1H-quinolizin-3(2H) –one.

Conclusion

In this research paper, Myanmar indigenous medicinal plant (Taw-thidin) was selected for detailed chemical analysis. The ethyl acetate extract of the root of Taw-thidin was separated by Thin Layer and Column Chromatograms applying SiO_2 as an adsorbent and n-hexane and EtOAc in various ratios as eluent. It produces a pure pale yellow needle shape crystal

and the yield percent is calculated as 0.08% based upon EtOAc crude extract. The melting point of this compound was found to be 198-199ºC. Moreover, the pure compound gave positive test for alkaloid by using Dragendroff's and Mayer's reagent. This alkaloid compound was tested for antibacterial activity on six selected organisms. In this test, it gave medium activity in all selected organisms.

Finally, the molecular formula of this potent alkaloid compound could be determined as ($C_{16}H_{30}O_3N_2$) applying some sophisticated spectroscopic methods, such as FT-IR, ^{1}H NMR, ^{13}C NMR, DEPT, HMQC, HMBC and EI mass spectrograms respectively.

Acknowledgements

Heartfelt gratitude and thanks are due to Professor Dr Mya Aye for his close supervision, invaluable advice and good suggestions throughout this research work. The author also wishes to express sincere gratitude to Dr Aye Kyaw, Rector, Magway University and Dr Aye Aye Wai, Professor and Head of Department of Chemistry, Magway University, for their encouragement and allowing to submit this research paper.

References

Harborne,J.B., (1993), "Phytochemical Methods -A Guide to Modern Techniques of Plant Analysis", Chapman and Hall Ltd, U.S.A

Johnson L. R., and Jankowski, W. C., (1972), "Carbon-13 NMR spectra, A Collective of Assigned, Coded, and Indexed Spectra", A Wiley- Interscience Publication.

Lemmens, and Bungapraphatsara,N., (2003), "Plant Resources of South East Asia, No.12(3)", Medicinal and poisonous plants 3", Bogor, Indonesia .

"Merck Index", (1983). 10th Edition, Merck and Co. Inc. U.S.A

Mnimh A. C., (1996), "The Encyclopedia of Medicinal Plants"

Nelson J. H., (2003), "Nuclear Magnetic Resonance Spectroscopic", Pearson Education, Inc. Upper Saddle River, NJ 07458.

Silverstein *et al*., (1989),"Spectrometric Identification of Organic Compound", 4h Edition, John Willy and Sons, Inc., Singapore.

Silverstein *et al.*, (1998), "Spectrometric Identification of Organic Compound", 6th Edition, John Willy and Sons, Inc., New York.

Some Chemical Analyses and Determination of Antioxidant Property of Neem Leaf (*Azadirachita indica* A.Juss*)*

Khine Khine Hla[1], Myat Mon Aye[2] and Ma Hla Ngwe[3]

Abstract

This research work deals with the study of some physicochemical properties and investigation of antioxidant activity of Neem (*Azadirachta indica* A. Juss) leaves. For this research work, Neem leaves were collected from Pyay Township and identified at Botany Department, Pyay University. After cleaning and drying, it was ground into powder. Then moisture content, ash content, crude fiber content, fat content, protein content and carbohydrate content of dry Neem leaves were determined by appropriate reported analytical methods. In order to determine the types of phytochemical organic constituents present in Neem leaves, preliminary phytochemical tests were carried out by reagent tests. In addition, qualitative EDXRF elemental analysis was also carried out on Neem leaves sample. Furthermore, antioxidant activity of 95% ethanol extract and watery extract from the dry Neem leaves was determined by DPPH free radical scavenging assay. Since the 50% oxidative inhibitory concentrations (IC_{50}) of 95% ethanol extract and watery extract were respectively found to be 0.26 and 3.99 µg/ml, the watery extract of Neem leaves possessed higher antioxidant activity than 95% ethanol extract of Neem leaves. Due to its antioxidant activity, the Neem leaves may be effective as antioxidant agent for the treatment of oxidative stress related diseases such as diabetes, cancers, tumors, aging, inflammatory etc.

Key words: Antioxidant activity, Neem (*Azadirachta inidca* A. Juss) leaves

Introduction

Medicinal plants are parts and parcel of human society to combat diseases, from the dawn of civilization. *Azadiachta indica* A. Juss (Syn. *Melia azadirachta*) is well known in Myanmar as well as in India and the neighboring countries for more than 2000 years as one of the most versatile medicinal plants having a wide spectrum of biological activity. Neem is an evergreen tree, cultivated in various parts of the Indian subcontinent. Every part of the tree has been used as traditional medicine for household remedy against various human ailments, from antiquity. Chemical investigation on

1. Assistant Lecturer, Dr, Department of Chemistry, Pyay University
2. Lecturer, Department of Chemistry, Pyay University
3. Professor, Dr, Department of Chemistry, Pyay University

the product of the Neem tree was extensively undertaken in the middle of the twentieth century (Kausik *et al*., 2002).

Botanical aspects of Neem

Scientific name	=	*Azadirachta indica* A.Juss
Family name	=	Meliaceae
Genus	=	*Azadirachta*
Species	=	*A. indica*
Common name	=	Neem
Myanmar name	=	Tamar
Parts used	=	leaves, flowers, fruits, barks, roots, oils, seeds

Chemical constituents of Neem

Neem is bitter in taste. The bitterness is due to an array of complex compounds called 'triterpenes' or more specifically 'limonoids'. Nearly 100 protolimonoids, limonoids or triterpenoids, hexanortriterpenoids and some nonterpenoid constituents have been isolated from various parts of the Neem tree; still more are being isolated. The most important bioactive principal is azadirachtin at least 10 other limonoids posses insect growth in regulation activity.

Biological activities and uses of Neem

Alcoholic extract of the leaves was found to possess a significant blood sugar lowering effect, which are very useful against diabetes. Neem also has shown antiviral, anti-fungal and anti-bacterial properties. Preparations from the leaves or oils of the tree are used as general antiseptics. Due to Neem's antibacterial properties, it is effective in fighting most epidermal dysfunction such as acne, psoriasis, and eczema, and it is also used in the manufacture of soap, mosquito repellent coil etc.

Traditionally, Indians bathed in Neem leaves steeped in hot water. Since there has never been a report of the tropical application of Neem causing an adverse side effect, this is a common procedure to cure skin ailments or allergic reactions. Neem also may provide antiviral treatment for smallpox, chicken pox and warts-especially when applied directly to the skin. Its effectiveness is due in part to its ability to inhibit a virus from

multiplying and spreading. Neem produces pain-relieving, anti-inflammatory and fever-reducing compounds that can aid in the healing of cuts, burns, sprains, earaches, and headaches as well as fevers. Several studies of Neem extracts in suppression malaria have been conducted, all supporting its use in treatment (Kausik *et al*., 2002).

Antioxidants and antioxidant activity

Antioxidants are the chemicals that reduce the rate of particular oxidation reaction. They help to protect the body from damage of cell by free radicals. Free radicals are chemical species possessing an unpaired electron that can be considered as fragment of molecules and which are generally very reactive. There is a report that the more the toxic metals in our body, the higher the free radical activity. Thus toxic metals are a cause of free radicals. They cause to oxidative damage of protein, DNA and other essential molecules and cause cancer, cardiovascular diseases and heart disease, and oxidative stress.

The methods for determination of antioxidant activity are :

(i)1,1-Diphenyl-2-Picryl-Hydrazyl (DPPH)Assay (ii) Conjugated Diene Assay (iii) Thiobarbituric Acid (TBA) Assay (iv) Lipid Peroxide (PD) Assay (v) Thiocyanate Assay and (vi) Active Oxygen Method. In the present work, the antioxidant activity of Neem leaves extracts was studied by using DPPH free radical scavenging assay method.

The following represents the reaction of DPPH with free radical scavengers, flavonoid compound.

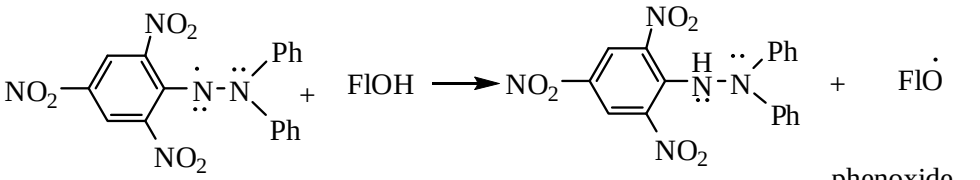

Here in, some chemical analyses and investigation of antioxidant activity on Neem leaves sample are reported.

Materials and Methods

For this research, Neem leaves were collected from Pyay Township in May, 2010. The sample was identified at Department of Botany, Pyay

University. The collected Neem leaves were washed with water and dried at room temperature. The dried samples were ground by using electric motor to obtain powder and stored in air-tight container to prevent moisture and other contaminations. The chemicals used in this research were "British Drug House Chemical Ltd., Poole, England", "Kanto Chemical Co., Inc., Japan", Hopkins and Williams Ltd., England".

Some chemical analyses of Neem leaves

Some nutritional values such as moisture, ash, fat, protein, crude fiber and carbohydrate contents of the Neem leaves sample were determined by appropriate reported methods (Vogel, 1966). The elements present in dried powdered sample were qualitatively determined by EDXRF (Energy Dispersive X-Ray Fluorescence) technique using Shimadzu EDX-700 spectrometer in Universities' Research Center, Yangon University. In order to find out the types of organic constituents present in the sample, preliminary phytochemical investigation: tests for alkaloids (Trease and Evans, 1980), α-amino acids (Marini-Bettolo *et al.*, 1981), carbohydrates (Molish's Test) (Shriner *et al*., 1980), cyanogenic glycosides (Trease and Evans, 1980), flavonoids (Robinson, 1983), glycosides (Marini-Bettolo *et al.*, 1981), organic acids (Robinson, 1983), reducing sugars (Finar, 1969), saponins (Shriner *et al*., 1980), steroids, tannins and terpenoids (Tin Wa, 1972) was carried out according to the appropriate reported methods.

Screening of Antioxidant Activity of Crude Extracts from Neem Leaves

DPPH (2, 2-diphenyl-1-picryl-hydrazyl) radical scavenging assay was chosen to assess the antioxidant activity of plant materials. This assay has been widely used to evaluate the free radical scavenging effectiveness of various flavonoids and polyphenols in food systems (Lee and Shibamoto, 2001).

In this experiment, the antioxidant activity was studied on 95% ethanol extract and watery extract from Neem leaves sample by DPPH free radical scavenging assay (Bicanic, 2001). Vitamin C was used as a standard.

(i) Preparation of 60 μM DPPH solution

To achieve 60 μM DPPH solution, 2.364 mg of DPPH were thoroughly dissolved in 95% ethanol (100 mL). This solution was freshly prepared in the brown colored flask. Then it must be stored in the fridge for no longer than 24 hours.

(ii) Preparation of test sample solution

2 mg of test sample and 10 mL of 95% EtOH were thoroughly mixed by vortex mixer. The mixture solution was filtered and the stock solution was obtained. Desired concentrations: 10 μg mL^{-1}, 5μg mL^{-1}, 2.5μg mL^{-1}, 1.25μgmL^{-1} and 0.625 μg mL^{-1} of solutions were prepared from this stock solution by serial dilution with appropriate amount of 95% ethanol.

(iii) Procedure

DPPH radical scavenging activity was determined by UV spectrophotometric method. Blank solution was prepared by mixing the test sample solution (1.5mL) with 95% ethanol (1.5 mL). The control solution was prepared by mixing with 1.5 mL of 60 μM DPPH solution and 1.5 mL of 95% ethanol using vortex mixer. The sample solution was also prepared by mixing thoroughly with 1.5 mL of 60 μM DPPH solution and 1.5 mL of test sample solution. The solutions were mixed thoroughly using vortex mixer for about 15 minutes and allowed to stand at room temperature for 15 minutes. After 30 minutes, the absorbance of each solution was measured at 517 nm by using UV-visible spectrophotometer. Absorbance measurements were done in triplicate for each solution and then mean values so obtained were used to calculate percent inhibition of oxidation by the following equation.

$$\% \text{ Inhibition} = \frac{A - B - C}{C} \times 100$$

where,

% Inhibition = % inhibition of test sample

A = absorbance of control solution (DPPH + solvent)

B = absorbance of blank sample (Sample + solvent)

C = absorbance of sample solution (Sample + DPPH + Solvent)

Then, IC_{50} (50% inhibitory concentration) values were also calculated by linear progressive excel program.

Results and Discussion

Chemical analyses showed that the dried Neem leaves powdered sample contained 5.14% of moisture, 8.70 % of ash, 1.6 % of fats, 10.54 % of proteins, 6.55% of fiber and 67.47 % of carbohydrates based on dry weight. According to qualitative EDXRF elemental analysis, Ca, K, Cl, Fe, Sr, Mn and Br were found to be present in the sample. Preliminary phytochemical investigation results indicated the presence of alkaloids, α amino acids, carbohydrates, flavonoids, glycosides, phenolic compounds, reducing sugars, saponins, steroids, tannins and terpenoids in Neem leaves sample. There is no cyanogenic glycosides found in this sample and it can be so inferred that Neem leaves may be free from harmful effect due to the toxic property of cyanogenic glycosides.

The antioxidant property of 95% ethanol crude extract and watery crude extract from the Neem leaves sample was studied by DPPH free radical scavenging assay method. This is based on the UV-visible absorption spectrophotometric method. DPPH free radical has violet colour and its maximum absorption wavelength is 517 nm. If the concentration of DPPH increases, the absorbance increases. Therefore, if a substance could reduce or quench the DPPH free radical, the concentration of the DPPH free radical will be decreased and the absorbance of this solution will also be decreased. This shows that the substance has the inhibitory effect on the oxidation formed due to the free radical.

From this experiment, the observed absorbance values of the DPPH in the presence of each crude extract with various concentrations (0. 156, 0.312, 0.625, 1.25, 2.50, 5.0, 10.0 μg/mL) were found to decrease, indicating the decrease of free radical DPPH concentrations and the increase of the free radical scavenging property of crude extracts. Therefore the higher the concentrations of crude extracts, the greater the oxidative inhibitory efficiency. They are described by percent oxidative inhibition as shown in Table 1. The percent oxidative inhibition of crude extracts was found to increase with increasing their concentrations as described in Figure 1.

The antioxidant activity of a substance is usually expressed by means of IC_{50} (50% oxidative inhibitory concentration). These IC_{50} values can be calculated from the plots of concentrations vs percent oxidative inhibition of the substance by using linear progressive EXCEL program.

The IC_{50} values for 95% ethanol extract and watery extract from Neem leaves sample were observed to be 3.99 and 0.26 µg/mL, respectively. Since the lower the µg/mL values, the higher the antioxidant activity of the sample, Neem leaves watery extract possessed higher antioxidant activity than ethanol extract. Ethanol extract from Neem leaves was found to be lower effective than standard vitamin C (IC_{50} = 0.2 µg/mL) in antioxidant activity and the antioxidant activity of Neem watery extract was observed to close to that of vitamin C.

Table 1. Percent oxidative inhibition and IC_{50} values of extracts from Neem leaves and standard ascorbic acid

Extracts of Neem leaves	% Oxidative inhibition in different concentrations of extracts (µg/mL)							IC_{50} (µg/mL)
	0.156	0.312	0.625	1.25	2.5	5	10	
EtOH	40.45	45.21	45.49	46.59	48.45	51.04	52.62	3.99
H_2O	42.35	51.56	54.29	57.55	58.59	60.94	71.74	0.26
Ascorbic Acid	47.85	55.45	57.18	65.60	75.35	90.80	92.10	0.20

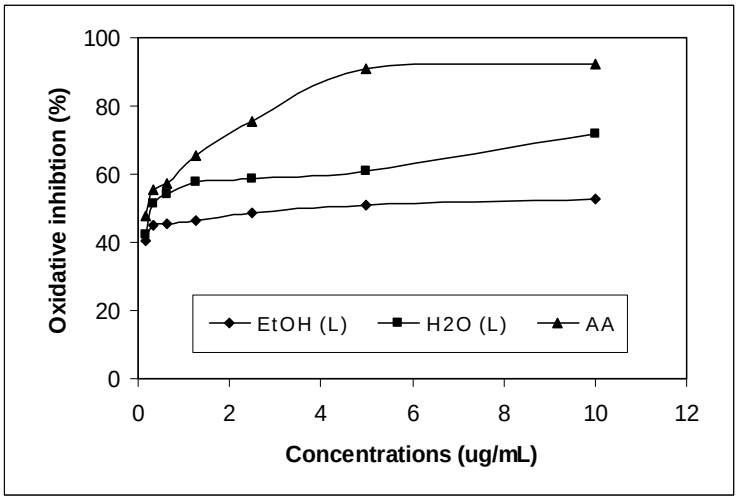

Figure 1. A plot of percent oxidative inhibition vs different concentrations of Neem leaves extracts and standard ascorbic acid

Conclusion

From the overall assessments of the present research work, the following inferences could be deduced.

The Neem leaves collected from Pyay Township were found to contain 5.14% of moisture, 8.70% of ash, 1.60% of fats, 6.55% of proteins, 10.54% of fiber and 67.47% of carbohydrates based on the dry weight. The classes of phytoorganic constituents present in Neem leaves are alkaloids, α–amino acids, carbohydrates, flavonoids, glycosides, phenolic compounds, reducing sugars, saponins, steroids, tannins and terpenoids. Not only the C, H and Mg, Neem leaves were found to contain Ca, K, Cl, Fe, Sr, Mn, Cu and Br determined by EDXRF technique.

DPPH free radical scavenging assay method showed that watery extract (IC_{50} = 0.26 μg/mL) of Neem leaves was more effective than 95% ethanol extract (IC_{50} = 3.99 μg/mL) in antioxidant activity and it was also observed to be comparable with the standard ascorbic acid IC_{50} = 0.20 μg/mL).

Consequently, due to its antioxidant activity, the Neem leaves may be useful as antioxidants for the treatment of oxidative stress related diseases such as diabetes, cancers, tumors, aging, inflammatory etc.

Acknowledgements

The authors wish to thank Rector U Win Myint and Pro-rector Dr. Than Than Win, University of Pyay and Professor Dr. Daw Hla Hla Than, Head of Department of Chemistry, Pyay University, for their kind provision of opportunity to submit this research paper.

References

Bicanic, D., (2001), “Evaluation of Antioxidative Activity of Some Antioxidants by Means of a Combined Optothermal Window and a DPPH Free Radical Colorimetry,” *J. Astrophys*, **17,** 544-545

Finar, I. L., (1973), "Organic Chemistry", 6th. Edn., **1**, Longmans Group Limited, London

Kausik, B., Ishita, C., Ranajit, K. B. and Uday, B., (2002), "Biological Activities and Medicinal Properties of Neem (*Azadirachta indica*)", *Current Science*, **82**, No. 11, 1336 - 1345

Lee, K.G. and Shibamoto, T., (2001), “Antioxidant Property of Aroma Extract Isolated from Clove Buds”, *Food Chemistry*, **74,** 443-448

Marini Bettolo G.B., Nicolettic, M. and Patamia, M. and Patamia, M., (1981), "Plant Screening by Chemistry and Chromatographic Procedure Under Field Conditions", *J. Chromato.*, 121**,** 213-214

Robinson, T., (1983), "The Organic Constituents of Higher Plants", 5th Edn., Cordus Press, North Amberst, 285-286

Shriner, R.L., Fuson, R.C., Curtin, D.Y. and Morrill, T.C., (1980), "The Systematic Identification of Organic Compounds - A Laboratory Manual", John Wiley and Sons, New York, 385-425

Tin Wa, (1972), "Phytochemical Screening Methods and Procedures", *Phytochemical Bulletin of Botanical Society of America Inc.*, **5**(3), 4-10

Trease, G. E. and Evans, W. C. (1980), "Pharmacognosy", 1st. Ed., Spottiswoode, Ballantyne Ltd., London, 108-529

Vogel, A.L, (1956), A Text Book of Practical Organic Chemistry Longman Group Ltd, London, 3rd Edition, 453.

Vogel, A.L, (1966), Qualitative Organic Analysis, 2nd Ed., Longman William and Sons Ltd.

Removal of Some Toxic Heavy Metals by means of Adsorption onto Biosorbent Composite (Coconut Shell Charcoal - Calcium Alginate) Beads

Chaw Su Hlaing,[1] Khaing Khaing Kyu[2] and Thida Win[3]

Abstract

Effective biosorbent composite beads have been successfully prepared by combining coconut shell charcoal and calcium alginate via sodium alginate at room temperature. The coconut shell charcoal, calcium alginate beads (CA) and coconut shell charcoal calcium alginate beads (CCA) have been applied for sorption studies on toxic heavy metals such as lead, cadmium and arsenic under the influence of various factors such as pH, contact time and dosage of these materials. Firstly, the optimum pH was determined to get high sorption capacity of these materials on Pb^{2+}, Cd^{2+} and As (V) ions solutions. At the optimum pH, the influence of contact time and dosage of these materials onto the sorption studies of Pb^{2+}, Cd^{2+} and As (V) ions have been examined. The prepared biosorbent materials and metal sorbed biosorbent materials were qualitatively and quantitatively characterized by FT IR, SEM, ED-XRF and TG-DTA. The removal of toxic heavy metals was dependent on pH, contact time, the adsorbent dose and competition between metal ions. Depending on the nature of the substrate the effective removal capacity was found to take place within a pH range from 5 to 6 at room temperature. Further batch adsorption tests were carried out at the optimal pH of 5 for lead and at pH 5.5 for cadmium and arsenic. The amount of toxic heavy metals adsorption increases rapidly with increasing shaking time and it tends to approach equilibrium within 60 min. The order of binding capacities of toxic heavy metals with prepared biosorbent materials was $Pb^{2+} > Cd^{2+} >$ As (V) ions in the individual and mixture of metal ions solution. The maximum percent removal for toxic heavy metals was 90% for lead, 79.4% for cadmium and 76.8% for arsenic at the initial concentration of 500 ppm. From this research, among three types of sorbent materials, CCA beads are more effective than CA beads and charcoal only in the removal of toxic metal ions from aqueous solutions.

Key words: biosorbent, calcium alginate, charcoal calcium alginate, FT IR, SEM, EDXRF, TG-DTA

Introduction

Toxic heavy metal contamination of the environment is a significant worldwide problem and conventional methods for removing toxic metals from contaminated water include chemical precipitation, chemical oxidation

1. Assistant Lecturer, Dr, Department of Chemistry, Yadanabon University
2. Associate Professor, Dr, Department of Chemistry, Kalay University
3. Pro-Rector, Dr, Kyaukse University

or reduction, ion exchange, adsorption, filtration, membrane technologies, and evaporation recovery. An alternative metal removal method, biosorption has been widely considered which is based on metal-sequestering properties of certain natural materials of biological origin. Biosorption processes can be based on plant biomass or animal polymers. However, biosorption studies typically have used microbial biomass. Of all the microbial species, algae have received the most attention in connection with metal bisorption and they have been extensively studied due to their ubiquitous occurrence in nature (Website 1) .

Coconut shell charcoal (biochar) is a type of charcoal produced from coconut shell (biomass) via pyrolysis. Due to its low cost and local availability, coconut shell charcoal has drawn attention in the wastewater treatment arena. Coconut shell charcoal, generated as a by-product from coconut shell pyrolysis, has been investigated for arsenic along with cadmium and lead. Alginic acid is a heteropolymer comprising polyuronic groups. It is derived from common commercial algae extracted commonly from brown seaweeds. The calcium alginate is a salt of alginic acid. Sodium salt has the ability to exchange multivalent cations. It is in fact the basis of their gelling properties. The metal ions easily linked to form covalent bonds yielding insoluble gels. In this study, the gelling property and the metal chelating property of alginate were combined to develop an alginate gel based adsorbent. To achieve a high application potential for the alginate gel adsorbent, coconut shell charcoal containing alginate bead adsorbent was developed. The coconut shell charcoal calcium alginate beads can be prepared simply by dropping sodium alginate solution containing coconut shell charcoal into $CaCl_2$ solution. It was successfully used for the removal of heavy metal ions (Website 2; Babel, 2003).

The aim of this research work was to prepare low-cost and highly efficient performance sorbent materials by the use of coconut shell charcoal and calcium alginate, and to investigate a deeper understanding about heavy metals adsorption onto the prepared biosorbent materials.

Materials and Methods

The chemicals used in the experimental work were from British Drug House Chemical Ltd., Poole, England and Kanto Chemical Co., Inc., Tokyo, Japan. Some of the instruments used in the experiments in this study

are balance, magnetic stirrer, pH meter, electric shaker, scanning electron microscope, atomic absorption spectrophotometer, thermoanalyzer: horizontal design and energy dispersive X-ray fluorescence.

Preparation of Three Types of Sorbent Materials

Carbonization of Coconut Shell Charcoal (Website 3; Costa and Leite, 1991)

The coconut shells were separated and cleaned from other materials, such as coconut fiber or soil and then dried in sunlight. The dried coconut shells were burned at burning sink or drum at 200 to 550°C for 3-5 hr to get charcoal. The charcoal was soaked in chemical solution ($CaCl_2$ or $ZnCl_2$, 25%) for 12-18 hr to become activated charcoal. The obtained activated charcoal was washed with distilled or clean water and spread on tray at room temperature to be drained. Then, it was dried in oven at temperature 110°C for 3 hr. This activated charcoal was ground and sieved to get the size range of 120 to 200 meshes. The obtained coconut shell charcoal is shown in Figure 1(a).

Preparation of Biosorbent Composite Beads (Website 4)

Various concentration of sodium alginate solution (2%, 4%, 6%, 8% w/v) were prepared, corresponding to constant amount 2 g of coconut shell charcoal and the prepared solution was stirred at constant rate (~150 rpm) at room temperature for 30 min. Using a syringe, the mixture was injected in droplets in 20% w/v of calcium chloride to form beads. The biocomposite beads were allowed to stay in calcium chloride solution with slow stirring for another 1 hr until it become harden. The beads were allowed to harden in this solution for 24 hr. After this time, hard spherical beads were dried at room temperature and collected in an air container. The results are presented in Table 1.

Calcium alginate beads were prepared by dissolving 6 g of sodium alginate in 100 mL of distilled water at room temperature. The gel was allowed to cool down at room temperature and the viscous solution was forced through a syringe. The resulting gel droplets were collected in a stirred reservoir containing 100 mL of a 20% w/v of a $CaCl_2$ solution. The beads were allowed to harden in this solution for 24 hr. After this time, the hard spherical calcium alginate beads were obtained.

A 6% (w/v) of sodium alginate gel solution was prepared by dissolving 6 g of sodium alginate into 100 mL distilled water at room temperature and 2 g of coconut shell charcoal was added to the gel solution with continuous stirring. Once the mixture was homogeneous, it was forced through a syringe. The resulting gel droplets were collected in a stirred reservoir containing 100 mL of a 20% w/v of a $CaCl_2$ solution. The beads were allowed to harden in this solution for 24 hr. After this time, hard spherical beads containing coconut shell charcoal calcium alginate were obtained. The prepared beads were allowed to dry at an ambient temperature. The beads obtained are shown in Figure 2 (b) and (c).

Characterization of Prepared Sorbent Materials

Prepared sorbent materials *viz*., coconut shell charcoal, calcium alginate beads and charcoal-calcium alginate beads were characterized by FT IR, TG-DTA, EDXRF and SEM analysis. The results are shown in Figures (2 a, b, c), (3 a, b, c), (4 a, b, c) and (5 a, b, c) respectively.

Removal of Metal Ions from Aqueous Solution (Website 3; Website 5)

The prepared sorbent materials were dried at room temperature (25°C) and these materials were used in sorption experiments. Stock solution containing 1000 mgL^{-1} of heavy metals ions were prepared by dissolving lead II nitrate, cadmium (II) sulphate and sodium arsenate respectively. Sample solutions were prepared from the stock solution by diluting appropriate aliquots with distilled water.The sorption experimental studies were carried out at room temperature using conical flasks containing 1 g of each dried sorbent materials and 100 mL each of heavy metal ions solution.

Effect of pH on Removal of Lead, Cadmium and Arsenic

The standard stock solutions (500 mg L^{-1}) of lead (II) nitrate, cadmium (II) sulphate and sodium arsenate at various pH (3, 4, 5, 6) were prepared by adding 0.1M hydrochloric acid and 0.1 M sodium hydroxide solution. A fixed amount of prepared sorbent materials (1 g) was added to 100 mL of 500 ppm each solution and the mixture was shaken with a shaker for 1 hr at room temperature. Then the mixture was filtered through filter paper Whatmann No.1 and the metal ions in the filtrate was determined by

complexometric titration using xylenol orange as indicator for lead and cadmium and iodometirc titration for arsenic.

Effect of Contact Time on Removal of Lead, Cadmium and Arsenic

Accurately weighed prepared sorbent material (1 g) each was placed in separate flasks. Then 100 mL of each metal stock solution (500 ppm), adjusted at pH 5 for lead and pH 5.5 for cadmium and arsenic were added into each flask. The flasks were placed on an electric shaker and were shaken to reach the equilibrium. The contact time was varied at interval of 10 min, 20 min, 30 min, 40 min, 50 min and 60 min. The sample solutions were separated by filtration. The resulting metal content in the solutions were determined by complexometric titration for lead and cadmium and iodometric titration for arsenic.

Effect of Dosage on Removal of Lead, Cadmium and Arsenic

Prepared sorbent material of various masses ranging from 1 g to 5 g were placed in the flasks and 100 mL of each metal solution (500 ppm) was added to each flask at optimum pH. And then the loaded flasks were placed on an electric shaker. In order to attain complete equilibrium, the solutions were shaken for one hour at room temperature. The sample solutions were removed from the sorbent by filtration. The residual content of metal ions in the solution were determined by complexometric titration for lead and cadmium and iodometric titration for arsenic.

Characterization of Sorption of Metal Ions on Prepared Three Types of Sorbent Materials

The FT-IR, TG-DTA, ED-XRF and SEM analyses were carried out for three types of sorbent materials after sorption of metal ions.

Results and Discussion

Preparation of Three Types of Biosorbent Materials

Figure 1 shows the prepared coconut shell charcoal, calcium alginate beads and coconut shell charcoal calcium alginate beads. In the preparation of the beads, sodium alginate concentration was very important, if the concentration of sodium alginate was very low, no formation of beads and if the concentration of sodium alginate was very high, the solution was

very viscous and difficult to pass through the syringe. The optimum condition was selected.

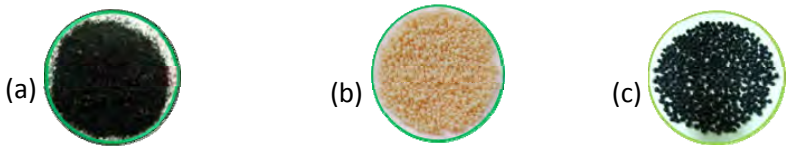

Figure 1. (a) Coconut Shell Charcoal, (b)Calcium Alginate Beads, (c) Charcoal-Calcium Alginate Beads

Table 1. Preparation of calcium alginate and coconut shell charcoal-calcium alginate beads

Charcoal ,W (g)	Sodium alginate solution, (% w/v)	$CaCl_2$, (% w/v)	Remark
0.5	6	20	no formation of beads
1.0	6	20	no formation of beads
1.5	6	20	Slightly viscous
2.0	6	20	fine beads

Characterization of Prepared Three Types of Sorbent Materials

FT IR Analysis

FT IR spectra of the adsorbent before and after sorption reaction possibly provides information regarding the surface groups that might have participated in the adsorption reaction and also indicates the surface sites on which adsorption have taken place.

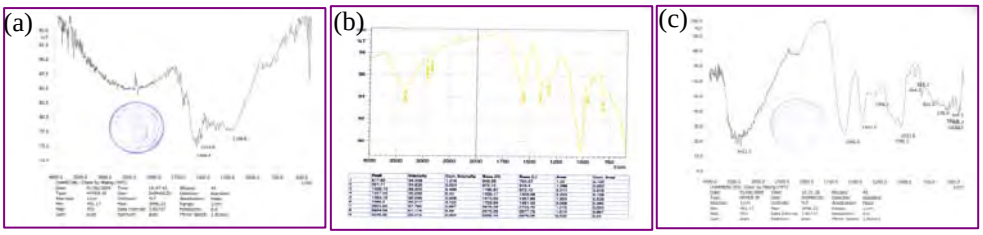

Figure 2 (a), (b), (c) FT-IR Spectra of Charcoal, CA beads and CCA beads

Thermal Analysis for Prepared Biosorbent Materials

On the basis of TG-DTA profiles, Figures 3 (a), (b) and (c) show the break in temperature corresponding to dehydration, deploymerization, decomposition and phase change temperature of charcoal, calcium alginate beads and charcoal-calcium alginate beads.

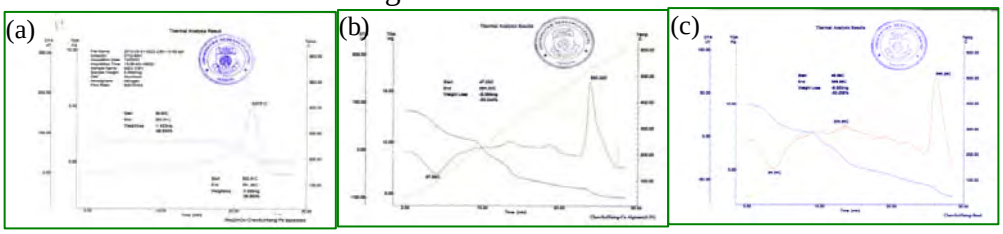

Figure 3 (a), (b), (c) Thermograms of Charcoal, CA beads and CCA beads

EDXRF Analysis

Figures 4 (a), (b) and (c) show the EDXRF spectra of three types of sorbent materials. The spectrum indicated that the calcium is the major constituent in the beads.

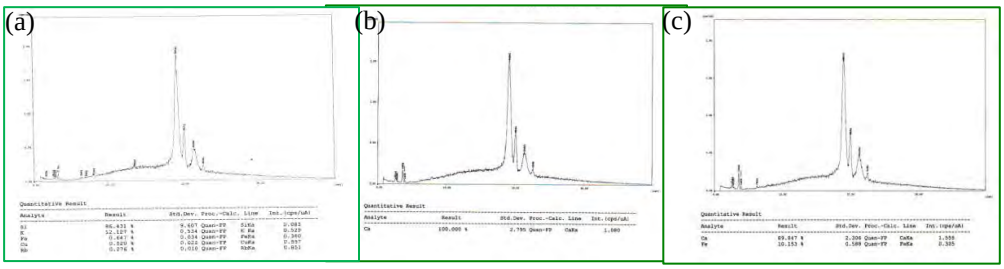

Figure 4 (a), (b) and (c) EDXRF Spectra of Charcoal, CA beads and CCA beads

SEM Analysis

Figures 5 (a), (b) and (c) show the surface morphology of prepared coconut shell charcoal, calcium alginate beads and charcoal calcium alginate beads.

SEM images of charcoal, calcium alginate beads and charcoal calcium alginate beads revealed a cluster form of aggregate with cavitated pores. It can be also found as the beads have foam-like and porous nature. Since micro and meso pores are observed on the surface of the biosorbent

materials, significant adsorption is likely to occur. Therefore, these beads may be responsible for the enhanced specific sorption properties.

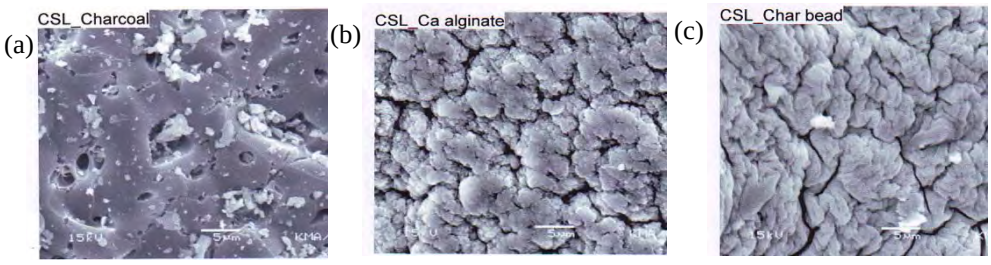

Figure 5 (a), (b) and (c) SEM micrographs of Charcoal, CA beads and CCA beads

Effect of pH on the Removal of Pb^{2+}, Cd^{2+} and As(V) Ions

The pH is an important process parameter on biosorption of metal ions from aqueous solution since it is responsible for protonation of metal binding sites. The removal of Pb^{2+} ions increased with increasing pH and the highest adsorption was observed at pH 5, Figure (6 a, b, c). Experiments were not performed beyond pH 5 because at higher pH, precipitation of metal was observed and the precipitate may be interfered with the biosorption process.

The removal of lead, cadmium and As (V) ions was dependent on pH, where optimal metal removal efficiency occurred at pH 5 for Pb^{2+}, pH 5.5 for Cd^{2+} and As (V) ions. As the results, the after adsorption experiments were performed at these pH values.

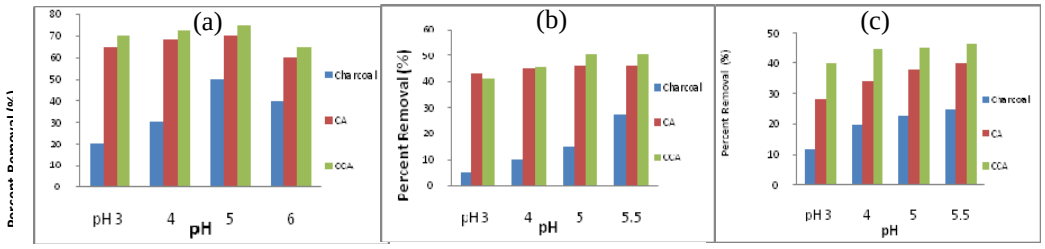

Figure 6 (a), (b) and (c) Effect of pH on the removal of Pb^{2+}, Cd^{2+} and As (V) ions by biosorbent materials

Effect of Contact Time on the Removal of Pb^{2+}, Cd^{2+} and As (V) Ions

The effect of contact time on the speciation of Pb^{2+}, Cd^{2+} and As (V) ions on prepared sorbent materials were investigated. It was found that the maximum adsorption occurred within 50 min for Pb^{2+}, 60 min for Cd^{2+} and 30 min for As (V) ions, Figure (7 a, b, c). Adsorption equilibrium time is defined as the time required for heavy metal concentration to reach a constant value.

Effect of Contact Time on the Removal of Pb^{2+}, Cd^{2+} and As (V) Ions by Prepared Biosorbent Materials

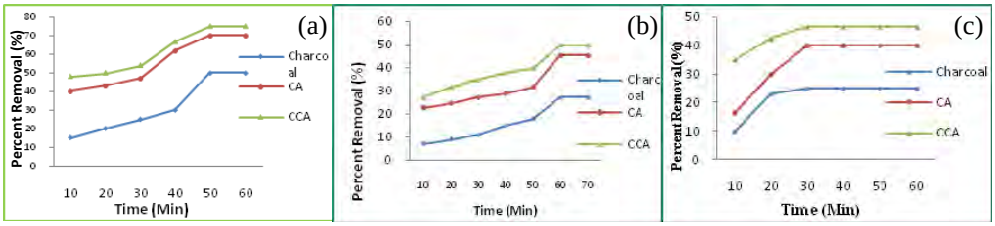

Figure 7 (a), (b) and (c) Effect of contact time on the removal of Pb^{2+}, Cd^{2+} and As(V) ions by biosorbent Materials

Effect of Dosage on the Removal of Pb^{2+}, Cd^{2+} and As (V) Ions

The effect of dosage on the speciation of Pb^{2+}, Cd^{2+} and As (V) ions on the prepared biosorbent beads were studied. It was found that the removal of Pb^{2+} ion from 500 ppm of model lead (II) nitrate solution increased from 35.5% to 76%, 56.5% to 87.5% and 66% to 90% with an increased in dose of charcoal, CA beads and CCA beads from $10gL^{-1}$ to $50gL^{-1}$, respectively. It was also found that the removal of Cd^{2+} ion increase from 18.2% to 51.82%, 40% to 73% and 43% to 79.4% with an increase in amount of charcoal, CA beads and CCA beads from $10gL^{-1}$ to $50gL^{-1}$, respectively.

The removal of As (V) ion from 500 ppm of sodium arsenate solution was increased from 14.3% to 48.8%, 33.4% to 71% and 37.5% to 76.8% with increase in dose of charcoal, CA beads and CCA beads from $10gL^{-1}$ to $50gL^{-1}$, respectively. It was apparent that the percent removal of metal ions increases rapidly with increase in dose due to great availability of the biosorbent. Figures (8 a, b, c) show the increase in percent removal when biosorbent dose was increased 1 to 5 g in 100 mL heavy metal solution. This may be attributed to reduction of total area of biomass surface

depending on the experimental condition such as pH, ionic strength and temperature.

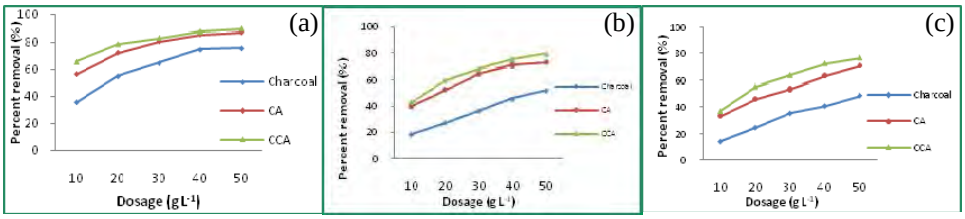

Figure 8 (a), (b) (c) Effect of dosage on the removal of Pb^{2+}, Cd^{2+} and As(V) ions by biosorbent materials

Characterization of Sorbed Metal Ions on Biosorbent Materials

FT IR Analysis

The spectra of each sorbent material and respective metal ion show the O-H stretching region around 3400 cm^{-1}. A band around 880 cm^{-1} which corresponds to metal -O stretching vibration confirms respective metal adsorption onto the metal-sorbed materials. Carboxyl group is supposed to be a characteristic group of alginic acid, which is the key compound found in calcium alginate and charcoal calcium alginate for making adsorption. The asymmetrical C=O stretching band for carboxylic group at 1600 cm^{-1} and the weaker symmetrical stretching band at around 1400 cm^{-1} observed for two biosorbent beads have shifted to different extents after contact with metal solutions, the differences between these two peaks all ranged from 4 to 25 cm^{-1}. These band changes indicate the involvement of carboxyl group in metal adsorption, probably through chelation or complexation.

Figure 9 (a), (b), (c) FT-IR spectra of Charcoal after adsorption of lead, cadmium and arsenic

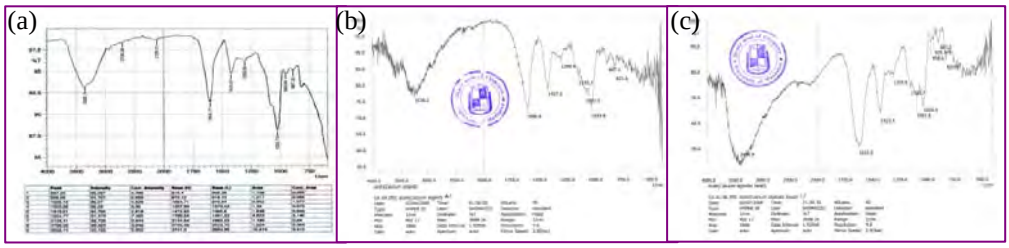

Figure 10 (a), (b) ,(c) FT-IR spectrum of CA Beads after adsorption of lead, cadmium and arsenic

Figure 11 (a), (b) , (c) FT-IR spectrum of CCA Beads after adsorption of lead, cadmium and arsenic

Thermal Analysis

On the basis of TG-DTA profiles, the figures show the break in temperature corresponding to dehydration, deploy-merization, decomposition and phase change temperature of charcoal, calcium alginate beads and charcoal –calcium alginate beads after adsorption of lead, cadmium and arsenic.

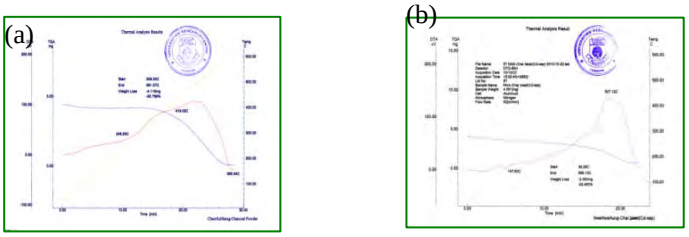

Figure 12 (a), (b) Thermograms of charcoal after adsorption of lead and cadmium

Figure 13 (a), (b), (c) Thermograms of CA beads after adsorption of lead, cadmium and arsenic

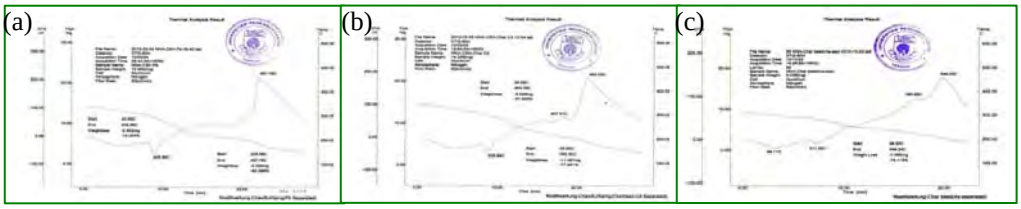

Figure 14 (a), (b), (c) Thermograms of CCA beads after adsorption of lead, cadmium and arsenic

EDXRF Analysis

The presence of Pb^{2+}, Cd^{2+} and As (V) ions individually sorbed on the prepared biosorbent materials are shown by the EDXRF spectra represented in Figures (15 a, b, c), (16 a, b, c) and (17 a, b, c) which are more semi quantitative and on the matrix basis. It can be observed that each spectrum indicates that the relevant metal ions was sorbed on the biosorbent materials. It can be inferred from the pronounced peaks that each spectrum had represented.

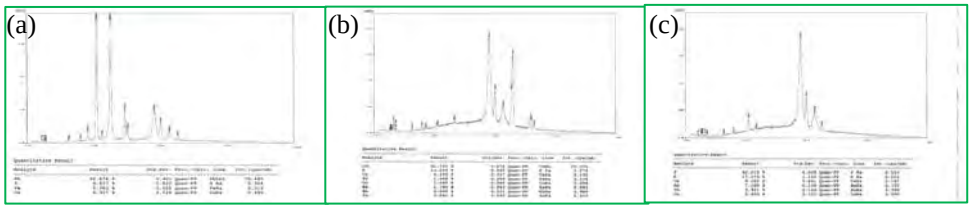

Figure 15 (a), (b), (c) EDXRF spectrum of charcoal after adsorption of lead, cadmium and arsenic

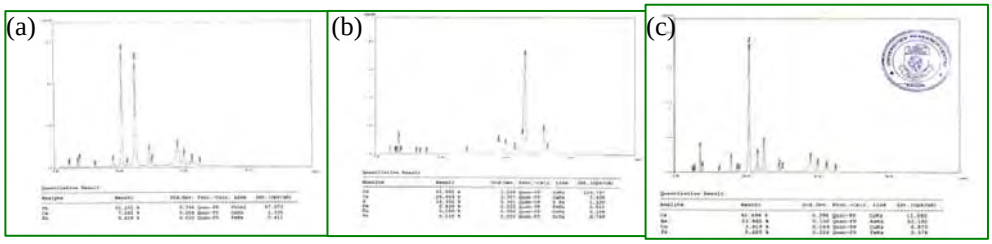

Figure 16 (a), (b), (c) EDXRF spectrum of CA beads after adsorption of lead, cadmium and arsenic

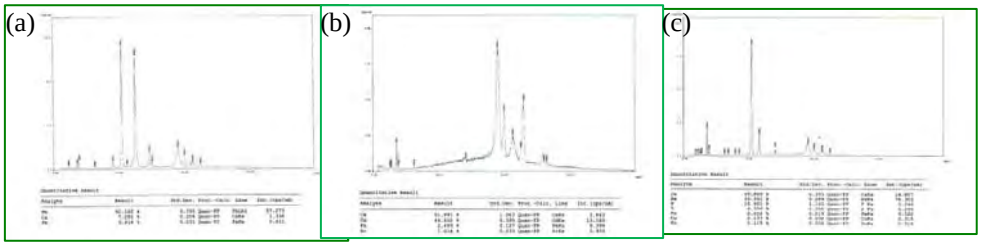

Figure 17 (a), (b), (c) EDXRF spectrum of CCA beads after adsorption of lead, cadmium and arsenic

SEM Analysis

Figures (18 a, b, c), (19 a, b, c) and (20 a, b, c) show the surface morphology of three types of sorbent materials after adsorption of lead, cadmium and arsenic.

After adsorption of lead, cadmium and arsenic ions on three types of sorbent materials are very different from one another. In all figures cavitated pores were closed by the sorption of lead or cadmium or arsenic. It is one way to explain the nature of images that co-precipitation of specified metal may take place.

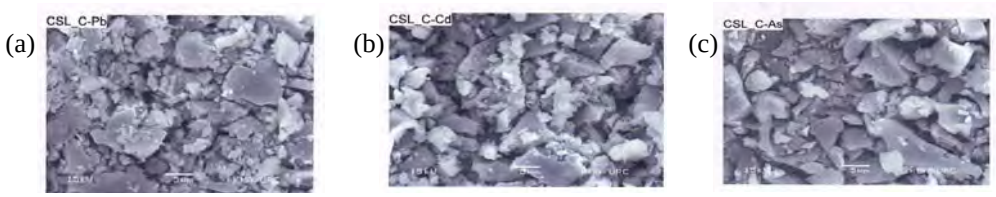

Figure 18 (a), (b), (c) SEM photographs of charcoal after adsorption of lead, cadmium and arsenic

Figure19 (a), (b), (c) SEM photographs of CA beads after adsorption of lead, cadmium and arsenic

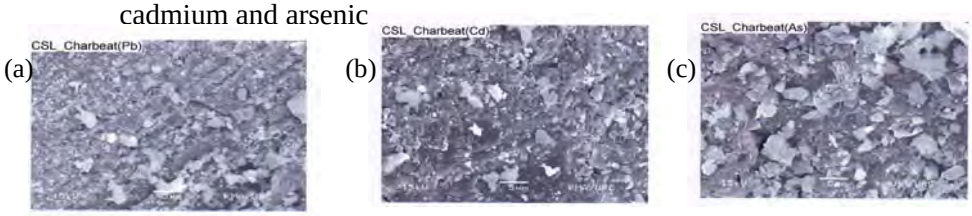

Figure 20 (a), (b), (c) SEM photographs of CCA beads after adsorption of lead, cadmium and arsenic

Conclusion

The present study indicates that all the prepared sorbent materials are effective adsorbents for heavy metals. The results show that effective biosorbent composite beads can be prepared by blending 2 g of coconut shell charcoal, 6% w/v of sodium alginate and 20% w/v of calcium chloride. On the aspect of removal of Pb^{2+}, Cd^{2+} and As (V) ions by charcoal, CA and CCA, the removal percent depends on pH, the mass of adsorbent used and the time contact between sorbent and sorbate. Sorption experiments were conducted based on the mass of adsorbent dose. It was observed that percent removal of metal ions increase with increase in mass of adsorbent dose however the increase dose of adsorbent will have to decrease metal uptake capacity. Thus, the adsorbent dose (10 gL^{-1}) was used in the whole experiments.

From the experiment, the maximum percent removal of Pb^{2+} ions by the coconut shell charcoal, calcium alginate and charcoal-calcium alginate beads were found to be 76%, 87.5% and 90% respectively. The highest percent removal of Cd^{2+} ions by charcoal, CA and CCA beads were observed at 51.8%, 73% and 79.4% respectively.

Similarly, the highest percent removal of As (V) ions by charcoal, CA and CCA beads were 48.8%, 71% and 76.8% respectively. From the above observations, it was found that sorption efficiency was in the order of

Pb^{2+} > Cd^{2+} > As (V) ions. The metal removal capacity of three types of sorbent materials was observed that CCA beads were more effective than that of CA beads and charcoal. The trend of metal removal capacities of prepared sorbent materials were found to be in the order of CCA > CA > charcoal.

Acknowledgements

The authors would like to express heartfelt gratitude to Rector Dr Khin Maung Oo, Yadanabon University for his interest and encouragement on this research work. The authors thank Dr Hlaing Hlaing Myat, Professor and Head, Department of Chemistry, Yadanabon University for her suggestions. Our thanks also to Dr Kyaw Myo Naing, Professor, Department of Chemistry, University of Yangon and Dr Win Pa Pa, Associate Professor, Nationality Youth Resources Development Degree College, Yangon for their helpful facilities and suggestions.

References

Babel, S. and Kuraniwan, T.A., (2003), "Low Cost Adsorbent for the Heavy Metal Uptake from Contaminated Water", *J.Hazard Matter*., **97**(1), 219-243

Costa, A.C.A. and Leite, S.C.G., (1991), "Metal Biosorption by Sodium Alginate Immobilized *Chlorerella homosphaera*", *Biotchnol. Letter*, **13**, 559-562

Online Materials

1.http:/www.elsevier.com/locate/procbio

2.http:/www.A-PDF.com to remove the watermark

3.http:/www.fftc.agnet.org

4.http:/www.google/Internets/CALCIUM/Alginate.htm

5.http:/www.bisorption.htm

Studies on Some Properties of Starch from Taro Corm

Tin Mya Mya Htwe

Abstract

Taro corms from Pyin Oo Lwin Township in Mandalay Region were collected for study on its properties. Experimental parameter such as pH, moisture and protein contents in taro starch were determined as 7.81,13.78 % and 5.61% respectively. Hydration capacity and moisture sorption capacity were 1.7 and 15.00 % respectively. Viscosity of taro starch solution (1.0%) was found to be 2.15 cP. Swelling power of taro starch increased with increasing temperature and rapid swelling was observed at 80^{o}C.Similar trend of increasing solubility of taro starch was also observed. By SEM, taro starch showed small, irregular shape and polygonal. Semi-crystalline nature of taro starch was shown by X-ray diffraction analysis. The degradation temperature of taro starch was observed as 310^{o}C by TG-DTA thermogram.

Key words : Taro starch, swelling power, solubility, SEM ,TG-DTA

Introduction

Taro is a common name for the corms and tubers of several plants in the family Araceae. Of these, *Colocasia esculenta* is the most widely cultivated.Taro is native to southeast Asia (Kolchaar, 2006). It is a perennial, tropical plant primarily grown as a root vegetable for its edible starchy corm, and as a leaf vegetable and is considered a staple food in African, Oceanic and Asian cultures. It is believed to have been one of the earliest cultivated plants.

A large number of starch resources are found in the tropic and subtropics regions which are being used as food while their properties remain to be determined. The taro (*Colocasia esculenta*) is one of those starch rich sources. Figure 1 shows the taro plants and corms.

Assistant Lecturer, Dr, Department of Chemistry, Kyaukse University

Figure 1. Taro plants and corms

Kingdom - Plantae

Order - Alismatales

Family - Araceae

Genus - *Colocasia*

Species - *esculenta*

Scientific name - *Colocasia esculenta* (L.) Schott

Taro corms contain considerable amount of starch (70-80 g/100g dry taro) (Quach *et al*., 2000). It has been reported that the carbohydrate content of taro cultivated in different locations varied (Jane *et al*., 1992).

Taro starch forms hard coating layer and its solution has clarity at even high solid concentration. It has high swelling power, high gel strength and peak viscosity (Adebayo and Itiola, 1998). Taro starch, in view of its small granule size (0.5 - 5 μm) form smooth textural gel and has been found to be easily digestible (Sugimoto *et al*., 1986). Due to ease of assimilation infants and the persons with digestive problems can use taro starch (May and Nip, 1983).

Taro starch has also been studied as a filling agent for the biodegradable polyethylene film and as a fat substitute (Daniel and Whistler, 1990; Jane *et al*., 1992).

Raw taro corms contain a considerable amount of oxalic acid ($H_2C_2O_4$) in forms of soluble oxalic acid and insoluble oxalate salts (Huang *et al*., 1992). Soluble oxalic acid can form complexes with calcium, magnesium (or) potassium and hence reduces mineral availability in the diet.

It has also been reported that insoluble oxalate salts cause skin irritation and a pungent odor in unwashed taro corms (Maga,1992). Continuing consumption of taro with a high oxalate salt content can lead to gallstone deposition in the gall-bladder. In a careful extraction of taro starch from its corm, both soluble and insoluble forms of oxalic acid can be removed.

The main aim of this study was to extract taro starch and to determine its physicochemical properties, morphological and thermal properties and semi-crystalline properties.

Materials and Methods

Sample Collection

Fresh taro corms in medium size, obtained upon harvest from Pyin Oo Lwin Township were purchased.

Extraction of Starch from Taro Corms

Taro starch was extracted from taro corm according to the procedure of Moorthy *et al*. (1993). Fresh taro corms were washed, peeled, and cut into small pieces and disintegrated in a blender at low speed using 0.03 M ammonia solution. The suspension was passed through 250 mesh screen twice and allowed to settle overnight. The supernatant was decanted off and this starch was subjected to a second washing and settled overnight. The starch cake formed was removed, powdered and dried at 45-50ºC for 24 hr. The starch obtained was analysed for its characteristics.

Determination of pH

Taro starch (1.0 g) was made into mucilage with 100 ml of distilled water and it was determined for pH with a pH meter (Oyster-15), which was previously calibrated with standard buffers of pH 4 and 7.

Determination of Moisture Content

Taro starch powder (5.0 g) was weighed and then dried in an oven at 110ºC for about 2 hr and then weighed again until constant weight was obtained and the percentage loss on drying was calculated.

Determination of Protein Content

Taro starch powder (1.0 g) was introduced to a Kjeldahl flask. The catalyst mixture (9.0 g anhydrous potassium sulphate and 1.0 g copper sulphate) and concentrated sulphuric acid (15 mL) were then added. The flask was partially closed by means of a funnel and then the contents were digested by heating the flask in an inclined position. At first, it was gently heated for about 30 min and then heating was continued vigorously for about 3 hr until the solution was totally digested and became clear. The flask was shaken occasionally during the digestion process.

Then the flask was allowed to cool and about 10 mL of distilled water were added and Kjeldahl distillation apparatus was set up. Into the flask, 70 mL of 40% sodium hydroxide solution was poured through the side arm together with 200 mL of distilled water. The contents were distilled by direct heating. The ammonia evolved was allowed to absorb in 25 mL of 4% boric acid solution that was in a receiver flask. The ammonia distillate was titrated with 0.05 M sulphuric acid, using methyl red as an indicator until a red colour just appeared.

Determination of Viscosity

Into 1.0 g of taro starch powder, a few mL of distilled water was added to make a paste. The paste was added into 100 mL boiling water and then boiled for 10 min to obtain 1 % starch solution. Using a U-tube viscometer the viscosity of starch solution was determined.

Determination of Hydration Capacity

Hydration capacity was determined according to the method of Kornblum and Stoopak (1973).

Taro starch powder (1.0 g) (Y) was placed in a centrifuge tube and covered with 10 ml of distilled water. The tube was shaken intermittently for about 2 hr and left to stand for 30 min before centrifugation at 3000 rpm for ten minutes. The supernatant was decanted and the weight of the powder after water uptake and centrifugation (X) was determined. Hydration capacity was calculated as;

$$\text{Hydration capacity} = \frac{X}{Y}$$

Moisture Sorption Capacity

Moisture Sorption Capacity was determined according to the method of Ohwoavworhua *et al*., (2004).

Taro starch powder (2.0 g)(W) was weighed and put into a Petri dish. The Petri dish was then placed in a desiccator containing distilled water at room temperature and the weight gained by the exposed sample at the end of a five-day period (W_g) was recorded and the amount of water absorbed (W_a) was calculated from the weight difference as;

$W_a = W_g - W$

Determination of True Density of Taro Starch

The true density (D_t), of taro starch powder was determined by the liquid displacement method using xylene as the immersion fluid and computed according to the following equation.

$D_t = W_p / [(a + W_p) - b] \times SG$

where W_p is the weight of powder, SG is specific gravity of solvent, 'a' is weight of bottle + solvent and 'b' is weight of bottle + solvent + powder.

Determination of Swelling Power and Solubility

Swelling power and solubility of taro starch were determined by the method described by Leach *et al*., (1959) over a temperature range of 50-90ºC.

In a graduated tube (15 mL), 2 g of starch was added to 50 mL distilled water followed by stirring for 1 min. The tube was placed in a water bath of desired temperature for 15 min, whereby the tube was mixed thoroughly every 5 min for 20s. After 15 min, the tube was cooled in an ice bath to 25ºC after which it was centrifuged at 3000 rpm for 25 min. The supernatant was carefully removed using a pipette and its amount as well as its dry matter content were determined. Starch solubility was calculated as the amount of dry matter present in the supernatant divided by the initial starch weight. The weight of the sedimented paste was also recorded and the swelling power was calculated as the weight of the sediment divided by the weight of the original sample.

Surface Morphology of Taro Starch

Surface morphology of the taro starch sample was examined using a scanning electron microscope (Jeol-JSM-5610LV, Japan) at Universities' Research Center, Yangon. The SEM image of taro starch was received at 15.5 kV accelerating voltage and magnified 5500 times.

X-Ray Diffraction Studies on Taro Starch

The structure of taro starch was investigated by using Rigaku X-ray powder diffractometer (Rigaku, Tokyo, Japan) at Universities' Research Center, Yangon.The powder taro starch was scanned using Cu K_α radiation (λ =1.54056 $\mathring{A}$) at 40 kV and 40 mA. The scanning region of the angles (2θ) was from 10^o to 70^o.

Thermal Stability

Thermal stability of taro starch was investigated by thermogravimetric differential analysis (TG-DTA) employing Shimadzu DTG 60H differential thermal analyzer at Universities' Research Center, Yangon.

Results and Discussion

Physicochemical Properties of Taro Starch

Table 1 shows the physicochemical properties of taro starch. The pH of taro starch was found to be 7.81, i.e, slightly alkaline. It was reported that maize starch has slightly acidic pH while rice and wheat starch was nearly neutral (Olayemi *et al*., 2008).

Moisture content of taro starch was 13.78%. It was greater than those of maize starch, rice starch and wheat starch which were reported as 4, 6 and 12 respectively (Olayemi *et al*., 2008).The moisture content of taro starch was higher than maize, rice and wheat starch. This may be due to its larger pore sizes and this may trap water and result in high moisture contents. Protein content of taro starch was found to be 5.61%.

Hydration capacity of taro starch is 1.70. It means that taro starch is capable of absorbing 1.7 times of its own weight of water. Moisture sorption capacity of taro starch was 15.00 %. The moisture sorption capacity is a measure of moisture sensitivity of a material. True density of taro starch was 1.81 and viscosity of 1% taro starch solution was 2.15 cP.

Table 1. Physicochemical properties of taro starch

No	Parameter	Composition
1	pH	7.81
2	Moisture content (%)	13.78
3	Protein content (%)	5.61
4	Hydration capacity	1.70
5	Moisture sorption capacity (%)	15.00
6	True density	1.81
7	Viscosity (1% solution)(c P)	2.15

Effect of Temperature on Swelling Power and Solubility

The swelling power is contributed by the content of amylopectin and the solubility is contributed by the content of amylose (Tester and Morrison,1990).

The swelling power of taro starch was found to be a function of temperature(Table 2 and Figure 2). Prior to gelatinization, there was some increase in swelling capacity of starch. At 50ºC and 60ºC, swelling power of taro starch was only 2.05% and 2.90 % respectively. However, once the gelatinization process sets in at 80ºC, swelling power increased rapidly with increasing temperature. At 70ºC and 80ºC, the swelling power is 6.40% and 14.15% respectively. At 90ºC the swelling power increased about 8.5 fold over its initial value.

Solubility of taro starch was observed to be a function of temperature between 50ºC-90ºC as shown in Table 3 and Figure 3 and. It followed a pattern similar to that of swelling power characteristic. Below the gelatinization temperature taro starch was less soluble. From 50°C to 70ºC, the solubility of taro starch was less than 10%. However, as the temperature increased to 80ºC, the solubility increased markedly and found to be 29.2%. When the temperature was raised to 90ºC, more increase in solubility of taro starch was observed. This may be attributed to loss of granular structure and release of amylose fraction of the starch as the amylose molecules are preferentially solubilized and leached from swollen

starch granules (Stone *et al.*, 1984). At 80ºC and 90ºC, complete gelatinization was also observed.

Starch could not be dissolved in cool water due to the starch crystal structure. The starch molecule started to disintegrate in water as the temperature increased. Amylose and amylopectin were dissociated in suspension, and the solubility of starch was increased. The insoluble starch started to swell because of hydration.

Table 2.Relationship between temperature and swelling power of taro starch

Temperature(^{o}C)	Swelling power (%)
50	2.05
60	2.90
70	6.40
80	14.15
90	16.90

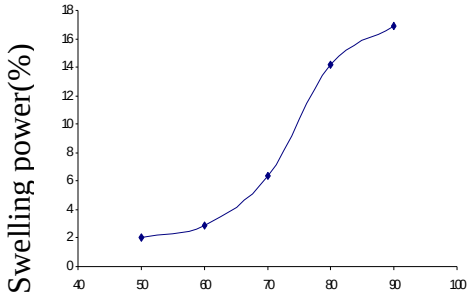

Figure 2. Effect of temperature on swelling power of taro starch

Table 3. Relationship between temperature and solubility (%)of taro starch

Temperature(^{o}C)	Solubility (%)
50	2.4
60	3.2
70	7.6
80	29.2
90	39.0

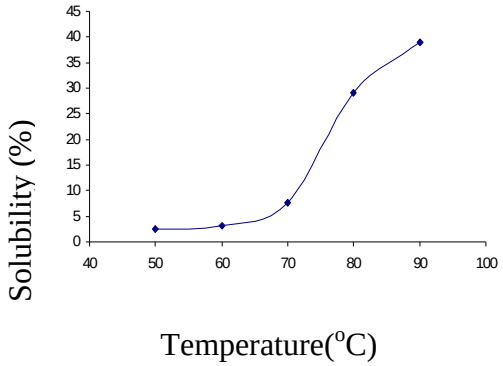

Figure 3. Effect of temperature on solubility (%) of taro starch solution

Morphology of Taro Starch

Scanning electron micrograph (Figure 4) shows that taro starch granules were small, irregular shapes, and polygonal.

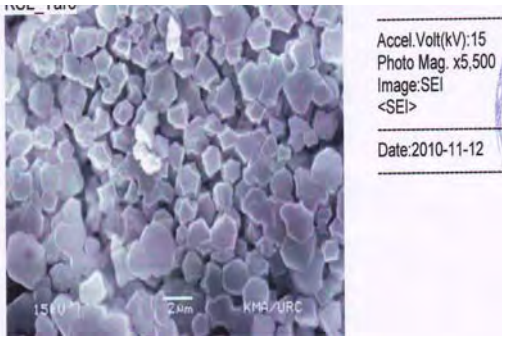

Figure 4. Scanning electron micrograph of taro starch

X-Ray Powder Diffraction

Semi-crystalline nature of taro starch was observed in X-ray diffractogram (Figure 5) because of the presence of both sharp and diffuse diffraction peaks.Taro starch showed strong diffraction peaks at 15.3^o, 17.9^o, 23.4^o,and 24.5^o of 2θ. Parallel double amylopectin molecules result in the formation of crystalline regions, while amylose molecules result in the formation of amorphous regions in the starch structure.

Thermogravimetric Differential Thermal Analysis (TG-DTA)

TG-DTA thermogram of taro starch is shown in Figure 6. It was noted that initial weight loss began at approximately 50ºC and reached a constant weight plateau after losing about 19.665 % of its initial weight. The weight loss corresponds to the loss of moisture content from the taro starch. Between 140 ºC and 290 ºC, taro starch was found to be thermally stable. DTA curve shows an endothermic peak at 70.9ºC. Moreover, another weight loss was started at approximately 310ºC. At this temperature the taro starch began to degrade. This temperature is the degradation temperature of taro starch. DTA curve shows two exothermic peaks at 386.41ºC and 550.54ºC due to degradation of starch. At the end of the experiment (559.72ºC), weight loss % was 81.684% and thus 18.316% residue was left. The nature and remarks regarding the TG-DTA thermogram profile is presented in Table 4.

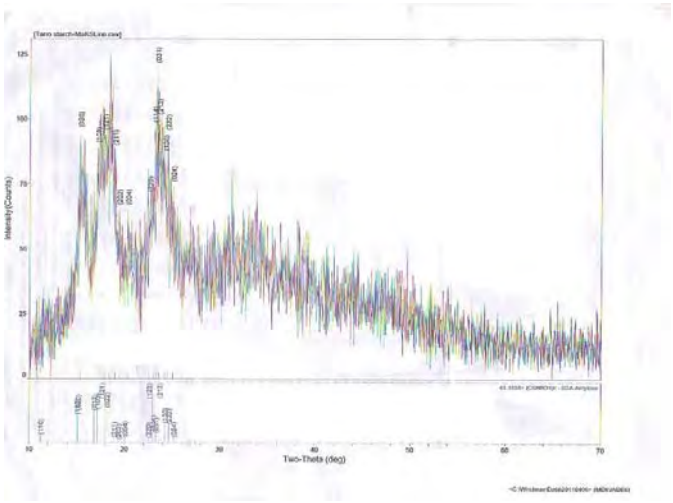

Figure 5. X-ray diffractogram of taro starch

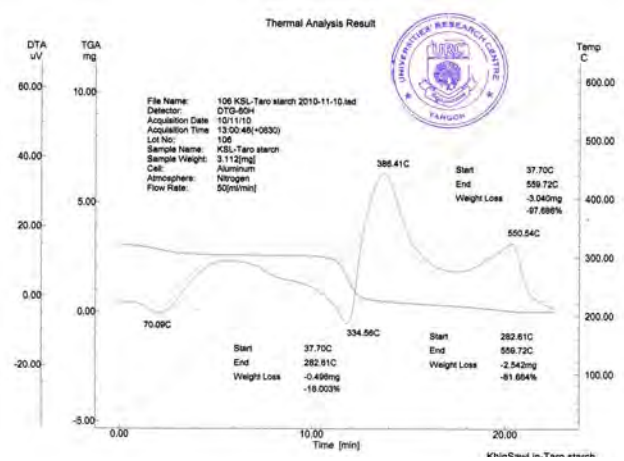

Figure 6. TG-DTA thermogram of starch

Table 4.Thermal analysis data of taro starch

Temperature range(°C)	TGA	DTA		Remark
	weight loss (%)	Break in temperature	Nature of peak	
37.70-282.61	16.003	70.09ºC	endothermic peak	Loss of moisture
282.61-559.72	81.684	386.41ºC 550.54ºC	exothermic peak	Degradation of starch

Conclusion

Fresh taro corms in medium size, obtained upon harvest from Pyin Oo Lwin Township in Mandalay Region, were purchased. Physicochemical investigations revealed that pH of taro starch was 7.81 and found to be slightly basic. Moisture content was observed as 13.78% and protein content was determined as 5.61%.The hydration capacity and moisture sorption capacity were 1.70 and 15.00 % respectively. The true density of taro starch was found to be 1.81.

Swelling power of taro starch increased with increasing temperature, however, it increased rapidly when the gelatinization process set in.

Moreover, the solubility of the taro starch increased with increasing temperature and at 80°C and 90°C complete gelatinization was observed. Surface morphology of taro starch was examined by SEM at 5500 X magnification and found to be small, irregular shapes and polygonal. Taro starch showed characteristic crystalline peaks at 15.3°, 17.9°, 23.4°, and 24.5° of 2θ. From TG-DTA thermogram the degradation temperature of taro starch was 310°C. By DTA one endothermic and two exothermic peaks were observed due to the loss of moisture and degradation of starch respectively.

This research contributes information on the physicochemical, morphological and thermal properties of taro starch. These findings would be useful in the handling of taro starch for its applications.

Acknowledgements

The author would like to acknowledge Dr Myint Lwin, Rector in-charge and Dr Thidar Win, Pro-rector, Kyaukse University, for their kind provision of the research facilities. The author would also wish to express grateful thank to Dr Ni Ni Sein, Professor and Head , Department of Chemistry, Kyaukse University for her sound suggestion.

References

Adebayo,A.S. and Itiola,O.A.,(1998),“ Properties of Starches Obtained from *Colocasia esculenta* and *Artocarpus communs*” , *Nigerian J.Naturae Prod.Med*.,**2** :29

Daniel.J.R. and Whistler.R.L.,(1990),“Fatty Sensory Qualities of Polysaccharides” , *Cereal Foods World*, **35**:825

Huang,AS. and Tanudjaja,L.S.,(1992), “ Application of Anion Exchange High-Performance Liquid Chromatography in Determining Oxalates in Taro (*Colocasia esculenta*) Corms”, *J.Agri. Food Chem*. **40**:2123-6

Jane J.L., Shen, L.,Chen J., Lim,S.,Kasemsuwan,T., and Nip, W.K., (1992), “ Physical and Chemical Studies of Taro Starches and Flours”, *Cereal Chem*, **69**: 528-35

Kolchaar .K.,(2006), “ Economic Botany in the Tropics”, Macmillan, India.

Kornblum,S.S.and Stoopak,S.B.,(1973), “A New Tablet Disintegrant Agent:Crosslinked Polyvinylpyrollidone.*J.Pharm.Sci*., **62**(1):43-49

Leach,H.W., Mccoven, L.D.,& Schoch,J.I.,(1959), “ Swelling and Solubility Patterns of Various Starches”, *Cereal Chem*., **36**:534

Maga, J.A., (1992), “ Taro: Composition and Food Uses”, *Food Rev Int*.,**8**:443-73

May,J.H. and Nip,W.K., (1983), " Processed Food", In " Taro: A Review of *Colocasia esculenta* and its Potentials",J.K.Wang ed. University of Hawaii Press,Honolulu

Moorthy,S.N., Thankamma, P.K., and Unnikrishnan, P.M., (1993), " Variability in Starch Extracted from Taro", *Carbohydrate Polymers*, **20**:169-173

Ohwoavworhua, F.O., Kunle,O.O. and Ofoefule, S.I. (2004), "Extraction and Characterization of Microcrystalline Cellulose Derived from *Luffa cylindrica* Plant ",*Afri.J.Pharamaceu.Res.Dev*., **1**(1):1-6.

Olayemi, O.J., Oyi, A.R. and Allagh, T.S.(2008), " Comparative Evaluation of Maize, Rice and Wheat Starch Powders as Pharmaceutical Excipients", *Journ.Pharm*., **7**(1):131-138

Quach M.L., Melton,.L.D., Harris, P.J., Burdon ,J.N., and Smith,B.G.,(2000), " Cell Wall Compositions of Raw and Cooked Corms of Taro (*Colocasia esculenta*)", *J. Sci Food Agri*., **81**:311-8

Stone, L.A., Loenz, K. and Collins, F., (1984), " The Starch of Amaranthus : Physicochemical Properties and Functional Characteristics",*Starch/ starke*, **36**(7):232

Sugimoto, Y., Nishihara, K., and Fuwa, H., (1996), "Some Properties of Taro and Yam Starches", *J.Jap Soci Starch Sci*., **33**;169

Tester, R. F. and Morrison,W.R.,(1990), " Swelling and Gelatinization of Cereal Starches –Effect of Amylopectin,Amylose and Lipids", *Cereal Chemistry*,**67**: 551-557

Snake Venom Inhibition Activity of Rosmarinic acid from *Argusia argentea*

Hnin Thanda Aung

Abstract

A methanolic extract of *Argusia argentea* significantly inhibited hemorrhage induced by crude venom of *Protobothrops flavoviridis* (Habu). The extract was then separated according to antivenom activity by using silica gel column chromatography and HPLC equipped with an octadecylsilanized silica gel (ODS) column to afford rosmarinic acid (RA) (1) as an active principle. Anti-hemorrhagic activity was assayed by using several kinds of snake venom. RA (1) significally inhibited the hemorrhagic effect of crude venoms of *P. flavoviridis*, *Crotalus atrox*, *Gloydius blomhoffii*, *Bitis arietans* as well as purified snake venom metalloproteinases, HT-*b* (*Crotalus atrox*), bilitoxin-2 (*Agkistrodon bilineatus*), HT-1 (*Bitis arietans*) and Ac_1-proteinase (*Deinagkistrodon acutus*). Inhibition against fibrinogen hydrolytic and collagen hydrolytic activities of *P. flavoviridis* venom were examined by SDS-PAGE. A histopathological study was done by microscopy after administration of venom in the presence or absence of RA (1). RA (1) was found to markedly neutralize venom-induced hemorrhage, fibrinogenolysis, cytotoxicity, lethality, edema and digestion of type IV collagen activity. Moreover, RA (1) inhibited both hemorrhage and neutrophil infiltrations caused by *P. flavoviridis* venom in pathology sections. These findings indicate that RA (1) can be expected to provide therapeutic benefits in neutralization of snake venom accompanied by heat stability.

Key words: *Argusia argentea*, rosmarinic acid, snake venom, hemorrhage, metalloproteinase

Introduction

Globally snakebite affects the lives of some 4.5 million people every year, and conservative estimates suggest that at least 100,000 people die from snakebite, and another 250,000 are permanently disabled (University of Melbourne, 2008). Envenomation resulting from snakebite is an important public health hazard in many regions, particularly in tropical and

Assistant Lecturer, Dr, Department of Chemistry, Kengtung University

subtropical areas (Gutiérrez *et al*., 2006). There are two main types of snake venoms namely neurotoxins, which attack the central nervous system and haemotoxins which target the circulatory system. They are usually complex mixtures of proteins including hemorrhagic metalloproteases, phospholipases A_2 (PLA_2), myotoxins, and other proteolytic enzymes, cytotoxins, cardiotoxins and others. Snake envenomation causes pathophysiological changes such as inflammation, increase in body temperature, hemorrhage, necrosis, nephrotoxicity, cardiotoxicity, haemostatic changes and ultimately death (Theakston and Reid, 1983) Envenomations due to snakebites are commonly treated by parenteral administration of horse- or sheep-derived polyclonal antivenoms aimed at the neutralization of toxins (Panfoli et al.,2010). Although antiserum is the only available medical antidote against snakebite, it does not provide enough protection against venom-induced hemorrhage, edema, necrosis, or nephrotoxicity, and it often produces adverse hypersensitivity reactions (Calmette,1984; Stahel *et al*., 1985; Sutherland, 1992; Cruz *et al*., 2009) Hemorrhage is one of the most conspicuous consequences of snake envenoming, and it is sometimes lethal. Unfortunately, the only clinical treatment is antiserum against snake venoms. Snakebites often occur outdoors, far from medical institutions. Because of this, drugs to treat snakebites must be transported to remote locations ahead of time, requiring them to be stable against light, oxygen, and other forms of decomposition without the aid of refrigeration or a special container. It is therefore important to search for other compounds which can effectively neutralize the hemorrhagic and other harmful activities of snake venoms.

The use of natural products, especially plants, for healing is as ancient and universal as medicine itself. One of the main traditional herbal plants called *Argusia* (or *Messerschmidia* or *Tournefortia*) *argentea* (Japanese name: Monpanoki) which is locally used in Okinawa as an antidote for poisoning from jellyfish and snakes venoms, was used for analysis in this research. A methanolic extract of the plant leaves was found to neutralize crude venom of *Protobothrops flavoviridis* which causes hemorrhage. The methanolic extract was further separated and rosmarinic acid (RA) (1) could be isolated as an active compound which can inhibit the hemorrhagic effect of crude venoms of *P. flavoviridis*. Moreover, the compound was submitted to venoms of *P. flavoviridis*, *Crotalus atrox*, *Gloydius blomhoffii*, *Bitis arietans* as well as purified snake venom metalloproteinases, HT-*b* (*Crotalus atrox*), bilitoxin-2 (*Agkistrodon*

bilineatus), HT-1 (*Bitis arietans*) and Ac_1-proteinase (*Deinagkistrodon acutus*). To investigate mechanistic evidence of RA's neutralization effects of snake venom, various pharmacological activities like lethality, hemorrhagic, fibrinogenolysis, cytotoxicity, edema and digestion of type IV collagen activity were studied. Moreover, histopathological study for myonecrosis was done by using microscope after administration of venom with or without RA (1).

Materials and Methods

General

IR spectra were recorded on FT-IR-410 spectrophotometre. ^{1}H- and ^{13}C-NMR spectra were recorded on a JEOL ECA-500 (^{1}H: 500 MHz and ^{13}C: 125 MHz). Chemical shifts for ^{1}H- and ^{13}C-NMR are given in parts per million (δ) relative to solvent signal (methanol-d_4: δ_H 3.30 and δ_C 49.0) as internal standard. EI- and FAB-MS were obtained with a JEOL JMS MS-700 and HX-110, respectively. *m*-Nitrobenzyl alcohol was used as a matrix for FAB-MS. Optical rotations were recorded on a JASCO P-1020 polarimeter (cell length 100 mm). Analytical TLC was performed on Silica gel 60 F_{254} (Merck). Column chromatography was carried out on silica gel BW-820MH (Fuji Silysia Chemicals, Co. Ltd, Seto, Japan). Develosil ODS UG-5 (ϕ4.6 x 250 mm, Nomura Chemical, Seto, Japan), and Cosmosil Cholester (ϕ4.6 x 250 mm, Nacalai Tesque, Kyoto, Japan) columns were used for the analytical HPLC. Develosil ODS UG-5 (ϕ20 × 250 mm, Nomura Chemical, Seto, Japan), and Cosmosil Cholester (ϕ20 × 250 mm, Nacalai Tesque, Kyoto, Japan) columns were used for preparative HPLC.

Plant material

Fresh twigs and leaves of *A. argentea* were collected on Okinawa Islands, and they were moved to the laboratory below 4 °C.

Venoms and chemicals

P. flavoviridis (habu) venom (Okinawa), *P. elegans* venom, *Gloydius blomhoffii* venom and *Bitis arietans* venom were purchased from Japan Snake Institute, Gunma. *Crotalus atrox* venom was purchased from Sigma-Aldrich. Hemorrhagic toxin b (HT*b*), Bilitoxin-2 and Ac_1-proteinase were kindly provided by Dr Toshiaki Nikai and Dr Komori. Hemorrhagic toxin-1 (HT-1) was obtained from *Bitis arietans* venom. Human and bovine fibrinogens were supplied by Sigma-Aldrich, Tokyo, Japan. Type IV

collagen was purchased from Nitta Gelatin Inc. Cryo-preserved human umbilical vein endothelial cells (HUVEC), its respective cell culture media (HuMedia EB-2), other cell culture supplements, and reagents were obtained from Kurabo (Osaka, Japan).

Extraction of *A. argentea* and purification of antivenom compounds

Fresh twigs and leaves of *A. argentea* (wet 7 kg) were extracted with methanol. The methanolic extract was concentrated in vacuo, and dried extract (72 g) was obtained. The extract was then partitioned with ethyl acetate and 1-butanol against water successively to give ethyl acetate (16 g), 1-butanol (16 g) and water soluble fractions (40 g). The ethyl acetate extract (16 g) was fractionated by using a silica gel column with mixed solvents of chloroform and methanol (19:1 – 1:1) to give 21 fractions (H-1 – H-21). Among them, H-13 (1.39 g, elute with chloroform–methanol = 8: 2) was further separated with silica gel column using ethyl acetate–chloroform–formic acid (9: 1: 0.3 – 1: 1: 0.3) as eluents. H-13-10 (236 mg) possessing antihemorrhage activity was purified by HPLC with octadecylsilanized silica gel (ODS) column with methanol–water–formic acid (5: 4: 0.1) as a mobile phase. Then a compound (142 mg) was isolated and identified by NMR analysis.

Antihemorrhagic activity

Anti-hemorrhagic activity was assayed by the modified method of Bjarnason and Tu (1978) using ddY mice of 20 g average weight. Two groups of four mice were used for the experiment. All crude venom solutions of *P. flavoviridis* venom, *Crotalus atrox* venom, *G. blomhoffii* venom and *Bitis arietans* venom, were prepared at a concentration of 0.14 mg/mL in saline. Concentrations of purified hemorrhagic toxin solutions were as follows: HT*b* (0.41 mg/mL), bilitoxin-2 (0.0028 mg/mL), HT-1 (0.29 mg/mL), and Ac_1-proteinase (1.04 mg/mL). A test solution was prepared by mixing the venom solution or the toxin solution (50 µL) and RA (1) (0.5 mg/mL in 10% DMSO-saline, 50 µL) followed by 10 min incubation at 37 °C. These test solutions (100 µL) were injected subcutaneously (s.c.) in the abdomen of mice. Similarly, a group of mice which were injected with a venom solution without RA (1) was used as a control group, and also a group which was only injected with 10% DMSO-saline (50 µL) served as a blank group. Prior to this study, effects of DMSO at several concentrations were investigated, and DMSO at less than 10% was found to cause no significant inactivation of venom. After 24 hr, mice

were euthanized by inhalation of chloroform, the skin covering the abdomen was removed and hemorrhagic lesions were analyzed as follows. The area of the lesion was estimated by major and minor axes measurements, since the shape of the lesions are always amorphous, like an ellipse.

Collagen hydrolytic activity assay

Collagen hydrolytic activity was assayed as follows. 0.1 M Sodium hydrogen carbonate (60 µL, pH 12) was added to 0.3% type IV collagen (0.9 mL) and adjusted to pH 8. Aliquots of type IV collagen were incubated with *P. flavoviridis* venom (0.21 µg/mL) in the presence or absence of RA (1) (0.5 mg/mL). At various time intervals, aliquots of 100 µL of denaturing solution (10 mM phosphate buffer, pH 7.2, containing 10 M urea, 4% SDS, and 4% β-mercaptoethanol) were added. This solution was boiled for 3 min and run on SDS-PAGE using a 7.5% polyacrylamide slab gel electrophoresis.

Fibrinogen hydrolytic activity assay

Fibrinogen hydrolytic activity was assayed by the method of Ouyang and Teng (1976). A solution of 0.1% human fibrinogen in 50 mM Tris-HCl buffer (pH 7.5) (1 mL) and a venom solution (50 µL of 0.21 mg/mL of *P. flavoviridis* venom or 5.5 µg/ml of bilitoxin-2) were incubated in the presence or absence of RA (1) (0.5 mg/mL) at 37 °C. At various time intervals, aliquots of 100 µL of denaturing solution (10 mM phosphate buffer, pH 7.2, containing 10 M urea, 4% sodium dodecyl sulfate (SDS), and 4% β-mercaptoethanol) were added. This solution was incubated at 37°C for 6 h and then run on 10% polyacrylamide slab gel electrophoresis. Electrophoresis was carried out for 2 hr with a current of 25 mA per slab gel. Bromophenol blue (BPB) solution was used as an indicator.

Histopathological study

Histopathological study for RA (1) was performed by intramuscular (i.m.) injection of *P. flavoviridis* venom solution into the medial aspect of the thigh muscle of ddY strain white mice. Histopathological study of muscle was conducted in three groups. Group A was injected with the venom (0.21 mg/mL, 100 µL), while group B was injected with RA (1) (0.5 mg/mL, 100 µL). Group C was injected with a mixture of the venom (0.41 mg/mL, 50 µL) and RA (1) (0.25 mg/mL, 50 µL). Test solutions were preincubated at 37 °C for 10 min before injection. The mice were killed by

chloroform inhalation 24 hr after injection. Tissue samples were immediately fixed in buffered formate fixative for 24 hr at room temperature. The tissue was then washed for 4 hr in running water, dehydrated in an autotechnicon, and stained with hematoxylin and eosin for observation under light microscope.

Cytotoxic action on HUVEC

The effects of RA (1) and *P. flavoviridis* venom on cultured human umbilical vein endothelial cells (HUVEC) were investigated using colorimetric cell viability assay (Ishiyama *et al*., 1997 ; Tominaga *et al*., 1999). Frozen HUVEC were cultured and maintained in commercially available media, HuMedia-EB2, supplemented with fetal calf serum (2% v/v), hEGF (10 ng/mL), hFGF-B (5 ng/mL), hydrocortisone (1 µg/mL), heparin (10 µg/mL), gentamicin (50 µg/mL), and amphotericin B (50 ng/mL). At confluency, cells were trypsinized, washed with the same medium and then resuspended in growth media. These cells were seeded in 96-multiwell plates (5×10^3 cells per well in 100 µL medium) and were allowed to attach and reach log phase of growth. Aliquots of venom and RA (1) to be assayed were diluted in saline and were sterilized by filtration with cellulose acetate 0.22 µm membrane filters. Various concentrations of RA (1) (0.5, 0.25, 0.125, 0.06, and 0.03 mg/mL in 10% DMSO-saline) in the presence or absence of *P. flavoviridis* venom (0.14 mg/mL) were added to each well in 100 µL medium. The plate was incubated at 37 °C under 5% CO_2 atmosphere for 17 h. Ten microliters of cell counting kit-8 was added to each well, and the microplate was incubated for 1 hr, after which cell densities were measured at 450 nm using Bio-RAD Model 550 Microplate Reader.

Assay for edema activity

Hind-paw edema activity was assayed by the method of Ho *et al*., 1993. Four ddY strain white mice (20–23 g) were individually injected in the right foot pad with *P. elegans* venom (12.5 µg in 50 µL of 10% DMSO-saline). An equal volume of 10% DMSO saline was injected into the left paws as control. Inhibition assays were performed by preincubated RA (1) (0.5 mg/mL in 10% DMSO saline) with toxin for 10 min at 37 °C. The volume of each paw was measured with a slide caliper. The degree of paw swelling was expressed as % increase of the initial paw volume.

Inhibition of venom lethal effect

The lethal toxicity of *P. flavoviridis venom* (LD_{50}) was assayed by i.p. administration of different concentrations of venom dissolved in 10 % DMSO saline to groups (n = 4) of ddY strain white mice (20 g). For venom inhibition study, various doses of venom were preincubated with 0.96 mg of RA (1) at 37 °C for 30 min followed by injection into the mice to test the inhibition of lethality.

Results

Extraction of *A. argentea* and purification of antivenom compounds

Twigs and leaves of *A. argentea* were extracted with methanol and the resulting extract was partitioned to afford ethyl acetate, 1-butanol, and water-soluble fractions, successively. Among them, the ethyl acetate fraction (2.5 mg/mL) showed significant antihemorrhagic activity against *P. flavoviridis* venom (final concentration 0.14 mg/mL in test solution). The fraction was fractionated by silica gel column chromatography to afford 21 fractions (H-1 to H-21), and their antihemorrhagic activity was examined. H-13, which inhibited hemorrhage induced by the venom, was further fractionated by repeated chromatography by using chromatography by using silica gel column and HPLC to afford H-13-10-1 as an antidote active compound against crude venom of *P. flavoviridis*. Its NMR and mass spectral data revealed the compound to be rosmarinic acid (RA) (1).

(+)-(*E*)-RA (1): Amorphous solid. $[\alpha]_D^{25}$ + 41.2° (*c* 0.058, MeOH). ^{1}H-NMR (500 MHz, methanol-d_4) δ: 7.55 (1H, d, *J* = 15.9 Hz; H-7), 7.04 (1H, br s; H-2), 6.95 (1H, d, *J* = 7.7 Hz; H-6), 6.78 (1H, d, *J* = 7.7 Hz; H-5), 6.76 (1H, s; H-2´), 6.70 (1H, d, *J* = 7.8 Hz; H-5´), 6.62 (1H, d, *J* = 7.8 Hz; H-6´), 6.26 (1H, d, *J* = 15.9 Hz; H-8), 5.19 (1H, br. d, *J* = 3.7 Hz; H-8´), 3.10 (1H, br. d, *J* = 13.4 Hz; H-7´a), 3.01 (1H, m; H-7´b). ^{13}C-NMR (125 MHz, methanol-d_4) δ: 169.3 (C-9), 150.5 (C-4), 148.4 (C-7), 147.6 (C-3), 146.9 (C-3´), 146.0 (C-4´), 130.2 (C-1´), 128.5 (C-1), 123.9 (C-6), 122.6 (C-6´), 118.4 (C-2´), 117.3 (C-5), 117.1 (C-5´), 116.0 (C-2), 115.4 (C-8), 75.7 (C-8´), 38.8 (C-7´). HRFAB-MS (positive) *m*/*z*: 361.0881 $[M+H]^+$ (*m*/*z* 361.0923 calcd for $C_{18}H_{17}O_8$).

Antidote activities of RA (1) and fractions from *A. argentea* against *P. flavoviridis* venom were investigated as shown in Table 1.

Table 1. Antivenom activities of fractions from methanol extract of *A. argentea* against crude venom of *P. flavoviridis*.

Fractions	Concentration (mg/ml)	Activity[a] / IC_{50} (μm)
Methanol extract	2.5	+++
Ethyl acetate fraction	2.5	+++
	1.0	++
1-Butanol fraction	2.5	–
Water fraction	2.5	+
H-13	0.5	+++
H-13-10	0.5	+++
RA (1)		0.60

Concentration of venom was 0.14 mg/ml. +++; 100–75% inhibition, ++; 75–50% inhibition, +; 50 to >0% inhibition. All experiments were carried out with four mice[a].

(a) (b)

(c)

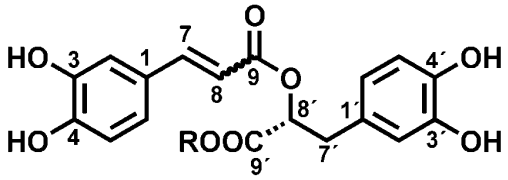

R = H, Rosmarinic acid (1)

Figure 1. (a) *A. argentea* (Japanese name – Monpanoki) in Okinawa Islands, (b) *Protobothrops flavoviridis* (Habu), (c) Structure of rosmarinic acid (1**).**

Inhibitory activity of RA (1) on crude snake venoms and purified hemorrhagic toxins

Antihemorrhagic activity of RA (1) was studied by using crude venoms and purified hemorrhagic toxins. When crude venom (*P. flavoviridis* venom, *Crotalus atrox* venom, *Gloydius blomhoffii* venom, and *Bitis arietans* venom) or purified toxin, (HT*b*, bilitoxin-2, HT-1 and Ac_1-proteinase) was injected subcutaneously (*s.c.*) in the abdomen of mice, a distinct hemorrhagic lesion was observed (Figure 2b). No hemorrhagic spots were produced after *s.c.* injection of crude venom or purified toxin with RA (1) (Figure 2a). RA (1) effectively inhibited the hemorrhagic activities of crude venoms as well as purified hemorrhagic toxins (Table 2).

Table 2. Inhibition of hemorrhage by RA (1) against crude snake venoms and hemorrhagic metalloproteinases.

Origins	Venoms	Concentrations of venoms (mg/ml)	Inhibitory activity of hemorrhage by RA (1) [a,b]
Crude venoms			
P. flavoviridis		0.14	+++
Crotalus atrox		0.14	+++
Gloydius blomhoffii		0.14	+++
Bitis arietans		0.14	+++
Hemorrhagic metalloproteinases (purified venoms)			
Crotalus atrox	Ht-*b*	0.41	+++
Agkistrodon bilineatus	bilitoxin 2	0.0028	+++
Bitis arietans	HT-1	0.29	+++
Deinagkistrodon acutus	Ac_1-p	1.04	+++

[a] Concentration of RA (1) for all experiments was 0.5 mg/ml.

[b] +++: 100 – 75% inhibition, ++: 75 –50% inhibition, +: 50 – >0% inhibition. All experiments were carried out with four mice.

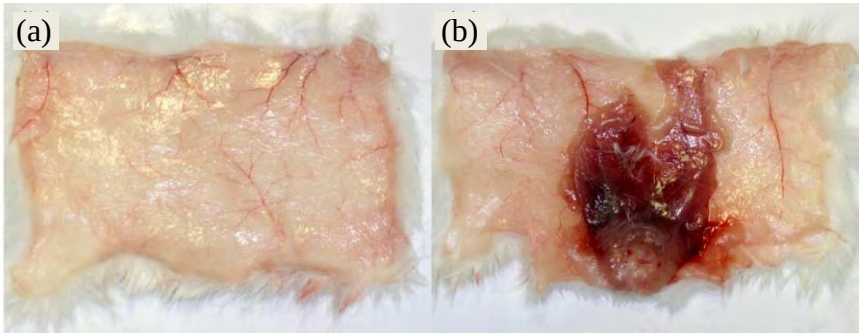

Figure 2. Inhibitory activity of RA (1) on *P. flavoviridis* venom (a) *P. flavoviridis* venom with RA (1), (b) *P. flavoviridis* venom without RA (1).

Inhibition of type IV collagen hydrolytic activity

Type IV collagen was incubated with *P. flavoviridis* venom for different periods of time. The venom completely degraded type IV collagen (104 kDa), especially over 1 h, and degradates with smaller molecular weights (43 and 35 kDa) appeared, as shown in Figure 3a. In the presence of RA (1) (0.5 mg/ml), type IV collagen was not digested by incubation with the venom (Figure 3b).

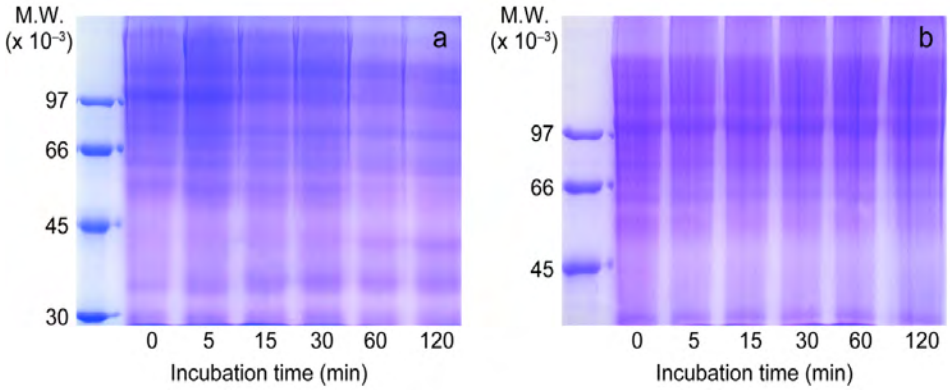

Figure 3. Effect of RA (1) on type IV collagen hydrolytic activity of *P. flavoviridis* venom.

7.5% SDS-PAGE of time-dependent digestion of type IV collagen by *P. flavoviridis* venom in the presence or absence of RA (1). (a) venom without RA (1), (b) venom with RA (1). Molecular weight makers of 97, 66, 43, and 30 kDa were used.

Inhibition of fibrinogen hydrolytic activity

To investigate the inhibition of fibrinogen hydrolytic activity, *P. flavoviridis* venom in the presence or absence of RA (1) was incubated with human fibrinogen at various time intervals. When human fibrinogen was incubated with *P. flavoviridis* venom, the Aα-band of the fibrinogen disappeared on SDS-PAGE, whereas the Bβ-chain and γ-chain were essentially unaffected (Figure 4a). The venom with RA (1) did not reveal any apparent degradation of human fibrinogen (Figure 4b). RA (1) also inhibited Aα-chain hydrolysis by bilitoxin-2 (Figure 4c and 4d).

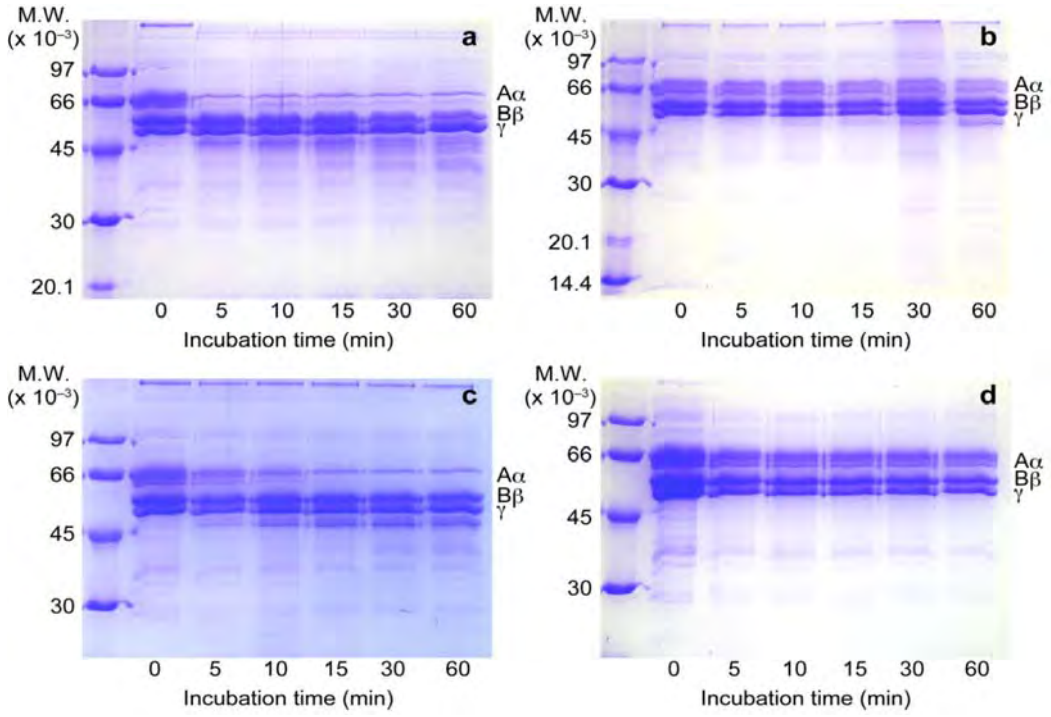

Figure 4. Effect of RA (1) on human fibrinogen hydrolytic activities by *P. flavoviridis* venom and bilitoxin-2.

10% SDS-PAGE of time-dependent digestion of human fibrinogen by *P. flavoviridis* venom and bilitoxin-2 in the presence or absence of RA (1). (a) *P. flavoviridis* venom without RA (1), (b) *P. flavoviridis* venom with RA (1), (c) bilitoxin-2 without RA (1); (d) bilitoxin-2 with RA (1). Molecular weight makers of 97, 66, 43, 30, 20.1, and 14.4 kDa were used.

Histopathological study of *P. flavoviridis* venom and the effect of rosmarinic acid

Histopathological study for RA (1) was conducted by intramuscular (*i.m.*) injection of *P. flavoviridis* venom solution into the medical aspect of the thigh muscle of ddy strain white mice. Both hemorrhage and neutrophil infiltrations were observed in a wide area (in the circle) after injection of *P. flavoviridis* venom (0.21 mg/mL) (Figure 5a). The result showed normal musculature devoid of hemorrhage and neutrophils in the muscle fibers after injection of RA (1) (0.5 mg/mL) (Figure 5b). There was no hemorrhage or neutrophil infiltration in the muscle fibers after injection of a mixture of the venom (0.41 mg/mL) and RA (1) (0.25 mg/mL; Figure 5c).

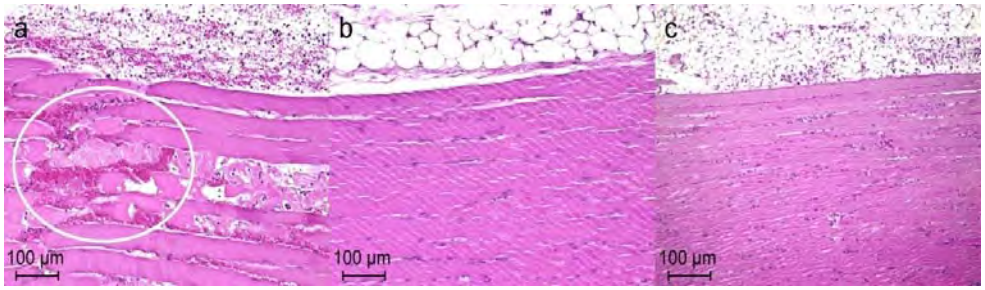

Fig. 5. Histopathological results of thigh muscle after (a) injection of *P. flavoviridis* venom (0.21 mg/ml) alone (b) injection of RA (1) (0.5 mg/ml) alone (normal muscle), (c) injection of a mixture of RA (1) (0.25 mg/ml) and the venom (0.41 mg/ml).

Inhibition of venom cytotoxic action on HUVEC

The inhibitory effect of RA (1) and *P. flavoviridis* venom on cultured human umbilical vein endothelial cells (HUVEC) were investigated using colorimetric cell viability assay. RA (1) alone had no effect on the viability of HUVEC, but it markedly protected HUVEC from the toxic effects of *P. flavoviridis* venom (0.14 mg/mL) at all concentrations of RA (1) tested (0.50, 0.25, 0.125, 0.06, and 0.03 mg/mL) (Table 3, Fig. 6). The maximum (84.2%) protective effect of RA (1) was exhibited at 0.5 mg/mL.

Table 3. Effects of rosmarinic acid (**1**) against the cytotoxic actions of *P. flavoviridis* venom on HUVEC

Treatment	*n*	cell survival (%)
Control (no treatment)	4	100 ± 5.4
RA (0.5 mg/ml) alone	4	100 ± 4.5
RA (0.5 mg/ml) + venom (0.14 mg/ml)	4	84.2 ± 5.2
RA (0.25 mg/ml) + venom (0.14 mg/ml)	4	82.3 ± 2.9
RA (0.125 mg/ml) + venom (0.14 mg/ml)	4	62.1 ± 12.4
RA (0.06 mg/ml) + venom (0.14 mg/ml)	4	39.0 ± 10.4
RA (0.03 mg/ml) + venom (0.14 mg/ml)	4	37.3 ± 9.4

Note: no viability on HUVEC with venom alone (0.14 mg/ml).

RA; rosmarinic acid (**1**), venom; *P. flavoviridis* venom

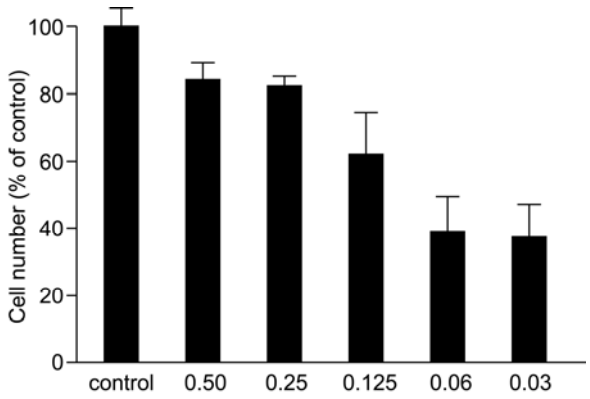

Figure 6. Effects of RA (1) against the cytotoxic actions of *P. flavoviridis* venom on HUVEC.

Inhibition of venom-induced edema

The edema-forming activity was assayed using four mice. *P. elegans* venom induced an edema of 30 % in the mouse footpad, at a dose of 12.5 µg. When *P. elegans* venom was preincubated with RA (1) (0.5 mg/mL), the edema-forming was reduced approximately by two-third.

Inhibition of venom lethal effect

The lethal toxicity (LD_{50}) of *P. flavoviridis* venom was assessed by using 20 g of ddy mice. The venom of *P. flavoviridis* is highly lethal to mice with (*i.p.*) of 0.2 mg/20 g mouse. The control group died within 3 h after envenomation. All of the mice survived for 24 hr after administration of a mixture of the venom and RA (1) (0.96 mg/20 g mouse). *P. flavoviridis* venom-induced lethality was significantly antagonized by RA (1) (0.96 mg/20 g mouse).

Discussion

This is the first scientific proof of antivenom activity of *A. argentea* which has been traditionally used as a folk medicine in the Okinawa Islands. In this study, the inhibitory activities of RA (1) from *A. argentea* against the action of snake venom were investigated. RA (1) effectively inhibited snake venom induced hemorrhage by crude venoms of *P. flavoviridis, Crotalus atrox, Gloydius blomhoffii,* and *Bitis arietans* or purified toxins (HTb, bilitoxin-2, HT-1 and Ac_1-proteinase). Envenomation by snakebites often produces persistent hemorrhage due to considerable degradation of fibrinogen and other coagulation factors, thus preventing clot formation. The pathogenesis of venom-induced hemorrhage involves direct damage to endothelial cells in microvessels by hemorrhagic toxins. Snake venom metalloproteinases (especially snake venom metalloproteinase from *P. flavoviridis* venom) degrade the most important components of the basement membrane, such as laminin, type IV collagen and nidogen/ entactin. In this study, an attempt was made to determine the protective effects of RA (1) on digestion of human fibrinogen, digestion of type IV collagen and cytotoxic action on HUVEC induced by *P. flavoviridis* venom. The pure compound showed antifibrinogenolytic activity by inhibiting the digestion of the Aα-chain of human fibrinogen. RA (1) also effectively inhibited HUVEC against the toxic action of *P. flavoviridis* venom at various concentrations and digestion of type IV collagen. Moreover, the pathological study of thigh muscles showed that RA (1) inhibited

hemorrhage and neutrophil infiltrations. *P. flavoviridis* venom-induced lethality was significantly antagonized by RA (1) (0.96 mg), whereas the venom is highly lethal to mice with 0.2 mg. The compound inhibited the edema-forming effect of *P. elegans* venom and lethal action induced by *P. flavoviridis* venom. This is the first report of RA (1) that demonstrates the inhibitory mechanism for snake venom-induced hemorrhage and protection from snakebite envenomation. Further studies are needed to investigate post-administration of RA (1), and the effects of different methods of administration. After these issues are resolved, RA (1) could become a potent alternative antidote compound for snake envenomation.

Conclusion

The antivenom active compound, RA (1), from the methanolic extract of *A. argentea* significantly inhibited hemorrhage induced by *P. flavoviridis* venom. RA (1) was found to markedly neutralize venom-induced lethality, paw edema, hemorrhage, fibrinogenolysis, cytotoxicity and digestion of type IV collagen activity. Moreover, RA (1) inhibited both hemorrhage and neutrophil infiltrations caused by *P. flavoviridis* venom in pathology sections. These results demonstrate that RA (1) possesses potent snake venom neutralizing properties. Snake venom inhibitors from plants may become helpful alternative or supplemental tools for the treatment of envenomings, as well as important leads for the synthesis of new drugs of medical interest.

Acknowledgements

The author would like to acknowledge Rector Dr. Thar Tun Aung for his great help in academic progress and research pursuits. Special thanks are due to Prof. Dr. Ni Ni Oo and Prof. Dr. Lwin Lwin Myint for their emotional support and insightful suggestions. Warmest thanks are extended to Professor Dr Mya Aye and Professor Dr. Myint Myint Sein for their endless support, insightful suggestions and guidance. The author would like to thank Dr. Aye Aye Cho, Dr. Khine Khine Lwin, Dr. Myint Myint Khnie, Dr. Thein Soe, U Tun Thein and U Myo Min Oo for sharing their academic knowledge, kindness and help.

References

Bjarnason, J.B.and Tu, A. T. (1978), "Hemorrhagic toxins from western diamondback rattlesnake (*Crotalus atrox*) venom: Isolation and characterization of five toxins and the role of zinc in hemorrhagic toxin" e. *Biochemistry*, **17**, 3395-3404.

Calmette, A., (1984), "Contribution a l'etude du venin desserpents. Immunization des animaux et traitement de l'envenimation", *Ann. Inst. Pasteur*, **8**: 275-291.

Cruz, L. S., Vargas, R., and Lopes, A. A., (2009), " Snakebite envenomation and death in the developing world" *Ethn Dis.*, **19**: 42-46.

Gutiérrez, J. M., Theakston, R. D. G.,and Warrell, D. A., (2006), "Confronting the neglected problem of snake bite envenoming: The need for a global partnership" *PloS Med*, **3**:e150.

Ho, C. L., Hwang, L. L., and Chen, C. T., (1993), "Edema-inducing activity of a lethal protein with phospholipase A_1 activity isolated from the black-bellied hornet (*Vespa basalis*) venom" *Toxicon*, **31**: 605-613.

Ishiyama, M., Miyazono, Y., Sasamoto, K., Ohkura, Y., and Ueno, K., (1997), "A highly water-soluble dislfonated tetrazolium salt as a chromogenic indicator for NADH as well as cell viability", *Talanta*, **44**: 1299-1305.

Ouyaung, C., and Teng, C. M., (1976), "Fibrinogenolytic enzymes of *Trimeresurus mucrosquamatus* venom", *Biochim. Biophys. Acta*, **420**: 298-308.

Panfoli, I., Calzia, D.,Ravera, S., and Morelli, A., (2010), "Inhibition of hemorrhagic snake venom components: old and new approaches", *Toxins*, **2**: 417-427.

Stahel, E., Wellauer, R.; Freyvogel, T. A., (1985), "Vergiftungem durch einheimische (*Vipera vipera berrus* and *Vipera aspis*) Eine retrospective studies on 113 patients", *Schweiz. Med. Wochenschr*, **115**: 890-896.

Sutherland, S. K., (1992), "Premedication, adverse reactions and the use of venom detection kits", *Med. J. Aust.*, **157**: 734-739.

Theakston, R. D. G.,and Reid, H. A., (1983), "Development of simple standard assay procedures for the characterization of snake venom", *Bull. World Health Organ.*, **61**: 949-956.

Tominaga, H., Ishiyama, M., Ohseto, F., Sasamoto, K., Hamamoto, T., Suzuki, K., and Watanabe, M., (1999), "A water soluble tetrazolium salt useful for colorimetric cell viability assay", *Anal. Commun.*, **36**: 47-50.

University of Melbourne, (2008), "Developing a global antidote for snake bites: 100,000 people die from snake bites each year" *ScienceDaily*. Retrieved October 20, 2010.

Study on the Reaction between Ninhydrin and Cyanide and its Analytical Applications

Amy Hlaing[1], Kyaw Naing[2], San San Myint[3] and Ye Myint Aung[3]

Abstract

In this research, ninhydrin was used to react with cyanide in aqueous medium to form hydrindantin, which decomposes in the presence of sodium carbonate to give a red colour product which has a maximum absorbance at 450 nm. When sodium hydroxide was added to the red colour solution an intense blue colour product was obtained with a strong bathochromic shift of 450 nm to 590 nm with increased intensity. Standard calibration curve for cyanide determination showed the straight line passing the origin; therefore Beer's law was well obeyed. Sandell's sensitivity is 0.00148μgcm^{-3} and limit of detection is 0.0653μgcm^{-3}. The optimum parameters (concentration of ninhydrin, Na_2CO_3 and NaOH) for cyanide determination were determined using various concentrations. The optimum concentrations were found to be 0.009 M (1.6x10^3 ppm), 0.075 M (8.0x10^3 ppm) and 3.5M (140x10^3 ppm), for ninhydrin, Na_2CO_3 and NaOH respectively. In this research, determinations of cyanide content in some plant samples were carried out by reaction with ninhydrin.The analyzed samples were bamboo shoot of kya-kat-wa, cassava root, lima bean, sweet potato and potato. Among the samples bamboo shoot of kya-kat-wa sample showed the highest cyanide content (2609.3 ppm), whereas potato (A-lu) sample showed the lowest cyanide content (1.56 ppm).

Key words: cyanide, ninhydrin, hydrindantin, cyanogenic glycoside, bamboo shoot, cassava root

Introduction

Cyanide is a chemical compound that consists the 'cyano group' (C≡N), which consists of a carbon atom triple bonded to a nitrogen atom (Greenwood and Eanshaw, 1997). Cyanide is a rapidly acting, potentially deadly chemical that can exist in various forms. Cyanide is salts and esters of hydrocyanic acid (Bellamy and Zajtchuk, 1997). Cyanide can be a colourless gas, such as hydrogen cyanide (HCN) or cyanogenic chloride (CNCl), or a crystal form such as sodium cyanide (NaCN) or potassium cyanide (KCN). Cyanide sometimes is described as having a 'bitter almond' odor, but it does not always give off an odor, and not every can detect this odor. Many organic compounds were derived from cyanide, and they are usually called nitriles. Many kinds of cyanide compounds exist ; some are

1. Demonstrator, Dr, Department of Chemistry, University of Yangon
2. Professor, Dr, Department of Chemistry, University of Yangon
3. Lecturer, Dr, Department of Chemistry, University of Yangon

gases, and other are solids or liquids. Some are molecular, some ionic and many are polymeric.

Although cyanides are present in small concentrations in plants and microorganism, their large scale presence in the environment is attributed to human activities because cyanide compounds are extensively used in industry. The analytical considerations are important for cyanides because these easily form complexes with many materials. Cyanide can form complexes with different affinities. Those that can release the cyanide ion CN^- are highly toxic. Complex cyanide is generally less toxic, while free cyanide is the most toxic of all the cyanide species (Nagaraja, *et al*., 2002).

Human Health Effects

Cyanide is produced in the human body and exhaled in extremely low concentrations with each breath. It is also produced by over 1,000 plant species including bamboo and cassava. Relatively low concentrations of cyanide can be highly toxic to people and wildlife. Cyanide is acutely toxic to human. Liquid or gaseous hydrogen cyanide and alkali salts of cyanide can enter the body through inhalation, ingestion or absorption through the eye and skin. The rate of skin absorption is enhanced when the skin is cut, abraded or moist; inhaled salts of cyanide are readily dissolved and absorbed upon contact with moist mucous membranes (Chistison and Rohrer, 2006).

The toxicity of hydrogen cyanide to human is dependent on the nature of the exposure. Due to the variability of dose-response effects between individuals, the toxicity of a substance is typically expressed as the concentration or dose that is lethal to 50% of the exposed population (LC 50 or LD 50). The LC 50 for gaseous hydrogen cyanide is 100-300 parts per million. Inhalation of cyanide in this range results in death within 10-60 minutes, with death coming more quickly as the concentration increases. Inhalation of 2,000 parts per million hydrogen cyanide cause death within one minute. The LD 50 for ingestion is 50-200 milligrams, or 1-3 milligrams per kilogram of body weight, calculated as hydrogen cyanide. For contact with unabridged skin, the LD 50 is 100 milligrams (as hydrogen cyanide) per kilogram of body weight (website 1).

The effects of ingesting or breathing in cyanide containing materials depend on the concentration. Small amounts are simply broken down and

passed out through urine. In toxic concentrations, cyanide blocks the cell from receiving oxygen, in effect suffocating the person or animal (website 2).

The cyanide found in plants can usually be cooked out, thereby making them safe to eat. Certain plants such as elderberries should never be eating raw, but only cooked. Heating released the cyanide gas into the air from the sugar molecule. The gas is quickly diluted into the air and rendered harmless. Smoking cigarettes releases more cyanide into the air than almost any other sources (website 3).

Cyanide Can Cause no Cancer

The EPA has determined that cyanide is not classifiable as to its human carcinogenicity (website 4). There is no evidence that chronic cyanide exposure has teretogenic, mutagenic, or carcinogenic (website 1).

Permissible Exposure Limit

The EPA has set a maximum contaminant level of cyanide in drinking water of 0.2 milligrams cyanide per liter of water (0.2 mg/L). The EPA require that spills or accidental releases into the environment of one pound or more of hydrogen cyanide, potassium cyanide, sodium cyanide, calcium cyanide or copper cyanide be reported to the EPA. The Occupational Safely Health Administration (OSHA) and the American Conference of Governmental Industrial Hygienists (ACGIH) have set a permissible exposure limit of 5 milligrams of cyanide per cubic meter of air (5 mg/m^3) in the workplace during 8 hours work day, 40 hours work week (website 1).

Reaction of Ninhydrin with Cyanide

Ninhydrin (I) reacts with cyanide in a neutral aqueous medium to form colourless hydrindantin(II). This hydrindantin gives a stable deep-red colour in a sodium carbonate medium.When sodium hydroxide is added to the red-coloured solution, it turns to a deep-blue colour in an aqueous sodium hydroxide medium. The red (IV) and blue (V) colour of hydrindantin are attributed to two anionic forms of 2-hydroxy-1, 3-indanedione, the monovalent ion of the enolic form being responsible for the red colour and the two possible divalent ions for the blue colour. The red colour is formed in the pH range 8-12 and turns to blue colour in the

pH range 12-12.8. In this reaction, cyanide ion can act as a specific base catalyst. A possible reaction mechanism is shown in Figure1 (Nagaraja, *et al*., 2002).

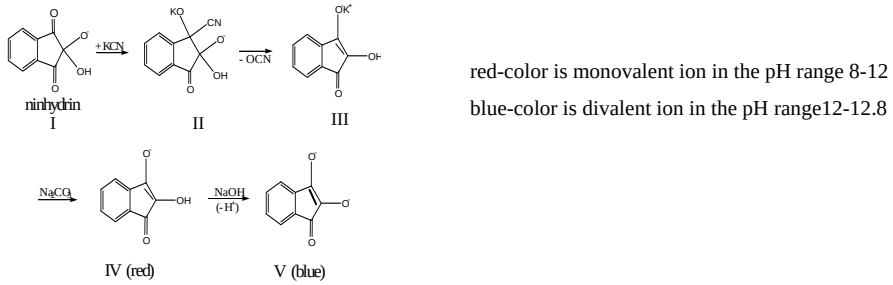

Figure 1. Proposed reaction sequences for the formation of hydrindantin

Bamboo Shoot

Nearly 1500 plants are known to contain cyanide, generally in the form of sugar or lipids (Noller, 2008). In plants, cyanides are usually bound to sugar molecules in the form of cyanogenic glycosides and defend the plant against herbivores. The bamboo shoot contains the highest amount of cyanogenic glycoside or cyanide sugar (Vetter, 2000).

Cassava Root

Cassava roots, an important potato-like food grown in tropical countries, also contain cyanogenic glycoside (Jones, 1998). The most widely distributed major food crop with a content of cyanogenic glycosides is cassava. Cassava is a staple food in human diets in over 80 countries, and it is sometimes added to animal feeds as a substitute for more expensive cereal grains (Gomez, *et al*., 1988). In cassava, for example, more than 90% of the cyanide is present as linamurin, a cyanogenic glycoside, and the remainder occurs as free (nonglycoside) cyanide (Eisler, 1991). Hydrolytic enzymes capable of breaking down these cyanogenic glycosides to hydrocyanic acid (HCN) are also present in the plant, however, separated from the substrate. Any process that ruptures the cell walls will bring the enzyme into contact with the glycosides and will thus release free cyanide (Brian, *et al*., 1991). High cyanide intake from the consumption of insufficiently processed cassava has been advanced as a possible etiologic factor in some disease such as ‘Konzo’ or upper motor neuron diseases

iodine deficiency disorder and tropical ataxic neuropathy (Osuntokun, 1981).

Materials and Methods

Samples Collection

In the present work, Kya-kat-wa (*Bambusa arundinacea* Will.), Pilaw-pinan-u (*Manihot esculenta* Crantz.), Pe-leik-pya (*Phaseolus lunatus* Linn.), Kazun-u (*Ipomoea batatas* Poir.) and A-lu (*Solanum tuberosum* Linn.) were chosen for cyanide determination. Kya-kat-wa and Pilaw-pinan-u were collected from Mingalar Don Township, Yangon Region. Pe-leik-pya, Kazun-u and A-lu were collected from Kyeemyindaine market, Kyeemyindaine Township, Yangon Region. After collection, the scientific names of these plant samples were identified by authorized botanist at Department of Botany, University of Yangon.





Bamboo shoot (kya-kat-wa) s**ample A**

C**assava root sample B**

Lima bean sample C

Sweet potato sample D

Potato sample E

Construction of Standard Calibration Curve

A 1-6 mL of standard cyanide solution, 4 mL of 1% ninhydrin solution and 4 mL of 5% sodium carbonate solution were added into each 25 ml volumetric flask.The solution was shaken for 30 min for completion of the reaction to give a deep red colour and then diluted to the mark with 10% sodium hydroxide solution. The deep blue colour developed instantaneously was stable for 30 min. The wavelength of maximum absorption was found at 590 nm (Nagaraja, *et al*., 2002).

The sample solutions were placed in 1.0 mL glass rectangular cell and the distilled-deionized water was used as reference. The absorbance was measured at 590 nm.

Sample Preparation for Cyanide Determination in Bamboo Shoot Samples

A 10 g of pieces of bamboo shoot was placed in the round-bottomed flask and 50 mL of distilled-deionized water was added, and then boiled in a water bath for 30 min. After boiling,the solution was cooled and filtered (filtrate I). A 1 mL of solution I (1 mL of filtrate I + 19 mL of distilled-deionized water), 4 mL each of 1% ninhydrin and 5% sodium carbonate solution were added into a 25 mL volumetric flask.The remaining procedure was the same as that mentioned above. Residue was placed in the round bottomed flask and, 50 mL of distilled-deionized water was added and then boiled in water bath for 30 min.The solution was cooled and filtered (filtrate II).The residue was placed in the round bottomed flask and the above procedure was carried out until cyanide ion was not found. Same procedures were used for determinations of cyanide in cassava root, lima bean, sweet potato and potato.

Results and Discussion

Visible Spectrophotometric Study on the Reaction between Cyanide and Ninhydrin

Figure 2 showed the absorption spectra of product from reaction between cyanide and ninhydrin. The absorption spectra (a) to (f) represent the following reaction;

CN^- + ninhydrin + Na_2CO_3 + NaOH $\longrightarrow$ blue colour

The product is blue colour and λ_{max} was found at 590 nm. Curve (g) showed the following reaction; CN^- + ninhydrin+ Na_2CO_3 $\longrightarrow$ red colour

The product is red colour and λ_{max} was found at 450 nm. Curve (h) showed the following reaction; ninhydrin + Na_2CO_3 $\longrightarrow$ yellow colour

The product is yellow colour. Curve (i) showed the following reaction;

ninhydrin + Na_2CO_3 + NaOH $\longrightarrow$colorless

The product is colourless. When NaOH is added into red-coloured solution, an intense blue-coloured product was obtained with a strong bathochromic shift of 490 to 590 nm with increased intensity. Based on this observation, determination of cyanide in the samples was carried out spectrophotometrically at 590 nm.

590 nm

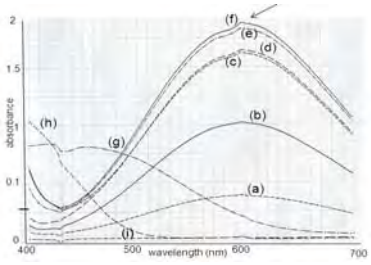

Figure 2. Absorption spectra of colour product

Standard Calibration Curve for Cyanide Determination

In this research, standard cyanide solutions (0.4 to 2.4 ppm) were used for the construction of standard calibration curve (Table1). The plot of absorbance versus concentration of cyanide gives the straight line passed through the origin (Figure 3). Therefore, Beer's law was obeyed.

There are evidently two factors involved in the sensitivity thus defined: first, the intrinsic sensitivity which is proportional to the extinction coefficient of the coloured product in solution and second, the ability of the observer, directly or indirectly, to detect small differences in the light transmission of a solution (Skoog *et al.*, 1992)

The smallest amount of an element detectable in the more sensitivity colour reaction by spectrophotometry usually lies in the range 0.001 to 0.01μg cm^{-3}. Very exceptionally it may lie below 0.001μg cm^{-2}(Sandell, 1959). Table 2 showed the properties of CN^- ninhydrin system. Sandell's sensitivity is 0.0653μgcm^{-3} and limit of detection is 0.00148μgcm^{-3}.

Table 1. Relationship between absorbance at 590 nm and concentration of cyanide

No.	[CN^-] (10^{-5} M)	Absorbance at 590nm
1	0.616	0.267
2	1.232	0.524
3	1.841	0.782
4	2.464	1.053
5	3.080	1.280
6	3.696	1.573

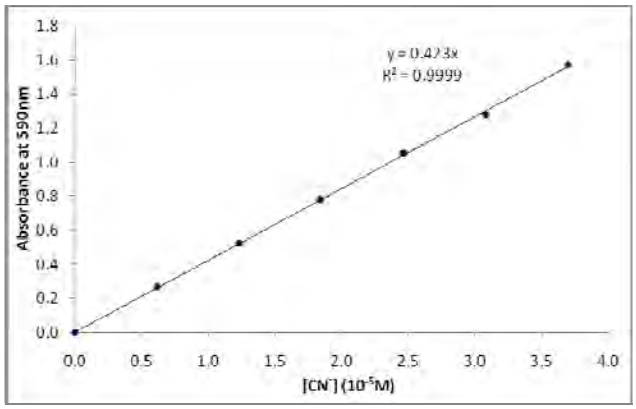

Table 2. The properties of CN^- ninhydrin system

Properties	Value
Colour of the product	Blue
λ max (nm)	590
Stability (min)	5
Beer's law range (μgcm-3)	0.4-2.4
Molar absorptivity (dm3mol-1cm-1)	4.3x104
Sandell's sensitivity (μg cm-3)	0.00148
Limit of detection (μg cm-3)	0.0653
R2 (linear regression)	0.9999

Effect of Ninhydrin Concentration on the Reaction between Cyanide and Ninhydrin

In this research, effect of ninhydrin concentration on the reaction between cyanide and ninhydrin was studied (Table 3). In this case cyanide concentration (40 ppm) was kept constant, while ninhydrin concentrations were varied between 400 to 2200 ppm. The absorbance at 590 nm that related to hydrindantin increased linearly with ninhydrin concentration up to 1600 ppm (0.009 M). After that absorbance becomes nearly constant (Figure 4).

Table 3. Effect of ninhydrin concentration on the absorbance of hydrindantin

No	Ninhydrin concentration (ppm)	Absorbance at 590nm
1	0.4×10^3	0.026
2	0.8×10^3	0.406
3	1.2×10^3	1.244
4	1.4×10^3	1.451
5	1.6×10^3	1.638
6	1.8×10^3	1.641
7	2.0×10^3	1.643
8	2.2×10^3	1.643

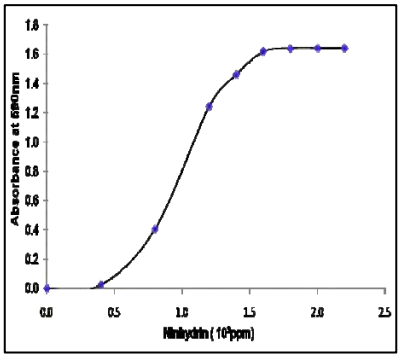

Figure 4. Plot of absorbance at 590 nm as a function of ninhydrin concentration

Effect of Sodium Carbonate Solution Concentration on the Reaction between Cyanide and Ninhydrin

In this research, effect of Na_2CO_3 concentrations on the reaction between cyanide and ninhydrin was studied (Table 4).

Table 4. Effect of sodium carbonate concentration on the absorbance of hydrindantin

No.	$[Na_2CO_3]$ (ppm)	Absorbance at 590 nm
1	1.0×10^3	1.121
2	2.0×10^3	1.493
3	3.0×10^3	2.072
4	4.0×10^3	2.412
5	5.0×10^3	2.816
6	6.0×10^3	2.876

No.	$[Na_2CO_3]$ (ppm)	Absorbance at 590 nm
7	7.0×10^3	3.121
8	8.0×10^3	3.765
9	9.0×10^3	2.783
10	10.0×10^3	2.785
11	11.0×10^3	2.783
12	12.0×10^3	2.780

In this case cyanide concentration (40 ppm) and ninhydrin concentration (1600 ppm) were kept constant, while Na_2CO_3 concentrations were varied from 1000 to 12000 ppm. The absorbance of the hydrindantin at 590 nm increased with an increase in Na_2CO_3 concentration up to 8000 ppm (0.075 M), then the absorbance decreased to lower value. At higher concentration of Na_2CO_3, the formation of hydrindantin was hindered and consequently the absorbance becames low (Figure 5).

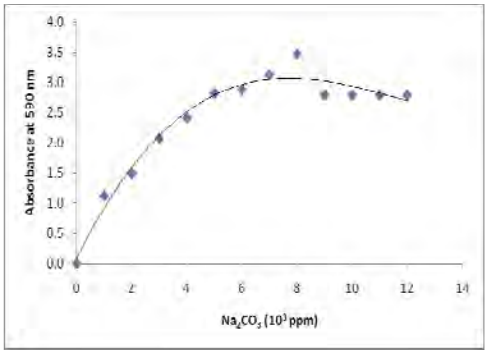

Figure 5. Plot of absorbance at 590nm as a function of sodium carbonate concentration

Effect of Sodium Hydroxide Solution Concentration on the Reaction between Cyanide and Ninhydrin

In this research, effects of NaOH concentrations were on the reaction between cyanide and ninhydrin was studied (Table 5).

Table 5. Effect of sodium hydroxide concentration on the absorbance of hydrindantin

No.	NaOH concentration(M)	Absorbance at 590 nm
1	2.0	2.078
2	2.5	2.257
3	3.0	2.304
4	3.5	2.474
5	4.0	2.204
6	4.5	2.137
7	5.0	1.969

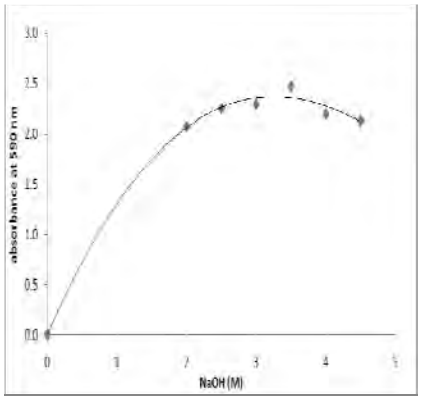

Figure 6. Plot of absorbance at 590 nm as a function of sodium hydroxide concentration

In this case cyanide concentration (40 ppm), ninhydrin concentration (1600 ppm) and Na_2CO_3 concentration (8000 ppm) were kept constant while NaOH concentrations were varied from 2 to 5 M. The absorbance of the hydrindantin at 590 nm increased with an increase in NaOH

concentration up to 3.5 M ($140x10^5$ ppm). More than this concentration can increase the basicity of the solution and side effect can be occurred (Figure 6).

Cyanide Contents in Bamboo Shoot Samples

The determination of cyanide contents in kya-kat-wa was carried out by reaction with ninhydrin. Figure 7 showed the absorption spectrum of hydrindantin developed from standard cyanide solution. Figure 8 showed the absorption spectrum of hydrindantin developed from cyanide in bamboo shoot sample A (1^{st} time boiling).

Table 6 showed the successive determinations of cyanide content in bamboo shoot of kya-kat-wa sample A.

Figure 8. The absorption spectrum of hydrindantin developed from standard cyanide solution

(CN^- + ninhydrin + Na_2CO_3 + NaOH ⟶ hydrindantin)

Figure 9. The absorption spectrum of hydrindantin developed from cyanide in bamboo shoot sample A (1^{st} time boiling)

(sample + ninhydrin + Na_2CO_3 + NaOH ⟶ hydrindantin)

Table 6. Successive determinations of cyanide content in bamboo shoot of kya-kat-wa sample A

Series	Absorbance at 590nm	CN^- content (mg)	Total amount of CN^- in 10 g of sample (mg)	CN^- content (ppm)
1	1.101	19.126	26.067	2606.7
2	0.685	5.950		
3	0.903	0.784		
4	0.213	0.185		
5	0.017	0.015		
6	0.008	0.007		

Cyanide Contents in Cassava Root

The determination of cyanide contents in cassava root was carried out. Figure 9 showed the absorption spectrum of hydrindantin developed from cyanide in cassava root sample B. Table 7 showed the successive determinations of cyanide content in cassava root (pilaw-pinan-u) sample B.

(sample + ninhydrin + Na_2CO_3 + NaOH ⟶ hydrindantin)

Figure 9. The absorption spectrum of hydrindantin developed from cyanide in cassava root sample B

Table 7. Successive determinations of cyanide content in cassava root(pilaw-pinan-u) sample B

Series	Absorbance at 590nm	CN^- content (mg)	Total amount of CN^- in 20 g of sample (mg)	CN^- content (ppm)
1	0.951	4.13	6.75	337.5
2	0.918	1.60		
3	0.851	0.74		
4	0.303	0.26		
5	0.014	0.01		
6	0.010	0.01		

Cyanide Contents in Lima Bean

In this research, determination of cyanide contents in lima bean was done. Table 8 showed the successive determinations of cyanide content in lima bean (pe-leik-pya) sample C.

Table 8. Successive determinations of cyanide content in lima bean (pe-leik-pya) sample C

Series	Absorbance at 590nm	CN^- content (mg)	Total amount of CN^- in 20 g of sample (mg)	CN^- content (ppm)
1	0.545	0.118	0.235	11.75
2	0.480	0.104		
3	0.052	0.011		
4	0.015	0.003		

Cyanide Contents in Sweet Potato

In this research, determination of cyanide contents in sweet potato was done. Table 9 showed the successive determinations of cyanide content in sweet potato (kazun-u) sample D.

Table 9. Successive determinations of cyanide content in sweet potato (kazun-u) sample D

Series	Absorbance at 590nm	CN^- content (mg)	Total amount of CN^- in 20 g of sample (mg)	CN^- content (ppm)
1	0.173	0.038	0.059	2.95
2	0.093	0.020		
3	0.003	0.001		

Cyanide Contents in Potato

In this research, determination of cyanide contents in potato was done. Table 10 showed the successive determinations of cyanide content in potato (A-lu) sample E.

Table 10. Successive determinations of cyanide content in potato (A-lu) sample E

Series	Absorbance at 590nm	CN^- content (mg)	Total amount of CN^- in 20 g of sample (mg)	CN^- content (ppm)
1	0.132	0.023	0.030	1.50
2	0.008	0.002		

Cyanide Contents in Various Plant Samples

Table 11 showed the cyanide content in various plant samples. Totally, 5 samples were analyzed for cyanide determination. Among them cyanide content of bamboo shoot of kya-kat-wa sample A (2609.3 ppm) was found to be the highest. The cyanide content of potato (A-lu) sample E 1.56 ppm was observed to be the lowest.

Table 11. Cyanide contents in various plant samples

No.	Sample	CN^- content (ppm) ($\bar{x} \pm s$)
1	Bamboo shoot of Kya-kat-wa,(A)	2609.3 ± 9.48
2	Cassava root (pilaw-pinan-u), (B)	337.03 ± 2.43
3	Lima bean (pe-leik-pya), (C)	11.30 ± 0.14
4	Sweet potato (kazun-u), (D)	2.86 ± 0.49
5	Potato (A-lu), (E)	1.56 ± 0.39

Conclusion

In this research, standard calibration curve for cyanide determination showed the straight line passing the origin; therefore Beer's law was well obeyed. Sandell's sensitivity is 0.00148 μgcm^{-3} and limit of detection is 0.0653 μgcm^{-3}. By using the optimum concentrations of ninhydrin, Na_2CO_3 and NaOH the maximum absorbance at 590 nm was obtained for cyanide determination. If ninhydrin concentration is greater than 0.009 M, deviations from Beer's law was observed in the system. The concentration of Na_2CO_3 greater than 0.075 M lead to the competitive reaction between cyanide and CO_3^{2-} with ninhydrin and therefore the absorbance at 590 nm decreased. If NaOH concentration is greater than 3.5 M, basicity of the solution increased and consequently the absorbance at 590 nm decrease. Highest cyanide content was found in bamboo shoot of kya-kat-wa sample A (2609.3 ppm) followed by cassava root (pilaw-pinan-u) sample B (337.03ppm), lima bean (pe-leik-pya) sample C(11.30 ppm), sweet potato (kazun-u) sample D(2.86 ppm) and potato (A-lu) sample E (1.56 ppm) . The cyanide found in plants can usually be cooked out, thereby making them safe to eat.

Acknowledgements

The authors would like to mention their sincere thanks to Professor Dr. Nilar, Head of Department of Chemistry, University of Yangon for her kind encouragement.

References

Bellamy, R. and Zajtchuk, R., (1997), "Textbook of Military Medicine", Medical Aspects of Chemical and Biological Warfare, Walter Reed Medical Center, Washington, DC, 46-63

Brian, G.M., Taylor, A.J. and Poulter, N.H., (1991), "Improved Enzymic Assay for Cyanogens in Fresh and Processed Cassava", J. *Sci. Food Agric*., **56**, 277-289

Chistison, T.T. and Rohrer, J.S., (2006), "Direct Determination of Cyanide in Drinking Water by Ion Chromatography with Pulsed Amperometric Detection", Dionex Corporation, Sannyvale, CA, 1-7

Eisler, R., (1991), "Cyanide Hazards to Fish, Wildlife, and Invertebrates", *Biological Report*, **85**, 1-5

Gomez, G., Aparicio, M.A. and Willhite, C.C., (1988), "Relationship between Dietary Cassava Cyanide Levels and Broiler Performance", *Nutrient Report*, **37**, 63 - 75

Greenwood, N.N. and Eanshaw, A., (1997), "Chemistry of the Elements", 2nd Edition, Pergamon Press, New York, 621-625

Jones,D.A.,(1998),"Why are many Food Plants Cyanogenic?", *Phytochemistry*, **47**(2), 155-162

Nagaraja,P., Kumar,M.S.H., Yathirajan,H.S. and Prakash,J.S.,(2002), "Novel Sensitive Spectrophotometric Method for the Trace Determination of Cyanide in Industrial Effluent", *Ana. Sci.*, **18**, 1027-1030

Noller, B., (2008), "Cyanide Management", Developing Program for the Mining Industry, Department of Resource Energy and Tourism, Australia, 137-154

Osuntokun, B.O., (1981), "Cassava Diet, Chronic Cyanide Cyanide Intoxication and a Degenerative Neuropathy in Nigeria", PhD Dissertation, Ibadan, Nigeria

Sandell, E. B., (1959), "Colorimetric Determination of Traces of Metals", Interscience Publishers Inc., New York, 269-301

Skoog, D.A.,West, D.M., and Holler, F.J.(1992), "Fundamental of Analytical Chemistry", Saunders College Pub., London, 168-176

Vetter, L., (2000), "Plants Cyanogenic Glycosides", *Terricon*, **38**(1), 11-36

Websites

1. Environmental and Health Effect, (2004), International Cyanide Management Institude

   (http://www. cyanidecode. Org/ cyanide_ environmental.php)

2. Heuberger,C.,Farah,Z. and Amado,R.,(2009), "Cyanide Content of Cassava Roots and the Fermerted Product"

   (http://www. cassava/ethz/ch)

3. Esser, A. J. A, (2009), "Removal of Cyanogens from Cassava Root" (http://www.processing/cyano/gluco/tox.)

4. ToxFAQs for cyanide, (2006), "Agency for Toxic Substances and Disease Registry

   (http://www. atsdr. cdc. gov /tfacts 8.html)

The Effect of Reducing Agents on Electroless Copper Plating Process

May Zin Oo[1], Sandar Tun[2] and Kyaw Myo Naing[3]

Abstract

This work is aimed mainly at the studies of zerovalent copper deposition on a selected plastic ABS (Acrylonitrile Butadiene Styrene), basis of electroless plating process using different classes of reducing agents. Palladium chloride and gold chloride were used as activators in electroless plating process. Firstly, electroless copper plating process using formaldehyde as reducing agent designated as Cu-ELP-1 was carried out. The deposited mass per unit area and thickness of finished products were calculated and compared. The optimized products using palladium chloride activator designated as Cu-ELP-1-(a) and using gold chloride activator designated as Cu-ELP-1-(b).In the second electroless plating process, sodium hypophosphite was used as reducing agents. It was denoted as Cu-ELP-2. The third process, Cu-ELP-3, the reducing agent used was phenyl hydrazine. In the investigation, the surface morphology of the copper coated film was characterized by SEM and semi quantitatively relative composition of deposited copper was characterized by ED-XRF. It was found that the use of palladium chloride as an activator in the electroless plating process served an efficient and effective activator than gold chloride in all electroless process. Of the reducing agent the use of sodium hypophosphite improvises is more durable deposited copper whereas formaldehyde improvises a brighter copper deposit. Bright copper depositions provide an efficient copper circuit than the durable copper deposition of using sodium hypophosphite.

Keywords: electroless plating, reducing agent, copper coated film

Introduction

This work is mainly concerned with the studies of the zerovalent copper deposition on a selected plastic ABS (Acrylonitrile Butadiene Styrene) basis of electroless plating process using different classes of reducing agents. The first electroless solutions were developed around 1840 for use in silvering mirror. The well-known solution is a mixture of ammonical silver nitrate and glucose or methanol (formaldehyde) (Warshawsky and Upson, 1989).

This was the first developed process of silvering glass mirrors, replacing the centuries-old (pre-1500) method of using a tin-mercury

1. Demonstrator, Dr, Department of Chemistry, University of Yangon
2. Lecturer, Dr, Department of Chemistry, University of Yangon
3. Professor, Dr, Department of Chemistry, University of Yangon

amalgam. However, further progresses on the process of silvering glass mirror were developed only after 1945 (after math of 2nd world war). Use of efficient reducing agents, such as hydrazine, boron hydride etc. were successfully carried out (Krulik,1978).

Today electroless process is one of the low cost which is generally employed without energy consumption. Based on the electroless plating process, metallization of copper or nickel on a desired functional polymer (poly acrylamide), i.e., copper or nickel clad beads were prepared and utilized in making electronic device like cut-off sensor (Khin Khin Swe, 2006).

In this study, the electroless copper plating on ABS (Acrylonitrile Butadiene Styrene) plastic using different reducing agents such as formaldehyde, sodium hypophosphite and phenyl hydrazine was investigated (Basdekis, 1964).

The role of palladium chloride and gold chloride activators on the deposition of copper was found out. The overall kinetic nature of the bulk process as well as on the enhance appearance of the finish items were figured out. It also include the optimum conditions for copper electroless plating such as complete coverage , smoothness and maximum deposited mass were determined by varying the weight ratio of different agents. Use of activators i.e., catalysts to achieve well adhered coherent smooth film were investigated.

The order to achieve a well adhered coherent smooth film, the detail mechanism controlled by various reducing agents, activators and other factors, was investigated.

Materials and Methods

The baths were prepared from reagent-grade chemicals and distilled water. The complexing agent used in this experiment was sodium potassium tartrate. After many experiments, the bath composition and operation condition shown in Table 1 was developed. A bath using formaldehyde, sodium hypophosphite and phenyl hydrazine as reducing agent is also listed in two kinds of activator (palladium chloride and gold chloride). The procedure for surface pretreatment of ABS plastic was as follows: clean, roughen, sensitize, activate and electroless copper plate (Horkans, *et al*.,

1984). After each step, the sample should be carefully rinsed. The solution components and operating parameters are shown in Table 2.

Table 1. Bath Composition and Operating Conditions for Electroless Copper Plating

Parameter	Cu-ELP-1 (HCHO)	Cu-ELP-2 (NaH_2PO_2)	Cu-ELP-3 ($C_6H_5NHNH_2$)
$CuSO_4\,5H_2O$ (g/L)	7	7	20
SPT(g/L)	6	6	10
NaOH (g/L)	8	8	5
EDTA (g/L)	-	4	42
Na_2CO_3	6	6	10
Time (min)	25	60	15
Temp: (ºC)	30	60	60
Formaldehyde (% v/v)	1.5	-	-
Sodiumhypophosphite (g/L)	-	35	-
Phenyl hydrazine (% v/v)	-	-	2

Table 2. Solution Components and Operating Parameters for Pretreatment of ABS Plastic

Cleaning	Etching	Sensitizing	Activation	
NaOH 50 g/L	$K_2Cr_2O_7$ 50 g/L	$SnCl_2$ 5 g/L	$PdCl_2$ 1g	$AuCl_3$ 1g
Na_2CO_3 30 g/L	H_2SO_4 350 ml/L	HCl 5 ml/L	HCl 1L (0.024M)	HCl 1ml

Cleaning	Etching	Sensitizing	Activation	
Detergent 10 g/L	-	-	-	H_2O 600mL
Time 10 min	Time 4o min	Time 10 min	Time 15 min	Time 15 min
Temp 60ºC	Temp 60ºC	Temp 30ºC	Temp 30ºC	Temp 30ºC

Results and Discussion

The experimental investigation is to study the deposition of zero valence copper using various types of reducing agents such as formaldehyde Cu-ELP-1, sodium hypophosphite Cu-ELP-2 and phenyl hydrazine Cu-ELP-3 are used to modify in copper electroless plating for good bath stability and cost effective. Moreover, two types of activators (palladium chloride and gold chloride) are used to achieve the formation of smooth coherent bright durable copper coverage. In Cu-ELP-1-(a), palladium chloride activator, the controlling factors on thickness of copper deposited such as concentration of formaldehyde solution, effect of concentration of sodium potassium tartrate (SPT), effect of operation time and effect of operation temperature were carried out. The optimum condition for Cu-ELP-1-(b) i.e., gold chloride activator system are the almost the same as palladium chloride activator system, that is, Cu-ELP-1-(a). This observation can attributed no change in mechanistic path way has taken place in Cu-ELP-1-(b) system compared to Cu-ELP-1-(a) system.

Moreover, one distinct point is that Cu-ELP-1-(a) possess more thickness of deposited, better appearance and more durable nature than that of Cu-ELP-1-(b) system. The optimum thickness of copper deposited in Cu-ELP-1is 1.793μm for palladium chloride activator and 1.760μm for gold chloride activator.

In Cu-ELP-2 system the effect of concentration of sodium hypophosphite, the concentration of sodium potassium tartrate (SPT), the effect of concentration of EDTA (ethylene diamine tetra acetic acid), the effect of operation time and the effect of operation temperature were investigated by using palladium chloride activator. In this system gold chloride cannot be used as activator; no effect of gold chloride activation on copper deposition at plastic substrate was observed (Gan *et al*., 2006). In Cu-ELP-3, concentration of phenyl hydrazine, the concentration of sodium potassium tartrate (SPT), concentration of EDTA (ethylene diamine tetra acetic acid), the effect of operation time and the effect of operation temperature were investigated. In this process palladium chloride activators were marked deposition than gold chloride activator on ABS substrate (Figure 1).

From the data of the output current at various applied voltage, the minimum resistance gives off the Cu-ELP-1-(a). Since the current flowing through the conductor is inversely proportional to the resistance of conductor,Cu-ELP-1-(a) which gives off minimum resistance has the greater conductivity than the other (Figure 2,3 and 4). Scanning Electron Microscopy (SEM) examination on the morphological feature of before and after of prepared Cu-ELP were also investigated. The EDXRF spectra analyses of Cu-ELP by using three different kinds of reducing agents (formaldehyde, sodium hypophosphite and phenyl hydrazine) based on palladium chloride activator as compared to gold chloride activators, the qualitative major constituent of copper is 97.047% in Cu-ELP-1-(a), 90.520 % in Cu-ELP-1-(b), 96.587 % in Cu-ELP-2, 87.287 % in Cu-ELP-3-(a) and 86.050 % in Cu-ELP-3-(b) respectively. Based on the two types of activator in three types of reducing agents, the formaldehyde reducing agent (Cu-ELP-1) of palladium chloride activator is the most copper deposited on ABS substrate.

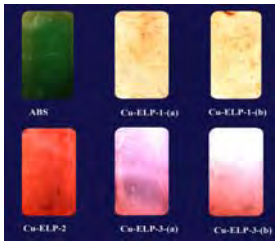

Figure 1.Three type of reducing agent on ABS plastic before and after coating of copper

Figure 2.Photograph of LED bulb Lighting

Figure 3. Photograph of circuit board showing copper grip line

Figure 4. Proof of electric circuit board switch on position

Conclusion

In this research, the electroless plating of copper on the ABS (Acrylonitrile Butadiene Styrene) substrate was studied by using three types of reducing agent (formaldehyde, sodium hypophosphite and phenyl hydrazine) accompanied with two kinds of activators and one complexing agent in this electroless deposition process.

The significant active nature of the activator was evaluated based on the controlling parameters; time, temperature, complexing agent and reducing agents apart from the morphological clean surfaces nature of the substrate.

The alkaline condition of the bath solution is the most feasible to take place for three electroless copper plating process.The active nature of the activator of palladium chloride and gold chloride were evaluated on the basis of mass of copper coated layer on the substrate. No matter what reducing agent is used, palladium chloride was found to be a more significant and efficient activator than using gold chloride. On a qualitative basis the aesthetic quality such as smoothness, brightness, durability etc. were evaluated. The brightness and mass deposition are two parameters which can be considered as prime factor regarding the active nature of the reducing agent. It was found that the use of formaldehyde as the reducing agent in Cu-ELP-1 process improvised the aesthetic quality of brightness and mass deposition of the copper coated plastic.

In the application of deposited copper, it was found that the preparation of circuit is more appropriate when bright copper plating processes are used. The durable copper plating processes Cu-ELP-2 was found not to improvise an effective circuit. In the case of bright copper

deposition it is very possible that elemental copper was deposited which was capable of making an efficient circuit whereas in the deposition of durable copper using sodium hypophosphite it is possible that elemental phosphorus i.e. P_4 was deposited together with copper. That is why the impregnation of phosphorus in the matrix of copper may have somehow impeded the electric character of prepared circuit.

Acknowledgements

The authors would like to mention their sincere thanks to Professor Dr Nilar, Head of Department of Chemistry, University of Yangon for her kind encouragement.

References

Basdekis, C.H., (1964), "ABS Plastic", Reinhold, New York

Horkans., J., Sambucetti ,C, and Markovich ,V., (1984), "Initiation of Electroless Copper Plating on Nonmetallic Surfaces", *ibmj, redevelop*, **28**, 6-9

Gan, X., Wu,Y., Shen, L., and Wenbin, S., (2006) , " Electroless Copper Plating using Hypophosphite as Reducing Agent" , *Surface and Coating Technology*, **201**, 7018-7023

Khin Khin Swe, (2006), "Studies on the Preparation, Characterization and Application of (Copper, Nickel) Metal Clad Beads", PhD, Dissertation, Department of Chemistry, University of Yangon

Krulik, A., (1978), "The Catalytic Process in Electroless Plating", 63rd A. E. S. Technical Conference, *J, Chem. Educ.*, **55**, 361

Warshawsky, A., and Upson, D.A.,(1989), "Metallization of Metal Oxide Surface", *J.Polym.Sci.Part A:Polym.chem.*,**27**, 3015-304

Determination of Stability Constant of Lead-Dithizonate Complex and its Application for the Determination of Lead in Industrial Wastewater

Lwin Moe Moe Aye[1], Kyaw Naing[2] and San San Myint[3]

Abstract

In this research, the complex formation between lead ion and dithizone ligand was studied in the presence of cationic surfactant cetyltrimethylammonium bromide (CTAB). The wavelength of maximum absorption of lead-dithizonate complex was found at 500 nm. The standard calibration curve was constructed using standard lead II solution. The effects of acidity on the formation of lead-dithizonate complex were studied from 0.1 to 2.08 $\times 10^{-3}$ M. It was found that the maximum complex formation was attained at 0.4×10^{-3} M.Then effects of CTAB surfactant concentration were studied from 0.03 to 0.195 M. The maximum complex formation was found at 0.12 M CTAB. The colour stability of lead-dithizonate complex was studied. The effect of foreign ions (Cu^{2+} , Fe^{2+} , Cd^{2+} , Hg^{2+}) were studied on the lead-dithizonate formation. The tolerance limits and tolerance ratios was also determined. Stability constant of lead-dithizonate complex was determined spectrophotometrically at 500 nm using Bunton equation. In this study, ten industrial wastewater samples were collected and spectrophotometric determinations of lead contents were carried out. Lead contents (as determined by spectrophotometric method) in industrial wastewater samples near Toyo battery factory, Shwepyithar battery factory, United Paint Group paint factory, Sein Diamond paint factory, Dyeing and Printing Textiles factory in South Dagon Township, South Dagon pulp factory, Sittaung paper mill, Tharyarwady plate factory, Thanlyin glass mill and No(4) fertilizer factory in Hmawbi Township were found to be 4.096, 1.845, 0.761,0.423, 0.304, 0.135, 0.118, 0.118, 0.084 and 0.078 ppm, respectively whereas lead contents by AAS technique were found to be 4.147, 1.810, 0.745, 0.411, 0.298, 0.127, 0.114, 0.112, 0.079 and 0.073 ppm, respectively. According to Australian and New Zealand Guidelines, the contents of lead in all the waste water sample were found to be below than that of acceptable level (12.5 ppm).

Key words: Lead, dithizone, CTAB, tolerance limits tolerance ratio, foreign ions, stability constant

1.Demonstrator, Department of Chemistry, Dagon University

2.Professor, Dr, Department of Chemistry, University of Yangon

3.Lecturer, Dr, Department of Chemistry, University of Yangon

Introduction

Lead is a very soft bluish-white metal. It is very malleable and ductile. Lead is found on the earth crust, mainly in lead bearing minerals such as galena or vanadite (Greenberg *et al*., 1989).

Lead is a toxic heavy metal that appears in the environment mainly due to industrial processes. Lead pollution is one of the most serious environmental problems because of their stability in contaminated sites and the complexity of the mechanism for biological toxicity (Pipat *et al*., 2010). Lead is a serious cumulative body poison. It enters the body system through air, water and food. Short-term exposure to high levels of lead can cause serious health problems including vomiting, diarrhea, convulsions, coma or even death. Exposure to even small amounts of lead can be harmful especially to infants and young children (Andrews, 1992).

In this research, the complex formation between lead II and dithizone was studied in order to develop a rapid analytical method for lead determination in environmental samples.

Application of Lead

Lead is used in ammunition, metal casting, bearing metals, brass and bronze billets. It is also used as oxides in glass and ceramics, sheet lead, covering for cable and caulking lead. (Andrews, 1992).

Materials and Methods

Reagents and Solutions

All chemicals were of analytical-reagent grade and was provided by BDH, unless stated otherwise, and all solutions were prepared using deionized water. A stock standard lead II solution (0.05M) was prepared by dissolving 4.14g of lead II nitrate in 100mL distilled water, then 1 drop of 0.01M nitric acid was added and diluting to 250ml with distilled water. A 1.95×10^{-4}M 1,5-diphenylthiocarbazone (dithizone) solution was prepared by dissolving 0.0025g of dithizone in 50mL 2-propanol. A 0.3M cetyltrimethylammonium bromide (CTAB) was prepared by dissolving 5.467g of CTAB in 50mL of doubly distilled deionized water. A 4×10^{-3}M hydrochloric acid solution was used (Vogel, 1961). All the polyethylene containers and glasswares used for aqueous solutions containing metallic cations were cleaned in 1:1(v/v) nitric acid and then all were rinsed with

distilled water before use. Absorbance measurements were made on a Shimadzu UV-visible spectrophotometer (UV-240 and PD-303).

Results and Discussion

Absorption Spectra

The complex formation between lead ion and dithizone ligand was studied in the presence of cationic surfactant cetyltrimethylammonium bromide (CTAB). The wavelength of maximum absorption of lead-dithizonate complex was found at 500 nm (Figure 1). The standard calibration curve was constructed using standard lead II solution (Table 1). The straight line was in the range of 0.5 to 3.5×10^{-4}M Pb^{2+} passed through the origin and therefore Beer's law was obeyed (Figure 2). Molar absorption coefficient and Sandell's sensitivity were found to be 3.99×10^{5} dm^3 mol^{-1} cm^{-1} and 0.2236 µg/ cm^2, respectively (Table 2).

Effect of Concentration of Hydrochloric Acid

Figure 3 showed a plot of absorbance of the lead-dithizonate complex at 500 nm as a function of hydrochloric acid concentration. The maximum complex formation was attained at 0.4×10^{-3} M.

Effect of Concentration of Surfactant Cetyltrimethylammonium Bromide (CTAB)

Figure 4 showed a plot of absorbance of the lead-dithizonate complex at 500 nm as a function of surfactant concentration (CTAB). The maximum complex formation was found at 0.12 M CTAB.

Effect of Reaction Time

Figure 5 showed a plot of absorbance of the lead-dithizonate complex at 500 nm as a function of reaction time. The maximum absorbance of colour stability was obtained at 15 minutes. After that absorbance decreased slowly.

Effect of Foreign Ions

The effect of foreign ions (Cu^{2+} , Fe^{2+} , Cd^{2+} , Hg^{2+}) were studied on the lead-dithizonate formation. The tolerance limits and tolerance ratios were also determined (Tables 3, 4, 5, 6 and 7).

Stoichiometric Composition and Stability Constant

Table 8 showed relationship between log ($\Delta A_{int}/ \Delta A_{com}- \Delta A_{int}$) and log [Pb]. Figure 6 showed a plot of log ($\Delta A_{int}/ \Delta A_{com} -\Delta A_{int}$) vs log [Pb] at 500 nm. The stability constant of lead-dithizonate complex was determined spectrophotometrically at 500nm using Bunton equation (Hossein and Elham, 2010). Stoichiometric composition of the lead-dithizonate complex was ML_2 and stability constant was calculated to be 1.29×10^9.

Determination of Lead Contents in Wastewater Samples

In this study, ten industrial wastewater samples were collected and spectrophotometric and AAS determinations of lead contents were carried out (Table 9). Table 10 showed comparison of lead contents between spectrophotometric method and AAS technique (Lang *et al*., 2008). There is no significant difference in lead contents between spectrophotometric method and AAS technique.

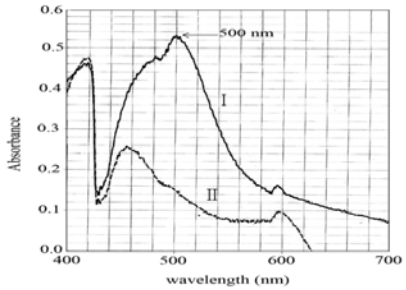

I = Pb^{2+} - dithizone complex

II = dithizone ligand

Figure 1. Wavelength of maximum absorption of lead-dithizonate complex

Table 1 Relationship between standard Pb(II) concentration and absorbance of lead-dithizonate complex at 500 nm

No.	$[Pb^{2+}](\times 10^{-4}M)$	Absorbance at 500nm
1	3.5	0.576
2	3.0	0.502
3	2.5	0.382
4	2.0	0.320

No.	$[Pb^{2+}](\times 10^{-4}M)$	Absorbance at 500nm
5	1.5	0.262
6	1.0	0.202
7	0.5	0.092

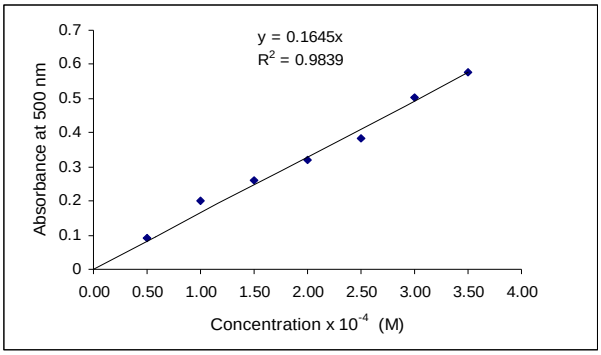

Figure 2 Standard calibration curve for lead-dithizonate complex

Table 2 The optical characteristics of lead-dithizonate complex

No.	Optical characteristics	Lead-dithizonate complex
1	Color	pink
2	λ_{max}(nm)	500
3	Color stability	> 24 h
4	Beer's law range (M)	$0.5 - 3.5\times10^{-4}$
5	Molar absorption coefficient ($dm^3\ mol^{-1}\ cm^{-1}$)	3.99×10^5
6	Sandell's sensitivity (µg/ cm^2)(for 0.001 Absorbance)	0.2236
7	R^2	0.9839

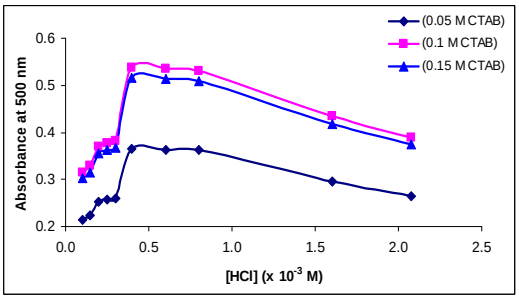

Figure 3. A plot of absorbance of the complex at 500 nm as a function of hydrochloric acid concentration

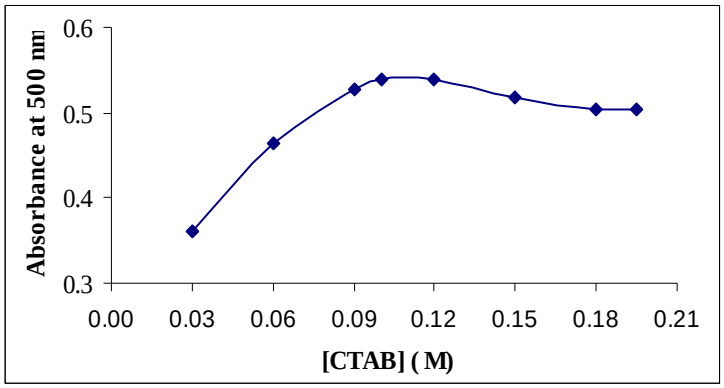

Figure 4. A plot of absorbance of the complex at 500 nm as a function of surfactant

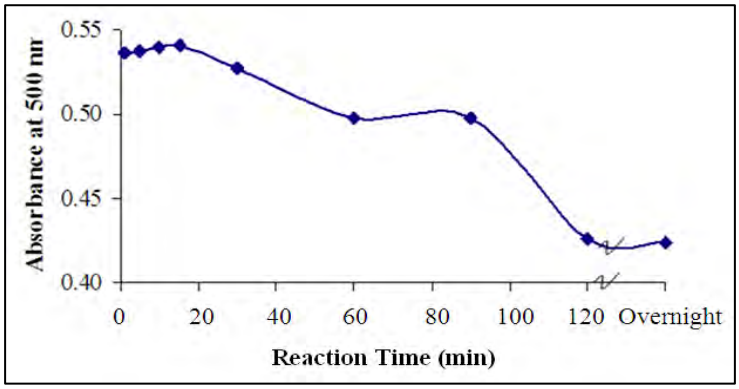

Figure 5. A plot of absorbance of the complex at 500 nm as a function of reaction time

Table 3 Effect of Cu^{2+} on the formation of lead-dithizonate complex

No	$[Pb^{2+}]$ added (ppm)	$[Cu^{2+}]$ (ppm)	Absorbance at 500 nm	$[Pb^{2+}]$ found (ppm)	Error %
1	20.72	-	0.374	20.7200	-
2	20.72	10	0.372	20.6091	-0.534
3	20.72	50	0.367	20.3321	-1.871
4	20.72	100	0.350	19.3903	-6.417

Table 4 Effect of Fe^{2+} on the formation of lead-dithizonate complex

No	$[Pb^{2+}]$ added (ppm)	$[Fe^{2+}]$ (ppm)	Absorbance at 500 nm	$[Pb^{2+}]$ found (ppm)	Error %
1	20.72	-	0.374	20.7200	-
2	20.72	10	0.382	21.1632	+2.139
3	20.72	50	0.390	21.6064	+4.278
4	20.72	100	0.392	21.7172	+4.812

Table 5 Effect of Cd^{2+} on the formation of lead-dithizonate complex

No	$[Pb^{2+}]$ added (ppm)	$[Cd^{2+}]$ (ppm)	Absorbance at 500 nm	$[Pb^{2+}]$ found (ppm)	Error %
1	20.72	-	0.374	20.7200	-
2	20.72	50	0.373	20.6645	-0.267
3	20.72	100	0.383	21.2186	+2.406

Table 6 Effect of Hg^{2+} on the formation of lead-dithizonate complex

No	$[Pb^{2+}]$ added (ppm)	$[Hg^{2+}]$ (ppm)	Absorbance at 500 nm	$[Pb^{2+}]$ found (ppm)	Error %
1	20.72	-	0.374	20.7200	-
2	20.72	50	0.385	21.3294	+2.941
3	20.72	100	0.390	21.6064	+4.278

Table 7. Tolerance limit[a] and tolerance ratio[b] of foreign cations on the formation of lead-dithizonate complex

No	Foreign ions	Tolerance ratio	Tolerance limit (ppm)	Error %
1	Na^{+}	9.7	200	+1.336
2	Mg^{2+}	9.7	200	+1.870
3	Zn^{2+}	9.7	200	+4.278
4	K^{+}	9.7	200	+4.010
5	Ni^{2+}	4.8	100	+4.545
6	Cu^{2+}	2.4	50	-1.871
7	Fe^{2+}	4.8	100	+4.812
8	Cd^{2+}	4.8	100	+2.406
9	Hg^{2+}	4.8	100	+4.278
10	Ca^{2+}	9.7	200	+2.673

a = Tolerance limit was defined as ratio that causes less than 5% interference

b = tolerance ratio = [species]/$[Pb^{2+}]$ = 200/20.72 = 9.7

Table 8. Relationship between log ($\Delta A_{int}/ \Delta A_{com}- \Delta A_{int}$) and log [Pb]

No	[Pb]×10^{-5} (M)	log[Pb]	Absorbance at 500 nm	ΔA at 500nm	Log ($\Delta A_{int}/\Delta A_{com}-\Delta A_{int}$)
1	2.0	-4.6989	0.410	0.048	-0.1995
2	2.5	-4.6021	0.417	0.055	-0.0984
3	3.0	-4.5229	0.426	0.064	0.0280
4	4.0	-4.3979	0.441	0.079	0.2444
5	5.0	-4.3011	0.445	0.083	0.3062
6	7.0	-4.1549	0.459	0.097	0.5554
7	9.0	-4.0458	0.466	0.104	0.7160
8	10.0	-4.0000	0.468	0.106	0.7700
9	12.5	-3.9031	0.473	0.111	0.9313
10	15.0	-3.8239	0.480	0.118	1.2937
11	17.5	-3.7569	0.484	0.122	1.7853

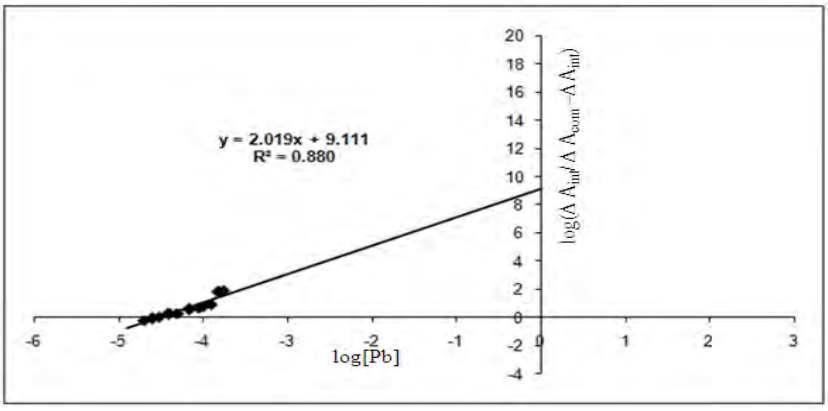

Figure 6 Plot of log ($\Delta A_{int}/ \Delta A_{com} - \Delta A_{int}$) vs log [Pb]

Calculation of stability constant by Bunton equation (1991)

$$\log\left(\frac{\Delta A_{int}}{\Delta A_{com}-\Delta A_{int}}\right) = \log K + n \log [Pb^{2+}]$$

ΔA_{int} = $A_{complex} - A_{free\ ligand}$ of lead-dithizonate complex

ΔA_{com} = $A_{complex} - A_{free\ ligand}$ of lead-dithizonate complex at maximum complex formation

K = Stability constant

n = Ligand number

From the graph, log K = 9.111

K = 1.2912×10^9

n = $2.019 \approx 2$

Pb^{2+} : Dithizone = 1:2

Table 9. Lead contents in industrial wastewater samples

No	Sample location	Abs at 500nm	[Pb] (ppm)	Mean ±SD(ppm)	AAS (ppm)
1	Toyo Battery Factory	0.082 0.080 0.080	4.164 4.062 4.062	4.096 ±0.059	4.147
2	Shwepyithar Battery Factory	0.035 0.037 0.037	1.777 1.879 1.879	1.845 ±0.059	1.810
3	United Paint Group Paint Factory	0.013 0.016 0.016	0.660 0.812 0.812	0.761 ±0.090	0.745
4	Sein Diamond Paint Factory	0.003 0.007 0.008	0.152 0.355 0.507	0.423 ±0.077	0.411
5	Dyeing and Printing Textiles Factory in South Dagon Township	0.003 0.005 0.006	0.152 0.254 0.355	0.304 ±0.050	0.298

No	Sample location	Abs at 500nm	[Pb] (ppm)	Mean ±SD(ppm)	AAS (ppm)
6	South Dagon Pulp Factory	0.002 0.003 0.003	0.101 0.152 0.152	0.135 ±0.029	0.127
7	Sittaung Paper Mill	0.001 0.003 0.003	0.050 0.152 0.152	0.118 ±0.061	0.114
8	Tharyarwady Plate Factory	0.002 0.002 0.003	0.101 0.101 0.152	0.118 ±0.029	0.112
9	Thanlyin Glass Mill	0.001 0.001 0.003	0.050 0.050 0.152	0.084 ±0.058	0.079
10	No(4) Fertilizer Factory in Hmawbi Township	0.001 0.004 0.005	0.050 0.082 0.103	0.078 ±0.026	0.073

Table 10. Comparison of lead contents between spectrophotometric method and AAS technique

No	Sample location	Pb contents (ppm)	
		spectrophotometric	AAS
1	Toyo Battery Factory	4.096 ±0.059	4.147
2	Shwepyithar Battery Factory	1.845 ±0.059	1.810
3	United Paint Group Paint Factory	0.761 ±0.090	0.745
4	Sein Diamond Paint Factory	0.423 ±0.077	0.411

Table 10. Comparison of lead contents between spectrophotometric method and AAS technique (Con'd)

No	Sample location	Pb contents (ppm)	
		spectrophotometric	AAS
5	Dyeing and Printing Textiles Factory in South Dagon Township	0.304 ±0.050	0.298
6	South Dagon Pulp Factory	0.135 ±0.029	0.127
7	Sittaung Paper Mill	0.118 ±0.061	0.114
8	Tharyarwady Plate Factory	0.118 ±0.029	0.112
9	Thanlyin Glass Mill	0.084 ±0.058	0.079
10	No(4) Fertilizer Factory in Hmawbi Township	0.078 ±0.026	0.073

Conclusion

The complex formation between lead ion and dithizone ligand was studied in the presence of cationic surfactant cetyltrimethylammonium bromide (CTAB). The wavelength of maximum absorption of lead-dithizonate complex was found at 500 nm. The standard calibration curve was constructed using standard lead II solution. The straight line was in the range of 0.5 to 3.5 × 10^{-4}M Pb^{2+} passed through the origin and therefore Beer's law was obeyed. Molar absorption coefficient and Sandell's sensitivity were found to be 3.99 × 10^5 dm^3 mol^{-1} cm^{-1} and 0.2236 µg/ cm^2, respectively. Maximum absorbances of the lead-dithizonate complex were attained under 0.4×10^{-3} M HCl, 0.12 M CTAB concentrations and 15 minutes reaction time. The lower tolerance ratio was 2.4 for Cu^{2+} ion. Stability constant of lead-dithizonate complex was determined spectrophotometrically at 500nm using Bunton equation. Stoichiometric composition of the lead-dithizonate complex was ML_2 and stability constant was calculated to be 1.29×10^9. Lead contents (as

determined by spectrophotometric method) in wastewater samples near Toyo battery factory, Shwepyithar battery factory, United Paint Group paint factory, Sein Diamond paint factory, Dyeing and Printing Textiles factory in South Dagon Township, South Dagon pulp factory, Sittaung paper mill, Tharyarwady plate factory, Thanlyin glass mill and No(4) fertilizer factory in Hmawbi Township were 4.096, 1.845, 0.761,0.423, 0.304, 0.135, 0.118, 0.118, 0.084 and 0.078 ppm, respectively. Lead contents (as determined by AAS technique) in wastewater samples near Toyo battery factory, Shwepyithar battery factory, United Paint Group paint factory, Sein Diamond paint factory, Dyeing and Printing Textiles factory in South Dagon Township, South Dagon pulp factory, Sittaung paper mill, Tharyarwady plate factory, Thanlyin glass mill and No (4) fertilizer factory in Hmawbi Township were 4.147, 1.810, 0.745, 0.411, 0.298, 0.127, 0.114, 0.112, 0.079 and 0.073 ppm, respectively. There is no significant difference in lead contents between spectrophotometric method and AAS technique. According to Australian and New Zealand Guidelines for industrial waste water, Pb^{2+}concentration up to12.5 ppm is acceptable level. However this level cannot allow to use in irrigation and general purposes.

Acknowledgements

The authors are thankful to Professor Dr. Nilar (Head of Department, Department of Chemistry, University of Yangon) and Professor Dr. Cho Cho Win (Head of Department, Department of Chemistry, Dagon University) for their kind encouragement.

References

Andrews, S.L., (1992), "Lead and Our Environment", *Food Safety Series*, **35**, 26-31

Greenberg, E.A., Trussell, R.R., and Clesceri, S.L., (1989), "Table of International Relative Atomic Weights", American Public Health Association, Boston, 110-112

Hossein, T., and Elham, A., (2010), "Sensitive Determination of Lead in Soil and Water Samples by Cloud Point Extraction-Flame Atomic Absorption Spectrometry Method", *International Journal of ChemTech Research*, **2**, 1731-1737

Lang,L.,Konghwa,C.,and Qingyong, L., (2008), " Spectrophotometric Determination of Lead*", Pharmaceutical Technology*, **64**, 1-13

Pipat,C., Puchong, W.,and Chalermpol, I., (2010), "Determination of Trace Levels of Lead II in Tap water by Anodic Stripping Voltammetry with Boron-Doped Diamond Electrode", *Science Asia*, **36**, 150-156

Vogel,A.I., (1961), "A Text Book of Quantitative Inorganic Analysis', Lowe & Brydone Printers, Ltd., London, 435-448

Particleboards Derived from Rattan Fiber Waste

Hnin Yu Wai[1], Sandar Tun[2] and Kyaw Myo Naing[3]

Abstract

The purpose of this report was to produce the cost effective particleboard from renewable natural fibers especially modified rattan waste fibers. This study investigates the quality grade particleboards by using renewable natural fibers especially untreated rattan fiber as well as treated rattan fiber by hot pressing molding method. Rattan fiber (RF) was obtained from rattan stem. In the particleboard preparation, polyvinyl chloride (PVC) powder was used as binder. The study was based on the optimal conditions of PVC (Polyvinyl chloride), applied temperature and applied pressure. Hydrochloric acid (A) and sodium hydroxide solution (B) were used as modifiers of the fibers. Five types of rattan fiber based particleboards such as RFPVC, MRFAPVC, MRFBPVC, MRFABPVC and MRFBAPVC had been prepared. All these boards were characterized by physicochemical, physico-mechanical properties and modern techniques such as TG-DTA and SEM. Among them, the quality grade particleboard MRFBPVC was prepared based on the optimum compositions of 50 % (w/ v) PVC and 10% (w/v) sodium hydroxide as modifier. From the results obtained, MRFBPVC particleboard was found to have 3555.34 psi of modulus of rupture, 0.70 cm of thickness, 17.14% of swelling thickness, 7.1044 % of moisture content, 11.05% of water absorption, 94 D of hardness and 1.2320 gcm^{-3} of density. On comparison of the different types of modified fiber particleboard based on physico-mechanical properties, the particleboard via base treated rattan fiber showed to possess the highest MOR value indicating that this board was the most significant and the best among all these boards.

Key words: rattan fiber, modified rattan fibers, PVC powder, particleboards, modulus of rupture

Introduction

Natural fibers such as sisal, jute, banana and coil, have been used as not only toughness modifiers but also reinforcing fillers in particleboard. It has emerged as a renewable and cheaper substitute to synthetics such as glass and carbon in making structural components. In addition, reinforcement plastics and cement using cellulose materials as filler are also lightweight enhanced with mechanical properties and free from health

1. Demonstrator, Dr, Department of Chemistry, University of Yangon
2. Lecturer ,Dr, Department of Chemistry, University of Yangon
3. Professor, Dr, Department of Chemistry, University of Yangon

hazards while synthetics are high cost and high-energy requirement in their production. Since cellulose based natural fibers are relatively inexpensive and there are abundantly available (Chawia, 1998).

Particleboard products lies in the enormous quantity of waste produced when the exploitation of the agricultural harvest is restricted to timber and veneer only. The earliest man-made boards were plywood and blackboard, but even the latter required relatively high class waste. In 1930, when fiberboard process proved to be a less wasteful way of using logs, and the incorporation of waste wood become possible. However, processing costs were relatively high and together with the limitations to board properties still left, the field wide open to a board based essentially on wood waste (Mitlin,1969).

Particleboards are produced from non-chemical processed using fiber particles mixed with filler. The hot press is the key item in determining the rate of particleboard production (Moslemi, 1974).In the production of particleboard, the two main components involved are filler and the other is a fibrous material. The filler plays an important role to obtain good strength of the board and also for low cost products.

Organic fillers used for making composite boards such as polystyrene foam waste adhesive (Cho Cho Mar,2002) and fiber reinforced polymer –clay composite (Khin Aye Tue, 2008) are reported before. In the present work, the particleboards were prepared using rattan fiber and modified rattan fiber together with polyvinyl chloride. The prepared boards were characterized according to the physicochemical and physico-mechanical properties as well as TG-DTA and SEM analyses. The prepared rattan fiber particleboards were utilized as the wood based panel for housing utilities and furniture.

Materials and Methods

All chemicals used in this work were the products from British Drug House Chemical Ltd., Poole, England and from the Kanto Co. Ltd., Japan unless otherwise stated.

Equipment employed in this work consist of lab ware, glassware and other supporting facilities. Some of the instruments used in the experiment are E-Mettler balance (LA – 310 S), pH meter (Jenway 4330, Lab quip, England) Viscometer (Reomat 15 T, Germany), Muffle

furnace (Range 100-1100 ºC Gallenkamp, England), TG-DTA (Hi-TGA 2950, DTG-60 H Thermo gravimetric analyser), Hydraulic hot press (Apex Construction Ltd., Gravesend England) Electro-hydraulic tensile tester (Thwing-Albert Instrument Company Philadelphia, USA), Mixer machine (Henschel Mischer, Germany) , Veneer clipper (or) screw gauge Sieves (US Series Equivalent, The Tyler Std. Screen Scale), Scanning Electron Microscope (No. JSM-5610, JEOL Ltd., Japan), Thermal control status oven (H 053, 240 V, England), Specific gravity balance (Wallace Test Equipment) and Hardness tester (H.W Wallace and Co. Ltd., England).

Screening of the Rattan Fiber

Raw samples were cut by cutting machine. After cutting, they were screened to pass the sieve aperture of 10 meshes (0.165 cm) and to retain on the sieve aperture of 25 meshes (0.0594 cm) obtained. The fiber obtained in size as about (-1.3 cm and +0.7 cm). The screened fibers were taken and dried in an oven at 70± 5°C)

Modification of Rattan Fiber

The experimental work was carried out in four categories. The first involves the treatment of rattan fiber with hydrochloric acid. The second involves the treatment of rattan fiber with sodium hydroxide. The third consists of the treatment of rattan fiber with hydrochloric acid followed by sodium hydroxide. The fourth include the treatment of rattan fiber with sodium hydroxide followed by hydrocholoric acid. The prepared samples were characterized by physicochemical and physico-mechanical properties.

Preparation of Particleboards

In this research, all of the particleboards were prepared by compressing molding method. Each rattan fiber (120 g) and 50% of PVC (polyvinyl chloride) were mixed by Henschel mixer for 2 min. The complete mixture was laid in a mold. It was necessary to get a uniform surface of the mixture in cold press section and later this was slowly transferred to the hydraulic press machine for 15 min. The boards from hydraulic press were kept cooled for at least 24 hr and then go through a sanding process. The boards were kept at room temperature for one week and then the edge and both sides of the boards were trimmed and sanded. The prepared particleboards were characterized by physicochemical and physico-mechanical properties.

Results and Discussion

RFPVC Particleboards

The results of the physicochemical and physico-mechanical properties of RFPVC particleboards are presented in Table 1, Figures 1 and 2.

Table 1. Physicochemical and physico-mechanical properties of RF particleboards at various percentages of polyvinyl chloride (PVC)

Particle Boards	PVC (wt.%)	MOR (psi)	Thinkness(cm)	Density (g/mL)	Water Absorption *(%)	Swelling Thickness * (%)	Hardness Shore (D)
RFPVC 1	10	1285.58	0.49	1.0667	29.68	40.51	90
RFPVC 2	20	1783.05	0.62	1.0124	64.27	65.60	89
RFPVC 3	30	1152.27	0.63	1.0346	74.22	66.63	90
RFPVC 4	40	2054.32	0.68	0.9237	83.33	67.26	90
RFPVC 5	50	2430.58	0.65	1.1115	14.88	18.43	92
RFPVC 6	60	1636.59	0.72	1.0187	38.29	21.86	90

*After 24 hr Applied temperature - 150 ºC
PVC – polyvinyl chloride Applied pressure - 3000 psi

RFPVC 1 = rattan fiber with 10 % (w/v) PVC
RFPVC 2 = rattan fiber with 20 % (w/v) PVC
RFPVC 3 = rattan fiber with 30 % (w/v) PVC
RFPVC 4 = rattan fiber with 40 % (w/v) PVC
RFPVC 5 = rattan fiber with 50 % (w/v) PVC
RFPVC 6 = rattan fiber with 60 % (w/v) PVC

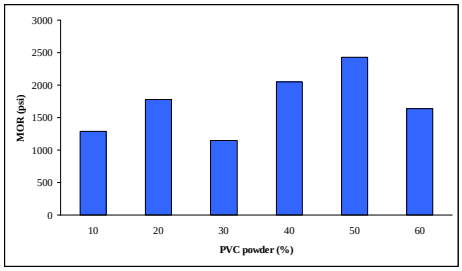

Figure 1 Modulus of rupture of rattan fiber particleboards as a function of percentage of polyvinyl chloride

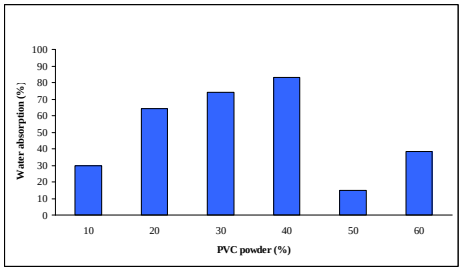

Figure 2 Water absorption of rattan fiber particleboards as a function of percentage of polyvinyl chloride

MRFAPVC Particleboards

The results of the physicochemical and physico-mechanical properties of MRFAPVC particleboards are presented in Table 2, Figures 3 and 4. From the results, MRFAPVC3 particleboard made with 2% (v/v) HCl was found to have the greatest modulus of rupture (3224.14 psi). Therefore, these conditions are the most suitable for making particleboards.

Table 2 Physicochemical and physico-mechanical properties of MRFA particleboards with polyvinyl chloride (MRFAPVC)

Particle Boards	HCl (% v/v)	MOR (psi)	Thickness (cm)	Density (g/cm^3)	Water Absorption *(%)	Swelling Thickness * (%)	Hardness Shore (D)
MRFAPVC 1	0	2430.58	0.65	1.1115	14.88	18.43	90
MRFAPVC 2	1	2213.70	0.53	1.1665	71.13	71.67	92
MRFAPVC 3	2	3224.14	0.67	0.9817	31.19	31.68	94
MRFAPVC4	3	1329.93	0.69	1.0463	72.76	71.74	93
MRFAPVC 5	4	Brittle ready to damage not detect					

*After 24 hr Applied temperature -150 ºC

PVC – polyvinyl chloride Applied pressure -3000 psi

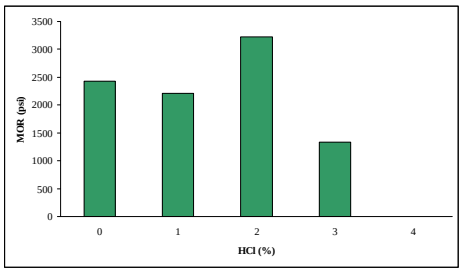

Figure 3 Modulus of rupture of rattan fiber polyvinyl chloride particleboards as a function of percentage of HCl

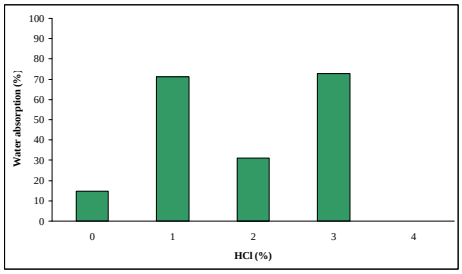

Figure 4 Water absorption of rattan fiber polyvinyl chloride particleboards as a function of percentage of HCl

MRFBPVC Particleboards

The results of the physicochemical and physico-mechanical properties of MRFBPVC particleboards are presented in Table 3 and Figures 5 and 6. It can be observed that MRFBPVC 3 particleboard made with NaOH (10 % w/v) was found to have 3555.34 psi of modulus of

rupture (MOR) and hardness of 94 D. These values are the highest among others. Pre-treatment of the rattan fiber is required mainly to remove the black particles of rattan fiber which remain adhered to the surface. Treatment with base has the beneficial effects of increasing the porosity and the creation of active sites for rattan fiber. Modified rattan fiber with 10 % NaOH (w/v), 50 % PVC at 150 ºC and under pressure of 3000 psi were the most suitable conditions for preparation of particleboards.

Table 3 Physicochemical and physico-mechanical properties of MRFB particleboards with polyvinyl chloride (MRFBPVC)

Particle Boards	NaOH (%w/v)	MOR (psi)	Thickness (cm)	Density (g/mL)	Water Absorption *(%)	Swelling Thickness * (%)	Hardness Shore (D)
MRFBPVC 1	0	2430.58	0.65	1.1115	14.88	18.43	90
MRFBPVC 2	5	1202.13	0.78	0.8746	65.64	37.17	92
MRFBPVC 3	10	3555.34	0.70	1.2320	11.05	17.14	94
MRFBPVC 4	15	1883.39	0.71	1.01625	53.07	38.26	93
MRFBPVC 5	20	1190.09	0.69	0.9954	84.44	59.28	90

*After 24 hr Applied temperature - 150 ºC

PVC – polyvinyl chloride Applied pressure - 3000 psi

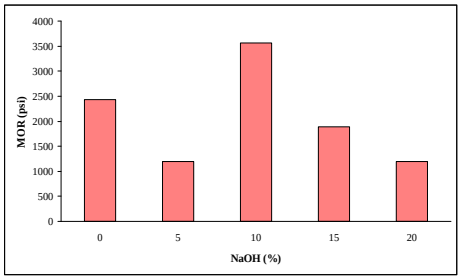

Figure 5 Modulus of rupture of rattan fiber polyvinyl chloride particleboards as a function of percentage of NaOH

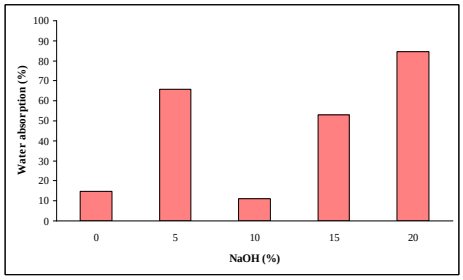

Figure 6 Water absorption of rattan fiber polyvinyl chloride particleboards as a function of percentage of NaOH

MRFABPVC and MRFBAPVC Particleboards

MRFABPVC particleboard was prepared by blending modified rattan fiber (fiber treated with HCl followed by NaOH) with 50 % PVC and alternatively MRFBAPVC particleboard was prepared by blending modified rattan fiber (fiber treated with NaOH followed by HCl) with 50 %

PVC according to the hot pressing method. In this method the applied pressure and temperature were 3000 psi and 150 ºC temperature. The results of the physicochemical and physico-mechanical properties of MRFABPVC particleboard are presented in Table 4.

Comparison of Rattan Fiber Particleboards with Different Ingredients

Physicochemical and physico-mechanical properties

All of the rattan fiber particleboards were made with different ingredients. Mechanical properties focused on bending strength, durometer absorption test of fibers and water absorption test of particleboards. Photographs of prepared rattan fiber particleboards with different ingredients are shown in Figure 6. Table 4, Figures 7 and 8 show the physicochemical and physico-mechanical properties of rattan fiber particleboard with the composition of different ingredients.

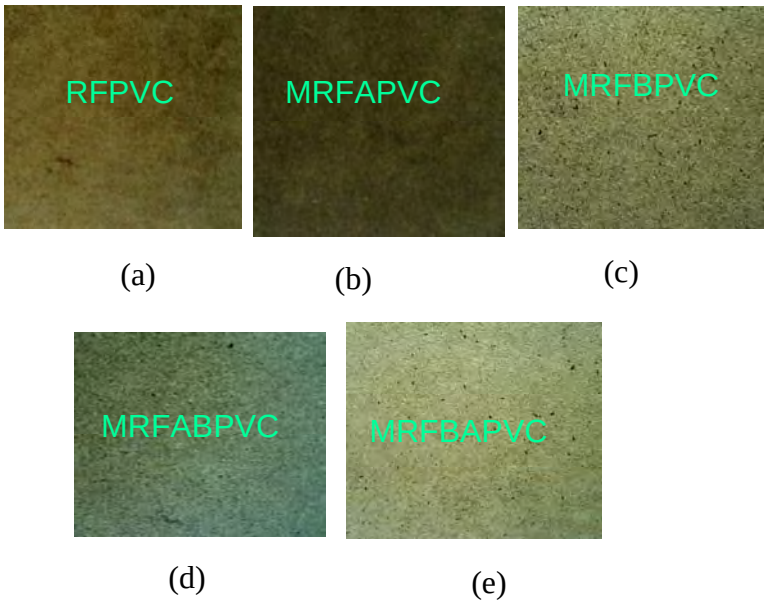

Figure 7 Photographs of rattan fiber particleboards with different ingredients

(a)RFPVC = rattan fiber with 50 % w/v PVC

(b)MRFAPVC = acid treated modified rattan fiber with 50 % w/v PVC

(c)MRFBPVC = base treated modified rattan fiber with 50 % w/v PVC

(d)MRFABPVC = acid treated followed by base treated modified rattan fiber with 50 % w/v PVC

(e)MRFBAPVC = base treated followed by acid treated modified rattan fiber with 50 % w/v PVC

It can be found that modulus of rupture (MOR) of the chemical treated MRFBPVC particleboard is greater than that of others. It was investigated that boards is more stiffness than other rattan fiber particleboards.

Table 4 Physicochemical and physico-mechanical properties of rattan fiber particleboards with different compositions of ingredients

Particle Boards	Moisture content (%)	MOR (psi)	Thickness (cm)	Density (g/mL)	Water Absorption *(%)	Swelling Thickness * (%)	Hardness Shore (D)
RFPVC	8.0517	2430.58	0.65	1.1115	14.88	18.43	92
MRFAPVC	7.1306	3224.14	0.67	0.9817	31.19	31.68	94
MRFBPVC	7.1044	3555.34	0.70	1.2320	17.14	11.05	94
MRFABPVC	7.1569	1402.05	0.65	1.0794	30.20	38.46	85
MRFBAPVC	7.2219	1022.11	0.70	1.0534	82.30	64.28	90

*After 24 hr Applied temperature - 150 ºC

PVC – polyvinyl chloride Applied pressure - 3000 psi

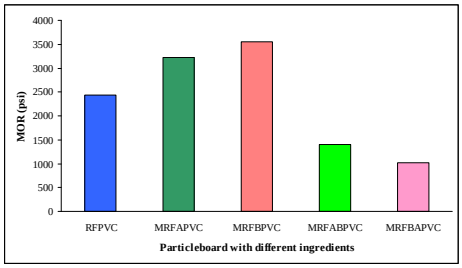

Figure 8 Modulus of rupture of rattan fiber particleboards as a function of rattan fiber particleboards with different ingredients

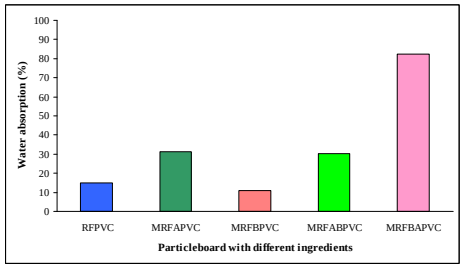

Figure 9 Water absorption of rattan fiber particleboards as a function of rattan fiber particleboards with different ingredients

RFPVC = RF particleboard with 50 % PVC

MRFAPVC = MRFA particleboard with 50 % PVC

MRFBPVC = MRFB particleboard with 50 % PVC

MRFABPVC = MRFAB particleboard with 50 % PVC

MRFBAPVC = MRFBA particleboard with 50 % PVC

TG-DTA analysis

The thermal stabilities of rattan fiber particleboards with the composition of different ingredients were determined by TG-DTA analysis. All these particleboards had similar temperature dependencies, however, gave different mass retentions after thermal decomposition. Figure 10 shows the TG-DTA thermogram of MRFBPVC particleboard . The thermal decomposition was found to take place in the programmed temperature range of 50^{o}C to 600^{o}C. The first decomposition was observed at nearly 250^{o}C and completed at about 530^{o}C.

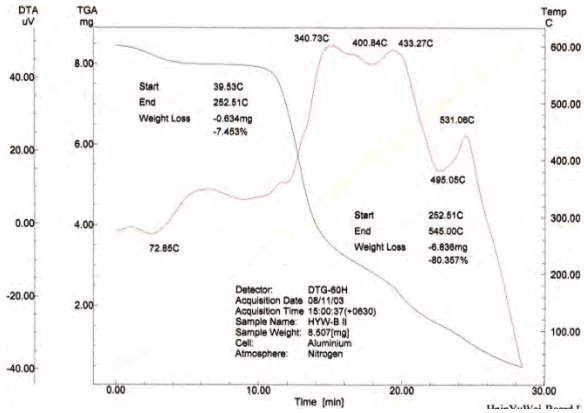

Figure 10 TG-DTA thermogram of MRFBPVC particleboard

Surface morphology of modified rattan fiber particleboards

Scanning electron microscopic analysis examined the surface morphology of untreated and treated fibers and polyvinyl chloride as a binder. The removal of surface impurities on plant fibers is advantageous for fiber and binder as it facilitates both mechanical interlocking and the

bonding reaction due to the exposure of the hydroxyl groups to the chemicals used in treatment. SEM photomicrographs of MRFAPVC, MRFBPVC, MRFABPVC, and M RFBAPVC particleboards are shown in Figures 11-14. On studying the surface morphology of Figure 12 MRFBPVC particleboard was found to be more compatible than others. When manufacturing the particleboard materials, compatibility of the binder and fibers are important. The more compatibility between the fiber and the binder the greater the modulus of rupture.

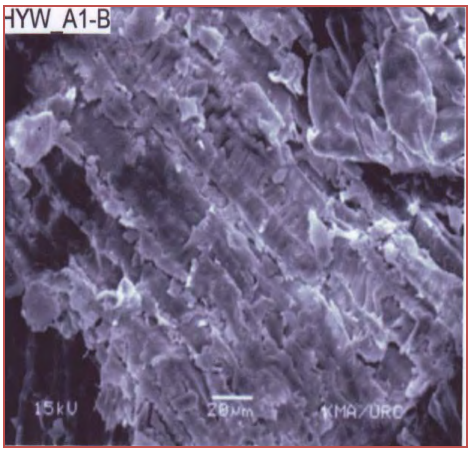

Figure 11 SEM microphotograph of MRFAPVC

Figure 12 SEM microphotograph of MRFBPVC particleboard

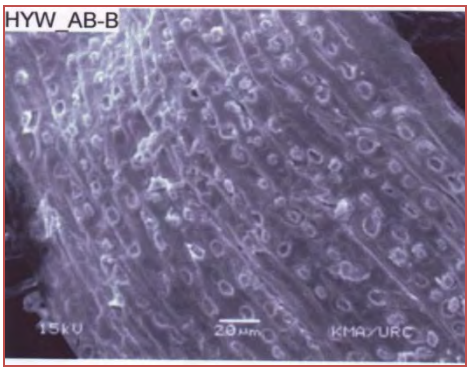

Figure 13 SEM microphotogroph of MRFABPVC particleboard

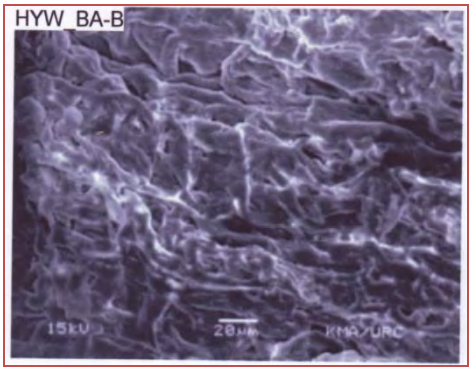

Figure 14 SEM microphotograph of MRFBAPVC particleboard

Application of Particleboards

Prepared particleboards were done by saw-drilled, and then coated with lacquer, e.g., polyurethane, melamine. The modified saw-drilled boards can be used as floor underpayment, housing cabinets, stair treads, shelving table tops, furniture, vanities, speakers, lock blocks, sliding doors, interior sings, displays, pool tables, electronic game consoler, table tennis tables, isolation panels, furniture decorative applications, and packaging. Figure 15 shows the photographs of application of particleboards derived from rattan fiber.

Figure 15 Application of particleboards

Conclusion

The production of particleboard was derived from rattan waste, obtained from rattan inner core, and modified waste. Particleboards were fabricated by using modified rattan waste (120 g) with 50 % PVC, 150 ºC and 3000 psi depending on modulus of rupture (MOR).

Various concentrations of hydrochloric acid (A) and sodium hydroxide (B) were used for surface modifiers. Particleboards were fabricated by using modified rattan fiber with hydrochloric acid (HCl), sodium hydroxide (NaOH), HCl followed by NaOH as well as NaOH followed by HCl. It was observed that 2 % of HCl and 10 % of NaOH were chosen as the optimum conditions for the treatment of fiber (modification of fiber) related to prepare particleboards because of the improvement of physico-mechanical properties modulus of rupture (MOR). MOR of MRFAPVC particleboard is 3224 psi whereas MOR of MRFBPVC particleboard is 3555 psi. By using the optimum concentration of HCl as well as that of NaOH alternatively, four different modified particleboards

such as MRFAPVC, MRFBPVC, MRFABPVC and MRFBAPVC were obtained.

Among them, MRFBPVC particleboard, made of 120 g of modified rattan with 10 % (W/V) of sodium hydroxide as modifier and 50 % PVC was found to be the best. It gave 0.70 mm of thickness, 17.14 % of swelling thickness, 11.05 % of water absorption, 1.2320 gcm^{-3} of density, 94 D of hardness and 3555 psi of modulus of rupture. On studying the surface morphology of rattan fiber particleboards, MRFBPVC board is good compatible. It indicates the effect of the improvement of modulus of rupture.

It was investigated that MRFBPVC particleboard has higher MOR value than that of other particleboards. Therefore, MRFBPVC particleboard was observed as the most feasible to make the particleboard for local needs. In addition to this, making particleboard is helpful in protecting the environment by means of recycling the by-products and in manufacturing cost effective particleboards. These boards will be a feasible replacement for housing components and furniture in wood based panel product. This research will support the technological needs for Myanmar and reduce the non-biodegradable pollution.

Acknowledgements

The authors would like to thank the Department of Higher Education (Lower Myanmar), Ministry of Education, Yangon, Myanmar, for the permission to do this research. Special thanks are extended to Dr. Nilar, Professor and Head, Department of Chemistry, University of Yangon, and also to the Polymer Department, Myanmar Science and Technological Research Department (MSTRD), Ministry of Science and Technology, for providing the research facilities and their invaluable suggestion, and co-operation.

References

Chawia, K.K., (1998), “Fibrous Materials”, London, Cambridge University Press, **7**, 60-65

Cho Cho Mar, (2002), “ Polystyrene Foam Waste Adhesive for Particleboard”, PhD Dissertation , Yangon Technological University, Myanmar

Khin Aye Tue,(2008), “ Study on the Fiber Reinforced Polymer – Clay Composite”, PhD Dissertation , Yangon Technological University, Myanmar

Mitlin, L., (1969), “Particleboard Manufacture and Application”, Novella & Company Ltd., Great Britain, 74-105

Moslemi, A.A., (1974), “Particleboard”, Southern Illinois University Press, USA, **1**, 53, 83

Preparation of Beverages Powder from Fruits

Pansy Kyaw Hla[1] and Thin Thin Khaing[2]

Abstract

This research work describes the process for preparing fruit juices in powder form. The beverage powder has an improved storage stability which can retain their organoleptic properties, such as flavor, taste and aroma, substantially unaltered with the course of time. Dried powder can be transported easily due to its lightweight and volume. The emphasis was places on preparing fruit juices in powdered form possessing its natural flavor and aroma when rehydrated and a longer shelf-life. To compare the quality of products with that of different branded powders from local supermarkets, the powders were characterized for physical and chemical properties such as acidity, pH, ash content (%), soluble solid content (%), total solid content (%), moisture content (%), specific gravity and protein content (%). Some work should be done to further lower the moisture content of the present fruits powders and also reduce its hygroscopic nature, fibre content should also be measured for the prepared fruits powders.

Key words : caking, solubility, stability.

Introduction

Our country, Myanmar is in the tropical zone. It has three seasons and various kinds of seasonal fruits can be found in different parts of Myanmar. Some common fruits are pineapple, mango, banana, papaya, orange, jackfruit, lime, lemon, pear and so on. Some of these fruits are seasonal ones and some are available all the year round. Some fruits are produced more than our consumption, it should avoid to reduce fruits loss and to develop new value products. The farmers also would have new sources of income, not only from fruit and vegetable the farmers have income, but also can have income by making the juices and other food products.

Myanmar being a developing country, agricultural is the mainstay of the economy. Of the various types of agriculturally based, the production of fruits and vegetables are among the most important. The main objective of fruit processing is to supply wholesome, safe, nutritious and acceptable food to consumers throughout the year. Fruit processing also aims to replace

1. Professor, Dr., Department of Industrial Chemistry, University of Yangon.
2. Lecturer, Dr., Department of Industrial Chemistry, University of Yangon

imported products like squashes, jams, jellies, etc; besides earning foreign exchange exporting finished or semi-processed product. Several kinds of fruit juices are consumed for food value but rather for thirst quenching. Naturally the juices were used for medicinal and refreshing qualities (Potter,1996). Fruit juices are manufactured for two main purposes: (a) for preparing pleasant-tasting "soft-drink" and (b) as a contribution of vitamin C to the diet. Commonly manufactured fruit juices are citrus, pineapple, strawberry, mango and tomato juice. Prune, grape and apple juices are produced in lesser amount. (Pyke, 1976).

Fruit juices are products for direct consumption and are obtained by the extraction of cellular juice from fruits. The technology of fruit juice processing covers two finished products categories: juice without pulp (clarified cordials) or squash. Fruits and fruit products are the enigma of food in modern society. Fresh fruits are perishable and have limited shelf life. To prolong shelf life, various processing and preservation methods such as drying, chemical treatments and various packaging methods are used. Drying is the major food processing operation to increase the shelf life.

The purpose of drying of fruit and vegetable juices is to produce a stable and easily handled form of the juice, which reconstitutes rapidly to a quality product resembling the original juice as closely as possible. Dried juice products today are used mainly as convenience foods and has long storage life at ordinary temperatures. Completely dried fruit powders are often used for making many delicious food products. Fruit powders less than 4% (wet basis) moisture content can be used to make candy, toffee, fudge and hard candy. There are several drying techniques for production of food powders. They are: hot air, vacuum, freeze and spray drying. Among them spray drying is the simplest and commercially used method for transforming a wide variety of liquid food products into powder form. Spray dryer uses hot air and can use fairly high air temperatures because the drying temperature drops drastically as water evaporates from the product being dried. The drying process can be completed within a short period of time, thus enabling to prepare dried fruit powder without heat degradation even at comparatively high air temperatures.

In this research, Mango Powder, Orange Powder, Lemon Powder and Pineapple Powder were prepared using locally available raw materials. For fruit juice powder production two complex problems were available,

stickiness of powder and its handling and the other was related to fruit juice natural characteristic that caused no powder production. For preventing of stickiness and production of powder two ways were using of drying agent material and using of specific equipment to facilitate the powder handling (Chegini.G.R,2004). Citrus fruit juice hygroscopic reduction required drying agent materials. The agent materials with changing of physical properties of fruit juice aided to drying. These agent materials include corn syrup, natural gums, sucrose, malto dextrin, etc., caused powder production and prevent cohesion of particle on spray dryer wall. (Bahandari, B.R, 1993).

The quality of pineapple fruit is dependent upon a number of important factors, including (1) variety, (2) nutrition, (3) exposure to light, (4) weather, (5) ripeness and (6) freedom from blemishes, insects or diseases. Pineapple is the most popular tropical fruit. It is sweet and has a pleasant aroma. Pineapples have special properties that distinguish it from all other fruits. Pineapples contain valuable vitamins and minerals. This fruit is low in fat and cholesterol. Pineapple is eaten as a fresh fruit throughout the tropics and sub-tropics. As the fruit deteriorates rapidly after harvest, much of the crop that is sold as canned within the country in which it is grown. The fruit is chopped and added to the other fruits and canned juice is also produced. It is also processed into marmalades, jam, jellies or candies. Pineapple oil or essence is also used as flavouring for confectionery. The outer shell of the fruit and the central core are removed and the residue is sliced, cut into chunks or diced. It is sterilized and hot syrup is added. Crushed pineapple, juice and mixed fruits are also canned and jam is also made from the fruit. (Gibbon, D., 1985)

A lemon is a yellow fruit with an aromatic rind and a tangy and acidic flavor. Though many assign its origin to India and China, the exact history of the fruit remains a mystery till date. Squashed either as lemonade, or simply used as a cooking or garnishing ingredient; lemons are very high nutritional value. Besides, many spirit-lovers will love to swear by lemons, when it comes to mixing and matching cocktails and mocktails. Due to their therapeutic powers, lemons are also popular in the field of traditional medicines.

One of the most delicious and most fattening fruits, mango is truly called the ‘King of Fruits’. A tropical fruit, it comes in as many as 1000 different varieties, each of them totally delectable. Though native to

Southern and Southeast Asia, the fruit is now also grown in Central and South America, Africa and the Arabian Peninsula also. Apart from being high in calories, mangoes are also rich in a large number of nutrients and hold great nutritional value. In fact, they have been known to have positive effects in case of a number of ailments.

Orange is a citrus fruit, considered to be a hybrid, of ancient cultivated origin, between pomelo (Citrus maxima) and tangerine (Citrus reticulata). Native to the countries of Southeast Asia, it is today cultivated in almost all the warm climate countries of the world. Its consumption is as popular in the raw, peeled form, as in the juice form. Even the rind of orange is used by people in recipes, either for flavoring or for garnishing purposes. Being a rich source of nutrients, orange has been associated with a number of health and nutrition benefits.

One of the juiciest fruits that is absolutely a delight to eat is the pineapple. It can be taken with whipped cream, custard or just like that. Pineapple juice is equally yummy and refreshing and is one of the favorite drinks of many people during hot weather. The best part about pineapples is that it is loaded with nutrients and beneficial enzymes, which ensures that not only have a healthy body but also a glowing complexion.

Material and Methods

The fruits for preparing the juice (or) puree were chosen from the following regions of Myanmar. Pineapple from Thibaw (Northern Shan State), Orange from Aungpan (Sourthern Shan State), Mango (sein-te-lone) from Hmawbi (Township) and Lemon from Htan-ta-bin (Yangon Region) were collected from Hledan Market.

Maltodextrin / dry glucose syrup

Maltodextrin (also called dry glucose syrup) are starch hydrolysis products of less than 25 D.E. (Dextrose Equivalent), produced by hydrolysis of corn starch or waxy maize starch by enzyme techniques. The final product is spray dried to a moisture level of 3% to 5 %. A wide variety of maltodextrins with different D.E values is commercially available. They are frequently used as binders (or) drying agents for drying processes. (Marchal, L.M. et al., 1999). It may serve as carriers and facilitate drying.

Sucrose/Sugar

Sucrose or table sugar is the commonest of the sugar, a white, crystallize solid disaccharide with a sweet taste, melting and decomposing at 186°C. It has the same empirical formula ($C_{12}H_{22}O_{11}$) as lactose and maltose but differs from both in structure (isomer). Sucrose is obtained from the juice of sugarcane or the sugar beet and from the sap of the sugar maple (Columbia Electronic Encyclopedia, 2000).

Glucose/ Dextrose

Glucose, Dextrose, or grape sugar, is a monosaccharide with the empirical formula $C_6H_{12}O_6$. It can be obtained by hydrolysis of a variety of carbohydrates, e.g., milk and cane sugars, maltose, cellulose, or glycogen, but it is usually manufactured by hydrolysis of corn-starch with steam only about and dilute acid. Glucose taste is only about sucrose three-fourth as sweet as table sugar (Columbia Electronic Encyclopedia, 2000).

Carboxymethylcellulose

Carboxymethylcellulose (CMC) is a cellulose derivative with carboxymethyl groups (-CH_2-COOH) bound to some of the hydroxyl groups of the glucopyranose monomers that make up the cellulose backbone. It is often used as its sodium salt, sodium CMC. CMC is used in beverage powder as a viscosity modifier or thickener, and to stabilize emulsions in the product.

Trisodium citrate

Trisodium citrate has the chemical formula of $Na_3C_6H_5O_7$. It is chiefly used as a food additive, usually for flavor or as a preservative. It is also used as an acidity regulator. Appearance: white crystalline powder.

Tricalcium phosphate

Tricalcium phosphate has the chemical formula of $Ca_3(PO_4)_2$. It is amorphous, odourless, tasteless powder, insoluble in water, slightly soluble in dilute acetic acid.

Modified starch

Modified starch is a food additive which is prepared by treating starch or starch granules, causing the starch to be partially degraded. It is used as a thickening agent, stabilizer or an emulsifier.

Xanthan gum

Xanthan gum is a polysaccharide used as a food additive and rheology modifier. One of the most remarkable properties of xanthan gum is its ability to produce a large increase in the viscosity of a liquid by adding a very small quantity of gum, on the order of 1%.

Citric acid

Citric acid is a weak organic acid, and it is a natural preservative and is also used to add an acidic, or sour, taste to foods and soft drinks. Citric acid exists in greater than trace amounts in a variety of fruits and vegetables, most notably citrus fruits. At room temperature it is a white crystalline powder. It can exist either in an anhydrous (water-free) form or as a monohydrate. As a food additive, citric acid is used as a flavoring and preservative in food and beverages, especially soft drinks.

Methods

Processing of Pineapple Powder

Pineapple powder produced by ripening, extracting, pulping, dosing the green banana carrier (20%) and sieving the mixture. Then drying in hot air oven for several hours, most of the moisture was driven off leaving behind solid lumps. It was then cooled in a desiccator, weighed and powdered in a Hammer Mill.

Processing of Mango Powder

Mango powder produced by ripening, blanching, extracting, dosing the green banana carrier (15%) and sieving the mixture. Then drying in hot air oven for several hours, most of the moisture was driven off leaving behind solid lumps. It was then cooled in a desiccator, weighed and powdered in a Hammer Mill.

Processing of Orange Powder

Orange juice powder processing has been done on washing, cutting, squeezing and filtering off seed to get fresh orange juice. Maltodextrin of 10 DE was used as the carrier drying aid agent. Experiments performed with adding maltodextrin to orange concentrated. With this agent material, yield was better.

Processing of Lemon Powder

Lemon juice powder processing has been done on washing, cutting, squeezing and filtering off seed to get fresh lemon juice. Maltodextrin of 10 DE was used as the carrier drying aid agent. Experiments performed with adding maltodextrin to lemon concentrated. With this agent material, yield was better.

Preparation of Beverage Powder

The fruit powder (mango or orange or lemon or pineapple) was mixed thoroughly with appropriate amount of glucose, sugar, trisodium citrate, xanthan gum, tricalciumphosphate, modified starch and citric acid. Fruit flavor and salt were added if it was necessary.

Results and Discussion

A comparative study based on the chemical composition (protein, soluble solids content, ash content) of pineapple juice with the literature data, and other results of juices (mango, orange and lemon) were shown in Tables (1) and (5). The measured soluble solid content and total solid content of pineapple juice are higher than that of mango, orange and lemon juices. The amount of protein is nearly the same as mango, orange and lemon juice. Amongst the different concentrating times of pineapple juice as shown in Table (2) and Figure (1), 30 minutes was found to be the optimum concentrating time as it gives the soluble solid content of 56°Brix which is in agreement with the literature value (50-60°Brix). Variation in moisture content and acidity stored at room temperature were shown in Tables (3) and (4) and Figures (2) and (3). It is clear that the pH values of juices from the freshly prepared and preserved juices were nearly the same as shown in Table (6). The next important factor prior to grinding (the dried lump of each fruit product) is the amount of moisture of the material, and as much the moisture

have to be reduced. The minimum moisture content that could be reduced to 4.2%, 3.8%, 4.4% and 4.5% for mango powder, orange powder, lemon powder and pineapple powder respectively at a drying time of 8 hours shown in Table (9) and the relevant graph in Figure (6), but it should not be further dried above (8) hours as case hardening and scorching (overcooked) took place. The qualitative nature of the fruits powder were tested as shown in Table (10) and the results quite clearly indicated that the powdered form still retained some good properties of the initial juice, soluble solid content 12.6 to 3.03°Brix (mango) by about moisture content lowered from 82.8% to 4.2%. Similarly for orange juice, lemon juice and pineapple juice soluble solid content 10.4 to 2.63°Brix, 9.64 to 2.73°Brix and 14.8 to 2.93°Brix by about moisture content lowered from 83.6% to 3.8%, 86.2% to 4.4% and 88.2% to 4.5% respectively. It was found that the values of pH, acidity and soluble solid content from the research samples and brand samples were nearly the same as shown in Table (11). The relatively low moisture content obviously assist the shelf-life that is, an extension of shelf-life from six months to ten months. The type of packing materials, whether tightly sealed or not, played an important role as shown by the results in Table (16). The powder packed in ordinary plastic packets exhibit caking but no caking was observed for fruit powder packed in laminated plastic sachet packets.

Table (1) Composition of Pineapple Juice

Sr. No.	Characteristics	Sample	Literature
1	Acidity (%)	0.78	0.7 – 0.8
2	Protein (%)	0.42	0.36 – 0.50
3	Ash Content (%)	0.44	0.27 – 0.45
4	pH	3.7	3.5 – 4.07
5	Soluble Solid Content (°Brix)	14.8	13.4 – 15.1
6	Total Solid Content (%)	33.4	-
7	Moisture Content (%)	88.2	-
8	Specific Gravity	1.06	1.045 – 1.0805
9	Yield (%)	64.5	-

Table (2) Relationship of Concentrating Time of Pineapple Juice to Soluble Solids Content

Operating Temperature - 50 ± 2°C

100 ml of Pineapple Juice

Sr. No.	Time (min)	Soluble Solids Content (°Brix)	Observation
1	0	14	Acceptable flavour, dilute solution
2	10	18	Acceptable flavour, dilute solution
3	20	32	Good flavour, dilute solution
4	30	56	Good flavour, concentrated solution
5	40	75	Good flavour, viscous liquid
6	50	80	Scorching smell, solid mass
7	60	82	Scorching smell, solid mass

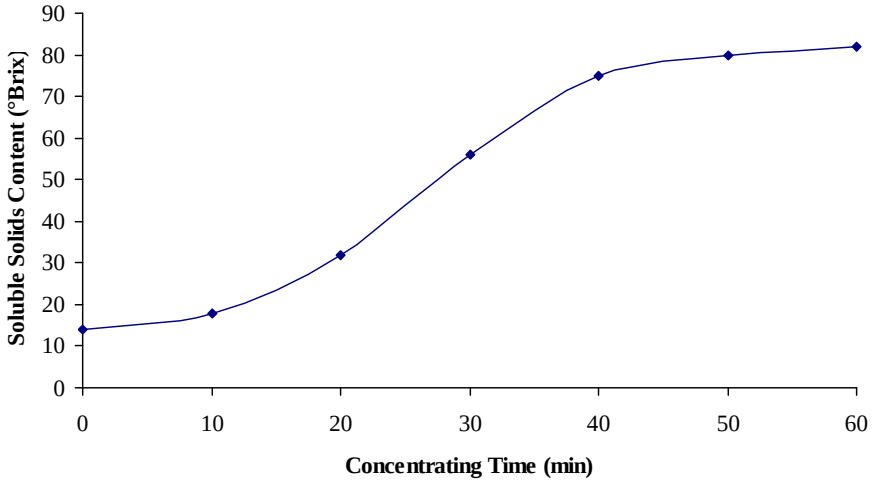

Fig. (1) Effect of Concentrating Time on Soluble Solids Content for Pineapple Juice

Table (3) Variation in Moisture Contents of Fruit Juices with Storage Period

Storage Period (month)	Moisture (%)			
	Mango Juice	Orange Juice	Lemon Juice	Pineapple Juice
1	82.8	83.6	86.2	88.2
2	82.6	83.4	86.0	88.0
3	82.3	83.0	85.8	87.6
4	81.8	82.8	85.7	87.4
5	81.6	82.7	85.5	87.2

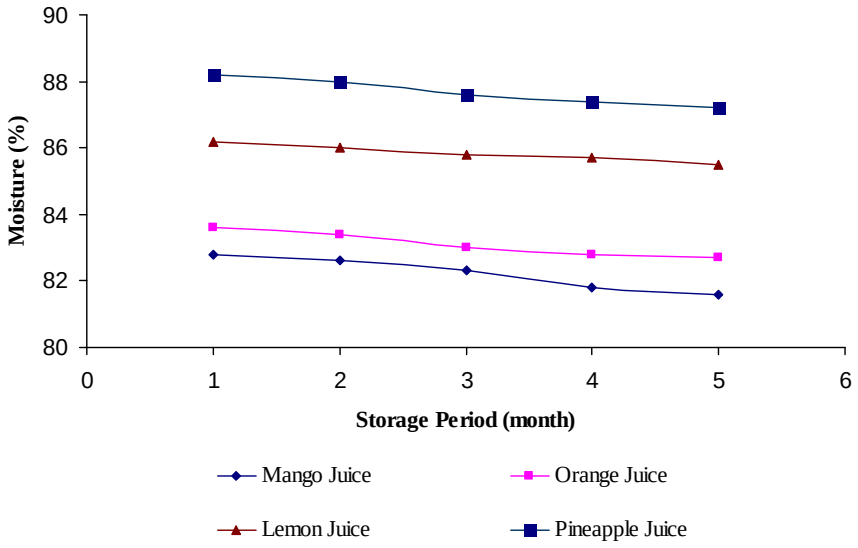

Fig. (2) Variation in Moisture Contents of Fruit Juices with Storage Period

Table (4) Variation in Acidity of Fruit Juices with Storage Period

Storage Period (month)	Acidity (%)			
	Mango Juice	Orange Juice	Lemon Juice	Pineapple Juice
1	1.02	1.18	4.2	0.78
2	1.06	1.20	4.3	0.90
3	1.07	1.24	4.36	0.96
4	1.07	1.27	4.4	1.01
5	1.08	1.28	4.48	1.03

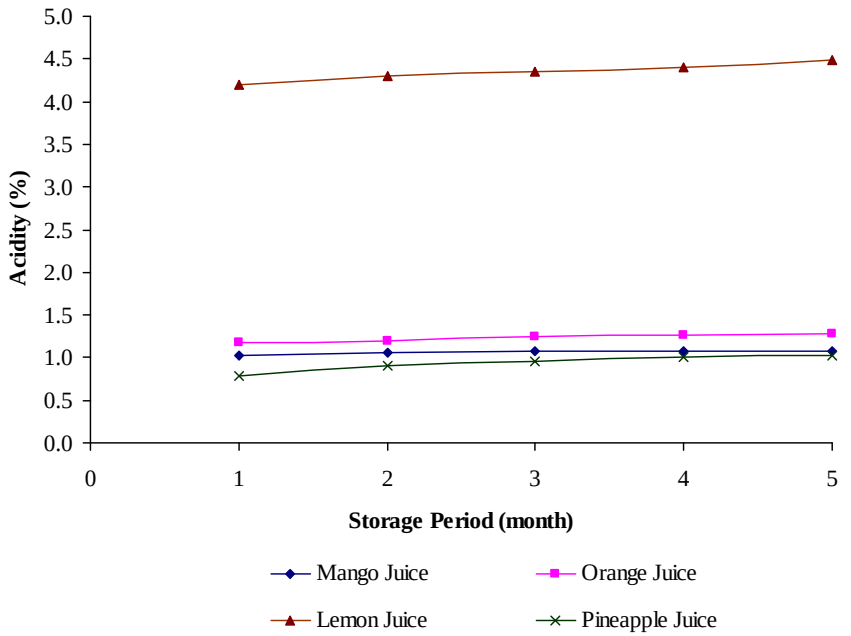

Fig. (3) Variation in Acidity of Fruit Juices with Storage Period

Table (5) Comparison of four Fruit Juices Composition

Sr. No.	Characteristics	Mango Juice	Orange Juice	Lemon Juice	Pineapple Juice
1	Acidity (%)	1.02	1.18	4.2	0.78
2	Protein (%)	0.44	0.43	0.40	0.42
3	Ash Content (%)	0.36	0.38	0.42	0.44
4	pH	3.5	3.6	2.2	3.7
5	Soluble Solid Content (°Brix)	12.6	10.4	9.64	14.8
6	Total Solid Content (%)	33.2	32.6	14.6	35.4
7	Moisture Content (%)	82.8	83.6	86.2	88.2
8	Specific Gravity	1.03	1.06	1.025	1.06
9	Yield (%)	55	40.5	52	64.5

Table (6) Comparison of Fresh Juices and Preserved Juices

Type	Specific Gravity	pH
Mango Fresh Juice	1.03	3.5
Mango Preserved Juice	1.04	3.6 – 3.7
Orange Fresh Juice	1.06	3.6
Orange Preserved Juice	1.06	3.6 – 3.7
Lemon Fresh Juice	1.025	2.2
Lemon Preserved Juice	1.03	2.3 – 2.4
Pineapple Fresh Juice	1.06	3.7
Pineapple Preserved Juice	1.07	3.7 – 3.8

Table (7) Effect of Drying Time on Moisture Liberated (Orange Juice Powder)

Sr. No.	Drying Time (min)	Moisture Liberated (%)
1	0	0
2	3	2.522
3	6	2.907
4	9	3.047
5	12	3.117
6	15	3.222

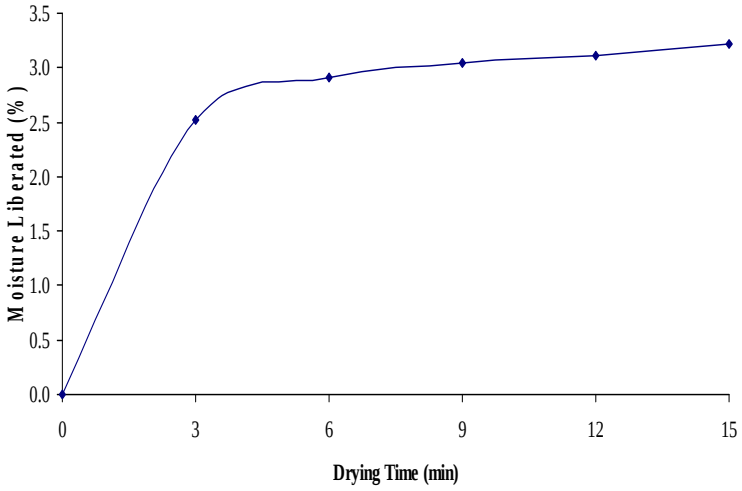

Fig. (4) Effect of Drying Time on Moisture Liberated (Orange Juice Powder)

Table (8) Effect of Drying Time on Moisture Liberated (Lemon Juice Powder)

Sr. No.	Drying Time (min)	Moisture Liberated (%)
1	0	0
2	3	2.540
3	6	3.133
4	9	3.274
5	12	3.359
6	15	3.415

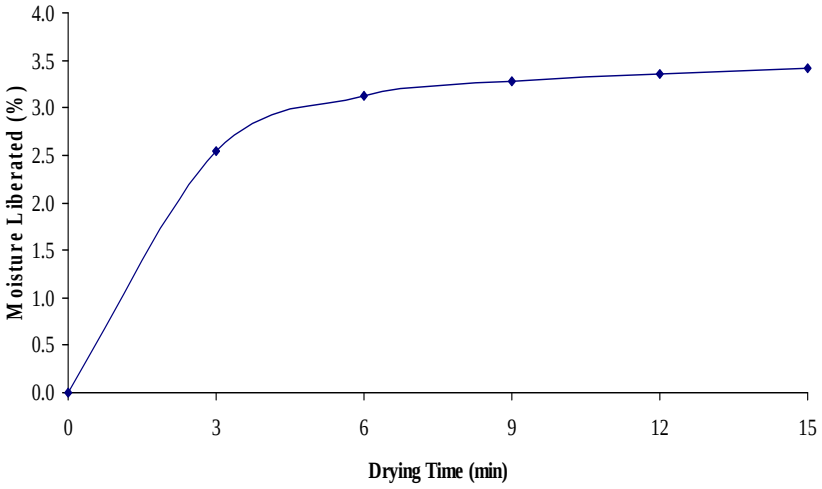

Fig. (5) Effect of Drying Time on Moisture Liberated (Lemon Juice Powder)

Table (9) Effect of Drying Time on Moisture Content

Sr. No.	Drying time (hour)	Moisture content (%)			
		Mango	Orange	Lemon	Pineapple
1	0	48.6	48.1	47.4	47.1
2	1	37.3	36.8	37.1	35.4
3	2	28.6	27.4	27.7	25.8
4	3	15.5	16.0	15.3	15.2
5	4	8.7	8.9	8.4	8.1
6	5	7.5	7.7	7.1	6.9
7	6	5.3	5.5	5.0	5.0
8	7	4.3	4.0	4.5	4.7
9	8*	4.2	3.8	4.4	4.5
10	9	4.2	3.8	4.3	4.4

* Optimum condition

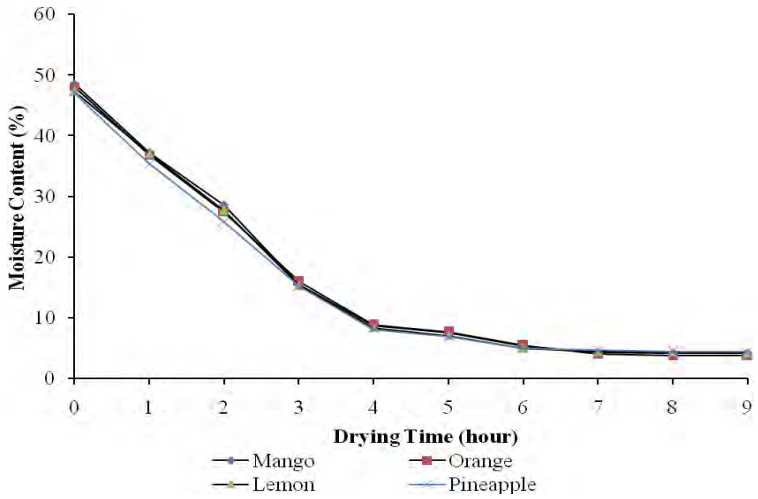

Fig. (6) Effect of Drying Time vs Moisture Content

Table (10) Comparison of the Fruit Juices and its Powdered Form

Type	Moisture Content (%)	Ash Content (%)	Soluble Solid Content (°Brix)	Solubility (%)	Specific Gravity
Mango juice	82.8	0.36	12.6	0.1807	1.03
Orange juice	83.6	0.38	10.4	0.1876	1.06
Lemon juice	86.2	0.42	9.64	0.1897	1.025
Pineapple juice	88.2	0.44	14.8	0.1841	1.06
Mango powder	4.2	1.84	3.03	0.8	-
Orange powder	3.8	1.2	2.63	0.9	-
Lemon powder	4.4	1.86	2.73	0.8	-
Pineapple powder	4.5	2.2	2.93	1.0	-

Table (11) Comparison of Beverages Sample and Brand Samples

Sample	pH	Acidity	Soluble solid content (°Brix)
Mango mix	3.64	2.17	7.4
Orange mix	3.88	2.9	7.3
Lemon mix	3.59	1.2	7.4
Pineapple mix	3.61	2.2	7.5
Brand-Mango mix	3.32	2.9	7.4
Brand-Orange mix	3.57	3.1	7.3
Brand-Lemon mix	2.9	1.4	7.18
Brand-Pineapple mix	3.4	2.2	8.5

Table (12) Moisture Levels During Storage Period at Room Temperature Sealed in Normal Plastic Bags

Sample – mango fruit powder

Storage Period (days)	Moisture Content (%)	Remark
0	4.2	Good appearance
10	4.5	"
20	4.8	"
30	5.2	"
40	5.6	"
50	6.2	Caking condition
60	6.8	Sticky condition

Table (13) Moisture Levels During Storage Period at Room Temperature Sealed in Normal Plastic Bags

Sample – orange fruit powder

Storage Period (days)	Moisture Content (%)	Remark
0	3.8	Good appearance
10	4.0	"
20	4.2	"
30	4.6	"
40	4.8	Caking begins
50	5.1	Caking condition
60	5.4	Sticky condition

Table (14) Moisture Levels During Storage Period at Room Temperature Sealed in Normal Plastic Bags

Sample – lemon fruit powder

Storage Period (days)	Moisture Content (%)	Remark
0	4.4	Good appearance
10	4.5	"
20	4.7	"
30	5.0	Caking begins
40	5.2	Caking condition
50	5.5	Sticky condition
60	5.7	"

Table (15) Moisture Levels During Storage Period at Room Temperature Sealed in Normal Plastic Bags

Sample – pineapple powder

Storage Period (days)	Moisture Content (%)	Remark
0	4.5	Good appearance
10	4.6	"
20	4.8	"
30	5.0	"
40	5.1	Caking begins
50	5.3	Caking condition
60	5.5	Sticky condition

Table (16) Moisture Levels during Storage Period at room Temperature Sealed in Aluminium foil (laminated plastic sachet packets) bag

Storage Period (months)	Moisture content (%)				Remark
	Mango	Orange	Lemon	Pineapple	
0	4.2	3.8	4.4	4.5	Desired colour and good appearance
1	4.2	3.8	4.4	4.5	"
2	4.2	3.8	4.4	4.5	"
3	4.2	3.8	4.4	4.5	"
4	4.2	3.9	4.5	4.5	"
5	4.3	4.1	4.6	4.6	"
6	4.3	4.1	4.6	4.6	"
7	4.3	4.1	4.7	4.6	"
8	4.4	4.1	4.7	4.6	"

Conclusion

In Myanmar, citrus fruits like lime, lemon are available seasonally in abundant quantities and quite cheap during its season. To be economical juices are extracted during the citrus season, properly preserved and stored to extend its availability all year round. Undesirable physical change, such as colour and absorption of water, in juice powder is the absorption of moisture, these results in caking. It can occur either as a result of poor selection of packaging material in the first place, and failure of the packaging during storage. The storage temperature has an important role on the dried powder and maintenance of the dried sample of its taste, colour, and water dehydration ratio and also to some extent for vitamin C, should be kept below 25°C.

Acknowledgements

The authors wish to thank the Department of Higher Education (Lower Myanmar), Ministry of Education, Yangon for the financial support of this research work. The authors are grateful to Dr. Khin Thet Ni, Professor and Head of Department of Industrial Chemistry, University of Yangon, for her permission to use research facilities in the Department during the tenure of the research work.

References

Bahandari, B.R.,et al., 1993. **Effect of spray-drying condition on physical properties of organic juice powder,** Drying Technology 23:657-668

Chegini, G.R., et al., 2005. **Spray drying of concentrated fruit juices**, Drying Technology 11: 1081-1092

Dauthy, M.E., 1995. **Fruit and Vegetable Processing**, FAO Agricultural Service.

Gibbon, D., 1985. **Crops of the Drier Regions of the Tropics,** English Language Book Society.

Marchal, L.M., et al.,1999. **Food Science and Technology**. 10, 345-355

Potter, N., 1986. **Food Science**,4th edition

Pyke, M., 1976. **Food Science and Technology**, W & J Mackay limited, Chatman The Columbia Electronic Encyclopedia, sixth edition, copyright @2000, Columbia University Press

A Study on Purification of Soybean Oil

Thin Thin Khaing[1], Cho Cho Oo[2] and Myint Pe[3]

Abstract

Crude edible fats and oils contain variable amounts of nonglyceride impurities, such as free fatty acids, non-fatty materials generally classified as gum and colour pigments. The purification treatment was designed to remove free fatty acids, phosphaties, gums and other impurities in the oil. Soybean oil was purified by degumming, neutralization and bleaching. Physical characteristics (viscosity, specific gravity, colour, and refractive index) and chemical characteristics (acid value, iodine value, saponification value and unsaponifiable matter) of crude soybean oil and purified oil were determined.

Key words : soybean oil, purified, free fatty acid, phosphatides

Introduction

Soybean oil contains a large percentage of unsaturated fatty acids. They are rich in linoleic acids.The botanical name of soybean is *Soja max*, the leguminous plant. In Myanmar, soybean is cultivated in Shan and Kayar States, and Ayeyawady Division. The composition of soybean oil in terms of fatty acids content are as follows: lauric acid 0.2%, myristic acid 0.1%, palmitic acid 9.8%, stearic acid 2.4%, arachidic acid 0.9%, oleic acid 28.9%, linoleic acid 50.7%, linolenic acid 6.5% and hexadecenoic acid 0.4% . (Bailey, 1964)

Triglycerides consist mainly of glycerol and fatty acids as esters. Vegetable oils in general, contain triglycerides and some minor components such as gums, steroids, sterols, coloring materials, sugar, waxes, partial glycerides, free fatty acids and phosphatides are also present.

Degumming with warm water removes hydratable phospholipids and metals. Addition of a small amount of phosphoric acid converts the remaining non-hydratable phospholipids into hydratable phospholipids. Byproducts of degumming are usually removed by plate and frame filter press by centrifuge. (Carr, 1976)

1. Lecturer, Dr., Department of Industrial Chemistry, University of Yangon
2. Professor, Dr., Department of Industrial Chemistry, Dagon University
3. Part-time Professor, Department of Industrial Chemistry, University of Yangon

Neutralization also results in removal of phosphatides, removal of free fatty acids and removal of color bodies. Removal of traces of soap and moisture occur in the washing and drying step. (Carr, 1976)

Neutralization involves adding moderately strong solutions of caustic soda (12-20ºBe') or alkaline salts, such as soda ash or sodium carbonate. Alkali refining effects an almost complete removal of free fatty acids, which are converted into oil-insoluble soaps. Other acidic substances likewise combine with the alkali, and there is probably some removal of impurities from the oil by adsorption on the soap formed in the operation. (Bailey, 1964)

The emulsion is then thermally shocked by heating to about 75ºC to break out the soap stock which is then centrifugally separated from the neutral oil. (Carr, 1976)

The neutral oil is washed by water or brine solution to avoid formation of insoluble or unwashable soaps. Sodium soaps from refining steps are readily washable and easily removed from the neutral oil by either as single or double water washing operation. The water-washed refined oil is continuously dried and is now ready for bleaching. (Erickson, 1980)

Pigments present in vegetable oils include carotene, xanthophylls, chlorophyll, gossypol, chroman-quinone and diketones and browning products. Most of coloured bodies present in soybean oil include the carotenese and xanthophylls that impart yellow and red colours to the oil, and the chlorophylls or a derivative, pheophytin that give the oil a greenish colour. (Cowan, 1976)

The removal of the effect of pigments can be carried out in several ways:

(1) Adsorption of pigments by clay, carbon black, or other suitable material.

(2) Heating the oil particularly in the presence of oxygen or hydroperoxides that may have been formed by previous exposure of the oil to air.

(3) Heating in the absence of air.

There is the possibility that oxygen and moisture can be dissolved from the surrounding atmosphere during degumming. To eliminate dissolved oxygen and moisture in the degummed oil sample, deaeration and demoisturization are applied. A deaerated feed stock is desirable to reduce

oxidation losses in the subsequent distillation. These objectives are most satisfactorily achieved by heating the feed stock to a temperature of 83 to 110ºC, while under a vacuum of 650 to 700 mm Hg. (Berger, 1952)

Material and Methods

In this research, soybean was obtained from Hinthada Township, Ayeyarwady Division. The crude oil was obtained from Yadanar Zaw Oil Mill, Hlaing Tharyar Township at Industrial Zone (5), Yangon Division.

Determination of Acid Value

Acid value was determined by the method shown in AOCS (1984) standard.

Determination of Iodine Value

Iodine value was determined by the method shown in AOCS (1984) standard.

Determination of Saponification Value

Saponification value was determined by the method shown in AOCS (1984) standard.

Determination of Unsaponifiable Matter

Unsaponifiable matter was determined by the method shown in AOCS (1984) standard.

Determination of Kinematic Viscosity

Kinematic viscosity was determined by ASTM standard test method (ASTM D 445).

Degumming Process

370.3 g of prefiltered soybean oil was first heated to 80ºC, followed by addition of 2% (v/w) hot water. The mixture was agitated by magnetic stirrer, at 200 rpm for 15 min. The hydratable phosphatides or gums were separated by centrifuge, running at 3000 rpm for 15 min.

After water degumming, the soybean oil was heated to 80ºC. Concentrated phosphoric acid, 0.35 ml of 0.1% (v/w) was added dropwise into 354.1 g of water degummed soybean oil and agitated by magnetic stirrer at 200 rpm for 15 min. The nonhydratable gums were converted to hydratable gums, by the reaction with phosphoric acid and settled at the bottom of the beaker. The gums were separated under similar experimental condition as in water degumming. The experiments were further carried out by varying the amount of phosphoric acid as (0.2%, 0.3% and 0.4%) respectively.

Neutralization Process

The degummed soybean oil was first analyzed for free fatty acid content by AOCS method. 347.7 g of degummed soybean oil of acidity 17.5 was heated to 80ºC. 18.5 ml of 20º Be' caustic soda including 5% excess solution was added drop by drop with continuous stirring. The oil and soap mixture was stirred with a magnetic stirrer at 200 rpm for 30 min. Soap and neutralized oil were separated by centrifuge running at 3000 rpm for 15 min.

The portion of neutralized oil separated from soap was washed with brine solution to remove traces of soap particles. Several washings of neutralized oil with hot water were carried out to remove last traces of soap particles. The washed water was tested with phenolphthalein indicator to ensure that it was free from soap particles. The washed oil was taken for deaeration and demoisturization under 200-300 mm Hg at 80-100ºC. The experiments were further carried out by varying the concentration of caustic soda as 16ºBe' and 18ºBe' respectively.

Bleaching Process

Bleaching of soyean oil was carried out after neutralization. 239.4 g of degummed, neutralized, deaerated and demoisturized soybean oil was heated in 1L round bottomed flask to 90ºC. 2.39 g of 1% (w/w) bleaching earth was preheated to 60ºC and added to oil sample. The oil mixture was agitated by magnetic stirrer spinning at the rate of 200 rpm for 30 min under 200-300 mmHg. The spent bleaching earth was separated by filtration. The experiments were further carried out by varying the amount of bleaching earth as (2%, 3% and 4%) respectively.

Deaeration and Demoisturization Process

Purification of triglyceride carried out under different steps was effective only when deaeration and demoisturization were applied after each step. The purpose of deaeration and demoisturization is to prevent undesirable reactions and by-products. Deaeration, usually carried out under vacuum to eliminate traces of moisture and dissolved oxygen in the oil refining process is technically termed as vacuum drying. The vacuum pump installed in refining process is of a separate unit and operated under 200-300 mmHg at 80-100ºC for 30min.

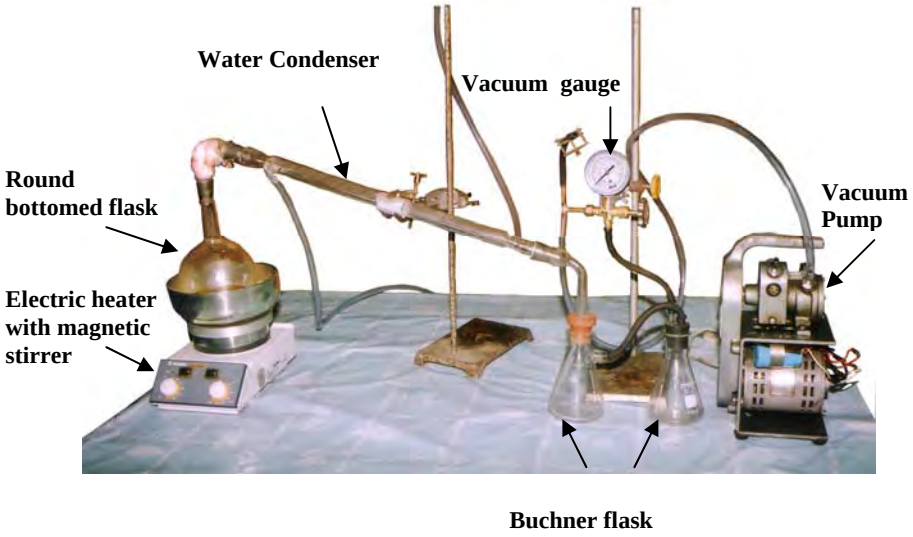

Fig (1) Deaeration and Demoisturization Apparatus

Results and Discussion

Soybean oil was subjected to various purification processes to prevent deterioration affected by the presence of impurities such as dissolved oxygen, moisture, steroid, sterol, gums and high melting waxes. Filtration, degumming, neutralization, bleaching and demoisturization were carried out except deodorization. The first purification step is hot water and phosphoric acid degumming. Table (1) indicates water degumming and condition of soybean oil.

In the acid degumming process of soybean oils, four different phosphoric acid concentrations, 0.1%, 0.2%, 0.3% and 0.4% (wt%) were used as shown in Table (3). Among these concentrations of phosphoric acid, 0.2% was found to be the most favourable condition with respect to acid value and unsaponifiable matter.

The corresponding change in viscosity, specific gravity, colour, refractive index, acid value, iodine value, saponification value and unsaponifiable matter after water degumming and acid degumming of oils are shown in Table (4).

In this research work, neutralization of degummed soybean oil was based on three concentrations of caustic soda (16ºBe', 18ºBe' and 20ºBe') to remove fatty acids. Table (5) shows neutralization condition, oil losses, soap obtained and yield percent of neutralized oil. Thus in the neutralization process undertaken, 16ºBe' of NaOH for soybean oil was found to be relatively more effective as they gave a lower acid value and relatively higher yield percent of refined oil.

Dissolved colour pigments were also partially removed. The neutralized soybean oil was then decolorized by using bleaching earth 1-4% (wt%) were used as shown in Table (7). 2% (wt%) of bleaching earth gave lower oil loss.

The data of Table (8) demonstrates the comparison of characteristics of neutralized and bleached oil.

Table (1) Water Degumming of Soybean Oil

Weight of sample	370.3 g
Temperature	80ºC
Volume of hot water added	7.4 ml (2% v/w)
Stirring rate	200 rpm
Stirring time	15 min
Speed of centrifuge	3000 rpm
Centrifugation time	15 min

Composition	Weight
Weight of gum (g)	16.2
Weight of water degummed oil (g)	354.1
Oil losses (wt%)	4.38
Yield % of water degummed oil (wt %)	95.62

Table (2) Comparison of Characteristics of Crude Soybean Oil and Water Degummed Soybean Oil

Chemical / Physical Characteristics	Crude oil	Water degummed oil	Literature value **
Acid value	15.3	16.3	0.5-3.0
Iodine value	140	139.9	120-143
Saponification value	193.68	193.5	189-195
Unsaponifiable matter	3.6	2.34	0.2-1.5
Viscosity (cP) at 30ºC	12.5	12.5	-
Specific gravity at 30ºC	0.9177	0.917	0.924-0.928 (15ºC)
Colour Y	49.1	49	-
R	9.9	9.9	-
B	4.8	4.6	-
Refractive index at 30ºC	1.472	1.4715	1.473- 1.477(20ºC)

** Specification for crude soya bean oil, British Standard, BS: 635

Table (3) Acid Degumming of Soybean Oil

Weight of sample	354.1 g
Temperature	80ºC
Volume of phosphoric acid added	0.71 ml (0.2% v/w)
Stirring rate	200 rpm
Stirring time	15 min
Speed of centrifuge	3000 rpm
Centrifugation time	15 min

Composition	H_3PO_4; % (v/w)			
	0.1%	0.2% *	0.3%	0.4%
Volume of phosphoric acid (ml)	0.35	0.71	1.06	1.42
Weight of gum (g)	3.8	4.9	6.3	9.8
Weight of acid degummed oil (g)	349	347.7	344.6	340.1
Oil losses (wt %)	1.44	1.81	2.68	3.95
Yield % of acid degummed oil (wt%)	98.56	98.19	97.32	96.05

* Optimum condition

Table (4) Comparison of Characteristics of Water Degummed Soybean Oil and Acid Degummed Soybean Oil

Chemical / Physical Characteristics	Water degummed oil	H_3PO_4 ; % (v/w)				Literature value **
		0.1%	0.2% *	0.3%	0.4%	
Acid value	16.3	16.7	17.5	18.3	22.6	0.5-3.0
Iodine value	139.9	139.7	139.5	138.5	138.4	120-143
Saponification value	193.5	193.2	192.8	192.5	192.2	189-195
Unsaponifiable matter	2. 34	2.1	1.68	1.47	1.37	0.2-1.5
Viscosity(cP) at 30ºC	12.5	12.5	12.5	12.5	12.5	-
Specific gravity at 30ºC	0.917	0.9169	0.917	0.917	0.9167	0.924-0.928 (15Cº)
Colour Y	49	49	49	49	49	-

Chemical / Physical Characteristics	Water degummed oil	H_3PO_4 ; % (v/w)				Literature value **
		0.1%	0.2% *	0.3%	0.4%	
R	9.9	9.9	11	11	11	-
B	4.6	4.5	4.2	4.1	4.2	-
Refractive index at 30ºC	1.4715	1.472	1.4725	1.472	1.472	1.473- 1.477 (20Cº)

* Optimum condition

Table (5) Neutralization of Acid Degummed Soybean Oil

Weight of sample	347.7 g
Temperature	80ºC
Stirring rate	200 rpm
Stirring time	30 min
Speed of centrifuge	3000 rpm
Centrifugation time	15 min

Composition	Neutralized oil			Remark
	20ºBe' NaOH	18ºBe' NaOH	16ºBe' NaOH*	
Volume of NaOH (ml)	18.5	24.2	33.4	16º Be' NaOH was required to obtain AV<1 and optimum yield %.
Acid value	0.5	0.5	0.5	
Weight of neutralized oil (g)	122.4	174.2	239.4	
Oil losses (wt %)	64.8	49.9	31.15	
Yield % of neutralized oil (wt %)	35.2	50.1	68.85	
Physical appearance	clear	clear	clear	

* Optimum condition

Table (6) Comparison of Characteristics of Acid Degummed Soybean Oil and Neutralized Soybean Oil

Chemical / Physical Characteristics	Acid degummed oil	Neutralized oil	Literature value **
Acid value	17.5	0.5	0.5-3.0
Iodine value	139.5	139.4	120-143
Saponification value	192.8	191.1	189-195
Unsaponifiable matter	1.68	1.3	0.2-1.5
Viscosity (cP) at 30ºC	12.5	12.5	-
Specific gravity at 30ºC	0.917	0.915	0.924-0.928 (15Cº)
Colour Y	49	31	-
R	11	8.9	-
B	4.2	2.7	-
Refractive index at 30ºC	1.4725	1.468	1.473- 1.477 (20Cº)

** Specification for crude soya bean oil, British Standard, BS: 635

Table (7) Bleaching of Degummed, Neutralized, Demoisturized and Deaerated Soybean Oil

Weight of sample	239.4 g
Temperature	90ºC
Stirring rate	200 rpm
Stirring time	30 min
Vacuum	200-300 mmHg

Composition	Bleaching earth; (wt %)			
	1%	2%*	3%	4%
Weight of bleaching earth (g)	2.39	4.79	7.18	9.58
Weight of bleached oil (g)	221	218	216	214
Oil losses (wt %)	7.66	9.06	9.88	10.7
Yield % of bleached oil (wt %)	92.34	90.94	90.12	89.3

* Optimum condition

Table (8) Comparison of Characteristics of Neutralized Soybean Oil and Bleached Soybean Oil

Chemical / Physical Characteristics	Neutralized oil (16ºBe' NaOH)	Bleaching earth; (wt %)				Literature value **
		1%	2%*	3%	4%	
Acid value	0.5	0.5	0.50	0.51	0.51	0.5-3.0
Iodine value	139.4	139.2	139.5	137.5	136.1	120-143
Saponification value	191.1	191.05	191.01	190.4	190.1	189-195
Unsaponifiable matter	1.3	1.28	1.25	1.22	1.9	0.2-1.5
Viscosity (cP) at 30ºC	12.5	12.5	12.5	12.5	12.5	-
Specific gravity at 30ºC	0.915	0.914	0.913	0.913	0.912	0.924-0.928 (15Cº)
Colour Y	31	14	13	10	10	-
R	8.9	4.1	3.4	3	3	-
B	2.7	0	0	0	0	-
Refractive index at 30ºC	1.468	1.468	1.468	1.468	1.468	1.473- 1.477 (20Cº)

* Optimum condition

** Specification for crude soya bean oil, British Standard, BS: 635

Table (9) Comparison of Characteristics of Crude and Refined Soybean Oil

Chemical / Physical Characteristics	Crude soybean oil	Refined soybean oil	Literature value **
Acid value	15.3	0.50	0.5-3.0
Iodine value	140	139.5	120-143
Saponification value	193.68	191.01	189-195
Unsaponifiable matter	3.6	1.25	0.2-1.5
Viscosity (cP) at 30ºC	12.5	12.5	-
Specific gravity at 30ºC	0.9177	0.913	0.924-0.928 (15Cº)
Colour Y	49.1	13	-
R	9.9	3.4	-
B	4.8	0	-
Refractive index at 30ºC	1.472	1.468	1.473- 1.477(20ºC)

** Specification for crude soya bean oil, British Standard, BS: 635

Conclusion

The removal of phosphatides prior to alkali refining is definitely advantageous in the case of soybean oil. In the phosphoric acid treatment, soybean oil is precipitated as insoluble phosphates with a high specific gravity. The bulk of gum is removed before alkali refining; the losses during the latter treatment depend on the condition. It was found that the physical and chemical properties purified soybean oil sample, like, viscosity, specific gravity, colour, refractive index, acid value, iodine value, saponification value and unsaponifiable matter were comparable to those of literature values.

Acknowledgements

The author is grateful to Professor Dr. Khin Thet Ni, Head of Industrial Chemistry Department, University of Yangon, for her guidance and kind encouragement.I would like to extend my thanks to my supervisor Dr. Cho Cho Oo, Professor, Industrial Chemistry Department, Dagon University, for her help and advice given to me while conducting the research work. I would also like to express my profound respect and deepest gratitude to my co-supervisor U Myint Pe, Deputy General Manager (Retired), Myanma Agricultural

Produces Trading, Ministry of Commerce, for his constructive advice, valuable suggestions and guidance throughout the research work until the completion of thesis.

References

Bailey, A.E., 1964. **Industrial Oil and Fat Products**, Interscience Publishers, Inc., New York. British Standard, 635 (1967).

Berger,R.W., 1952. **Improvements in the Simple Distillation of Fatty Acids by Continuous Methods,** Journal of American Oil Chemists' Society, Vol 30.

Cowan, C., 1976. **Degumming, Refining, Bleaching and Deodorization Theory**, Journal of American Oil Chemists' Society, Vol 53.

Carr, A., 1976. **Degumming, Refining, Practices in the U.S**., Journal of American Oil Chemists' Society, Vol 53.

Erickson, R., 1980. **Handbook of Soy Oil Processing and Utlization**, American Soybean Association and American Oil Chemists' society. Champaign, Illinois.

Kirk, R.E., and Othmer, D.F., 1978 Encyclopedia of Chemical Technology, John Wiley and sons, Inc., New York 3rd edition, Vol 2.

Preliminary Studies on the Preservation of Longan Fruit in Sugar Syrup

Khin Hla Mon

Abstract

This research work was emphasized on the preservation of longan fruit in sugar syrup. The main objective of this work is to supply wholesome, safe, nutritious and acceptable food to consumers throughout the year. In this research, longan fruits were pretreated by using different methods namely, blanching, soaking in each aqueous solution of citric acid, salt, potassium sorbate, sodium metabisulfite and finally dipping in sugar syrup. To assess their quality , the characteristics such as pH, ash, moisture, protein, fat, calcium, iron, organoleptic properties and shelf-life were determined.

Keywords: blanching, organoleptic properties

Introduction

In Myanmar, agriculture is the mainstay of the economy. However most types of fruit and vegetable are seasonal and are not available the whole year. Even in other seasons, they are not always available in the perfect condition due to poor transportation, weak infrastructure and their perishable nature. So, to be available anytime anywhere, they are preserved in the perfect condition using various methods and processes.

The major aim of preservation of fruit is to make it possible for consumers to have the nutritious processed fruits during the off-season and to reduce the fruit loss. Food preservation refers to any one of a number of techniques used to prevent food from spoilage. Fruits and vegetables begin to spoil as soon as they are harvested. Some spoilage is caused by microorganisms such as bacteria and mold. Other spoilage result from chemical changes within the food itself due to natural processes such as enzyme action or oxidation (Peter,1958).

Methods of preservation used to extend shelf-life include removal of moisture, temperature control, pH control, use of chemical preservatives and irradiation. Some preservation techniques involve the processes to inhibit natural aging and discoloration that can occur during food preparation such as enzymatic browning reaction in fruits (Dauthy,1995).

Lecturer, Dr., Department of Industrial Chemistry, Yadanabon University

Preservatives are substances added to foods to inhibit the growth of microorganisms, to facilitate the preparation, and to improve the keeping qualities and appearance. Many chemicals will kill or inhibit the growth of microorganisms, but most of these are not permitted in foods. Salt and Sugar have long been used as effective means of extending shelf-life of various products (Potter and Hotchkiss,1996).

Materials and Methods

Selection of Fruits

Good, sound, fresh and mature longan fruits grown in Sagaing Region were collected for this research.

Preparation of Fruits

Longans were washed thoroughly to remove dust and dirt. Then, the rinds were peeled and seeds were removed to obtain the flesh.

Preparation of Sugar Syrup

Sugar syrup was made using required amount of sugar and boiling water to get required specific gravity. And then, the sugar syrup was filtered to remove impurities and placed in each of the five beakers.

Methods of Pretreatment

Blanching

About 50g of prepared fruit sample was blanched in boiling water for 15 minutes. Then, they were filtered and dipped in cold water for 10 minutes.

Addition of Citric Acid

About 50g of each sample prepared as mentioned above was placed in each beaker containing 1% to 5% citric acid solution for 15 minutes. Then, they were filtered and soaked in water for 10 minutes

Addition of Salt

About 50 g of each prepared fruit sample was placed in individual beakers containing 0.2%, 0.4%, 0.6%, 0.8% and 1% of salt (sodium chloride) solution for 15 minutes. Then, they were filtered and soaked in water for 10 minutes.

Addition of Potassium Sorbate

About 50 g of each prepared longan fruit was put in separate beakers containing 0.2%, 0.4%, 0.6%, 0.8% and 1 % of potassium sorbate solution for 15 minutes. After that, it was taken out and soaked in water for 10 minutes.

Addition of Sodium Metabisulfite

About 50 g of each sample prepared, as mentioned in above section was placed in each beaker containing 0.2 %, 0.4 %, 0.6 %, 0.8 % and 1 % of sodium metabisulfite solution respectively for 15 minutes. It was taken out and soaked in water for 10 minutes.

Preservation of Longan Fruit

Pretreated samples mentioned above were placed carefully into sterilized bottles filling with hot sugar syrup having specific gravity 1.05, 1.10 and 1.15 respectively. After that, they were pasteurized at 100°C for half an hour using water bath. The pasteurized bottles were then labeled and stored in a cool, dry place. The results of preserved longan fruits for the various concentration of citric acid, salt, potassium sorbate, sodium metabisulfite are shown in Table (1) to Table (5).

Results and Discussion

In this research work, preservation of longan fruit was carried out by pretreatment using blanching, addition of food additives such as sodium metabisulfite, potassium sorbate, citric acid, salt and finally preserving in sugar syrup with different specific gravities of 1.05, 1.10 and 1.15.

In the present work, the ratio of raw material to sugar syrup was carried out in 1:2 and 1:3. When the ratio of raw material to sugar syrup (1:2) was used, small scum and bubbles were found on the surface of the product. Therefore, 1:3 (raw material: sugar syrup) was chosen as the optimum condition for preserved fruits.

The results from Table (1) show that when blanching method was used, the texture of product was found to be very soft and also the small amount of scum and bubbles were formed. These results point out that the product's shelf-life was found to be only two days. It is rather obvious from the results of Table (2) that among five different concentrations of citric

acid solution, the preserved longan using 1% citric acid in 1.10 specific gravity sugar syrup gave the best result due to its organoleptic properties, pH and prolonged shelf-life.

Table (3) shows that pretreatment of longan in salt solution containing less than 0.8% and 0.8% salt gave soft and brown flesh and fermentation began 10 days after treatment, formation of small bubbles and scum. Pretreatment in 1% salt solution, and especially 1.10 specific gravity of sugar syrup gave the product that resembles closely the original material in organoleptic properties and nutritional quality.

It is found that longan preserved in sugar syrup treated with 1% salt solution give normal and white flesh but the syrup is turbid. Using more than 1% salt gave hard and brown flesh, the product's shelf-life was found to be 2 months. The results from Table(3) indicate the different amounts of salt solution used. It is observed that the preserved longans treated in 1% salt solution in 1.10 specific gravity sugar syrup gave the best result due to its organoleptic properties, pH and prolonged shelf-life.

It can be seen that the pH decreased with increase in preservative concentration and specific gravity of syrup. The taste of the product was also poor with increasing the concentration of preservative. The color of the products were brown and the fleshes were shrinked at higher concentration of preservative. The optimum condition for preserved longan was found to be in 0.2% potassium sorbate in 1.10 specific gravity sugar syrup. In this condition, the shelf-life of preserved longan was found to be four months, and color, texture and taste were also the best for this duration. The results are shown in Table(4).

Table (5) shows that the optimum conditon of product was found to be 0.2% sodium metabisulfite in 1.05 specific gravity sugar syrup due to its organoleptic properties, pH and prolonged shelf-life.

From the results in Table (6), it is clear that protein content and fat content in preserved longan fruit was significantly lower than that of fresh longan fruit (literature value) due to the preservation in sugar syrup. The content of iron and calcium were lower than that of fresh pulp because of the loss of soluble mineral salt. The value of pH was acceptable values of health and safety for consumers.

Conclusion

Longan fruit is the excellent source of vitamins, minerals, carbohydrate and fiber. It can be consumed throughout the year by processing with some preservatives in sugar syrup. In this research work, the preservation of longan fruit in sugar syrup was prepared by the individual addition of potassium sorbate, sodium metabisulfite, salt, citric acid solution and finally dipped in sugar syrup.

Optimum conditions of preservation of longan fruit in sugar syrup related to the characteristics of preserved longan fruit were one of the most interesting points of this research. Among the different experiments, it is found that the optimum concentration of 0.2 % sodium metabisulfite solution in 1.05 specific gravity sugar syrup gave the best results.

Table (1) Characteristics of Preserved Longan Fruit by Pretreatment of Blanching

Sr. No	Raw Material (g)	Blanching Time (min)	Sugar Syrup (sp.gr)	Characteristics				
				Organoleptic Properties			pH	Shelf-life (days)
				Texture	Color	Taste		
1.	50	15	1.05	Soft	White	Slightly sour	4	2
			1.10	Soft	White	Slightly sour	4	2
			1.15	Soft	White	Slightly sour	5	2

Raw Material: Sugar Syrup = 1:3

Sugar Syrup (265g/1000 ml); sp.gr = 1.05

Sugar Syrup (340g/1000 ml); sp.gr = 1.10

Sugar Syrup (560g/1000 ml); sp.gr = 1.15

Table (2) Characteristics of Preserved Longan Fruit with Pretreatment in Citric Acid Solution

Sr. No	Raw Material (g)	Citric Acid (%) (w/v)	Sugar Syrup (sp.gr)	Characteristics				
				Organoleptic Properties			pH	Shelf-life (month)
				Texture	Color	Taste		
1.	50	1	1.05	Shrink	Yellow	Sweet	5	3
			1.10	∗Normal	Normal	Sweet	5	3
			1.15	Normal	Brown	Sweet	5	2
2.	50	2	1.05	Soft	Yellow	Sour	3	1
			1.10	Soft	Yellow	Sour	3	1
			1.15	Shrink	Yellow	Slightly sour	4	1
3.	50	3	1.05	Soft	Yellow	Sour	3	1
			1.10	Soft	Yellow	Sour	3	1
			1.15	Shrink	Yellow	Sour	2	1
4.	50	4	1.05	Soft	Yellow	Slightly sour	4	1
			1.10	Soft	Yellow	Slightly sour	4	1
			1.15	Shrink	Yellow	Sour	2	1
5.	50	5	1.05	Soft	Yellow	Slightly sour	4	1
			1.10	Soft	Yellow	Sour	3	1
			1.15	Shrink	Yellow	Sour	2	1

∗ Optimum condition

Raw material : Sugar Syrup = 1:3

Sugar Syrup (265g/1000 ml); sp.gr = 1.05

Sugar Syrup (340g/1000 ml); sp.gr = 1.10

Sugar Syrup (560g/1000 ml); sp.gr = 1.15

Table (3) Characteristics of Preserved Longan Fruit with Pretreatment in Salt Solution

Sr. No	Raw Material (g)	Salt (%) (w/v)	Sugar Syrup (sp.gr)	Characteristics				
				Organoleptic Properties			pH	Shelf-life (days)
				Texture	Color	Taste		
1.	50	0.2	1.05	Soft	Brown	Sour	3	20
			1.10	Soft	Brown	Sour	3	20
			1.15	Soft	Brown	Sour	3	20
2.	50	0.4	1.05	Soft	Brown	Sour	3	20
			1.10	Soft	Brown	Sour	3	25
			1.15	Soft	Brown	Sour	3	25
3.	50	0.6	1.05	Soft	Brown	Sour	3	30
			1.10	Soft	Brown	Sour	3	30
			1.15	Soft	Brown	Sour	3	30
4.	50	0.8	1.05	Soft	Brown	Sour	3	30
			1.10	Soft	Brown	Sour	3	30
			1.15	Soft	Brown	Sour	3	30
5.	50	1	1.05	Normal	Brown	Sweet	4	50
			*1.10	Normal	White	Sweet	4	60
			1.15	Normal	White	Sweet	4	60

* Optimum condition

Raw material : Sugar Syrup = 1:3

Sugar Syrup (265g/1000 ml); sp.gr = 1.05

Sugar Syrup (340g/1000 ml); sp.gr = 1.10

Sugar Syrup (560g/1000 ml); sp.gr = 1.15

Table (4) Characteristics of Preserved Longan Fruit with Pretreatment in Potassium Sorbate Solution ($C_6H_7KO_2$)

Sr. No	Raw Material (g)	O_2 (%) (w/v)	Syrup (sp.gr)	Characteristics				
				Organoleptic Properties			pH	Shelf-life (month)
				Texture	Color	Taste		
1	50	0.2	1.05	Normal	Brown	Sweet	5	4
			*1.10	Normal	White	Sweet	5	4
			1.15	Normal	Yellow	Sweet	4	4
2	50	0.4	1.05	Soft	Brown	Sweet	4	4
			1.10	Soft	Yellow	Sour	4	4
			1.15	Soft	Yellow	Sweet	4	4
3	50	0.6	1.05	Soft	Brown	Sour	4	5
			1.10	Soft	Yellow	Sour	4	5
			1.15	Soft	Yellow	Sweet	4	5
4	50	0.8	1.05	Shrink	Yellow	Sour	4	5
			1.10	Shrink	Yellow	Sour	4	5
			1.15	Shrink	Yellow	Sweet	4	5
5	50	1	1.05	Shrink	Yellow	Sour	4	5
			1.10	Shrink	Yellow	Sour	4	5
			1.15	Shrink	Yellow	Sour	4	5

* Optimum condition

Raw material : Sugar Syrup = 1:3

Sugar Syrup (265g/1000ml); sp.gr = 1.05

Sugar Syrup (340g/1000ml); sp.gr = 1.10

Sugar Syrup (500g/1000ml); sp.gr = 1.15

Table (5) Characteristics of Preserved Longan with Pretreatment in Sodium Metabisulfite Solution ($Na_2S_2O_5$)

Sr. No.	Raw Material (g)	$Na_2S_2O_5$ (%)(w/v)	Sugar Syrup (sp.gr.)	Characteristics				
				Organoleptic Properties			pH	Shelf-life (month)
				Texture	Color	Taste		
1	50	0.2	*1.05	Normal	White	Sweet	6	6
			1.10	Normal	White	Sweet	6	6
			1.15	Normal	White	Sweet	6	6
2	50	0.4	1.05	Normal	White	Sweet	6	6
			1.10	Normal	White	Sweet	6	6
			1.15	Normal	White	Sweet	6	6
3	50	0.6	1.05	Normal	White	Sweet	5	5
			1.10	Normal	White	Sweet	5	5
			1.15	Normal	White	Sweet	5	5
4	50	0.8	1.05	Hard	Brown	Sweet	5	5
			1.10	Hard	Brown	Sweet	5	5
			1.15	Hard	Brown	Sweet	5	5
5	50	1	1.05	Hard	Brown	Sweet	5	5
			1.10	Hard	Brown	Sweet	5	5
			1.15	Hard	Brown	Sweet	5	5

* Optimum Condition

Raw material : Sugar syrup= 1:3

Sugar Syrup (265 g/ 1000 ml); sp.gr = 1.05

Sugar Syrup (340 g/ 1000 ml); sp.gr = 1.10

Sugar Syrup (500 g/ 1000 ml); sp.gr = 1.15

Table (6) Physico-Chemical Analysis of Preserved Longan Fruit

Sr. No.	Composition	*Literature Value for Fresh Longan Fruit	**Prepared Longan Fruit
1.	Moisture (%) (w/w)	82.4	82.77
2.	Calcium (ppm)	10.0	46.8
3.	Ash (%) (w/w)	0.7	2.9
4.	Iron (ppm)	1.2	nil
5.	Fat (ppm)	0.1	nil
6.	pH	-	6
7.	Protein(%) (w/w)	1.0	-

* www.nutritive value of Longan from wikipedia

** These datas were measured at Myanmar Pharmaceutical Factory (Sagaing) and Cottage Industries Department.

Fig. (1) Longan Tree with Fruits

Fig. (2) Fresh Longan Before Preserving

Fig.(3) Preserved Longan in Sugar Syrup

Acknowledgements

We would like to express our gratitude to Dr Khin Maung Oo, Rector and Dr Si Si Hla Buu, Pro-Rector, Yadanabon University for their permission to publish the manuscript in the universities research journal and Dr Than Than Kyi, Professor and Head and Dr Yi Yi Myint ,Professor of Industrial Chemistry Department, Yadanabon University for reviewing the manuscript. Warmest thanks go to all the persons for their kind support in carrying out this research and editing this article.

References

Dauthy,M.E., (1995), Fruit and Vegetable Processing, FAO Agricultural Service, Rome.

Peter,(1958),The Technology of Food Preservation, Mc Graw Hill Company, Londan.

Potter, N.N and Hotchkiss,J.H., (1996), Food Science,Fifth Edition,CBS Publishers and Distributors.

Websites

http:// en. wikipedia. org/ wiki/ Sodium metabisulfite

http:// en. wikipedia. org / wiki/ food preservation

http:// www. nontosogardens. com/ dimocarpus-longan-htm

http:// www. wikipedia.org/wiki/ sugar

http:// nutrition about. com/od/hydration water/a/ water article.htm

Preparation of Bagasse - based Composite Materials

Khin Mar Hlaing[1] and Aye Nyunt Kyi[2]

Abstract

Composites are combination of two or more materials present as separate phases and combined to form desired structures so as to take advantage of certain desirable properties of each component. The constituents can be organic, inorganic, or metallic (synthetic or naturally occurring) in the form of particles, rods, fibers, plates, etc. Particleboards and fiberboards are produced by using different adhesives with different agricultural wastes (bagasse, bamboo, straw, coconut fiber, sawdust) with reasonable cost. The boards made from bagasse with different types of adhesives have been utilized successfully in making household articles such as show case, TV stand and side shelves. In this study, organic bonded bagasse fiberboards were prepared with various resins, such as phenol-formaldehyde, urea formaldehyde, polystyrene and polyethylene as adhesives. The physicochemical properties of the organic binders were determined. The boards were prepared with hot pressing method under different operating conditions. The amount of resin used, pressing time and applied pressure were varied. The prepared boards were characterized by determining the physicomechanical properties such as bending strength, thickness, density, water absorption, swelling thickness and hardness. Differential thermal analysis (TG-DTA) was performed on the adhesives as well as on the prepared fiberboards. SEM photomicrographs of the prepared boards were also taken. Phenol-formaldehyde was the most effective binder because amongst these different adhesives, fiberboard bonded with phenol-formaldehyde had the highest bending strength and least cold water absorption and swelling thickness. Pressing time of (15minutes.), applied pressure of (2000 psi), adhesive concentration of (15%) for urea-formaldehyde (UF) and phenol-formaldehyde (PF) boards and adhesive concentration of (30%) for polystyrene were found to be optimum based on the bending strength, water absorption and swelling thickness. The quality of polystyrene (PS) 30 (%w/w) bonded fiberboards were also as good as urea-formaldehyde and phenol-formaldehyde (15% w/w) bonded fiberboards.

Key words: bagasse, urea-formaldehyde, phenol-formaldehyde, polystyrene polyethylene

1. Assistant Lecturer , Department of Industrial Chemistry, Yadanabon University
2. Professor(Head) (Retired), Department of Industrial Chemistry, University of Yangon

Introduction

A composite material can be defined as a heterogeneous mixture of two or more homogeneous phases which have been bonded together. Provided that the existence of the two phases is not easily distinguished with the naked eye, the resulting composite can itself be regarded as a homogeneous material. Such materials are familiar: many natural materials are composites, such as wood; so are automobile tires, glass-fiber-reinforced plastics (GRP), the cemented carbides used as cutting tools, and paper, a composite consisting of cellulose fibers (sometimes with a filler, often clay). Paper is essentially a mat of fibers, with interfiber bonding being provided by hydrogen bonds where the fibers touch one another. (Anthony and Kelly, 1989). Composites are more versatile than metals and can be tailored to meet performance needs and complex design requirements.

Bagasse, a waste of sugar cane processing, is now considered to be the most promising lignocelluloses raw materials. Large quantities of this waste are left unused or burnt in developing countries. Its fiber length fulfils the requirements for the manufacture of boards, pulp and paper. Three types of board can be produced from bagasse fibers for use in construction: soft board, hardboard and particle/fiberboard. The technology for the production of board from bagasse would utilize the available adhesives like urea formaldehyde and phenolic resins.

In recent years, not only waste wood particles and flakes are utilized in making boards but also other lignocelluloses materials like rice husk, bagasse, cotton stalks etc. are also used as basic raw materials for making panel boards. On account of advancement of resin technology, a variety of boards with different types of raw materials mentioned above are available in the commercial market, bonded with different kinds of resins which have wide range of applications. Nowadays, different types of residential, commercial and industrial buildings are required for the development of Myanmar.

Materials and Methods

Collection and Preparation of Bagasse Sample

Non-wood plant fiber, Bagasse (sugarcane residue) was collected from Pyinmanar Sugar Mill, Mandalay Region under Ministry of Industry (1). Raw samples were cut by cutting machine and ground by Henschel

mixer for about five minutes. They were screened and dried in an oven at 70 ± 5 ºC till the moisture content of 15% (dry basis) was obtained.

Preparation of Fiberboards from Bagasse with Different Adhesives

Raw material (Bagasse) 120g was mixed with adhesive in Henschel mixer for 10 minutes. The mixture was then laid in a mold. Care must be taken to get uniform surface layer in pre-press section. Later, this mat was carefully transferred to the hydraulic hot press machine.

The hot pressing was performed at 150°C. The boards were cooled at room temperature for about five minutes and then the edges and both sides of the boards were trimmed and sanded. Table (1) illustrates the variations of parameters used in the preparation of fiberboards.

Table (1) Parameters Used in Preparation of Organic-bonded Bagasse Fiberboards

Parameters	**Value**
Particle size (mesh size)	(-10+20)
Moisture (%), w/w	≤10%
Length (cm)	15.24
Width (cm)	2.54
Thickness (cm)	0.5 - 0.9
Application method	Hot pressing
Pressing temperature (°C)	150
Pressing time (min.)	10,15,20
Applied pressure (psi)	1000, 2000, 3000
Adhesive concentration (%), w/w	5, 10, 15, 20, 25, 30

Determination of Bending Strength of Fiberboards

The boards were cut into (14cm x 2.54cm) pieces and bending strength of individual fiberboard was measured by Electro-hydraulic

Tensile Tester. (Dziurka, 2003). At least five references were measured for all the samples. Two references were taken from one and three references were taken from another of the same ingredient of composite boards.

Determination of Thickness of Fiberboards

The boards were cut into (14cm x 2.54cm) pieces and thickness of individual composite boards were measured by Vernier caliper in at least four points of each bundle.

Determination of Water Absorption of Fiberboards

The boards to be tested were cut into (2.54cm x 2.54cm) in size and weighed. Then the sample boards were placed in a container and immersed in distilled water for 24 hours. The swollen pieces were wiped with filter paper to remove water on the surface and then weighed. Five replicated specimens were tested from individual composite boards and the results were presented as average of the tested specimens. The same experiments were conducted in boiling water but the immersion time of 2 hours was employed.

Determination of Swelling Thickness of Fiberboards

The boards to be tested were cut into (2.54cm x 2.54cm) in size and placed in a desiccator. These pieces were immersed in distilled water for 24 hours. The wet swollen pieces were wiped with filter paper to remove water on the surface and then the thickness was measured with Vernier caliper. At least five references of individual composite boards were tested and average value was taken as the swelling thickness percentage. The same experiments were also conducted in boiling water but an immersion time of 2 hours was employed.

Determination of Density of Fiberboards

The boards to be tested were cut into (2.54cm x 2.54cm) in size. The length, width and thickness of each test piece was measured to an accuracy of $\pm$ 0.01cm. The weight in grams of each test piece was determined to an accuracy of $\pm$ 0.01g.

Determination of Hardness of Fiberboards

The fiberboards were cut into (1.7cm x 1.7cm) pieces. The surfaces of the boards were trimmed and sanded to get smooth surface. The hardness of the boards were measured by Wallace Micro Tester (DIN-Normen 1987).

Results and Discussion

A fixed quantity of bagasse was bonded with a fixed amount of adhesive at a constant temperature, at a fixed pressing time and pressure. Only the particle size was varied from 10 mesh to 30 mesh size. It can be noted from Tables (2 to 5) that as the particle size of bagasse became smaller, the density and thickness of fiberboards increased. Cold Water Absorption (CWA), Swelling Thickness (ST) and bending strength of UF bonded and PF bonded fiberboards decreased with decrease in particle size whereas a reverse phenomenon was noted in CWA, Boiling Water Absorption (BWA) and ST of Polystyrene (PS) and Polyethylene (PE) bonded boards. It can be seen from Figure(1) that PF was the most effective binder because amongst these different adhesives, the fiberboards bonded with PF had the highest bending strength and least CWA and ST.

The pressing time was also varied from 10 minutes to 20minutes. It can be noted from Table (6-9) that PF and PS bonded boards pressed for 15minutes had the least CWA, ST and highest bending strength. A pressing time of 15minutes also gave the least BWA and ST (2hours) and highest bending strength for UF bonded boards and least BWA for PS bonded boards. For PE, similar results were noted at a pressing time of 20 minutes. It can be seen from Figure (2), PF was the most effective binder because amongst these different adhesives, fiberboard bonded with PF had the highest bending strength and least CWA and ST. The pressure was also varied from 1000 to 3000 psi. It can be noted from Tables (10 to13) that with the exception of BWA (2 hours) for PF bonded board, increasing the pressure from 2000 to 3000 psi did not result significant reduction in CWA (24 hours), ST(24 hours), ST(2 hours) for UF and PF bonded boards. Slight changes in bending strength were also noted. It can be seen from Figure (3). For PS bonded boards, increasing the pressure from 2000 to 3000 psi resulted in a marked increase in bending strength whereas, CWA (24 hours) and ST (24 hours) increased slightly, ST (2hours) decreased slightly but BWA (2 hours) decreased sharply. But for PE, pressing at 3000 psi gave the lowest CWA, ST and highest bending strength. With the exception of PE

bonded board, a pressure of 2000 psi was found to be favorable for fiberboard production.

Table (2) Effect of Particle Size of Bagasse on Properties of Fiberboards Bonded with Urea-formaldehyde Resin

Characteristics	**Particle size of bagasse (Mesh size, Tyler screens)**		
	10	**20**	**30**
Thickness (cm)	0.6	0.62	0.65
Density (g/cm^{-3})	0.88	0.96	1.02
CWA (24hr.) (%w/w)	53.5	49.8	48.7
ST(24hr.) (%)	23.64	22.49	21.67
BWA(2hr.) (%w/w)	72.29	68.9	67.5
ST(2hr.) (%)	46.48	41.49	40.01
Bending strength (psi)	3140	2998	2840
Hardness (Shore D)	90	92	92

Table (3) Effect of Particle Size of Bagasse on Properties of Fiberboards Bonded with Phenol- formaldehyde Resin

Characteristics	**Particle size of bagasse (Mesh size, Tyler screens)**		
	10	**20**	**30**
Thickness (cm)	0.595	0.61	0.62
Density (g/cm^{-3})	0.99	0.97	1.01
CWA (24hr.) (%w/w)	36.1	23.35	20.12
ST(24hr.) (%)	25.35	18.99	17.87
BWA(2hr.) (%w/w)	53.6	48.91	47.81
ST(2hr.) (%)	39.9	29.82	28.72
Bending strength (psi)	3512	3412	3301
Hardness (Shore-D)	95	97	98

Table (4) Effect of Particle Size of Bagasse on Properties of Fiberboards Bonded with Polystyrene Powder

Characteristics	**Particle size of bagasse (Mesh size, Tyler screens)**		
	10	**20**	**30**
Thickness (cm)	0.68	0.71	0.72
Density (g/cm^3)	0.87	0.89	0.92
CWA (24hr.) (%w/w)	35.2	47.2	50.1
ST(24hr.) (%)	30.9	32.6	33.5
BWA(2hr.) (%w/w)	80.3	85.5	89.4
ST(2hr.) (%)	50.1	53.2	60.4
Bending strength (psi)	2852	2672	2190
Hardness (Shore-D)	80	82	82

Table (5) Effect of Particle Size of Bagasse on Properties Fiberboards Bonded with Polyethylene Powder

Characteristics	**Particle size of bagasse (Mesh size, Tyler screens)**		
	10	**20**	**30**
Thickness (cm)	0.70	0.83	0.88
Density (g/cm^3)	0.88	0.89	0.97
CWA (24hr.) (%w/w)	77.5	80.21	83.43
ST(24hr.) (%)	43.1	49.91	52.65
BWA(2hr.) (%w/w)	91.3	95.62	98.23
ST(2hr.) (%)	68.99	69.82	71.12
Bending strength (psi)	1064	1047	1033
Hardness (Shore-D)	68	69	70

Table (6) Effect of Pressing Time on Properties of Fiberboards Bonded with Urea formaldehyde Resin

Characteristics	Time (minute)		
	10	**15**	**20**
Thickness (cm)	0.58	0.60	0.62
Density (g/cm^{-3})	0.9110	0.7527	0.9364
CWA (24hr.) (%w/w)	46.84	44.11	39.66
ST(24hr.) (%)	21.73	19.64	17.68
BWA(2hr.) (%w/w)	78.96	60.42	69.20
ST(2hr.) (%)	91.17	45.00	61.68
Bending Strength (psi)	3158	3520	3139

Table (7) Effect of Pressing Time on Properties of Fiberboards Bonded with Phenol-formaldehyde Resin

Characteristics	Time (minute)		
	10	**15**	**20**
Thickness (cm)	0.60	0.70	0.56
Density (g/cm^{-3})	0.8836	0.8082	0.9943
CWA (24hr.) (%w/w)	20.76	10.84	59.19
ST(24hr.) (%)	16.78	12.35	13.43
BWA(2hr.) (%w/w)	45.99	40.11	39.89
ST(2hr.) (%)	22.27	16.93	18.41
Bending strength (psi)	3523	4099	3512
Hardness (Shore-D)	96	98	97

Table (8) Effect of Pressing Time on Properties of Fiberboards Bonded with Polystyrene Powder

Characteristics	Time (minute)		
	10	**15**	**20**
Thickness (cm)	0.42	0.79	0.49
Density (g/cm^{-3})	0.9256	0.6378	1.0341
CWA (24hr.) (%w/w)	27.19	18.28	23.11
ST(24hr.) (%)	18.80	8.99	13.96
BWA(2hr.) (%w/w)	30.28	29.11	35.50
ST(2hr.) (%)	19.78	11.16	13.95
Bending strength (psi)	2672	3150	2832
Hardness (Shore-D)	81	85	85

Table (9) Effect of Pressing Time on Properties of Fiberboards Bonded with Polyethylene Powder

Characteristics	Time (minute)		
	10	**15**	**20**
Thickness (cm)	0.58	0.88	0.51
Density (g/cm^{-3})	0.9393	0.6799	0.9581
CWA (24hr.) (%w/w)	48.45	57.50	36.71
ST(24hr.) (%)	31.49	33.10	26.95
BWA(2hr.) (%w/w)	69.03	77.52	67.88
ST(2hr.) (%)	35.94	42.10	32.98
Bending strength (psi)	1564	2351	2577
Hardness (Shore-D)	80	82	82

Table (10) Effect of Applied Pressure on Properties of Fiberboards Bonded with Urea-formaldehyde Resin

Characteristics	**Pressure (psi)**		
	1000	**2000**	**3000**
Thickness (cm)	0.91	0.83	0.61
Density (g/cm^{-3})	0.7570	0.8018	0.8823
CWA (24hr.) (%w/w)	35.20	24.51	24.46
ST(24hr.) (%)	22.79	16.91	14.43
BWA(2hr.) (%w/w)	59.05	56.42	56.13
ST(2hr.) (%)	48.33	39.01	32.83
Bending strength (psi)	1984	3579	3561
Hardness (Shore-D)	92	93	94

Table (11) Effect of Applied Pressure on Properties of Fiberboards Bonded with Phenol-formaldehyde Resin

Characteristics	**Pressure (psi)**		
	1000	**2000**	**3000**
Thickness (cm)	0.66	0.59	0.58
Density (g/cm^{3})	0.8636	0.8648	0.9910
CWA (24hr.) (%w/w)	20.98	10.74	10.69
ST(24hr.) (%)	11.02	7.43	7.28
BWA(2hr.) (%w/w)	54.82	42.01	26.19
ST(2hr.) (%)	28.16	15.54	14.89
Bending strength (psi)	2898	3636	3650
Hardness (Shore-D)	89	98	99

Table (12) Effect of Applied Pressure on Properties of Fiberboards Bonded with Polystyrene Powder

Characteristics	**Pressure (psi)**		
	1000	**2000**	**3000**
Thickness (cm)	0.71	0.68	0.57
Density (g/cm^{-3})	0.7570	0.8018	0.8823
CWA (24hr.) (%w/w)	21.305	16.19	17.87
ST(24hr.) (%)	9.85	8.32	9.11
BWA(2hr.) (%w/w)	43.40	39.88	28.26
ST(2hr.) (%)	20.63	18.99	16.76
Bending strength (psi)	2026	3159	3626
Hardness (Shore-D)	80	85	87

Table (13) Effect of Applied Pressure on Properties of Fiberboards Bonded with Polyethylene Powder

Characteristics	**Pressure (psi)**		
	1000	**2000**	**3000**
Thickness (cm)	0.79	0.72	0.53
Density (g/cm^{-3})	0.6852	0.7780	0.9314
CWA (24hr.) (%w/w)	25.19	23.88	19.34
ST(24hr.) (%)	16.89	12.13	9.78
BWA(2hr.) (%w/w)	45.59	43.39	29.87
ST(2hr.) (%)	23.11	21.28	9.67
Bending strength (psi)	1850	2119	2675
Hardness (Shore-D)	70	82	83

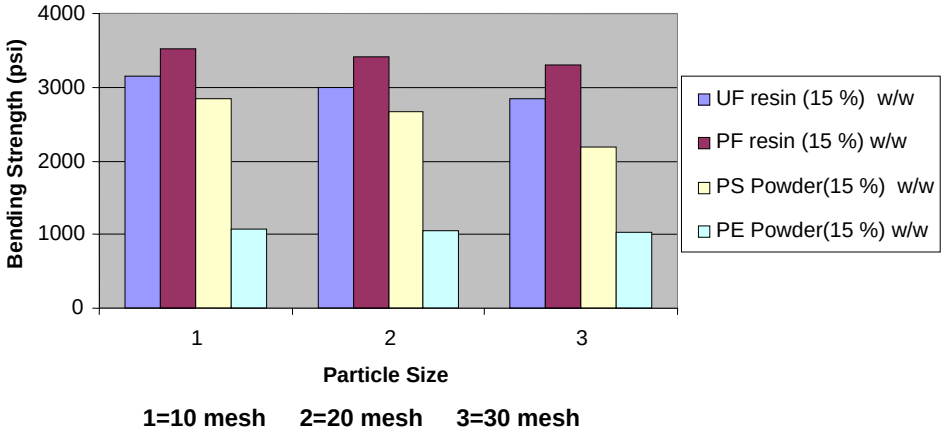

Figure (1) Effect of Particle Size on Bending Strength of Bagasse Fiberboard

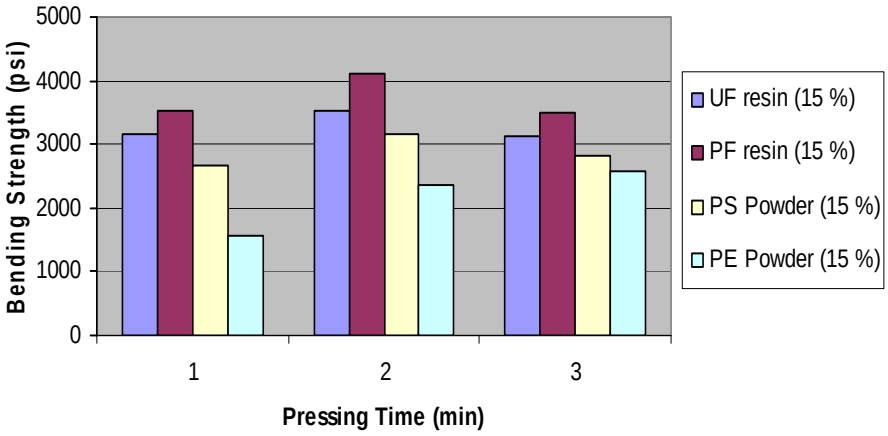

Figure (2) Effect of Pressing Time on Bending Strength of Bagasse Fiberboard

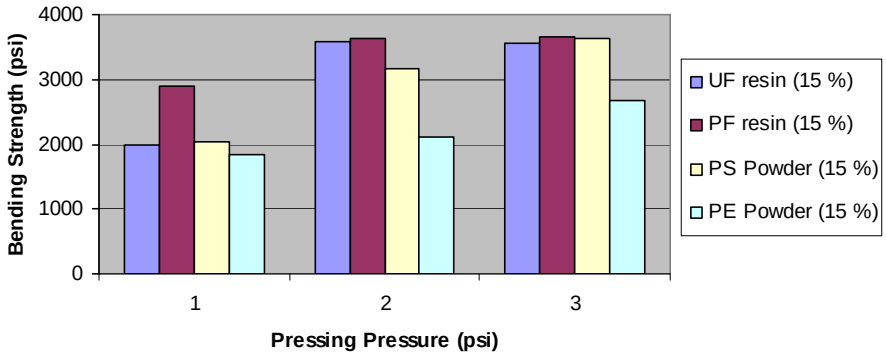

Figure (3) Effect of Applied Pressure on Bending Strength of Bagasse Fiberboard

Table (14) Thermal Analysis Data of Composite Boards

Sample	TG		DTA		Remark
	Break in temp	Weight loss(%)	Peak in temp	Nature of peak	
Bagasse and PF Fiberboard (BPF)	50-200	9.7	59.90	Endothermic	-loss in weight due to dehydration on residual water
	200-400	23.9	365.25	Exothermic	-due to combustion or decomposition
					-residual weight is 86.9%
Bagasse and UF Fiberboard (BUF)	50-250	24.3	121.2	Endothermic	-loss in weight due to dehydration on residual water
	250-400	69.8	224.93	Endothermic	-loss in weight due to combustion or decomposition
			301.17	Endothermic	-residual weight is 59.96%
Bagasse and Polystyrene					-loss in weight due to evaporation of

Sample	TG		DTA		Remark
	Break in temp	Weight loss(%)	Peak in temp	Nature of peak	
Fiberboard (BPS)	50-100	1.7	101.25	Endothermic	moisture
	400-500	97.2	377.04	Exothermic	-loss in weight due to combustion -residual weight is 51.29%
Bagasse and Polyethylene Fiberboard (BPE)	50-100	0.6	64.16	Endothermic	-loss in weight due to evaporation of moisture
	100-300	12.2	486.24	Exothermic	
	300-700	0.3	723.24	Exothermic	-loss in weight due to combustion -residual weight is 38.11%

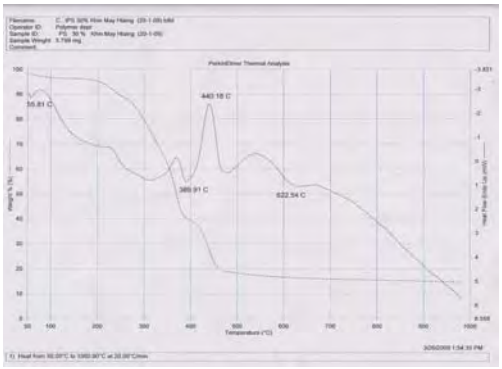

Figure(4)TG- DTA Thermogram of BPS Fiberboards

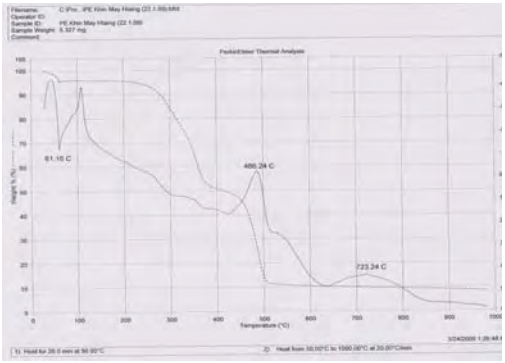

Figure (5) TG- DTA Thermogram of BPE Fiberboards

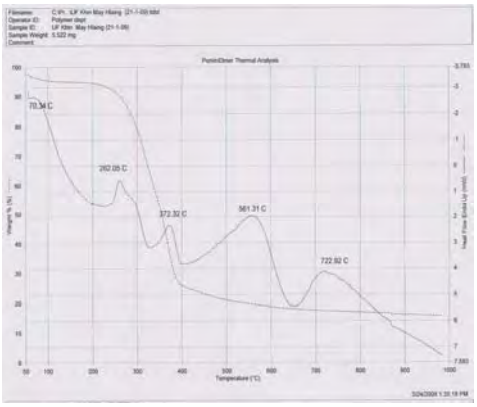

Figure (6) TG- DTA Thermogram of BUF Fiberboards

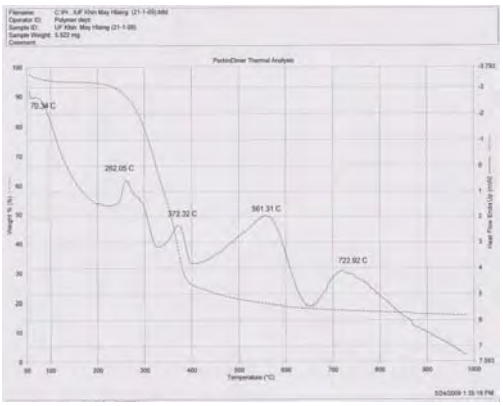

Figure (7) TG- DTA Thermogram of BPF Fiberboards

Study on Surface Morphology of Composite Boards

Scanning electron microscopic analysis examined the surface morphology of composite boards. The removal of surface impurities on plant fibers were advantageous of fiber, adhesive and binder as it facilitates both mechanical interlocking and the bonding reaction due to the exposure of chemicals used in treatment. SEM photomicrographs of BPF, BUF, BPS and BPE composite boards are shown in Figures (8-11).

Modification of the fibers by chemical treatment is conducted to improve compatibility. These chemical reactions modified the properties of the fiber and one of the roles of the cellulose fibers in composite is to give stiffness and strength to the polymer matrix.(Wang, B, 2004)

The scanning electron micrographs of the BUF, BPF, BPS and BPE fiberboards show that these boards are not uniform in the surface fracture. Poor compatibility of interfacial adhesion between bagasse fibers and organic binders was observed whereas good compatibility between cement and bagasse fiber was also noted.

When manufacturing the composite materials, compatibility of fibers and binders are important. More compatibility between fibers and binders can enhance the modulus of rupture.

Figure (8) SEM Photomicrograph of BPF Fiberboard

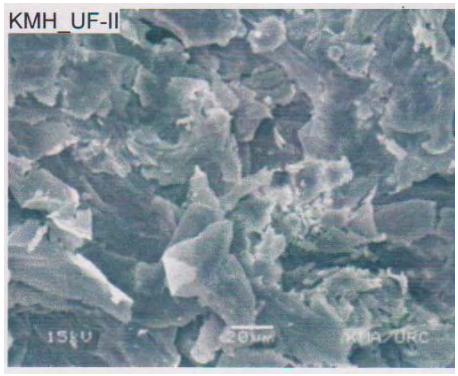

Figure (9) SEM Photomicrograph of BUF Fiberboard

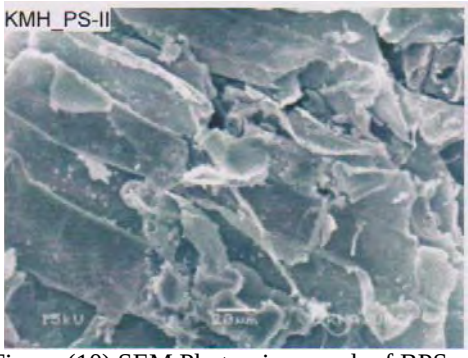

Figure (10) SEM Photomicrograph of BPS Fiberboard

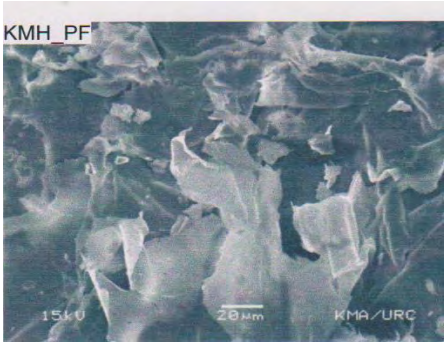

Figure (11) SEM Photomicrograph of BPS Fiberboard

Figure (12) Photographs of Tissue Box and Pen Holder Made from Bagasse Based Fiberboards

Figure (13) Photographs of Tray and CD Holder

Conclusion

Fiberboards were prepared from bagasse with different proportions of different adhesives (PF, UF, PS, PE**)** under various conditions. Four types of composite fiberboards such as BPF, BUF, BPS, and BPE bagasse cement board (BCB) had been fabricated. All these boards were characterized by their physicomechanical properties.

From the experimental results, pressing time (15min.), applied pressure of (2000 psi), adhesive concentration of (15%) for UF and PF boards and adhesive concentration of (30%) for PS were found to be optimum based on the bending strength, water absorption and swelling thickness.

The results of TG-DTA and SEM of composite fiberboards were also investigated. On the basis of residual weight, it can be concluded that BPF composite boards have more thermal stability than BUF, BPS, BPE composite boards because it had the highest residual weight.

The scanning electron micrographs of the BUF, BPF, BPS and BPE fiberboards show that these boards are not uniform in the surface fracture. Poor compatibility of interfacial adhesion between bagasse fibers and organic binders was observed whereas good compatibility between cement and bagasse fiber was also noted.

It is duly claimed that the following are my own contributions which is not found anywhere in the current literature. The quality of PS (30 %w/w) bonded fiberboards are as good as UF and PF (15% w/w) bonded fiberboards.

Since PS used in this work was available as waste material, it seems economical to use PS as adhesive in place of UF and PF. The qualities of fiberboard bonded with PE adhesive are found to be inferior in quality.

Acknowledgements

We would like to express our gratitude to Dr Khin Maung Oo, Rector, and Dr Si Si Hla Buu, Pro-Rector,Yadanabon University for their permission to publish the manuscript in the research journal and Dr Yi Yi Myint, Professor of Industrial Chemistry Department, Yadanabon University for reviewing the manuscript. Our Warmest thanks go to all the persons for their kind support in carrying out this research and editing this article.

References

Holiday, L., (1966), "Composite Materials," Elsevier Publishing Company, Amsterdam, London, New York.

Holister, GS., (1977), "Developments in Composite Materials," Applied Science Publishers, Ltd London.

Hurd, J., (1959), "Adhesives Guide," British Scientific Instrument Research Association, B.S.I.R.A Research, Report, London, 37, 39.

Ismail, H., Rosnah, N., and Rozman, H.D., (1997), "Curing Characteristics and Mechanical Properties of Short Oil Palm Fiber Reinforced Rubber Composites," Polymer, 38.

Jayne, B.A., (1972), "Theory and Design of Wood and Fiber Composite Materials," New York, Syracuse University Press.

John, A.Y., (1996), "Agricultural Fibres for Use in Building Components," Forest Products Laboratory and the Forest Product Society, United States.

Joseph, K., Mattoso, L.H.C., Toledo, R.D., Thomas, S., Carvalho, L.H., Pothen, L., Kala, S., and James, B., (2000), "Natural Fiber" Reinforced Thermoplastic Composites," San Carlos Brazil.

Joseph, K., Thomas, S. and Pavithran, C., (1995), "Composite Science Technology," Brazil, 52, 99.

Kelly, A., (1989), "Concise Encyclopedia of Composite Materials," Pergamon Press, New York.

Websites

1. http://www.tidco.com/tidodocs/tn/opportunities/poly20% viny120%Alchol.doc
2. http://www.fpl.fs.fed.us/documents,pdf1997/Young97a.pdf
3. http://www.dcchem.co.kr/english/products/p-petr/p-petr8-html
4. http://www.4.ipdl.ncipi.go.jp/Tokujitu/ticoitentdben.IpdI?
   NOOOO=21&NO400=image
5. http://www.jpdl.inpit.go.jp/homepg.e.ipdl
6. http://www.en.wikilib.com/wiki/gypsum
7. http://www.en.wikilib.com/wiki/plaster
8. http://www.cheque.uq.edu.au/ugrad/thesis/2002/pdf/Thesis-Dwin-pdf
9. http://www.competition.commission.org.uk/rep-pub/reports/1970-1975/futext/074co2.pdf.

Effectiveness of Design of Solar Dryers on Dehydration of Vegetables (Tomato, Green Onion Leaves)

Tin Lin Maung[1] and Yee Yee Win[2]

Abstract

Based on preliminary investigations under controlled conditions of drying experiments, solar tunnel dryer and solar cabinet dryer with turbo-ventilator were designed and constructed to dry tomato and green onion leaves. Solar tunnel dryer (STD) design uses direct sunlight and has low resistance to airflow. STD is weather protected food dehydration tunnel that can dry food economically and hygienically. Solar cabinet dryer with turbo-ventilator (SCD) is an innovative design with natural draught induced with turbo-ventilator. Turbo-ventilator runs on external wind and creates necessary draught and maintains good airflow through the solar dryer giving excellent performance. As the turbo-ventilator works on outside wind only, no power is required and unit is truly a renewable energy gadget. This paper describes the design considerations followed and presents the results of calculations of design parameters. A minimum of 6 ft^2 (0.557m^2) solar collector area is required to dry a batch of 2-5 kg sliced vegetables in 6-10 hours (~two days drying period). The average initial and final moisture content considered were ~95% and ~10% wet basis, respectively. The average ambient conditions are 35ºC air temperature and 56% relative humidity. The weather conditions considered are of Southern Yangon Region, Myanmar. Tomato and green onion leaves were chosen systematically prepared and dehydrated. Their characteristics such as pH, acidity, moisture content, color, ash content, fibre content, sugar content and rehydration ratio were determined.

Introduction

Sun drying is still the most common method used to preserve agricultural products in most tropical and subtropical countries. However, being unprotected from rain, wind-borne dirt and dust, infestation by insects, rodents and other animal, products may be seriously degraded to the extent that sometimes become inedible and the resulted loss of food quality in the dried products may have adverse economic effects on domestics and international markets. Some of the problems associated with open-air sun drying can be solved through the use of a solar dryer which comprises of collector, a drying chamber and sometimes a chimeny. The conditions in tropical countries make the use of solar energy for drying food practically

1. Assistant Lecturer, Dr., Department of Industrial Chemistry, East Yangon University.
2. Professor (Head), Dr., Department of Industrial Chemistry, East Yangon University.

attractive and environmentally sound. (Mulhlbauer, W., J. Mullere, and A. Esper, 1996)

Solar dryers have the principal advantage of using solar energy--a free, available, and limitless energy source that is also non- polluting. Solar dryers use the energy of the sun to heat the air that flows over the food in the dryer. As air is heated, its relative humidity decreases and it is able to hold more moisture. Warm, dry air flowing through the dryer carries away the moisture that evaporates from the surfaces of the food.

Solar dryers can be classified based upon the exposure of the crop to direct or indirect solar radiation, or the method of air flow through the dryer which may be by natural or forced convection. Natural convection solar dryer has low buoyancy induced air flow. Forced convection solar dryer have increased air flow induced with fan. Solar cabinet dryer with turbo-ventilator is the indirect forced convection solar dryer, whereas solar tunnel dryer is the direct natural convection solar dryer. (Bala B.K., 2009)

In this research work, the chosen fruits and vegetables for dehydration are tomato and green onion leaves. Dehydrated leaves in the form of flour, powder, flakes, and granulated are used in cookery as seasonings, condiments and also ingredient of instant- noodles.

Materials and Methods

Design of Solar Dryers

The two types of solar dryers constructed are solar tunnel dryer and solar cabinet dryer with turbo-ventilator.

Solar Tunnel Dryer

The dryer dimension is 3ft wide x 6ft (0.91m x 1.82m) long and is constructed with materials readily available in Southern Yangon Area. The frame consists of 3 ft x 6ft (0.91m x 1.82m) plywood sheet and two 1 x 4in (0.0254m x 0.1016m) side boards (Figures 1, and 2). Hoops made of 1in (0.0254m) bamboo sticks support a clear polyethylene film cover. The peak height of polyethylene cover is 1ft (0.3048m) above the drying tunnel. The bottom of the dryer is insulated with ⅓in (0.85cm) foam insulation board. The entire solar dryer frame is supported on a bunch. Drying trays, 3ft wide x 4ft (0.91m x 1.22m) long, have knitted polyethylene shade cloth attached to the bottom of the ¾ x 1½in (1.905cm x 3.81cm) wood frames.

Air ducts convey heated air from the 6 ft^2 (0.557m^2) solar collector to below the drying trays, allowing heated air to rise through the bottom of the polyethylene shade cloth.

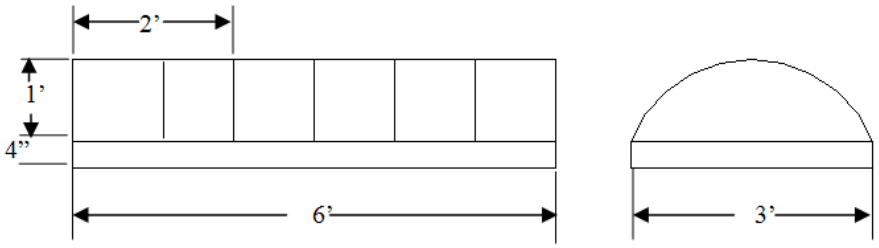

Figure (1) Views of Solar Tunnel Dryer

Fig (2) Solar Tunnel Dryer

Solar Cabinet Dryer with Turbo-ventilator

The solar cabinet dryer with turbo-ventilator consists of drying cabinet, solar collector and turbo-ventilator. 26in wide x 41.5in long (0.6604m x 1.0541m) corrugated galvanized sheet, painted black is fitted to the bottom of the drying chamber and tilted at 30 º. Galvanized sheet was covered with 26in wide x 47.5in long (0.6604m x 1.2065m) transparent glass plate. There are three trays in the drying chamber. 13.5in wide x 26in length x 2in height (0.3429m x 0.6604m x 0.0508m) trays are made of mosquito wire net. The height below the trays is 45in (1.143m). The top of the trays are covered with turbo-ventilator made of iron sheet.

The black colour of the corrugated galvanized sheet absorbs the sun rays and heats the air above. The warm air rises, flows through the drying

cabinet and leaves the drying chamber through the top turbo-ventilator. Cool environment air is sucked off through the bottom opening. Turbo-ventilator works on outside wind and exhausts air from drying cabinet inducing draught. The solar dryer only works with direct solar radiation and works best during dry periods when there is little humidity in the air.

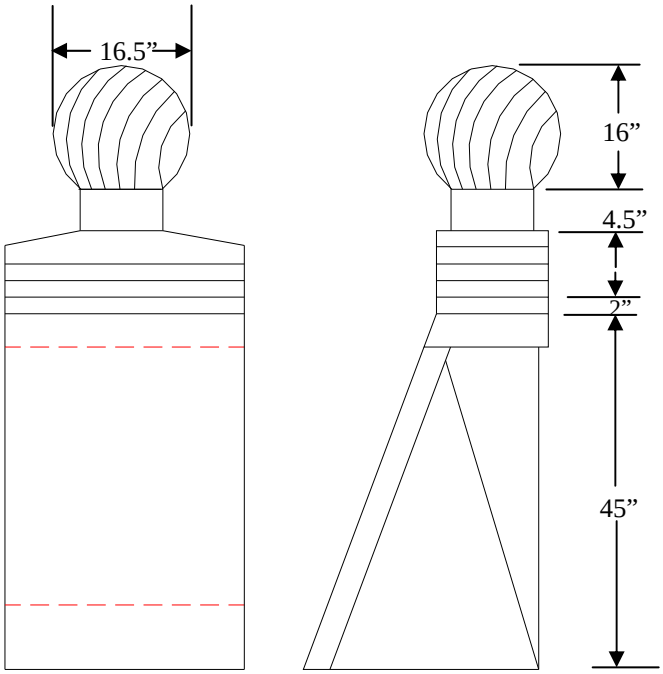

Fig (3) Views of the Solar Cabinet Dryer with Turbo-ventilator

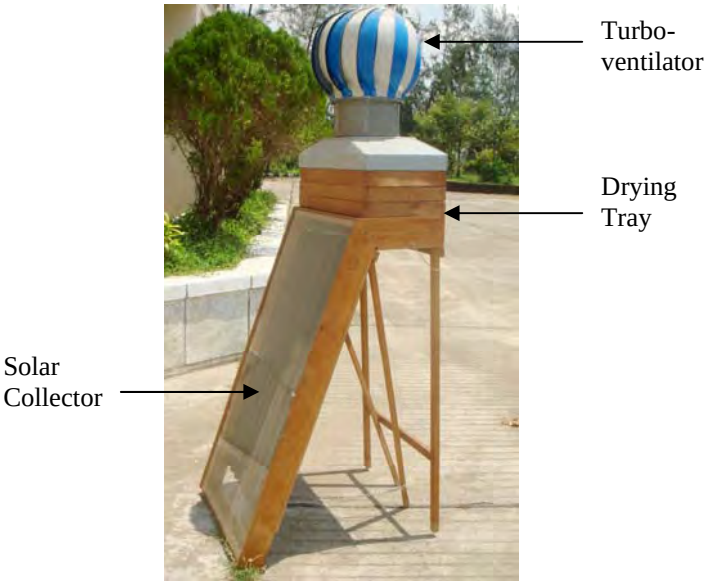

Fig (4) Solar Cabinet Dryer with Turbo-ventilator

Table (1) Design Conditions and Assumptions of Solar Tunnel Dryer for Tomato and Green Onion Leaves

Conditions	**Tomato**	**Green Onion Leaves**
Location	EYU Campus	EYU Campus
Drying Period	November	November
Loading Rate(m_p) (kg)	5	2
Initial Moisture Content (M_i) (%w/w)	95.86	96
Final Moisture Content (M_f) (%w/w)	14	7.94
Ambient Air Temperature (T_{am}) (ºC)	37	37
Ambient Relative Humidity (RH_{am}) (%)	56.7	42.8
Maximum Allowable Temperature (ºC)	48	46
Drying Time (t_d) (hr)	9.5	5.5
Wind Speed (m/s)	0.36	0.36
Thickness (mm)	5	5

Table (2) Design Conditions and Assumptions of Solar Cabinet Dryer with Turbo-ventilator for Tomato and Green Onion Leaves

Conditions	Tomato	Green Onion Leaves
Location	EYU Campus	EYU Campus
Drying Period	November	November
Loading Rate(m_p) (kg)	3	1
Initial Moisture Content (M_i) (%w/w)	95.86	96
Final Moisture Content (M_f) (%w/w)	12.5	10
Ambient Air Temperature (T_{am}) (^oC)	33	37
Ambient Relative Humidity (RH_{am}) (%)	42.3	42.8
Maximum Allowable Temperature (^oC)	45	46
Drying Time (t_d) (hr)	10	6
Wind Speed (m/s)	0.36	0.36
Thickness (mm)	5	5

Table (3) Values of Design Parameters for Solar Tunnel Dryer for Tomato and Green Onion Leaves

Parameters	Tomato	Green Onion Leaves
Initial Humidity Ratio ,w_i (kg H_2O/kg dry air)	0.015	0.018
Initial Enthalpy, h_i (kJ /kg dry air)	73.7	78.33
Equilibrium Relative Humidity ,RH_f (%)	59	46.5
Final Humidity Ratio ,w_f (kg H_2O/kg dry air)	0.024	0.025
Final Enthalpy, h_f (kJ /kg dry air)	86.1	100.9
Mass of Water to be Evaporated, m_w (kg)	4.76	1.91
Average Drying Rate, m_{dr} (kg H_2O/hr)	0.50	0.35
Air Flow Rate, m_a (kg dry air/hr)	71.4	50
Volumetric Air Flow Rate, V_a (m^3/hr)	59.5	41.6
Total Useful Energy, E (MJ)	18.55	8.95
Solar Collector Area, A_c (m^2)	0.557	0.557

Table (4) Values of Design Parameters for Solar Cabinet Dryer with Turbo-ventilator for Tomato and Green Onion Leaves

Parameters	Tomato	Green Onion Leaves
Initial Humidity Ratio ,w_i (kg H_2O/kg dry air)	0.015	0.014
Initial Enthalpy, h_i (kJ /kg dry air)	73.7	66.5
Equilibrium Relative Humidity ,RH_f (%)	56.4	51.4
Final Humidity Ratio ,w_f (kg H_2O/kg dry air)	0.021	0.024
Final Enthalpy, h_f (kJ /kg dry air)	89.1	106.78
Mass of Water to be Evaporated, m_w (kg)	2.86	0.95
Average Drying Rate, m_{dr} (kg H_2O/hr)	0.286	0.158
Air Flow Rate, m_a (kg dry air/hr)	47.7	15.8
Volumetric Air Flow Rate, V_a (m^3/hr)	39.75	13.2
Total Useful Energy, E (MJ)	7.34	1.434
Solar Collector Area, A_c (m^2)	0.696	0.696

Dehydration of Tomato and Green Onion Leaves

Materials

Sound ripe tomato and good, fresh and green onion leaves, from Thanlyin Township, Yangon Division were used. Sodium bicarbonate was purchased from local markets.

Method of Preparation of Dehydrated Tomato

Sound ripe tomatoes were thoroughly washed with water and removed stems and blemishes. These tomatoes were put in a large pot of boiling water for no more than 1 min (30 – 45 seconds is usually enough) and then plunged them into a waiting bowl of ice water. With a gentle tug, the skins were practically slide off the tomatoes. Tomatoes were then sliced into 5mm thickness. Olive oil was used to lightly grease the trays of solar dryer (this will prevent the tomatoes from sticking to the tray). Sliced tomatoes were arranged on the trays and then dried in solar tunnel dryer at 48ºC for (9.5) hr. As another

way, they were dried in solar cabinet dryer with turbo-ventilator at 45ºC for about 10 hours to obtain complete drying.

Method of Preparation of Dehydrated Green Onion Leaves

Mature green onion leaves were trimmed to remove the undesired portions (bulb and roots), followed by washing and cutting into small pieces (5mm). Consequently the weighed pieces were blanched for 15 minutes in steam vapour and then dipped in 1% sodium bicarbonate solution for about 5 minutes at room temperature (adapted from Yi Yi Myint et. al., (2007)**)**. Finally they were then dried in solar tunnel dryer (46ºC) for 5.5 hours and another way, they were dried in solar cabinet dryer with turbo-ventilator at 46ºC for about 6 hours to obtain complete drying.

Methods of Analysis

The essential determinants, showing the quality of each type of dehydrated leaves including, pH, moisture content, ash content, fibre content, colour, acidity, sugar content, total solid content, rehydration ratio and organoleptic properties were investigated.

Results and Discussion

The mean average day temperature in November at Southern Yangon Region, Myanmar is 35ºC and RH is 56 %. From the psychometric chart, the humidity ratio is 0.02kg H_2O/kg dry air. Since Southern Yangon Region is rainy and tropical district and also near the sea, the humidity is high. From the result of preliminary experiments on the crops, the drying temperature range for the two dryers is 40-50ºC and final moisture content of products for storage is ~10% w.b. The corresponding relative humidity is 50-60% (sorption isotherms equation).

Based on the results obtained during the test of dryer, temperature above 40ºC was recorded against the ambient temperature in the drying chamber. For solar tunnel dryer, design parameters and design conditions of tomato and green onion leaves are shown in Tables (1) and (3) whereas design parameters and design conditions of these two vegetables for solar cabinet dryer with turbo-ventilator are shown in Tables (2) and (4).

In solar tunnel dryer, ideal height of polyethylene cover is important and ranges between 8 to 16 inches (20-41cm) above the drying trays. A

solar tunnel dryer with taller peak height has a larger air volume to absorb water vapour but it takes longer to heat the volume of air. The taller peak height also has less wind resistance allowing faster air flow, but the path of airflow is higher above the drying trays with less mixing of moisture-laden air at the drying tray. A shallow peak height has a smaller volume to absorb water vapour but the smaller volume heats up faster and the airflow is directed closer to the drying tray to remove the moisture from the products. So, the peak height of 1ft (30.48cm) is chosen for this solar tunnel dryer. The amount of produce place in the dryer also affects the humidity in the dryer and the drying rate.

The solar cabinet dryer is an indirect dryer by inserting blackened galvanized plate directly beneath the clear glass cover and which removes the exposure of the crop to direct sunlight. If the drying trays are in any way over-packed, air flow is obstructed and crop spoilage occurs. Dryers of this type must be used with care. An exhaust fan such as turbo-ventilator, fitted at the top of the cabinet can facilitate air movement through such dryers. This unit does not require external power because of use of turbo-ventilator.

The characteristics of fresh and dehydrated (tomato and green onion leaves) such as colour, ash content, fibre content, pH, total solid content, sugar content and rehydration ratio can be seen in Tables (5) and (6). In Table (5), colour of the dehydrated tomato using SCD was nearly equal to fresh tomato. With STD, red and yellow color were reduced. Table (6) show that colour of dehydrated green onion leaves using SCD was nearly equal to those using STD. The increase of color intensity after dehydration was reduced in solar tunnel dryer than solar cabinet dryer. This was due to the direct heat and low resistance to air flow in solar tunnel dryer. Other characteristics of dehydrated products were increased because of dehydration. The effect of the type of dryer on the characteristics of dehydrated fruits and vegetables are recorded in Table (7). The results point out that solar cabinet dryer with turbo-ventilator was more favourable for dehydration of fruits and vegetables because indirect and forced convection can retain better characteristics than solar tunnel dryer. As solar tunnel dryer is direct and natural convection dryer, flavour of the products were slightly reduced than with solar cabinet dryer with turbo-ventilator.

Table (5) Characteristics of Fresh and Dehydrated Tomato

Characteristics	Fresh Tomato	Dehydrated Tomato	
		Solar Cabinet Dryer with Turbo-ventilator	Solar Tunnel Dryer
Colour	R 15.5, Y 3.9	R 15.4, Y 3	R 4.3, Y 1.7
Moisture (%)	95.86	12.5	14
Fiber (%)	1.123	-	-
Ash (%)	4.357	12.5	12.4
pH	4.12	4.45	4.57
Sugar Content (%)	4	10	11
Rehydration Ratio	-	9.44	9.32

Table (6) Characteristics of Fresh Green Onion Leaves and Dehydrated Green Onion Leaves

Characteristics	Fresh Onion Leaves	Dehydrated Green Onion Leaves		
		Solar Cabinet Dryer with Turbo-ventilator	Solar Tunnel Dryer	Shift-made Hot –air Dryer*
Colour	Y 60, B9	Y 20.7, B 10.9	Y 20.6, B 12	Y 20.6,B 60,R 2
Moisture (%)	91.68	10	7.94	15.59
Ash (%)	0.7292	11.78	11.67	10.0861
Total Solid Content (%)	7.4	90	92.06	-
Rehydration Ratio	-	9.44	9.32	10.6

* adapted from Yi Yi Myint et. al., (2007)

Table (7) Effect of Dryers on the Characteristics of Tomato and Green Onion Leaves

Vegetables	Dryers	Color	Smell	Shelf life
Tomato	STD	Pale red	Pleasant smell	6 months (browning occur)
	SCD with Turbo-ventilator	red	Pleasant and pungent smell	6 months (browning occur)
Green Onion Leaves	STD	green	Pleasant smell	1 year (do not change)
	SCD with Turbo-ventilator	Green	Pleasant and pungent smell	1 year (do not change)

(i)  (ii) 

Figure (7) Dehydrated Tomato Using (i) Solar Tunnel Dryer (ii) Solar Cabinet Dryer with Turbo-ventilator

(i)  (ii) 

Figure (8) Dehydrated Green Onion Leaves Using (i) Solar Tunnel Dryer (ii) Solar Cabinet Dryer with Turbo-ventilator

Conclusion

Solar dryers are very usable and it will help the community to have nutritious processed food. Solar driers are simple in construction and can be constructed using locally available materials such as glass, wood, galvanized plate, bamboo and plastic, by the local craftsman. Solar cabinet dryer with turbo-ventilator is an indirect, forced-convection solar dryer. Solar tunnel dryer is a direct, natural convection solar dryer.

The quality of the dehydrated products using solar cabinet dryer with turbo-ventilator is superior in color than those using solar tunnel dryer since solar cabinet dryer is indirect and good ventilation. Solar cabinet dryer with turbo-ventilator can be used for many types of fruits and vegetables with good quality in color and flavor. Solar tunnel dryer can also be used for fruits and vegetables whose quality is independent of color and flavor. Based on this research work, the farmers in rural areas can also use simple solar drying technique in their farm to preserve their home-grown vegetables after harvesting and the products can be used in off-season.

Acknowledgements

We would like to express our sincere gratitude to U Kyaw Ye' Tun, Rector, East Yangon University, Dr. Mar Lar Aung, Pro-Rector and Dr. Kyaw Kyaw Khaung, Pro-Rector, East Yangon University, for their permission and the financial support in this research work. We are deeply indebted to Dr. Yee Yee Win, Professor and Head of the Industrial Chemistry Department, East Yangon University, for giving permission to use research facilities in the department. We are grateful to Dr. Than Htaik, Director General (Retired), Department of Cottage Industry and Dr. Yi Yi Myint, Professor, Department of Industrial Chemistry, Yadanarbon Univeristy (Former Associate Professor, Department of Industrial Chemistry, East Yangon University) for their kind help in construction of solar cabinet dryer with turbo-ventilator. Thanks are also extended to the teaching staff, especially, Daw Naw Zar Htwe, Daw Aye Thida, Daw Soe Wai Phyo and Daw Myat Yu Maw, Demonstrators of Industrial Chemistry Department, East Yangon University for their help in carrying out this research.

References

Bala B. K. (2009), Solar Drying of fruits, vegetables, spices, medicinal plants and fish: Developments and Potentials, International Solar Food Processing Conference, 2009.

Ehiem J.C. and etal, (2009) Design and Development of An Industrial Fruit and Vegetable Dryer**,** Research Journal of Applied Sciences, Engineering and Technology 1, Maxwell Scientific Organization.

Mulhlbauer, W., Mullere J., and Esper A., (1996), Sun and Solar Crop Drying, Research and Development.

Yi Yi Myint et. al., (2007), Study on the Dehydration of Green Onions, Chive (Chinese Leek) Leaves and Green Mustard Leaves in Southern Yangon Area, Department of Industrial Chemistry, East Yangon University.

Study on the Preparation of Banana Chips and Banana Powder

Khin Swe Oo[1] and Yee Yee Win[2]

Abstract

In our country, a wide variety of bananas are available. Bananas from Thanlyin Township, Southern Yangon Division were selected for this research.The main objective of this work is to supply wholesome, safe, nutritious and acceptable food to consumers throughout the year. This research work also aims to replace imported products, to earn foreign exchange by exporting finished or semi-finished products, to develop new value-added products and to generate both rural and urban employment. This work involved preparation of banana products such as puree, chips, banana jam and banana powder. The present research placed its emphasis on preparing banana products retaining its natural flavor, aroma and a longer shelf-life. Their characteristics such as pH, acidity, viscosity, fiber content, ash content, color, soluble solids (Brix%), and organoleptic properties were determined. The effect of food additives such as salt, antioxidant and chemical preservatives on the quality of products were studied. The effect of drying time and drying temperature were also investigated in this research work. The results so obtained would in some way be helpful or supplement the local cottage industries.

Introduction

In developing countries, agriculture is the mainstay of the economy. Of the various types of activities that can be termed as agriculturally based, fruit and vegetable processing are among the most important. Among all our foods, fruits are unique in the way that they progress from inedibility to deliciousness. Both established and planned fruit processing projects aim at solving a very clearly identified development problem. This is due to insufficient demand, weak infrastructure, poor transportation and perishable nature of the fruits. In addition, advanced planning is necessary to process a large range of products. In varied weather and temperature conditions, each requires a special set of manufacturing and packaging formulae. Modern applied technique always seeks to improve the quality of better flavor and improved texture of the product. (M.E.Dauthy, 1995)

Fresh fruits are generally used in season, but all the year –round production can be maintained by the use of frozen, canned and dehydrated

1. Assistant Lecturer, Dr., Department of Industrial Chemistry, East Yangon University.
2. Professor(Head), Dr., Department of Industrial Chemistry, East Yangon University

fruits. (F.Aylward, 1999) Dried fruits and vegetables have certain advantages over those preserved by other methods. They are lighter in weight than their corresponding fresh produce and, at the same time, they do not require refrigerated storage. However, if they are kept at high temperatures and have high moisture content they will turn brown after relatively short periods of storage. (Homenauth, Oudho., Dr., 2010) In conclusion, stored dried food is prepared every growing season. Dried food should be used within the next months as the nutritional value slowly drops over time. (David E.Whitfield V., 2000)

Most fresh fruits are high in water content, low in protein and low fat. In these cases, water contents will generally be greater than 70 % and frequently greater than 85 %. Commonly protein content will not be greater than 0.5 %. In addition, fruits are important sources of both digestible and indigestible carbohydrates and are also the main sources of minerals and certain vitamins, especially vitamin A and C. Fruits also contain some free organic acids. Malic and citric acids occur in most of the fruits, but tartaric acid is a prominent constituent of grapes. Oxalic acid, when present, usually combines with calcium to form calcium oxalate. Fruits are good sources of vitamins. Naturally, citrus fruit are excellent sources of vitamin C. Carbohydrates are the main component of fruits and represent more than 90 % of their dry matter. From an energy point of view, daily adult should intake about 500 g carbohydrates per day. (M.E.Dauthy, 1995)

Banana is one of the vegetable fruit that grow well in the tropics. Since then, development of high yield, short-time growth, disease resistant banana varieties by institutions of agriculture have increased the volume of banana at harvest. These bananas are mainly transported to urban areas, where they would be eaten as fruit vegetables. However, unavoidable delay in transport, poor post harvest technology and fluctuating market demand result in overripe and senescence of fruits prior to market delivery. Hence, large amount of banana post- harvest losses serve as impetus to the study on processing and application of mature green bananas with view to diversify utilization of the crop. (Daramola, B. And Osanyinlusi, S.A, 2005)

The main commercial products made from bananas are canned or frozen puree, dried figs, banana powder, flour, flakes, chips (crisps), canned slices and jams. Banana products are used in most food manufacturing industry, for example, purees and powder. Many banana products are now produced on an industrial scale. One of the main problems encountered has

been the susceptibility of banana products to flavor deterioration and discoloration and in the past many products reaching the market have been of poor quality.

The most important agents of food spoilage are microorganisms; others are the reactions due to enzymes in the foods; direct oxidation; the desiccation of moist foods; the absorption of foreign odors and flavors; contamination with injurious chemicals; mechanical damage by animal and insect pests; and causes peculiar to a particular process of preservation, for example, the corrosion of container in canning. A great deal of research has been directed to overcoming these problems, however, good the resultant products are they cannot in flavor and other characteristics with the fresh banana fruit. Indeed, an important constraint on the large-scale development of banana products since the fresh fruit is available throughout the year in most part the world. (M.E.Dauthy, 1995)

Banana is the most important fruit in Myanmar based on production and value. It is grown in almost every State and Division of the country with a total area of 50586 ha and produced 92,486,000 bunches with a yield of 1826 bunches per ha in 2001. The total production increased steadily from 1996-2001. The largest banana-producing area in the country is the Ayeyarwady Region with 20065 ha followed by Sagaing Region with 61223 ha and Bago Division with 4208 ha. (Maung Maung Htwe, 2003)

> Finally, bananas are of great value to people who are on a reducing diet, and anxious to lose weight. They are low in calories, yet high in food value. Bananas contain practically no sodium, hence their suitability for overweight people, as also for dropsical people. These people are unable to utilize the sodium in the foods they eat; the consequence is it accumulates in the tissues causing overweight because of its power of attracting fluids. Thus, it is the liquid retained in the tissues, not the tissues themselves that cause the overweight. (Constance Mellor, M.C.S.P, 1975)

Table (1) Nutritional Value and Composition of Banana

(per 100 g edible portion)

Energy	371 kJ (89 kcal)
Carbohydrates	22.84 g
Sugars	12.23 g
Dietary Fiber	2.6 g
Fat	0.33 g
Protein	1.09 g
Vitamin A equivalent	3 µg (0%)
Thamine (Vitamin B_1)	0.031 mg (2%)
Riboflavin (Vitamin B_2)	0.073 mg (5%)
Niacin (Vitamin B_3)	0.665 mg (4%)
Pantothenic Acid (Vitamin B_5)	0.334 mg (7%)
Vitamin B_6	0.367 mg (28%)
Folate (Vitamin B_9)	20µg (5%)
Vitamin C	8.7 mg (15%)
Calcium	5 mg (1%)
Iron	0.26 mg (2%)
Magnesium	27 mg (7%)
Phosphorous	22 mg (3%)
Potassium	358 mg (5%)
Zinc	0.15 mg (1%)
Moisture	70.1 g
Ash	0.9 g

*From Wikipedia, the Free Encyclopedia

Materials and Methods

Selection and Preparation of Fruit for Banana Processing

In general, to obtain a good quality banana puree, the fruit is picked green artificially under controlled conditions. In addition, the fruit should be fully mature but not overripe. The sugar content must be as high as possibly, otherwise, the final product is liable to be tough and lacking in flavor. In this research, both mature green and ripe bananas were used. After reaching full ripeness, the fruit is washed to remove dirt and spray residues, inspected and any substandard fruit removed. After that, the fruit is peeled by hand using stainless steel knives, although a mechanical peeler for ripe bananas has been developed.

Preparation of Banana Chips

About 100 g of unripe bananas (Thi-hmwe) ***Musa Accuminata* (Colla sub-sp) Burmanica Simmonds (Herbs))** were peeled and sliced to 3mm size. Consequently, about 1.5 % of salt, 0.3 % of sodium metabisulphite, 0.6 % of soda, 0.03 % of food color were weighed and dissolved in 300 ml of water to obtain the osmotic solution. After that, they were immediately immersed in osmotic solution for 1 hour and then drained. The sliced bananas were blanched in boiling water bath at 95°C for 2 minutes. The bananas after blanching were immediately deep fat fried in vegetable oil and hydrogenated oil with 0.01 % butylated hydroxyl toluene (BHT), also called antioxidants, at 180 °C. The fried bananas were then dried on screen with made shift dryer at about 65 °C for 20 minutes. The dried bananas were fried again with the used oil for 3 minutes in order to get better crispness and then dried with made shift dryer. When the banana chips were dried, they were coated with sugar syrup of about 70 °Brix and then dried for 2 hours with made shift dryer. The finished products were packed in airtight plastic bags to prevent them absorbing moisture and losing their crispness.

Preparation of Banana Powder

For the preparation of banana powder, the bananas **(Hpee-gyan-nget-pyaw, *Musa Saba*)** were first washed and then peeled by hand. The peeled bananas were then dipped in 0.05 % sodium metabisulphite and 0.05 % salt solution for 30 minutes in order to prevent browning reaction. After dipping, the cores sin banana pulp were removed and then sliced with

stainless steel knife. The sliced bananas were then transferred to a solar cabinet dryer with turbo ventilator until the final moisture content to 7-10 %. Finally, the dried banana slices were milled in a blender and then screened with 100 mesh size screen. The finished products, packed in moisture proof plastic bags, were found good texture, color and flavor during storage at room temperature.

Figure (1) Banana (Thi-hmwe)

Figure (2) Banana (Hpee-gyan)

Methods of Analysis

Physicochemical characteristics showing the quality of' banana chips and banana powder such as moisture content, ash content, crude fibre content, protein content and acidity were determined by chemical analysis, pH by pH meter, colour by tintometer, and organoleptic properties by sensory tests.

Results and Discussion

Banana Chips

The effect of salt concentration on banana chips was studied and the results are indicated in Table (2). From these resultant values, it was seen that the sample using 1.5% of salt concentration was more suitable due to better color, taste and texture than others. Table (3) shows that the effect of metabisulphite concentration on organoleptic properties and shelf-life of banana chips. From the results of table (3), it was evident that the sample using 0.1% of sodium metabisulphite of storage. The effect of blanching time and temperature on banana chips are shown in Table (4) and Table (5)

respectively. Blanching of fruits and vegetables in hot or boiling water or steam as a pretreatment before drying can reduce the amount of microorganism present on the surface. From these tables, the optimum blanching time and blanching temperature were 2 minutes and 95 °C because of good texture of banana was found. Tables (6) and (7) describe that the effect of frying time and temperature. From these tables, frying time 8 minutes and frying temperature 180°C were the most favorable conditions because the more crispness and attractive color of banana chips were obtained at that condition. The effect of oil ratio on banana chips are described in Table (8). As a result from this table, the optimum ratio of vegeatable and hydrogenated oils was 1:0.2. In Table (9), the results are presented the effect of drying time on moisture liberated of fried banana chips. The characteristics of banana chips are displayed in Table (10).

Banana Powder

As an organoleptic property point of view, the effect of salt concentration on banana powder are presented in Table (11). In this Table, sodium metabisulphite concentration was fixed and salt concentration was varied. The salt concentration of 0.05 % was found to be the most favorable organoleptic properties. The effect of sodium metabisulphite concentration on organoleptic properties of banana powder are described in Table (12). As a results of this table, the optimum sodium metabisulphite concentration of 0.05 % gave the powder with pleasant taste and more attractive color. This optimum sodium metabisulphite concentration fall within the Food and Drug Administration (FDA) acceptable limit. The characteristics and shelf-life of banana powder at optimum conditions are shown in Table (13). Table (14) displays the effect of drying time on moisture liberated of banana powder with solar dryer equipped with Turbo Ventilator. From this table, it is clearly observed that how much moisture liberated during 12 hours drying. Figure (6) shows the drying curve of banana powders at different sodium metabisulphite concentration. From this figure, it is obvious that the curves between 8 to 12 hours become horizontal lines and represent constant rate period of drying.

Table (2) Effect of Salt Concentration on Banana Chips

Banana weight = 100, Antioxidant (wt%) = 0.01

Sample No.	Salt (wt%)	SMBS (wt%)	SB (wt%)	Food Color (wt%)	Organoleptic Properties	
					Flavor	Color
1	1	0.1	0.6	0.03	Slightly Salty	Yellow
*2	1.5	0.1	0.6	0.03	Pleasant Taste	Yellow
3	2	0.1	0.6	0.03	Salty	Yellow

*The most favorable salt concentration

SMBS = Sodium metabisulphite, SB = Sodium bicarbonate

Table (3) Effect of Sodium Metabisulphite Concentration on Banana Chips

Banana weight = 100 g, Antioxidant (wt%) = 0.01

Sample No.	Salt (wt%)	SMBS (wt%)	SB (wt%)	Food Color (wt%)	Organoleptic Properties	Shelf-life (months)
					Color	
1	1.5	0.05	0.6	0.03	Yellow	3
*2	1.5	0.1	0.6	0.03	Yellow	4
3	1.5	0.15	0.6	0.03	Yellow	4

*The most favorable SMBS concentration

SMBS = Sodium metabisulphite, SB = Sodium bicarbonate

Table (4) Effect of Blanching Time on Banana Chips

Banana weight = 100 g

Sample No.	Blanching Temperature (°C)	Blanching Time (min.)	Organoleptic Properties	
			Texture	Color
1	95	1	Slightly Soft	Yellow
*2	95	2	Good Texture	Yellow
3	95	3	Deform	Yellow

*The most favorable blanching time

Table (5) Effect of Blanching Temperature on Banana Chips

Sample No.	Blanching Temperature (°C)	Blanching Time (min.)	Organoleptic Properties	
			Texture	Color
1	85	2	Slightly Soft	Yellow
*2	95	2	Good Texture	Yellow
3	105	2	Deform	Yellow

*The most favorable blanching temperature

Table (6) Effect of Frying Time on Banana Chips

Sample No.	Frying Temperature (°C)	Frying Time (min.)	Organoleptic Properties	
			Crispness	Color
1	180	6	Crisp	Yellow
*2	180	8	More Crisp	Yellow
3	180	10	Hard	Yellow

*The most favorable frying time

Table (7) Effect of Frying Temperature on Banana Chips

Sample No.	Frying Temperature (°C)	Frying Time (min.)	Organoleptic Properties	
			Crispness	Color
1	170	8	Soft	Yellow
*2	180	8	Crisp	Yellow
3	190	8	Hard	Yellow

*The most favorable temperature

Table (8) Effect of Vegetable Oil and Hydrogenated Oil Ratio on **Banana Chips**

Sample No.	Frying Temperature (°C)	Frying Time (min.)	Vegetable Oil and Hydrogenated Oil Ratio	Organoleptic Properties	
				Crispness	Color
1	180	6	1 : 0.1	Crisp	Yellow
*2	180	8	1 : 0.2	More Crisp	Yellow
3	180	10	1 : 0.3	More Crisp	Yellow

*The most favorable oil ratio

Table (9) Effect of Drying Time on Moisture Liberated of Fried Banana Chips

Sample No.	Drying Time (min.)	Moisture Content (%)
1	10	27.8
*2	20	26.6
3	30	18.8

*The most favorable drying time

Table (10) Characteristic and Shelf-life of Banana Chips

Banana Chips wt: (g)	Characteristics of Banana Chips						Shelf-life (months)
	Moisture Content (%)	Acidity (%)	pH	Fiber Content (%)	Fat Content (%)	Ash Content (%)	
100	4	0.004	5.8	20.535	1.377	14.44	7

Ash content was conducted at the Industrial Chemistry Department, University of Yangon.Fat content was measured at the Laboratory of Development Centre for Food Technology (DCFT), Ministry of Industry (I). The others were carried out at the Industrial Chemistry Department, University of East Yangon.

Table (11) Effect of Salt Concentration on Organoleptic Properties of Banana Powder

Sample No.	Food Additives		Organoleptic Properties	
	Salt (wt %)	SMBS (wt %)	Flavour	Colour
*1	0.05	0.05	Pleasant Taste	Yellowish White
2	0.1	0.05	Slightly Salty	Yellowish White
3	0.15	0.05	Salty	Yellowish White

*The most favorable salt concentration , SMBS = Sodium metabisulphite

Table (12) Effect of Sodium Metabisulphite Concentration on Organoleptic Properties of Banana Powder

Sample No.	Food Additives		Organoleptic Properties	
	Salt (wt %)	SMBS (wt %)	Flavour	Colour
*1	0.05	0.05	Pleasant Smell and good Taste	White
2	0.05	0.1	Pleasant Smell and good Taste	Creamy White
3	0.05	0.15	Pleasant Smell and good Taste	Creamy White

*The most favorable sodium metanisulphite concentration.

Note: SMBS = Sodium metabisulphite

Table (13) Characteristics and Shelf-life of Banana Powder

Sample No.	Food Additives		Characteristics of Banana Powder						Shelf-life months
	Salt %wt	SMBS (%wt)	Moisture Content (%)	Ash Content (%)	Protein Content (%)	Solubility (%w/v)	Acidity	pH	
1	0.05	0.05	7-10	2.85	2.2	0.37	0.074	6.5	4

Ash content was conducted at the Industrial Chemistry Department, University of Yangon. Protein (%) was measured at the Laboratory of Development Centre for Food Technology (DCFT), Ministry of Industry (I). The others were carried out at the Industrial Chemistry Department, University of East Yangon.

Table (14) Effect of Drying Time on Moisture Liberated of Banana Powder with Solar Dryer equipped with Turbo Ventilator

Sample No.1	Food Additives		Drying Time (hr)						
	Salt (% w/w)	SMBS (% w/w)	0	2	4	6	8	10	12
* 1	0.05	0.05	71.6	65.4	30.2	11.6	11	10.6	8.2
2	0.05	0.1	68.6	55.6	41.8	15.6	12.2	9.4	9.3
3	0.05	0.15	69.2	59.4	40	34.2	20	10	9.3

*The most favorable drying condition, SMBS = Sodium metabisulphite

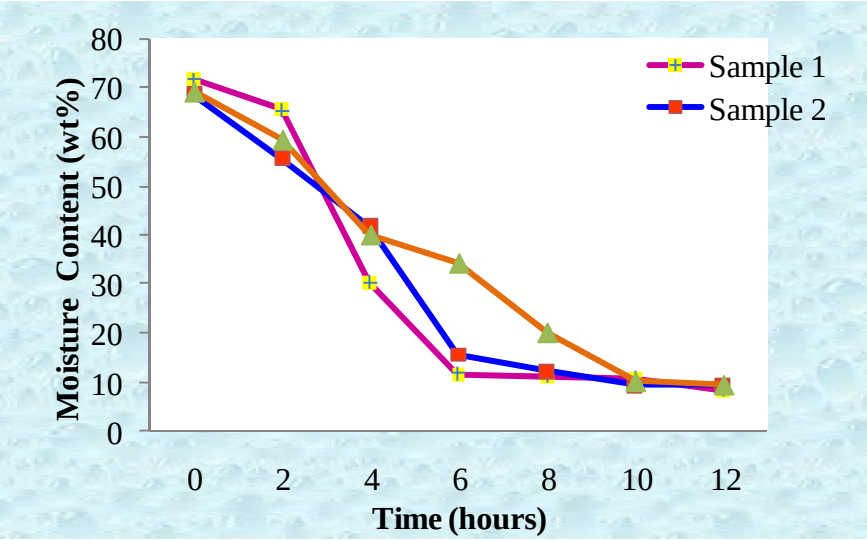

Figure (3) Drying Curve of Banana Powder

Figure (4) Banana Chips

Figure (5) Banana Powder

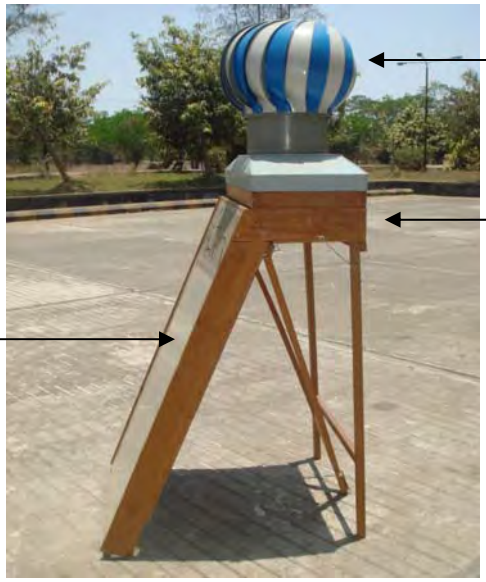

Figure (6) Solar Cabinet Dryer with Turbo-ventilator

Conclusion

In the preparation of banana chips, blanching of banana slices in hot water as a pretreatment before frying and drying can reduce the amount of microorganisms present on the surface, also preserve the natural colour in dried products and protect from oxidative breakdown during processing and storage.In addition, the crispness of banana chips and other organoleptic properties were increased due to the presence of hydrogenated oil in the

frying process. The banana chips must be packed in moisture proof bags to prevent them absorbing moisture and losing their crispness. Drying with solar cabinent turbo-ventilator dryer gave a product of more uniform quality than that dried in the sun. Banana powder is used chiefly in the baking industry for the preparation and filling for cubes and biscuits and is also used for invalid and baby foods.

Acknowledgements

I am thankful to the professors and teachers of Industrial Chemistry Department, East Yangon University for their kind support in carrying out this research wok.

References

Aylward, F., 1999, Food Technology Processing and Laboratory Control, Alliced Scientific Publishers, India.

Constance Mellor, M.C.S.P, 1975, Natural Remedies for Common Ailments.

Daramola, B., Osanyinlusi, S.A., 2005, Production, Characterization and Application of Banana (*Musa* spp) Flour in Whole Maize, Department of Food Science and Technology, Federal Polytechnic, Ekiki State, Nigeria.

Dauthy, M.E., 1995, Fruit and Vegetable Processing, FAO Agricultural Services Bulletin 119, Rome.

David E. Whitfield V., 2000, SOLAR DRYING, Solar Dryer Systems and the Internet: Important resources to improve food preparation, International Conference on Solar Cooking, Kimberly, South Africa.

Homenauth, Oudho., Dr., 2010, Compendium of Process Flow Technology in Fruit and Vegetable Preservation, Agro Processing Manual, Ministry of Agriculture, Georgetown, Guyana.

Hundley H.G and Chit Ko Ko, Trees, Shrubs, Herbs and Principal Climbers etc., Fourth Revised Edition.

Maung Maung Htwe, 2003, Myanmar Agricultural Sector Review and Investment Strategy Formulation Project Horticulture Development in Myanmar, National Consultant, Food and Agriculture Organization of the United Nations, Myanmar.

http://www.ikisan.com/links/ap.banana history.shtml.

http://www.banana.com/links/ap.health benefits of banana.shtml.

Observation on the Yield of Reducing Sugar from Rice for the Preparation of Bioethanol by Acid Hydrolysis

Hay Mar Soe[1] and Soe Soe Than[2]

Abstract

Rice is considered as a source of starch enriched material for the preparation of bioethanol. Conversion of rice into reducing sugar (i.e. fermentable sugar) prior to continuous fermentation process was carried out by acid hydrolysis. Starch hydrolysis such as liquefaction and saccharification of gelatinized rice, was conducted by using hydrochloric acid (HCl) and sulphuric acid (H_2SO_4) with various concentrations (1%, 3%, 6%, 9% and 12% (v/v)), volume of acid (50 ml, 100 ml, 150 ml, 200 ml and 250 ml) and duration of hydrolysis (5 hr, 6 hr, 7 hr, 15 hr and 30 hr). The maximum yield of reducing sugar by HCl and H_2SO_4 hydrolysis resulted at the acid concentration of 6% and 3%, volume of acid of 100ml each and duration of hydrolysis of 15 hr and 7 hr respectively.

Key words: Rice, Acid hydrolysis, liquefaction and saccharification

Introduction

In order to meet carbon reduction for fuelling bioethanol production from starchy materials has already been introduced since last decades. Three kinds of feedstock such as sugar crops, cereal and tuber crops, and cellulosic plants are used for bioethanol production. Because of the reduction of greenhouse gas emission and replacement in ever increasingly expensive petroleum supplies, ethanol is considered as an alternative fuel and used in automobiles as a fuel additive at 10% (Demirbas, 2005).

Rice is one of the starch enriched materials obtained from cereal grains. Starch is the commonest carbohydrate in plants and occurs in the form of granules. It comprises of two components: amylose and amylopectin. Amylose consists of long, unbranched chains of D-glucose units connected by (α-1,4) linkages. Its molecular weight varies from a few thousand to 500,000. Amylopectin is highly branched and has a high molecular weight (up to 1 million). The glycosidic linkages joining successive glucose residues in amylopectin main chains are (α-1,4), but the branch points, occurring in every 24 to 30 residues, connected with the main chains are (α-1,6) linkages (http://en.wikipedia.org/wiki/Starch).

1. MSc Student, Department of Industrial Chemistry, Dagon University
2. Lecturer, Department of Industrial Chemistry, Dagon University

Three stages involve in conversion of starch into sugar: gelatinization, liquefaction, and saccharification. Liquefaction and saccharification are also known as a process of starch hydrolysis and starch hydrolysis is the conversion of polysaccharide starch molecules into monosaccharide fermentable sugars (reducing sugars). It is achieved by acid or enzymatic hydrolysis. The combination of heat and acid or enzyme breaks up the long chain starch molecule, initially converting starch to a simple sugar hydrolysate (maltodextrin) which is next converted to fermentable glucose as the saccharification step. Maltodextrin are intermediate compounds resulting from incomplete hydrolysis of starch. On the one hand, the product of complete hydrolysis of starch is glucose (reducing sugar) (Marchal, 1999).

The present study investigated the opportunity for the obtainable maximum reducing sugar from rice starch through acid hydrolysis. The corresponding conditions for starch hydrolysis by HCl and H_2SO_4 were evaluated based on the yield of reducing sugar.

Materials and Methodology

Materials

Rice grain–Myaunmya pawsan was purchased from Sanchaung market, Yangon. Analar grade hydrochloric and sulphuric acids were purchased from local chemical dealers, Kemiko shop, Yangon.

Methodology

Starch Hydrolysis

Initially, ground rice grain 50 g (# 60 mesh) was suspended with 100 ml of distilled water and gelatinized by heating the mixture at 95°C for five min. The resultant gelatinized starch was further liquefied and saccharified by heating at 100°C at least for four hr. After that, starch hydrolysate was neutralized with 0.1 M sodium hydroxide solution and reducing sugar was determined.

Detection of Starch

Iodine–potassium iodide solution was prepared for detection of starch. 3 g of gelatinized rice was placed in a glass dish and three drops of

iodine–potassium iodide solution was added into it. The sample was observed for the presence of starch, indicating a dark blue color.

Determination of Reducing Sugar

Reducing sugar of starch hydrolysate was determined by using Lane and Eynon's method (Pearson, 1976). The mixture of 10 ml portions of Fehling's solution A (6.928% (w/v) of copper sulphate) and Fehling's B (34.6% (w/v) sodium potassium tartarate in 10% sodium hydroxide) were freshly prepared and it was titrated with starch hydrolysate using methylene blue as indicator.

Starch hydrolysate 10 ml was diluted with 50 ml of distilled water and filled into a 50 ml burette. 10 ml portions of Fehling's solutions A and B were placed into a 250 ml conical flask, stoppered and mixed thoroughly for 15 sec by swirling and boiled on an electric heater. After the solution had boiled for about 2 min, the diluted sample was added to the boiling solution from the burette and 3 drops of methylene blue was added into it. The titration was continued by adding the sample dropwisely until the blue color disappeared. At the end point the boiling liquid turned into the brick-red color by the precipitation of cuprous oxide. This procedure was repeated thrice and the average titre value was calculated. Fermentable sugar (reducing sugar) was calculated by using the following equation.

$$\text{Reducing Sugar} = \frac{\text{Factor}}{\text{Titre}} \times 100,$$ Where Factor is the product of titre volume of standard invert sugar solution required to titrate with 10 ml portions of Fehling's solution and mg of invert sugar in 1 ml of standard invert sugar solution.

Results and Discussion

The steps involved in the conversion of rice starch into reducing sugar are gelatinization, liquefaction and saccharification. Gelatinization is the swelling of starch granules to the slurrying water. Before gelatinization milling of rice grains was a necessary step to reduce the size of rice grain approximately 2 mm grains. The ground rice so obtained was slurried with water and gelatinized or cooked at 95°C for 5 min. At this step, viscous starch slurry was obtained by loosing its crystallinity and became gel. Thereafter, liquefaction and saccharification of starch slurry called starch

hydrolysis was carried out by acid hydrolysis with HCl and H_2SO_4 respectively.

In order to determine the conditions for maximum yield of reducing sugar in starch hydrolysis, different acid concentrations (1%, 3%, 6%, 9% and 12% (v/v)), acid volume (50 ml, 100 ml, 150 ml, 200 ml and 250 ml) and duration of hydrolysis (5 hr, 6 hr, 7 hr, 15 hr and 30 hr) were varied. Figures 1, 2 and 3 represent the effect of acid concentration, volume of acid and duration of hydrolysis on the yield of reducing sugar. These figures also indicate the respective conditions of starch hydrolysis by HCl and H_2SO_4. The conditions based on the maximum yield of reducing sugar were acid concentration of 6%, volume of acid of 100 ml and duration of hydrolysis of 15 hr for starch hydrolysis reaction by HCl while for starch hydrolysis reaction by H_2SO_4 3%, 100 ml and 7 hr respectively.

With respect to the optimal acid concentration as shown in Figure 1, both HCl and H_2SO_4 with the lowest acid concentration of 1% caused incomplete starch hydrolysis, resulting the lower yield of reducing sugar. Increase in reducing sugar occurred with increase in acid concentration, however, reducing sugar gradually decreased after getting the maximum yield at the acid concentration of 6% and 3% respectively. The results as indicated also in Figure 2 pointed out that the maximum yield of reducing sugar was obtained at the acid volume of 100 ml for both, but before and beyond this point decreased yield in reducing sugar has resulted. It was found that 15 hr and 7 hr of duration of hydrolysis have provided the maximum yield of reducing sugar for HCl and H_2SO_4 hydrolysis. As can be seen in Figure 3, shorter hydrolysis time supported lower yield of reducing sugar, meanwhile, longer duration of hydrolysis did not offer the greater yield. According to Borglum (1999), starch hydrolysis is a degradation process in which starch molecules are broken down and fermentable sugars such as glucose are formed as the product of complete hydrolysis. The process for converting the starch to maltodextrin is known as partial hydrolysis and complete hydrolysis furnishes the starch into fermentable glucose. Complete starch hydrolysis is preferable for maximum fermentable sugar. In this study, the process of starch hydrolysis– liquefaction and saccharification of starch after gelatinization was conducted as a simultaneous acid hydrolysis. Therefore, partial and complete hydrolysis could be occurred and the maximum yield of reducing sugar may depend on such reaction of partial or complete starch hydrolysis. Before the point that has reached to the maximum yield of reducing sugar, decreased value occurred would be related to partial hydrolysis which offers mostly maltodextrin with small amount of glucose.

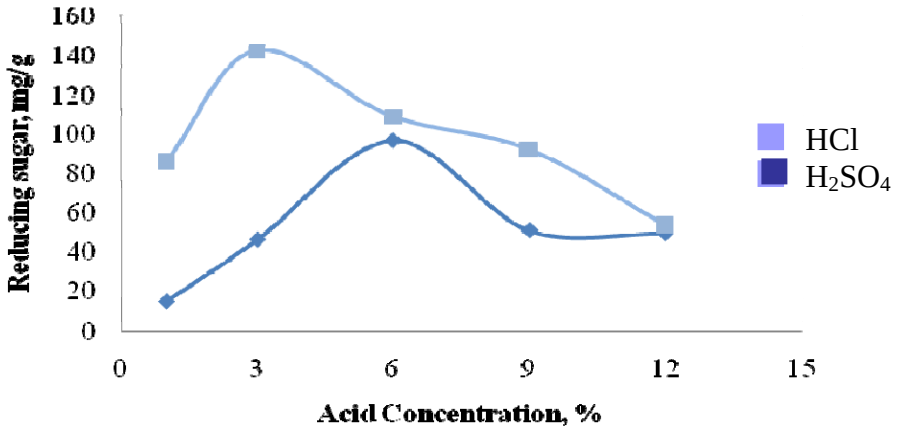

Figure 1 Effect of Acid Concentration on the Yield of Reducing Sugar

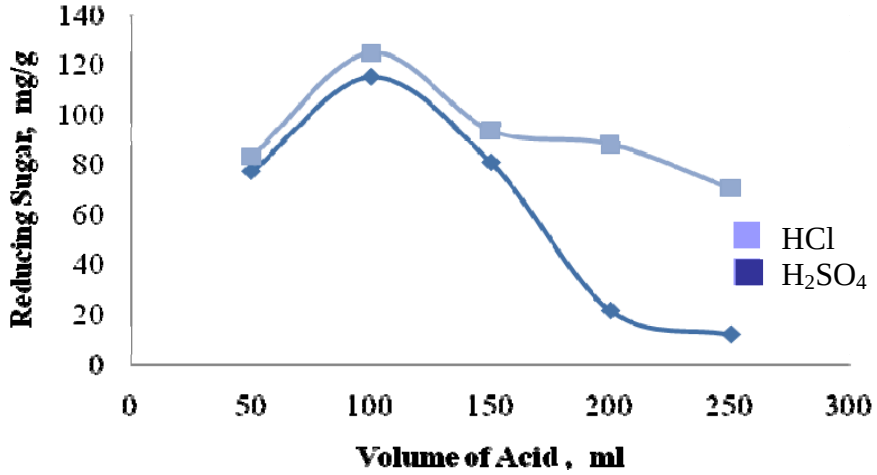

Figure 2 Effect of Acid Volume on the Yield of Reducing Sugar

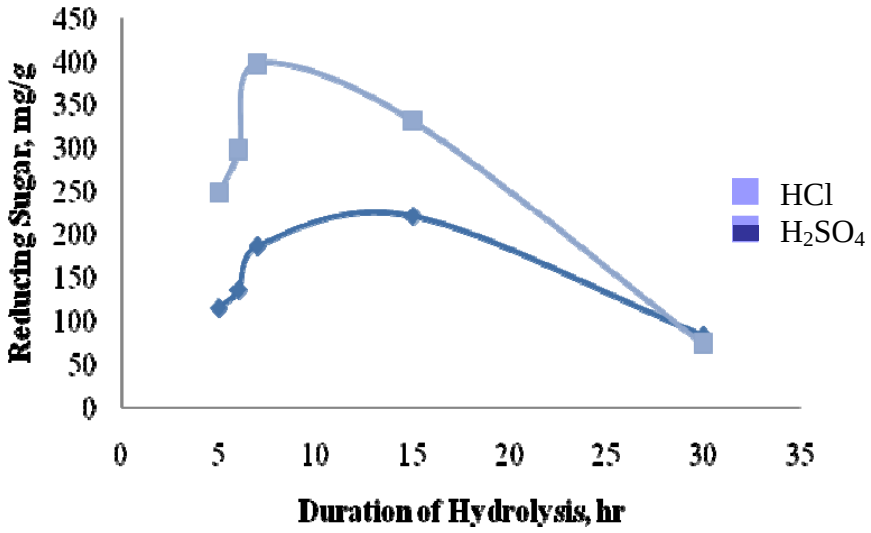

Figure 3 Effect of Duration of Hydrolysis on the Yield of Reducing Sugar

In addition, van Dam, Kieboom & van Bekkum (1986) found that glucose decomposed in acidic media under moderate reaction conditions and by then 5-hydroxymethylfuraldehyde (HMF) was formed. Therefore, the resulting glucose may decompose in acid media with longer hydrolysis time.

Figure 4 shows the comparison between starch hydrolysis by HCl and H_2SO_4 as regards the maximum yield of reducing sugar. It was apparent that starch hydrolysis by H_2SO_4 has resulted higher yield of reducing sugar of 399 mg/g than that by HCl in which 221.7 mg/g was obtained. Moreover, starch hydrolysis by H_2SO_4 occurred at lower acid concentration and shorter hydrolysis time when compared with starch hydrolysis by HCl.

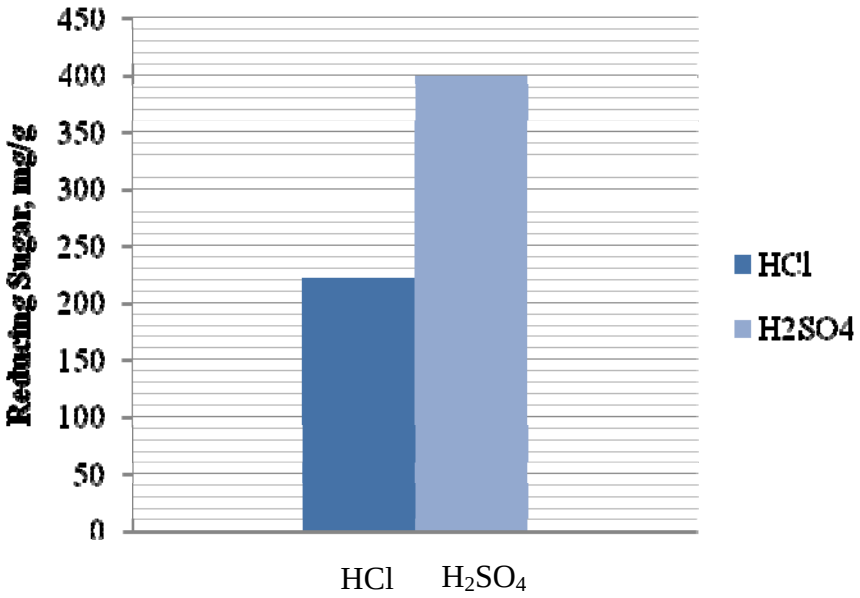

Figure 4 Comparison of the Yield of Reducing Sugar by HCl and H_2SO_4 in Starch Hydrolysis

Conclusion

Starch hydrolysis –liquefaction and saccharification of gelatinized rice was carried out as a simultaneous acid hydrolysis by HCl and H_2SO_4 respectively. Starch hydrolysis by H_2SO_4 has resulted the higher yield of reducing sugar at acid concentration of 3% (v/v), volume of acid of 100 ml and duration of hydrolysis of 7 hr whereas starch hydrolysis by HCl revealed at acid concentration of 6%, volume of acid of 100 ml and duration of hydrolysis of 15 hr.

Acknowledgement

I am very grateful to my research Supervisor Dr Soe Soe Than for her kind guidance.

References

Borglum, G.B., (1999). *Starch Hydrolysis for Ethanol Production*, Miles Laboratories Inc, Industrial Products Group, Elkhart, Indiana.

Carbohydrate Biotechnology Protocols, Edited by Department of Food Technology and Nutrition Science, Food and Bioprocess Engineering, University of Iowa, Iowa.

Damirbas, A., (2005). Bioethanol from Cellulosic Materials; A Renewable Motor Fuel from Biomass, *Energy Sources, 27*, 327-337.

Marchal, M.L., (1999). Partial Hydrolysis of Starch to Maltodextrins on the Lab Scale,

Pearson, D., (1976). *The Chemical Analysis of Foods*, 7th Edition, Churchill LivingStone Inc, Edinburgh, London.

Van Dam, H. E., Kieboom, A. P. G. and van Bekkum, H. (1986), The Conversion of Fructose and Glucose in Acidic Media: Formation of Hydroxymethylfurfural. Starch-Stärke, 38: 95–101, doi: 10.1002/star. 19860380308, Retrieved April 25, 2011 from www.pubmedcentral. nih.gov.

Wikipedia, The Free Encyclopedia, (2011). Starch. Retrieved March 20, 2011, from http://en.wikipedia.org/wiki/Starch.